DEVELOPMENT OF THE MGS APPROACH GUARDRAIL TRANSITION USING STANDARDIZED STEEL POSTS

Submitted by

Scott K. Rosenbaugh, M.S.C.E., E.I.T.
Research Associate Engineer

Karla A. Lechtenberg, M.S.M.E., E.I.T.
Research Associate Engineer

Ronald K. Faller, Ph.D., P.E.
Research Assistant Professor

Dean L. Sicking, Ph.D., P.E.
Professor and MwRSF Director

Robert W. Bielenberg, M.S.M.E., E.I.T.
Research Associate Engineer

John D. Reid, Ph.D.
Professor

MIDWEST ROADSIDE SAFETY FACILITY
Nebraska Transportation Center
University of Nebraska-Lincoln
130 Whittier Research Center
2200 Vine Street
Lincoln, Nebraska 68583-0853
(402) 472-0965

Submitted to

MIDWEST STATES REGIONAL POOLED FUND PROGRAM
Nebraska Department of Roads
1500 Nebraska Highway 2
Lincoln, Nebraska 68502

MwRSF Research Report No. TRP-03-210-10

December 21, 2010

TECHNICAL REPORT DOCUMENTATION PAGE

1. Report No. TRP-03-210-10	2.	3. Recipient's Accession No.
4. Title and Subtitle Development of the MGS Approach Guardrail Transition Using Standardized Steel Posts		5. Report Date December 21, 2010
		6.
7. Author(s) Rosenbaugh, S.K., Lechtenberg, K.A., Faller, R.K., Sicking, D.L., Bielenberg, R.W., and Reid, J.D.		8. Performing Organization Report No. TRP-03-210-10
9. Performing Organization Name and Address Midwest Roadside Safety Facility (MwRSF) Nebraska Transportation Center University of Nebraska-Lincoln 130 Whittier Research Center 2200 Vine Street Lincoln, Nebraska 68583-0853		10. Project/Task/Work Unit No.
		11. Contract © or Grant (G) No. SPR-3(017) TPF-5(193)
12. Sponsoring Organization Name and Address Midwest States Regional Pooled Fund Program Nebraska Department of Roads 1500 Nebraska Highway 2 Lincoln, Nebraska 68502		13. Type of Report and Period Covered Final Report: 2008 – 2010
		14. Sponsoring Agency Code RPFP-08-05 and RPFP-09-03

16. Abstract (Limit: 200 words)

A W-beam to thrie beam stiffness transition was developed to connect the Midwest Guardrail System (MGS) to a previously-approved thrie beam approach guardrail transition to bridge rail. This new stiffness transition was configured with standard steel posts commonly used by State Departments of Transportation. The system was crash tested and evaluated according to the Test Level 3 (TL-3) safety performance criteria specified in the Manual for Assessing Safety Hardware (MASH).

BARRIER VII computer simulation modeling, in combination with post-in-soil bogie tests, was used to evaluate multiple transition configurations. The optimal configuration was the shortest design to successfully eliminate excessive pocketing and wheel snag. The approach guardrail transition was attached to Missouri's thrie beam and channel bridge railing system. Three full-scale crash tests were conducted. During the first test, the upstream terminal anchor post failed prematurely, thus causing a loss of rail tension which ultimately led to vehicle pocketing. After inspection, the upstream anchor post was found to have a large knot located on its tension face at groundline that led to the wood fracture and failure of the test. The test was rerun given careful attention to the quality of the BCT anchor posts to ensure that the system design strength could be met. Following the successful containment and redirection of both the ½-ton Quad Cab pickup truck (2270P) and the small car (1100C) test vehicles, the safety performance of the stiffness transition between the MGS and a thrie beam approach guardrail transition system, including an asymmetrical guardrail element, was determined to be acceptable according to the TL-3 evaluation criteria specified in MASH.

17. Document Analysis/Descriptors Highway Safety, Roadside Appurtenances, Crash Test, Compliance Test, MASH, Asymmetric W-Beam to Thrie Beam Transition, Longitudinal Barrier, Approach Guardrail Transition, TL-3, Steel Post, and Midwest Guardrail System (MGS)		18. Availability Statement No restrictions. Document available from: National Technical Information Services, Springfield, Virginia 22161
19. Security Class (this report) Unclassified	20. Security Class (this page) Unclassified	21. No. of Pages 278 · 22. Price

DISCLAIMER STATEMENT

This report was conducted in part through funding from the Federal Highway Administration, U.S. Department of Transportation. The contents of this report reflect the views and opinions of the authors who are responsible for the facts and the accuracy of the data presented herein. The contents do not necessarily reflect the official views or policies of the state highway departments participating in the Midwest States Regional Pooled Fund Program nor the Federal Highway Administration, U.S. Department of Transportation. This report does not constitute a standard, specification, regulation, product endorsement, or an endorsement of manufacturers.

UNCERTAINTY OF MEASUREMENT STATEMENT

The Midwest Roadside Safety Facility (MwRSF) has determined the uncertainty of measurements for several parameters involved in standard full-scale crash testing and non-standard testing of roadside safety features. Information regarding the uncertainty of measurements for critical parameters is available upon request by the sponsor and the Federal Highway Administration.

INDEPENDENT APPROVING AUTHORITY

The Independent Approving Authority (IAA) for the data contained herein was Dr. John Reid.

ACKNOWLEDGEMENTS

Kansas Department of Transportation

Ron Seitz, P.E., Bureau Chief
Rod Lacy, P.E., Metro Engineer
Scott King, P.E., Road Design Leader

Minnesota Department of Transportation

Michael Elle, P.E., Design Standard Engineer

Missouri Department of Transportation

Joseph G. Jones, P.E., Engineering Policy Administrator

Nebraska Department of Roads

Amy Starr, P.E., Research Engineer
Phil TenHulzen, P.E., Design Standards Engineer
Jodi Gibson, Research Coordinator

Ohio Department of Transportation

Dean Focke, P.E., Road Safety Engineer (Retired)
Michael Bline, P.E., Standards and Geometrics Engineer

South Dakota Department of Transportation

Bernie Clocksin, Lead Project Engineer

Wisconsin Department of Transportation

Jerry H. Zogg, P.E., Chief Roadway Standards Engineer
John Bridwell, P.E., Standards Development Engineer
Erik Emerson, P.E., Standards Development Engineer

Wyoming Department of Transportation

William Wilson, P.E., Architectural and Highway Standards Engineer

Federal Highway Administration

John Perry, P.E., Nebraska Division Office
Danny Briggs, Nebraska Division Office

Dunlap Photography

James Dunlap, President and Owner

TABLE OF CONTENTS

LIST OF FIGURES

LIST OF TABLES

1 INTRODUCTION

1.1 Background and Problem Statement

Throughout the United States, State Highway Departments commonly use standard strong-post, W-beam guardrail systems to prevent errant vehicles from leaving the roadway and encountering safety hazards beyond or near the roadway edge. One of the more common applications for this barrier is to shield traffic from impacting the blunt ends of bridge rails and their associated drop offs. Although strong-post, W-beam barriers are generally considered to be "semi-rigid," these barriers are much more flexible than most bridge railing systems. In order to eliminate the potential for vehicle pocketing or wheel snag at the point of attachment to a rigid bridge rail end, an approach guardrail transition region is added between semi-rigid W-beam guardrail systems and stiff bridge railing systems to provide a more gradual change in lateral barrier stiffness.

Traditionally, approach guardrail transitions have been comprised of some combination of reduced post spacing, longer posts, additional rail elements, a curb incorporated under the barrier, and thrie beam guardrail. These additional elements provide increased stiffness in the approach guardrail transition system and prevent vehicles from impacting the upstream end of the bridge rail. However, the upstream end of the typical approach guardrail transition can also be a potential location for vehicle pocketing or wheel snag if the change in lateral stiffness occurs too rapidly. Further, prior full-scale crash tests involving impacts near the upstream ends of typical approach guardrail transitions have resulted in pocketing, rail ruptures, and vehicle instabilities [1-4].

In 2007, the Midwest Roadside Safety Facility (MwRSF) developed a new W-beam to thrie beam approach transition system to provide the gradual change in lateral barrier stiffness deemed necessary for a crashworthy approach guardrail transition [5-7]. This stiffness transition

utilized an asymmetrical W-beam to thrie beam transition element to connect the Midwest

Guardrail System (MGS) to one of the stiffest thrie beam transition systems used by the member

states of the Midwest States Pooled Fund Program. This barrier system was crash tested near the

upstream end of the approach guardrail transition and was deemed acceptable according to Test

Level 3 (TL-3) of National Cooperative Highway Research Program (NCHRP) Report No. 350,

Recommended Procedures for the Safety Performance Evaluation of Highway Features [8].

This new stiffness transition successfully adapted the 31-in. (787-mm) high, MGS to the

upstream end of a crashworthy thrie beam transition. However, the barrier system utilized three

post types, including "non-standard" W6x12 (W152x17.9) steel guardrail posts that were not

currently used by most State Departments of Transportation (DOTs). Therefore, the system was

viewed as too complicated. In addition, approach guardrail transitions had not yet been crash

tested and evaluated under the newly-adopted guidelines found in the *Manual for Assessing

Safety Hardware* (MASH) [9]. Thus, the MASH safety performance of W-beam to thrie beam

transitions was not known, including the potential for underride or wheel snag with the new

1100C small car vehicles as well as the propensity for pocketing, override, wheel snag, and

vehicle rollover with the new 2270P pickup truck.

1.2 Research Objective

The objective of the research project was to develop a simplified stiffness transition

between the MGS and a thrie beam approach guardrail transition using only two post types –

standard W6x15 (W152x22.3) and W6x9 (W152x13.4) steel posts. The simplified stiffness

transition was to be crash tested and evaluated according to TL-3 safety performance criteria set

forth in MASH. The safety performance of the W-beam to thrie beam transition element is

somewhat dependent upon the stiffness and strength of the approach guardrail transition system

adjacent to the end of the bridge rail. A stiffer downstream approach guardrail transition system

will increase the risk of pocketing, wheel snag, and vehicle underride. Thus, it was determined to examine the performance of the simplified stiffness transition when attached to a very stiff approach guardrail transition system developed for use with Missouri's thrie beam and channel bridge railing system [5-7,10-11].

1.3 Scope

The research objective was achieved through the completion of several tasks. First, a literature review was undertaken to review previous evaluations of W-beam to thrie beam transition sections. Second, dynamic component tests were conducted to verify the force vs. deflection characteristics of the standard steel posts used in the transition system. Next, BARRIER VII computer simulations were performed utilizing the post-soil behavior to determine the optimum, simplified transition design. Then, a modified guardrail system consisting of a new stiffness transition between the MGS and a stiff thrie beam approach guardrail transition was constructed. Three full-scale vehicle crash tests were performed according to the TL-3 impact conditions of MASH. The first two crash tests utilized a ½–ton Quad Cab pickup truck, weighing approximately 5,000 lb (2,268 kg). The target impact conditions for these tests were an impact speed and angle of 62 mph (100 km/h) and 25 degrees, respectively. The final test utilized a small car, weighing approximately 2,425 lb (1,100 kg). The target impact conditions for this test were an impact speed and angle of 62 mph (100 km/h) and 25 degrees, respectively. The results of these tests were analyzed, evaluated, and documented. Conclusions and recommendations were made that pertain to the safety performance of the stiffness transition between MGS and a crashworthy thrie beam approach guardrail transition system. Finally, guidance was provided for adapting the new, simplified stiffness transition to other crashworthy approach guardrail transitions.

2 LITERATURE REVIEW

2.1 NCHRP Report No. 230 Systems

Previous testing on various W-beam to thrie beam transition sections was conducted by the New York State Department of Transportation (NYSDOT) and was met with mixed results. When the unsymmetrical designs were initially crash tested, the full-size sedans were forced down under the W-beam rail element, resulting in severe snagging on the lower thrie beam corrugation which included a taper [1-2]. In the later tests on a symmetrical W-beam to thrie beam section, two out of three test vehicles were successfully redirected. Crash tests of the W-beam to thrie beam transition systems previously conducted at NYSDOT were evaluated according to the criteria provided in NCHRP Report No. 230 [12].

NYSDOT performed five full-scale vehicle crash tests on several W-beam to thrie beam transition configurations used to transition from a weak-post, W-beam guardrail system with reduced post spacing to a rigid thrie beam bridge railing. For the first design, a 50-in. (1,270-mm) long asymmetrical section was placed between the W-beam and thrie beam rails. At the upstream end of the transition section, the lower corrugation terminated with a 12-in. (305-mm) long taper toward the rail's mid-height. A 4,500-lb (2,041-kg) passenger-size sedan (test no. 67) impacted the rail 105 in. (2,667 mm) upstream from the tapered section at 58.8 mph (94.6 km/h) and 25 degrees. During the test, the right-front wheel and suspension snagged severely on the end of the lower thrie beam corrugation, and the test was determined to be unacceptable according to the NCHRP Report No. 230 requirements.

Following the failure of test no. 67, the transition section was modified to reduce the severe snagging at the end of the section. For the second design, a 75-in. (1,905-mm) long asymmetrical section was placed between the W-beam and thrie beam rails. At the upstream end of the transition section, the lower corrugation terminated with an increased taper length of 36 in.

(914 mm), as measured from the bottom of the rail to the rail's mid-height. A 4,499-lb (2,041-kg) passenger-size sedan (test no. 68) impacted the rail 55 in. (1,397 mm) upstream from the tapered section at 59.5 mph (95.8 km/h) and 24 degrees. During the test, the right-front wheel and suspension once again snagged severely on the end of the lower thrie beam corrugation, and the test was determined to be unacceptable according to the NCHRP Report No. 230 requirements.

After the failure of test nos. 67 and 68, the NYSDOT realized the termination of the lower tapered corrugation presented an insurmountable snag point. Therefore, the W-beam to thrie beam transition section was redesigned to include a symmetrical tapered section which could adapt W-beam rail directly to thrie beam rail. This transition section is the same design that now appears in the American Association of State Highway and Transportation Officials' (AASHTO's) *Standard Specifications for Transportation Materials and Methods of Sampling and Testing* [13].

Following the redesign of the symmetrical W-beam to thrie beam transition section, three additional full-scale crash tests were performed. For this design, a 4,601-lb (2,087-kg) passenger-size sedan (test no. 69) impacted the rail 82 in. (2,083 mm) upstream from the tapered section at 54.4 mph (87.5 km/h) and 26 degrees. During impact, the vehicle was smoothly redirected with only minor snagging on the posts, and the test was determined to be acceptable according to the NCHRP Report No. 230 requirements. A fourth test (test no. 70) was performed using a 1,980-lb (898-kg) small car (Subaru station wagon) impacting the rail 42 in. (1,067 mm) upstream from the tapered section at 57.8 mph (93.0 km/h) and 20 degrees. During the test, the right-front wheel and bumper snagged severely on the first W6x9 (W152x13.4) steel post which resulted in rapid vehicle yaw away from the rail and roll onto its side. As a result, the test was determined to be unacceptable according to the NCHRP Report No. 230 requirements.

After the failed small car test on the symmetric W-beam to thrie beam transition section, the depth of the steel wide-flange blockouts was increased from 6 to 14 in. (152 to 356 mm), and the small car crash test was rerun. This fifth test (test no. 71) was performed using a 1,799-lb (816-kg) small car (Honda) impacting the rail 34 in. (864 mm) upstream from the tapered section at 60.3 mph (97.0 km/h) and 19 degrees. During the test, the vehicle was smoothly redirected, and the test was determined to be acceptable according to the NCHRP Report No. 230 requirements. Although the system was redesigned following the successful passenger-size sedan test, a retest with the large car was deemed unnecessary. Thus, the symmetrical W-beam to thrie beam transition section, combined with 14¼-in. (362-mm) deep blockouts and used to connect weak-post W-beam guardrail to a thrie beam approach guardrail transition, met the requirements of NCHRP Report No. 230.

2.2 NCHRP Report No. 350 Systems

In 1999, the Midwest Roadside Safety Facility (MwRSF) conducted two full-scale vehicle crash tests on a symmetrical W-beam to thrie beam transition section [4]. The test installation consisted of four major structural components: (1) two nested 18-ft 9-in. (5.72-m) long 12-gauge (2.66-mm thick) thrie beam rail sections; (2) a 6-ft 3-in. (1.91-m) long 12-gauge (2.66-mm thick) W-beam to thrie beam transition section; (3) a 50-ft (15.24-m) long 12-gauge (2.66-mm thick) W-beam rail section attached to a simulated anchorage device; and (4) a 12-ft 6-in. (3.81-m) long thrie beam and channel bridge railing system with an attached simulated anchorage device. The tests were evaluated according to the safety performance criteria provided in NCHRP Report No. 350 [8].

For the first test, test no. MWT-1, a 1,810-lb (821-kg) small car impacted the system 48 in. (1,219 mm) upstream from the first post of the W-beam to thrie beam transition at a speed of

61.8 mph (99.5 km/h) and at an angle of 25.7 degrees. The vehicle was smoothly redirected, and the test was determined to be acceptable according to the NCHRP Report No. 350 requirements.

In the second test, test no. MWT-2, a 4,458-lb (2,022-kg) ¾-ton pickup truck impacted the system 7 ft - 4 in. (2.23 m) upstream from the first post of the W-beam to thrie beam transition at a speed of 61.1 mph (98.3 km/h) and at an angle of 25.3 degrees. During this test on the approach guardrail transition, the guardrail upstream of the transition element began to deform laterally, and the test vehicle slowly began to redirect. As the vehicle progressed into the barrier, a pocket began to develop at the downstream end of the transition element where it was connected to the nested thrie beam rail. As the test vehicle approached, the nested thrie beam rails, a sharp kink developed at the end of the transition element and eventually ruptured at this location. When the front of the test vehicle contacted the end of the largely undeformed nested thrie beam elements, it was forced up into the air and rolled over the traffic side of the barrier. Therefore, this test was determined to be unacceptable according to the NCHRP Report No. 350 requirements, as the vehicle did not remain upright after collision.

In 2002, the Materials Engineering and Testing Services of the California Department of Transportation (CALTRANS) designed and tested a symmetrical W-beam to thrie beam transition section [14]. The system consisted of nested thrie beam on the traffic-side face of the barrier and a single thrie beam on the backside. One of the thrie beams on the traffic side was 10 gauge (3.42 mm thick), while the other one and the rail on the backside were 12 gauge (2.66 mm thick). A 10-gauge (3.42-mm thick) symmetrical W-beam to thrie beam transition connected the W-beam to the thrie beam. The five posts closest to the bridge rail were 10-in. x 10-in. x 8-ft long (254-mm x 254-mm x 2.44-m) Douglas Fir posts with 8-in. x 8-in. x 22-in. (203-mm x 203-mm x 559-mm) blockouts. The sixth post was also 10 in. x 10 in. (254 mm x 254 mm) but only 6 ft (1.83 m) long.

In test no. 519, a 4,352-lb (1,974-kg) ¾-ton pickup truck impacted the transition at the third post upstream from the end of the concrete bridge rail, or 37 ½ in. (953 mm) downstream of the symmetrical transition element's downstream end, at a speed and angle of 62.1 mph (100.0 km/h) and 25.5 degrees, respectively. The vehicle was safely redirected without any indication of pocketing. Therefore, this test was considered acceptable according to the NCHRP Report No. 350 safety performance criteria.

In test no. 518, a 4,400-lb (1,996-kg) ¾-ton pickup truck impacted the transition 37.4 in. (950 mm) upstream from the beginning of the symmetrical transition element at a speed and angle of 62.1 mph (99.9 km/h) and 25.0 degrees, respectively. The vehicle was safely redirected without any indication of pocketing. Therefore, this test was considered acceptable according to the NCHRP Report No. 350 safety performance criteria.

In test no. 514, a 17,661-lb (8,011-kg) single-unit truck impacted the transition midway between the second and third posts upstream from the end of the concrete bridge rail, or approximately 56 in. downstream of the symmetrical transition element's downstream end, at a speed and angle of 46.9 mph (75.5 km/h) and 16.0 degrees, respectively. The vehicle was safely redirected without revealing any tendency toward pocketing. Therefore, this test was considered acceptable according to the NCHRP Report No. 350 safety performance criteria.

In 2007, MwRSF undertook another project to further evaluate the transition from W-beam guardrail to thrie beam guardrail [5-7]. All four test installations measured 87 ft – 6 in. (26.67 m) long and were comprised of five major structural components: (1) a 12-ft 6-in. (3.81-m) long thrie beam and channel bridge railing system with an attached simulated anchorage device; (2) two nested 12 ft - 6 in. (3.81 mm) 12-gauge (2.66-mm thick) thrie beam rail sections; (3) a 6 ft - 3 in. (1.91 m) long 12-gauge (2.66-mm thick) thrie beam rail section; (4) a 6-ft 3-in. (1.91-m) long, 12-gauge (2.66-mm thick) W-beam to thrie beam transition segment; and (5) a

8

50-ft (15.2-m) long 12-gauge (2.66-mm thick) W-beam guardrail attached to a simulated anchorage device.

During the first test, test no. MWT-3, the system was impacted by a 4,456-lb (2,021-kg) pickup truck 6 ft – 11 in. (2.11 m) upstream from the symmetrical W-beam to thrie beam transition element at a speed of 63.9 mph (102.9 km/h) and at an angle of 24.8 degrees. During impact, the pickup truck experienced a large amount of roll which ultimately led to the vehicle rolling over after it exited the barrier. Due to vehicle roll over, this test was determined to be unacceptable according to the NCHRP Report No. 350 requirements.

To prevent the vehicle rollover, the Midwest Guardrail System (MGS) was utilized in place of the standard W-beam guardrail. This switch raised the top height of the W-beam guardrail section from 27¾ in. (706 mm) to 31 in. (787 mm). Therefore, an asymmetrical transition piece was utilized to extend the bottom of the W-beam downward to meet the thrie beam element. This transition segment was fabricated by cutting a triangular piece from the bottom of a standard 12-gauge (2.66-mm thick) thrie beam rail and welding a 10-gauge (3.43-mm thick) plate along the cut region. All other elements for this system were identical to the previous test. The full-scale crash test, test no. MWT-4, consisted of a 4,448-lb (2,018-kg) pickup truck impacting the system 7 ft (2.1 m) upstream from the first post of asymmetrical W-beam to thrie beam element at a speed of 61.0 mph (98.1 km/h) and at an angle of 25.3 degrees. Due to stress concentrations in the fabricated transition element, the rail ruptured. Thus, this test was determined to be unacceptable according to the NCHRP Report No. 350 requirements. However, the basic design of the MGS transition element showed potential.

Consequently, a new asymmetrical W-beam to thrie beam transition element was developed that incorporated the same basic philosophy as a symmetrical transition element (i.e., the gradual introduction of a new peak between the two existing peaks in the W-beam). The new

9

element was manufactured from 10-gauge (3.43-mm thick) plate welded together. In addition, the system was stiffened to eliminate the pocketing observed prior to rail rupture in test no. MWT-4. The additional stiffness was achieved by changing several posts from W6x9 (W152x13.4) to W6x12 (W152x17.9) steel sections throughout the upstream transition region.

During test no. MWT-5, a 4,431-lb (2,010-kg) pickup truck impacted the transition system 7 ft – 4 in. (2.24 m) upstream from the first post of the asymmetrical W-beam to thrie beam segment at a speed of 61.5 mph (99.0 km/h) and an angle of 24.9 degrees. The vehicle was smoothly redirected, and the test was determined to be acceptable according to the NCHRP Report No. 350 requirements.

Test no. MWT-6 consisted of a 1,992-lb (904-kg) small car impacting the system 3 ft – 10¾ in. (1.19 m) upstream from the first post of the asymmetrical W-beam to thrie beam transition element at a speed of 65.5 mph (105.3 km/h) and at an angle of 20.4 degrees. The vehicle was smoothly redirected, and the test was determined to be acceptable according to the NCHRP Report No. 350 requirements.

3 COMPONENT TEST CONDITIONS

3.1 Purpose

In previous research, MwRSF has conducted numerous dynamic bogie tests of W6x9 (W152x13.4) steel posts embedded in strong soil. However, tests have not been conducted on the larger W6x15 (W152x22.3) steel posts used in the selected transition system [10-11]. Therefore, dynamic testing was undertaken to determine the dynamic properties of these larger steel posts.

3.2 Scope

Two dynamic bogie tests were conducted with W6x15 (W152x22.3) steel posts embedded 54 in. (1,372 mm) in soil. The soil was a compacted, coarse, crushed limestone material that met AASHTO standard soil designation M147 Grade B, as recommended by MASH [9]. The target impact conditions were 20 mph (32 km/h) at an angle of 0 degrees (i.e., through the strong axis of the post). The posts were impacted $24\frac{7}{8}$ in. (632 mm) above the groundline. The bogie test matrix and the test setup are shown in Figure 1.

3.3 Test Facility

Physical testing of the W6x15 (W152x22.3) steel posts was conducted at the MwRSF testing facility located at the Lincoln Air Park on the northwest side of the Lincoln Municipal Airport. The facility is approximately 5 miles (8 km) northwest from the University of Nebraska-Lincoln's city campus.

3.4 Equipment and Instrumentation

A variety of equipment and instrumentation was utilized to collect and record data during the dynamic bogie tests, including a bogie vehicle, accelerometers, pressure tape switches, and digital video and still cameras.

Number of Tests	Impact Speed (mph)	Impact Orientation	Post Placement	Post Length (ft)	Embedment Depth (in.)	Post Specifications
						W6x15
2	20	Strong Axis	Strong Soil	7	54	Southern Yellow Pine 8" x 8" Post
2	20	Strong Axis	Strong Soil	7	54	

MGS Transition Post Testing

Post Details &
Test Matrix

Midwest Roadside
Safety Facility

Sheet:	1 of 2
Date:	09/21/2007
By:	MJW
Rev:	KAP

Drawing Name:
MGSTransitionBogie.dwg   Scale: 1=25

Figure 1. Bogie Testing Matrix and Setup

3.4.1 Bogie

A rigid frame bogie was used to impact the posts. A variable height, detachable impact head was used in the testing. The bogie head was constructed of 8-in. (203-mm) diameter, ½-in. (13-mm) thick standard steel pipe, with ¾-in. (19-mm) neoprene belting wrapped around the pipe to prevent local damage to the post from the impact. The impact head was bolted to the bogie vehicle, creating a rigid frame with an impact height of 24⅞ in. (632 mm). The bogie with impact head is shown in Figure 2. The weight of the bogie with the addition of the mountable impact head was 1,810 lb (821 kg).

A pickup truck with a reverse cable tow system was used to propel the bogie to a target impact speed of 20 mph (32 km/h). When the bogie approached the end of the guidance system, it was released from the tow cable, allowing it to be free rolling when it impacted the post. A remote braking system was installed on the bogie allowing it to be brought safely to rest after the test.

Figure 2. Rigid Frame Bogie on Guidance Track

3.4.2 Accelerometers

Three environmental shock and vibration sensor/recorder systems were used to measure the accelerations in the longitudinal, lateral, and vertical directions. All of the accelerometers were mounted near the center of gravity of the test vehicles.

One triaxial piezoresistive accelerometer system, Model EDR-4 6DOF-500/1200, was developed and manufactured by Instrumented Sensor Technology (IST) of Okemos, Michigan and includes three differential channels as well as three single-ended channels. The EDR-4 6DOF-500/1200 was configured with 24 MB of RAM memory, a range of ±500 g's, a sample rate of 10,000 Hz, and a 1,677 Hz anti-aliasing filter. The "EDR4COM" and "DynaMax Suite" computer software programs and a customized Microsoft Excel worksheet were used to analyze and plot the accelerometer data.

The second system was a two-arm piezoresistive accelerometer system developed by Endevco of San Juan Capistrano, California. Three accelerometers were used to measure each of the longitudinal, lateral, and vertical accelerations independently at a sample rate of 10,000 Hz. The accelerometers were configured and controlled using a system developed and manufactured by Diversified Technical Systems, Inc. (DTS) of Seal Beach, California. More specifically, data was collected using a DTS Sensor Input Module (SIM), Model TDAS3-SIM-16M. The SIM was configured with 16 MB SRAM memory and 8 sensor input channels with 250 kB SRAM/channel. The SIM was mounted on a TDAS3-R4 module rack. The module rack was configured with isolated power/event/communications, 10BaseT Ethernet and RS232 communication, and an internal backup battery. Both the SIM and module rack were crashworthy. The computer software program "DTS TDAS Control" and a customized Microsoft Excel worksheet were used to analyze and plot the accelerometer data.

The third system, Model EDR-3, was a triaxial piezoresistive accelerometer system developed and manufactured by IST of Okemos, Michigan. The EDR-3 was configured with 256 kB of RAM memory, a range of ±200 g's, a sample rate of 3,200 Hz, and a 1,120 Hz low-pass filter. The computer software program "DynaMax 1 (DM-1)" and a customized Microsoft Excel worksheet were used to analyzed and plot the accelerometer data.

3.4.3 Pressure Tape Switches

Three pressure tape switches, spaced at approximately 18-in. (457-mm) intervals and placed near the end of the bogie track, were used to determine the speed of the bogie before the impact. As the left-front tire of the bogie passed over each tape switch, a strobe light was fired sending an electronic timing signal to the data acquisition system. The system recorded the signals and the time each occurred. The speed was then calculated using the spacing between the sensors and the time between the signals. Strobe lights and high-speed video analysis are used only as a backup in the event that vehicle speeds cannot be determined from the electronic data.

3.4.4 Photography Cameras

One high-speed AOS VITcam digital video camera and one JVC digital video camera were used to document each test. The high-speed AOS camera had a frame rate of 500 frames per second and the JVC digital video camera had a frame rate of 29.97 frames per second. Both cameras were placed 17 ft (5.2 m) from the center of the posts, with a view perpendicular to the bogie's direction of travel. Also, a Nikon D50 digital still camera was used to document pre- and post-test conditions of each test.

3.5 End of Test Determination

When the impact head initially contacts the test article, the force exerted by the surrogate test vehicle is directly perpendicular. However, as the post rotates, the surrogate test vehicle's orientation and path moves further from perpendicular. This introduces two sources of error: (1)

15

the contact force between the impact head and the post has a vertical component and (2) the impact head slides upward along the test article. Therefore, only the initial portion of the accelerometer trace may be used since variations in the data become significant as the system rotates and the surrogate test vehicle overrides the system.

Guidelines were established to define the end of test time using the high-speed video of the crash test. The first occurrence of any one of the following three events was used to determine the end of the test: (1) the test article fractures; (2) the surrogate vehicle overrides/losses contact with the test article; or (3) a maximum post rotation of 45 degrees.

3.6 Data Processing

The electronic accelerometer data was filtered using the SAE Class 60 Butterworth filter conforming to the SAE J211/1 specifications [15]. The pertinent acceleration signal was extracted from the bulk of the data signals. The processed acceleration data was then multiplied by the mass of the bogie to get the impact force using Newton's Second Law. Next, the acceleration trace was integrated to find the change in velocity verses time. Initial velocity of the bogie, calculated from the pressure tape switch data, was then used to determine the bogie velocity, and the calculated velocity trace was integrated to find the bogie's displacement. This displacement is also the displacement of the post. Combining the previous results, a force vs. deflection curve was plotted for each test. Finally, integration of the force vs. deflection curve provided the energy vs. displacement curve for each test.

4 COMPONENT TESTING RESULTS AND DISCUSSION

4.1 Results

The information desired from each component test was the relation between the force on the post and deflection of the post at the impact location. This data was then used to find total energy (the area under the force versus deflection curve) dissipated during each test.

Although the acceleration data was applied at the impact location, the data came from the center of gravity of the bogie. Error was added to the data, since the bogie was not perfectly rigid, thus causing vibrations in the bogie. Also, the bogie may have rotated during impact, thus causing differences in accelerations between the bogie center of mass and the bogie impact head. While these issues may affect the data, it was believed the data was not significantly influenced. Also, the accelerometer data may include influences from the post's inertial resistance when calculating the bogie's reaction force. This influence can be an important factor as the mass of the post can affect the inertial results.

The accelerometer data for each test was processed in order to obtain acceleration, velocity, and displacement curves, as well as force versus deflection and energy versus deflection curves. The values described herein were calculated from the EDR-3 raw data, since it was used during all of the tests. Individual accelerometer results for all tests are provided in Appendix A.

4.1.1 Test No. MGSATB-1 [W6x15 (W152x22.3) Steel Post]

During test no. MGSATB-1, the bogie impacted the post at a speed of 19.2 mph (30.9 km/h). As a result, the post rotated through the soil until it reached a maximum deflection of 19.5 in. (495 mm), as determined from the EDR-3 data. The bogie vehicle was brought to a stop at this maximum deflection before rebounding and rolling backward a short distance. Upon post-

test examination, the post had bent backward, resulting in yielding and compression flange buckling at approximately 6 in. (152 mm) below the groundline.

Force vs. deflection and energy vs. deflection curves are shown in Figure 3. Initially, inertial effects resulted in a peak force of 13.6 kips (60.5 kN) over the first 2 in. (51 mm) of deflection. An average force of around 15 kips (67 kN) was observed through the rest of the impact event, with a peak force of 20.1 kips (89.4 kN). The post absorbed 269 kip-in. (30.4 kJ) of energy and had a maximum deflection of 19.5 in. (495 mm).
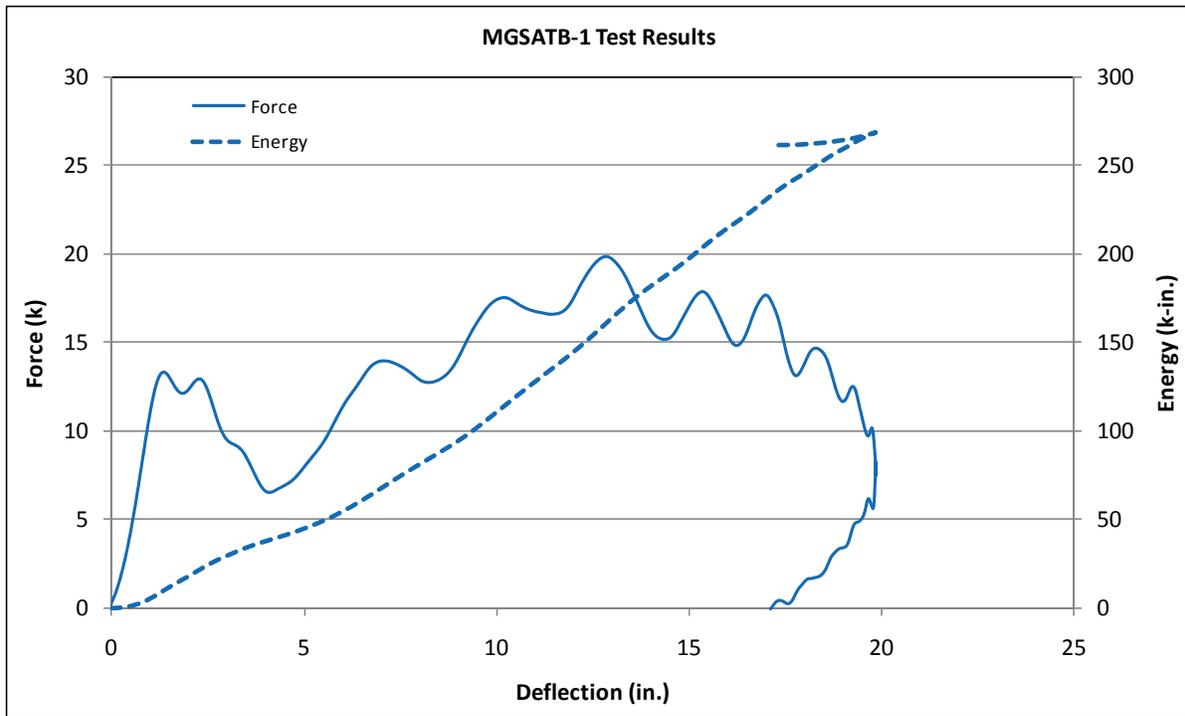
Figure 3. Force vs. Deflection and Energy vs. Deflection, Test No. MGSATB-1 [W6x15 (W152x22.3) Post]

IMPACT

0.050 sec

0.100 sec

0.150 sec

0.200 sec

0.250 sec

Figure 4. Time Sequential and Post-Impact Photographs, Test No. MGSATB-1

4.1.2 Test No. MGSATB-2 [W6x15 (W152x22.3) Steel Post]

During test no. MGSATB-2, the bogie impacted the post at a speed of 19.7 mph (31.7 km/h). As a result, the post rotated through the soil until it reached a maximum deflection of 19.3 in. (490 mm), as determined from the EDR-3 data. The bogie vehicle was brought to a stop at this maximum deflection before rebounding and rolling backward a short distance. Upon examination, the post had bent backward, resulting in yielding and compression flange buckling at approximately 6 in. (152 mm) below the groundline.

Force vs. deflection and energy vs. deflection are shown in Figure 3. Inertial effects resulted in a peak force of 14.2 kips (63.2 kN) over the first 2 in. (51 mm) of deflection. After a short drop in magnitude, the force increased and remained relatively constant near 18 kips (80 kN) between 10 in. and 18 in. (250 mm and 450 mm) of deflection. The peak force was 19.9 kips (88.6 kN). The post absorbed 283 kip-in. (32.0 kJ) of energy and had a maximum deflection of 19.3 in. (490 mm).

4.2 Discussion

Two bogie tests were performed on W6x15 (W152x22.3) steel posts embedded 54 in. (1,372 mm) in soil, as summarized in Table 1. Soil failure (i.e., post rotation) was the primary mode of failure in test nos. MGSATB-1 and MGSATB-2, even though both posts experienced post yielding and compression flange buckling. The data analysis for each test showed very similar results with maximum deflections of approximately 19.5 in. (495 mm) and peak forces around 20 kips (89 kN). The force vs. deflection curves, as shown in Figure 7, were similar in shape and magnitude. Both tests showed an inertial spike over the first 2 in. (51 mm) of deflection and a relatively constant force between 15 and 20 kips (65 and 90 kN) from 10 in. (250 mm) of deflection until reaching their respective maximum displacements. Detailed results from all accelerometers are shown in Appendix A.
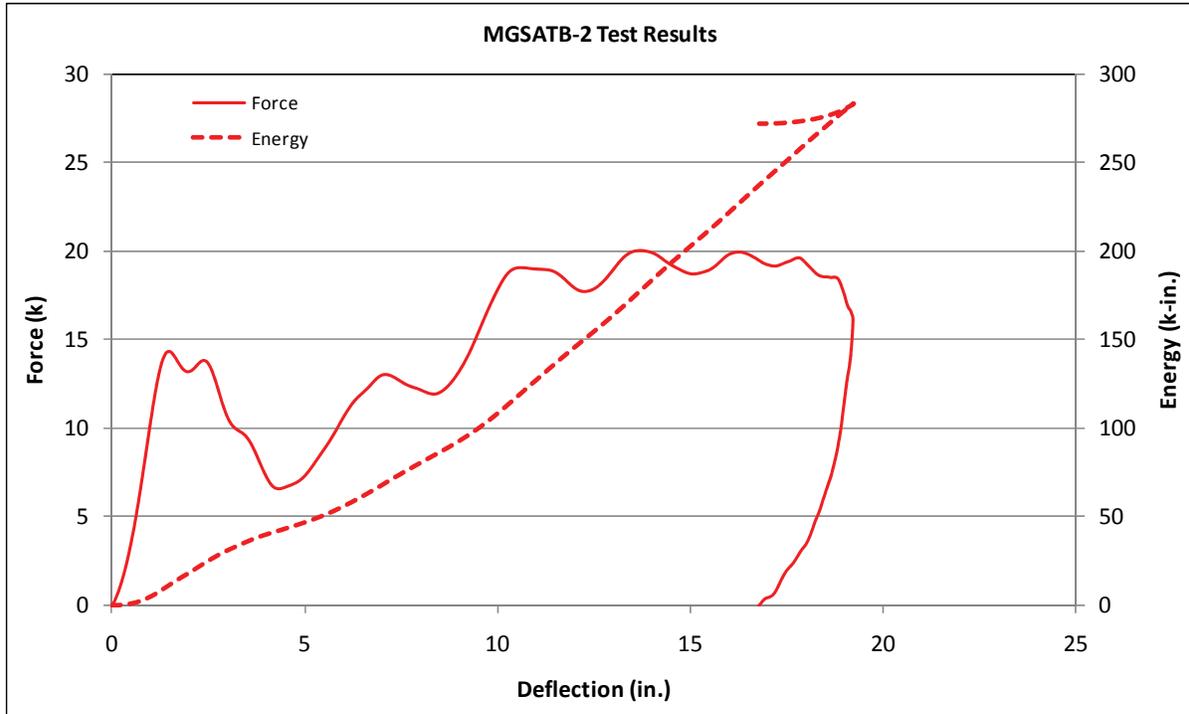
Figure 5. Force vs. Deflection and Energy vs. Deflection, Test No. MGSATB-2 [W6x15 (W152x22.3) Post]

With these two tests producing similar results, the researchers believed that the typical response of a W6x15 (W152x22.3) steel post embedded 54 in. (1,372 mm) in strong soil could be predicted by averaging the results. Therefore, further bogie testing was not conducted.
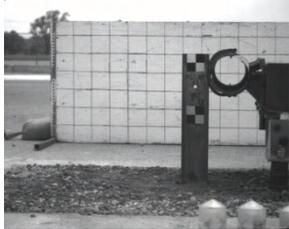
IMPACT
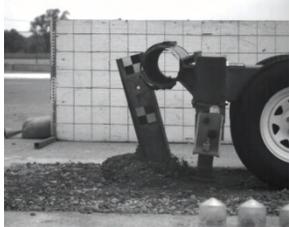
0.050 sec

0.100 sec

0.150 sec

0.200 sec

0.250 sec

Figure 6. Time Sequential and Post-Impact Photographs, Test No. MGSATB-2

Table 1. Bogie Testing Summary and Comparison

Test No.	Impact Velocity	Average Force					Max. Displ.	Total Energy	Failure Type
		@5 in. Displ.	@10 in. Displ.	@15 in. Displ.	@18 in. Displ.	@20 in. Displ.			
	mph (km/h)	kips (kN)	kips (kN)	kips (kN)	kips (kN)	kips (kN)	in. (mm)	kip-in. (kJ)	
MGSATB-1	19.2 (30.9)	9.11 (40.52)	11.19 (49.78)	13.35 (59.38)	14.38 (63.97)	12.94 (57.56)	19.5 (495)	269 (30.4)	Soil Rotation
MGSATB-2	19.7 (31.7)	9.26 (41.19)	10.61 (47.20)	13.41 (59.65)	15.11 (67.21)	13.60 (60.50)	19.3 (490)	283 (32.0)	Soil Rotation
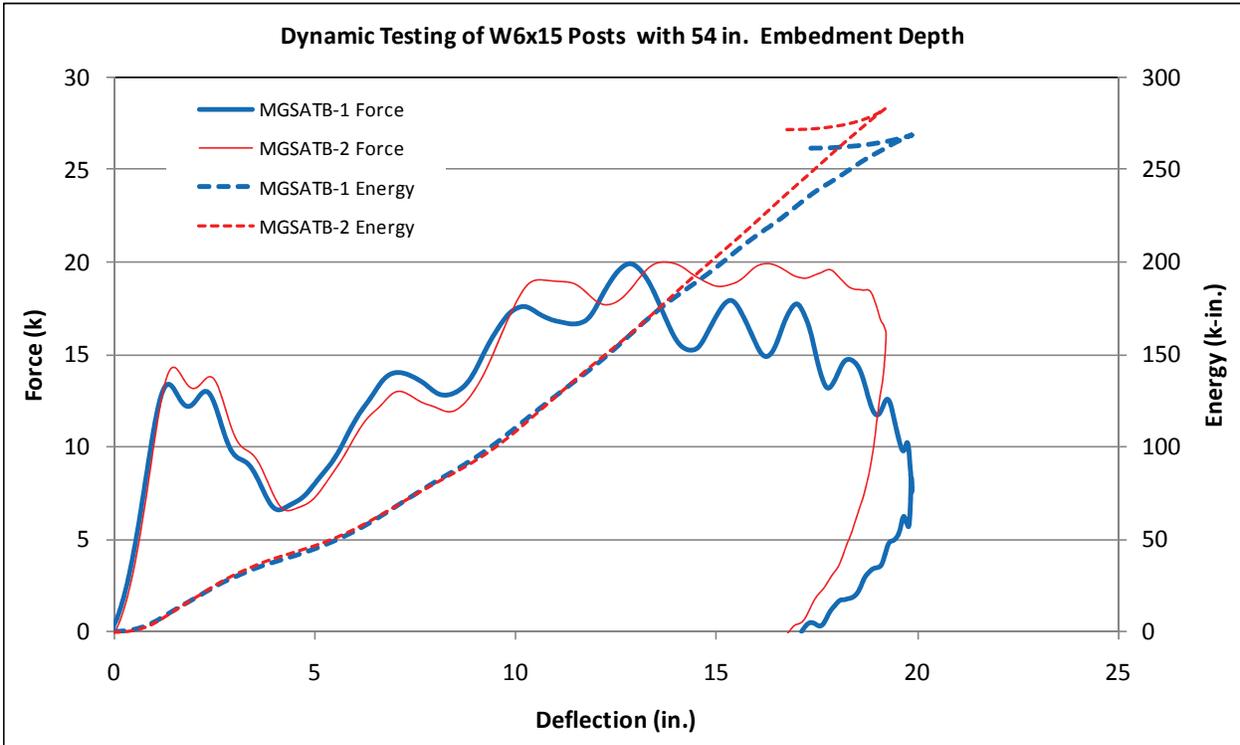
Figure 7. Force and Energy vs. Deflection Results Comparison

5 SYSTEM DESIGN USING BARRIER VII ANALYSIS

5.1 Design Criteria

As a vehicle approaches the stiffened, semi-rigid approach guardrail transition region from the relatively flexible guardrail region, a potential for rail pocketing exists. Pocketing occurs when the lateral deflection of one region of a guardrail system is much less than the adjacent region, thus creating a sharp bend in the guardrail system as the impacting vehicle approaches the stiffer region. This sharp bend produces a high longitudinal force on the vehicle that can create excessive decelerations or force the vehicle to override the barrier near the pocket and/or roll over.

A 2-D computer simulation program, BARRIER VII [16], was utilized to predict the severity of pocketing on various transition configurations by quantifying the pocketing angle associated with each configuration and impact condition combination. The pocketing angle was defined as the angle between the guardrail region just in front of the impacting vehicle and the downstream section of rail, as shown in Figure 8. The critical pocketing angle, θ_p, was defined such that at angles smaller than θ_p, the bend in the guardrail would not cause serious pocketing. However, at pocketing angles more severe than θ_p, where the difference between the guardrail and the transition regions was more abrupt, the vehicle would not be able to escape the pocket, and an undesirable vehicle response could be expected. This definition of θ_p is only applicable where there is a sharp bend in the guardrail, and the pocketing angle is essentially a measure of the magnitude of that angle. The depth of the pocket may also have a significant impact on the performance of a guardrail system. However, for the purposes of using BARRIER VII to design a guardrail stiffness transition, MwRSF researchers have assumed that the depth of the pocket will always be sufficient to create a problem, provided the critical pocketing angle is attained.
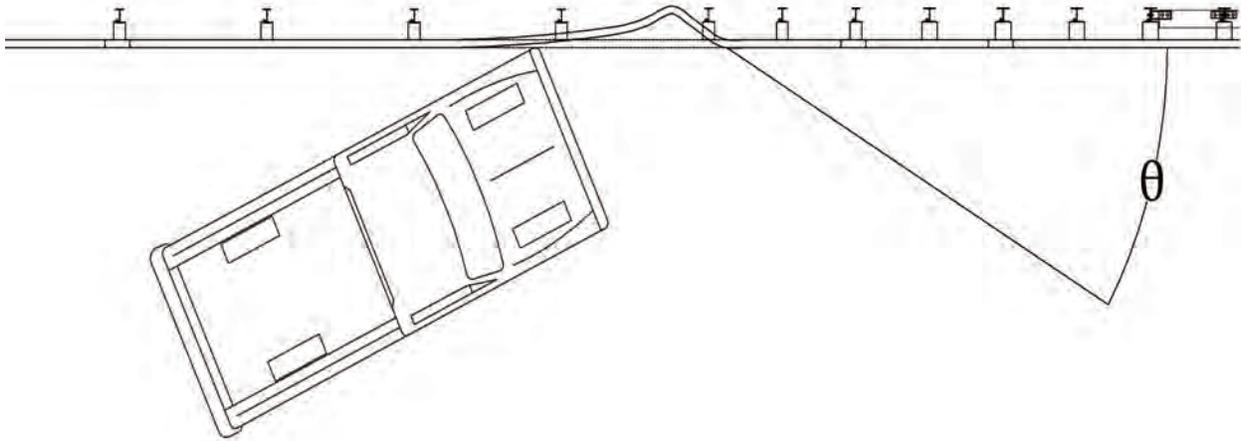
Figure 8. Critical Pocketing Angle

In 2007, MwRSF reviewed many guardrail and approach guardrail transition tests involving 2000P vehicles, the standard pickup truck in NCHRP Report No. 350 [8], in order to identify the critical pocketing angle. Based upon this analysis, the critical pocketing angle was estimated to be approximately 23 degrees [5]. However, this angle may not directly apply to the new standard pickup, 2270P, found in MASH [9]. Presently, limited data exists concerning 2270P vehicles impacting transition systems. However, it is believed that the larger 2270P is more stable than the previous 2000P. Taking into account this increase in stability, MwRSF researchers believed that the critical pocket angle for a 2270P vehicle was higher than 23 degrees and closer to 30 degrees. Therefore, multiple transition configurations were configured which had maximum pocket angles between 23 and 30 degrees, and it was left up to the Midwest States Pooled Fund Program member states to decide which design to subject to full-scale crash testing.

5.2 Approach Transition Configurations

Multiple approach guardrail transition configurations were analyzed under TL-3 impact conditions using BARRIER VII. The upstream and downstream ends remained constant in every

configuration. Each of the configurations began with the standard MGS which is composed of standard 12-gauge (2.66-mm thick) W-beam attached to W6x9 (W152x13.4) steel posts spaced at 75-in. (1,905-mm) intervals. The downstream end of each configuration consisted of a 12-gauge (2.66-mm thick) thrie beam bridge rail attached to W6x20 (W152x29.8) steel posts rigidly attached to a simulated concrete bridge deck and spaced at 37½-in. (953-mm) intervals. A thrie beam transition system, previously designed by MwRSF and accepted by the Federal Highway Administration (FHWA), was attached to the upstream end of the bridge rail [10-11,17-20]. The transition measured 12 ft – 6 in. (3.81 m) long and consisted of two nested 12-gauge (2.66-mm thick) thrie beam rails attached to W6x15 (W152x22.3) steel posts with a 37½-in. (953-mm) spacing. This transition was selected because it represented the worst case scenario, i.e., the stiffest of the previously-accepted FHWA approach transition systems. Thus, pending a successful test, it was believed that the new stiffness transition could be adapted to any other previously-accepted approach guardrail transition system.

The design configurations for the stiffness transition between standard MGS and the thrie beam approach guardrail transition using W6x15 (W152x22.3) steel posts were composed of varying combinations of similar guardrail elements. Every configuration utilized the asymmetric, 10-gauge (3.42-mm thick) W-beam to thrie beam transition section designed by MwRSF in 2007 [5-7]. The remaining rail segments consisted of varying lengths of 12-gauge (2.66-mm thick) W-beam, nested 12-gauge (2.66-mm thick) W-beam, and 12-gauge (2.66-mm thick) thrie beam. The remaining posts were all 6-ft (1.83-m) long W6x9 (W152x13.4) steel sections. However, each configuration utilized a different combination of post quantities, post spacing, and system lengths. The seven analyzed stiffness transitions are summarized in Table 2 and shown in Figure 9.

Table 2. Summary of Stiffness Transitions Combined with Thrie Beam Approach Guardrail Transitions

System Parameters	Design D	Design F	Design G	Design H	Design J	Design K	Design L
Length of Transition[1]	40 ft – 7½ in. (12.38 m)	40 ft – 7½ in. (12.38 m)	28 ft – 1½ in. (8.57 m)	34 ft – 4½ in. (10.48 m)	34 ft – 4½ in. (10.48 m)	28 ft – 1½ in. (8.57 m)	34 ft – 4½ in. (10.48 m)
Length of Nested W-Beam Rail	-	25 ft (7.62 m)	12 ft – 6 in. (3.81 m)	12 ft – 6 in. (3.81 m)	25 ft (7.62 m)	-	-
Length of 10-Gauge W-to-Thrie Rail	6 ft – 3 in. (1.91 m)	6 ft – 3 in. (1.91 m)	6 ft – 3 in. (1.91 m)	6 ft – 3 in. (1.91 m)	6 ft – 3 in. (1.91 m)	6 ft – 3 in. (1.91 m)	6 ft – 3 in. (1.91 m)
Length of Thrie Beam Rail	12 ft – 6 in. (3.81 m)	6 ft – 3 in. (1.91 m)	6 ft – 3 in. (1.91 m)	6 ft – 3 in. (1.91 m)	6 ft – 3 in. (1.91 m)	6 ft – 3 in. (1.91 m)	6 ft – 3 in. (1.91 m)
Length of Nested Thrie Beam Rail	12 ft – 6 in. (3.81 m)	12 ft – 6 in. (3.81 m)	12 ft – 6 in. (3.81 m)	12 ft – 6 in. (3.81 m)	12 ft – 6 in. (3.81 m)	12 ft – 6 in. (3.81 m)	12 ft – 6 in. (3.81 m)
No. of W6x9 Posts[2]	13	12	8	10	10	8	10
No. of W6x15 Posts	3	3	3	3	3	3	3
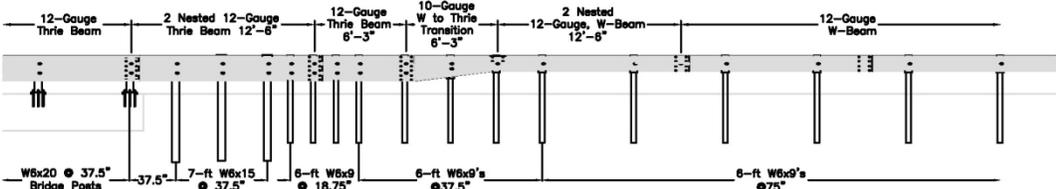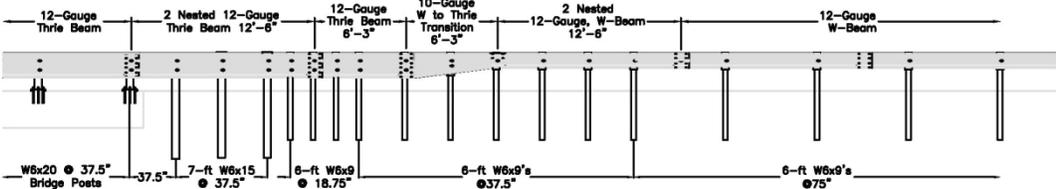
[1] – First reduced post spacing to first bridge post.
[2] – Post located within reduced spacing configuration.

27

Figure 9. Schematic of Stiffness Transitions to Thrie Beam Approach Guardrail Transitions

The thrie beam approach guardrail transition system selected to represent the stiffest of the FHWA-accepted transition systems had an option for using one 10-gauge (3.42-mm thick) thrie beam or two nested 12-gauge (2.66-mm thick) thrie beam segments to connect the W-beam to thrie beam transition element to the bridge rail. Nested 12-gauge (2.66-mm thick) thrie beam has roughly 50 percent more bending strength than a single 10-gauge (3.42-mm thick) thrie beam rail. Thus, the nested rail configuration was selected for use in order to develop and test a stiffness transition to the most critical approach guardrail transition.

The FHWA-accepted approach guardrail transition was original comprised of five W6x15 (W152x22.3) posts spaced at 37½-in. (953-mm) intervals between the standard guardrail system and the bridge rail [10-11,17-20]. However, in the interest of designing the shortest possible overall transition, two of the W6x15 (W152x22.3) steel posts were removed and replaced with four standard W6x9 (W152x13.4) steel posts at an 18¾-in. (476-mm) spacing. The proposed post alternative and use of nested thrie beam was analyzed to justify the shortening of the system.

BARRIER VII analysis was conducted to compare the performance of the original bridge rail approach guardrail transition to that obtained for the proposed alternatives described above. Impact conditions from the full-scale crash tests [17-20] on the original transition system (one pickup truck and one single-unit truck) were replicated in BARRIER VII in order to calibrate the barrier model. Then, two W6x15 (W152x22.3) steel posts on the upstream end were replaced with four W6x9 (W152x13.4) posts at an 18¾-in. (476-mm) spacing, and the new model was analyzed under the same impact conditions. The original system was crash tested with impacts near the downstream end (i.e., close to the bridge rail), and the impacting vehicles did not contact the two upstream W6x15 (W152x22.3) posts evaluated within this study. The analysis showed that barrier deflections for the simplified stiffness transitions were similar to, and in some

instances lower than, the barrier deflections observed for the original bridge rail transition design. Therefore, each upstream stiffness transition configuration analyzed consisted of three W6x15 (W152x22.3) steel posts at 37½-in. (953-mm) intervals, a minimum of four W6x9 (W152x13.4) steel posts at 18¾-in. (476-mm) intervals, and nested thrie beam rail located upstream from the bridge rail.

5.3 BARRIER VII Component Models

5.3.1 Rails

Input values for the various guardrail segments were determined from cross sectional properties, as shown in Table 3. A yield stress of 50 ksi (345 MPa) was used to calculate the elastic tensile and moment capacities. Each rail element in BARRIER VII was 9⅜ in. (238 mm) long. For nested rail sections, all strength and cross sectional input values were doubled. Properties for the 10-gauge (3.42-mm thick) W-beam to thrie beam transition piece were calculated at the center of each 9⅜ in. (238 mm) segment using a linear interpolation between the W-beam and thrie beam ends.

Table 3. Guardrail Cross Section Properties for BARRIER VII

Beam Properties	Beam Type			
	12-Gauge W-Beam	10-Gauge W-Beam	12-Gauge Thrie Beam	10-Gauge Thrie Beam
A (in^2)	1.99	2.56	3.10	4.00
I (in^4)	2.29	3.00	3.76	4.82
S (in^3)	1.37	1.76	2.19	2.80
Wt (lb/ft)	6.92	8.90	10.81	13.95
F_y (ksi)	50	50	50	50

5.3.2 W6x9 (W152x13.4) Steel Posts

In previous studies, MwRSF has preformed dynamic bogie tests on steel posts embedded in soil. Of particular interest are test nos. MGS2-1B18, MGS2-1B19, MGS2-1B20, and MGS2-1B21 from a 2007 study [21] and test nos. NPGB-2, NPGB-4, NPGB-9, and NPGB-10 from a 2001 study [22]. These eight tests consisted of W6x9 (W152x13.4) steel posts or W6x16 (W152x23.8) posts, embedded 40 in. (1,016 mm) in soil and impacted by a bogie vehicle at a height of 24⅞ in. (632 mm) and a velocity near 20 mph (32.2 km/h). Soil failure was the primary mode of failure for both test series and only minimal post deformations were observed. W6x16 (W152x23.8) posts have the same flange width as W6x9 (W152x13.4), thus produce the same force vs. deflection curves when rotating through soil. All eight tests were used to calculate an average force vs. deflection soil resistance curve for strong-axis rotation of a W6x9 (W152x13.4) post. Post deflection through the weak axis was expected to occur from post bending and not rotation through the soil. Therefore, the resistance in this direction was calculated from the cross-sectional properties, a 24 ⅞-in. (632-mm) moment arm, and a yield stress of 36 ksi (248 MPa).

5.3.3 W6x15 Steel Posts

Chapter 4 described the results of two dynamic bogie tests on W6x15 (W152x22.3) steel posts embedded 54 in. (1,372 mm) in soil and impacted at approximately 20 mph (32.2 km/h). The accelerometer data resulting from these tests was used to calculate an average force vs. deflection soil resistance curve for strong-axis rotation. Similar to the W6x9 (W152x13.4) post model, deflection through the weak axis was expected to occur from post bending and not rotation through the soil. Therefore, the resistance in this direction was calculated from the cross-sectional properties, a 24⅞-in. (632-mm) moment arm, and a yield stress of 36 ksi (248 MPa).

5.4 BARRIER VII Analysis and Results

Before BARRIER VII was utilized to analyze the proposed stiffness transition configurations, it was necessary to calibrate the model components. This calibration was accomplished by modeling three previous full-scale crash tests involving a pickup impacting the MGS installation. Test nos. NPG-4 and NPG-6 consisted of the MGS at standard post spacing, 75 in. (1,905 mm), and quarter post spacing, 18¾ in. (476 mm), respectively [23]. Test no. MWT-5 consisted of an approach transition utilizing the same asymmetric W-beam to thrie beam transition piece included in all of the proposed transition configurations [5-7]. BARRIER VII model components, including post deflection at failure and the effective coefficient of friction, were adjusted such that the system deflections, vehicle time to parallel, and vehicle exit time matched the results from the full-scale crash tests within 10 percent. The effective coefficient of friction was determined to be 0.45, and the W6x9 (W152x13.4) post deflection at failure was determined to be 16 in. (406 mm). An example BARRIER VII input deck and the design configuration layouts are shown in Appendix B.

The BARRIER VII analysis was conducted with a 2000P vehicle model and not a 2270P vehicle model even though the new simplified stiffness transition was designed to meet the MASH TL-3 performance criteria. This decision was made for several reasons. First, the calibration was being conducted on test no. MWT-5 which was the previously-designed stiffness transition using the asymmetrical W-beam to thrie beam rail element. Second, the prior test was performed with the 2000P as well as MwRSF researchers had significant experience with the 2000P vehicle model. Further, there had not been a prior full-scale crash test involving a 2270P vehicle impacting a guardrail transition in which a simulation could be calibrated. It was also believed that the mass increase from the 2000P vehicle to the 2270P vehicle would only provide minimal increases in the barrier deflection and vehicle pocketing within the guardrail system. In

fact, the difference in dynamic deflection between the two pickup trucks impacting the standard MGS has been similar in the past. Test no. 2214MG-2, conducted with a 2270P vehicle, had a maximum dynamic deflection of 44 in. (1,118 mm) [24], while test no. NPG-4, conducted with a 2000P vehicle, had a maximum dynamic deflection of 43 in. (1,092 mm) [23].

During the BARRIER VII analysis of the proposed stiffness transitions to thrie beam approach guardrail transitions, the pickup truck was given an initial velocity of 62.14 mph (100 km/h) at an angle of 25 degrees to the system. In order to analyze the entire approach transition, the impact point was moved along the length of the system at every rail node, or at 9⅜-in. (238-mm) intervals. The impact range began 150 in. (3,810 mm) upstream of the first reduced post spacing and continued downstream into the W6x15 (W152x22.3) steel posts. Recall, the W6x15 (W152x22.3) posts are a part of the original thrie beam bridge rail transition that was successfully crash tested and accepted by the FHWA [10].

The BARRIER VII simulation results were used to identify the maximum dynamic deflection, the maximum pocketing angle, the time in which the vehicle became parallel with the system, and the amount of wheel snag that occurred between the front tire and each post. The pocketing angle was taken as the average between five barrier nodes, or over a distance of 37½ in. (953 mm). The magnitude of wheel snag on each post was calculated using the methods described by Reid [25]. Simulation results for every design configuration and impact point are shown in Appendix C. For each stiffness transition configuration, the critical impact point was defined as the location causing the maximum pocketing angle. In design nos. D, F, and L, the maximum pocketing angle was located at the transition between full- and half-post spacing. However, MwRSF researchers did not believe that the half-post spacing region would provide enough stiffness to create a sharp pocketing angle; rather, the vehicle would deform the system as it moved down the rail and significantly flatten the pocket. Therefore, the pocketing angles at

the transition between full- and half-post spacing were not considered for the determination of the critical impact point. Critical impact points and their associated barrier deformations are described in Table 4.

Table 4. Critical Impact Points for the Transition Designs (2000P Impact Scenarios)

Transition Design	Critical Impact Point		Maximum Pocketing Angle		Maximum Dynamic Deflection in. (mm)
	Node No.	Description	(deg.)	Location Description	
Design D	85	75" (1,905 mm) US of W-to-thrie rail segment	22.9	28" (711 mm) US of ¼ spacing	32.6 (828)
Design F	113	37½" (953 mm) US of W-to-thrie rail segment	22.0	first post of ¼ spacing	27.3 (693)
Design G	94	65½" (1667 mm) US of W-to-thrie rail segment	28.9	first post of ¼ spacing	35.2 (894)
Design H	88	122" (3,099 mm) US of W-to-thrie rail segment	25.7	18¾" (476 mm) US of ¼ spacing	35.9 (912)
Design J	96	122" (3,096 mm) US of W-to-thrie rail segment	23.9	28" (711 mm) US of ¼ spacing	34.7 (881)
Design K	93	75" (1,905 mm) US of W-to-thrie rail segment	29.6	first post of ¼ spacing	36.4 (925)
Design L	108	9½" (241 mm) US of W-to-thrie rail segment	23.9	37½" (953 mm) into ¼ spacing	27.1 (688)

Design nos. K and L were identified as the two best stiffness transition alternatives. Both options were two of the shorter configurations, and neither required nesting of W-beam rail before the stiffness transition. Although only one additional post separated Design L from Design K, their maximum pocketing angles were 23.9 and 29.6 degrees, respectively, putting them on opposite sides of the design window established for the critical pocketing angle of 23 to 30 degrees, as set in Section 5.1.

The member states of the Midwest States Pooled Fund Program were given the option of selecting the configuration for full-scale crash testing. Design K was presented as an aggressive

design utilizing the shortest length and the highest pocketing angle. Design L was presented as a more conservative design utilizing an additional post, making it slightly longer than Design K, but having a greater chance of a successful crash test. Overwhelmingly, the member states selected Design K, while expressing the desire to make the transition as short and as cost efficient as possible.

6 DESIGN DETAILS

The 87-ft 6-in. (26.67-m) long test installation, as shown in Figure 10, consisted of five major structural components: (1) a 12-ft 6-in. (3.81-m) long thrie beam and channel bridge railing system; (2) 12 ft - 6 in. (3.81 m) of nested 12-gauge (2.66-mm thick) thrie beam guardrail; (3) 6 ft - 3 in. (1.91 m) of standard 12-gauge (2.66-mm thick) thrie beam guardrail; (4) a 6-ft 3-in. (1.91-m) long, asymmetrical 10-gauge (3.42-mm thick) W-beam to thrie beam transition element; and (5) 50 ft (15.24 m) of standard 12-gauge (2.66-mm thick) W-beam rail attached to a simulated anchorage device. Design details are shown in Figures 10 through 30.

The barrier system was constructed with three bridge rail posts and eighteen guardrail posts. Post nos. 1 and 2 were timber posts measuring 5½ in. wide x 7½ in. deep x 45½ in. long (140 x 191 x 1,156 mm) and were placed in 6-ft (1.8-m) long steel foundation tubes. The timber posts and foundation tubes were part of an anchorage system used to develop the required tensile capacity of a tangent guardrail terminal. Post nos. 3 through 15 were galvanized ASTM A36 W6x9 (W152x13.4) steel sections measuring 6 ft (1.83 m) long. Post nos. 16 through 18 were galvanized ASTM A36 W6x15 (W152x22.3) steel sections measuring 7 ft (2.1 m) long. Bridge post nos. 19 through 21 were galvanized ASTM A36 W6x20 (W152x29.8) steel sections measuring 29⅝ in. (752 mm) long.

Post nos. 1 through 8, 8 through 12, 12 through 16, and 16 through 19 were spaced 75 in. (1,905 mm), 37½ in. (953 mm), 18¾ in. (476 mm), and 37½ in. (953 mm) on center, respectively, as shown in Figure 10. Bridge post nos. 19 through 21 were spaced 75 in. (1,905 mm) on center. The soil embedment depths for post nos. 3 through 15 and 16 through 18 were 40 in. (1,016 mm) and 55⅛ in. (1,400 mm), respectively, as shown in Figures 16 through 18. The steel posts were placed in a compacted crushed limestone material that met AASHTO soil standard M147 Grade B, as recommended in MASH [9].

For post nos. 3 through 9, 6-in. wide x 12-in. deep x 14¼-in. long (152 x 305 x 362-mm) wood spacer blockouts were used to offset the rail away from the front face of the steel posts. Post nos. 10 through 15 utilized 6-in. wide x 12-in. deep x 19-in. long (152 x 305 x 483-mm) wood spacer blockouts. Post nos. 16 and 17 utilized 6-in. wide x 8-in. deep x 19-in. long (152 x 203 x 483-mm) wood spacer blockouts, while post no. 18 used a 6-in. wide x 8-in. deep x 15-in. long (152 x 203 x 381-mm) wood spacer blockout. For post nos. 19 through 21, a galvanized ASTM A36 W6x15 (W152x22.3) steel spacer measuring 13⅝ in. (346 mm) long was used to offset the rail away from the front face of the steel bridge post.

Standard 12-gauge (2.66-mm thick) W-beam rails were placed between post nos. 1 and 9, as shown in Figure 10. The W-beam's top rail height was 31 in. (787 mm) with a 24⅞-in. (550-mm) center mounting height. An asymmetrical 10-gauge (3.42-mm thick) W-beam to thrie beam transition element spanned between post nos. 9 and 11. Standard 12-gauge (2.66-mm thick) thrie beam rail spanned between post nos. 11 and 14 and also between post nos. 19 and 21. Two nested 12-gauge (2.66-mm thick) thrie beams were placed between post nos. 14 and 19, as shown in Figure 12. All thrie beam rails had a top rail height of 31 in. (787 mm) with a 21-in. (533-mm) center mounting height. All lap-splice connections between the rail sections were configured to reduce vehicle snag at the splice. The thrie beam channel bridge railing system was rigidly attached to the concrete tarmac located at the MwRSF's outdoor proving grounds, as shown in Figure 35.
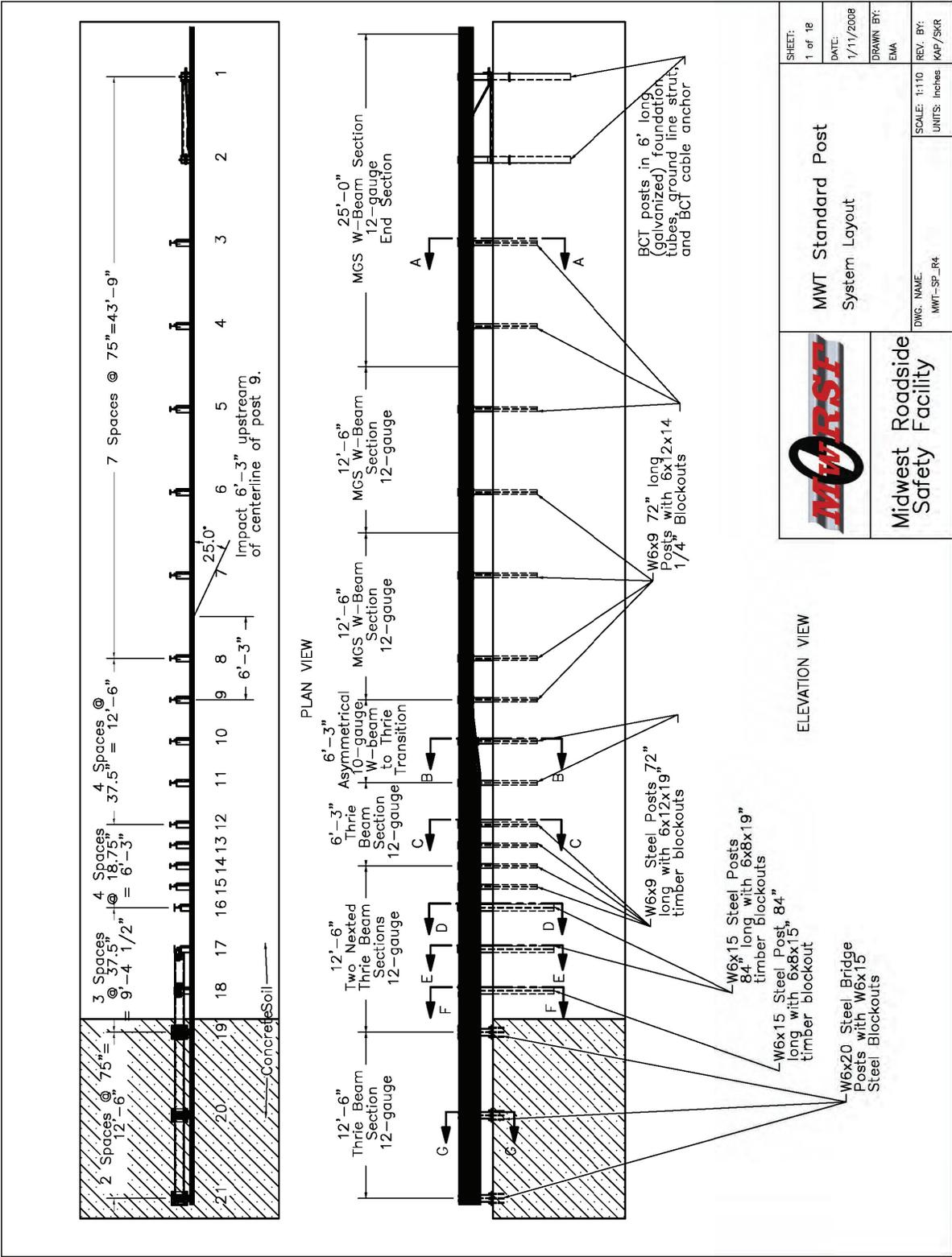
Figure 10. System Layout, Test Nos. MWTSP-1 and 2
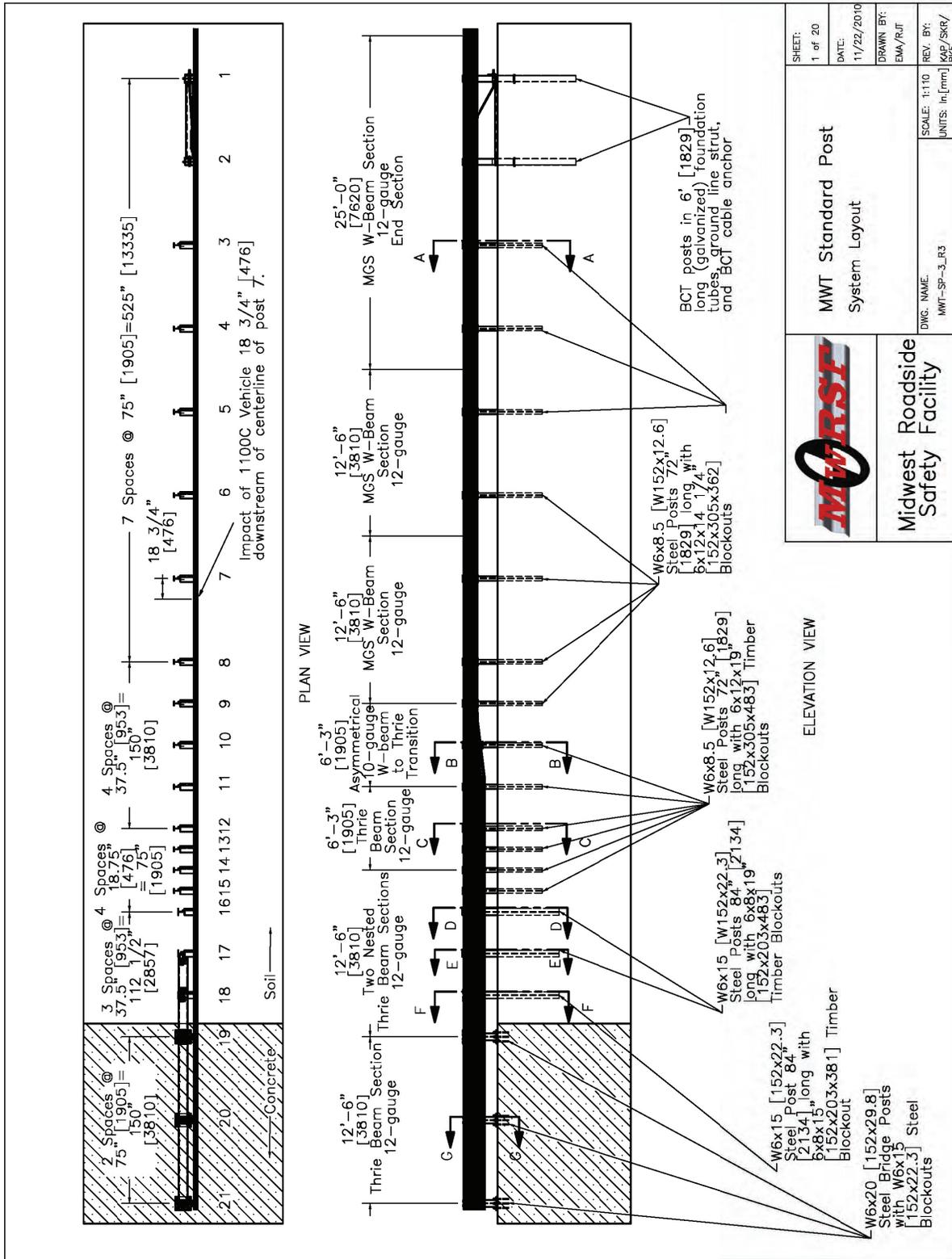
Figure 11. System Layout, Test No. MWTSP-3
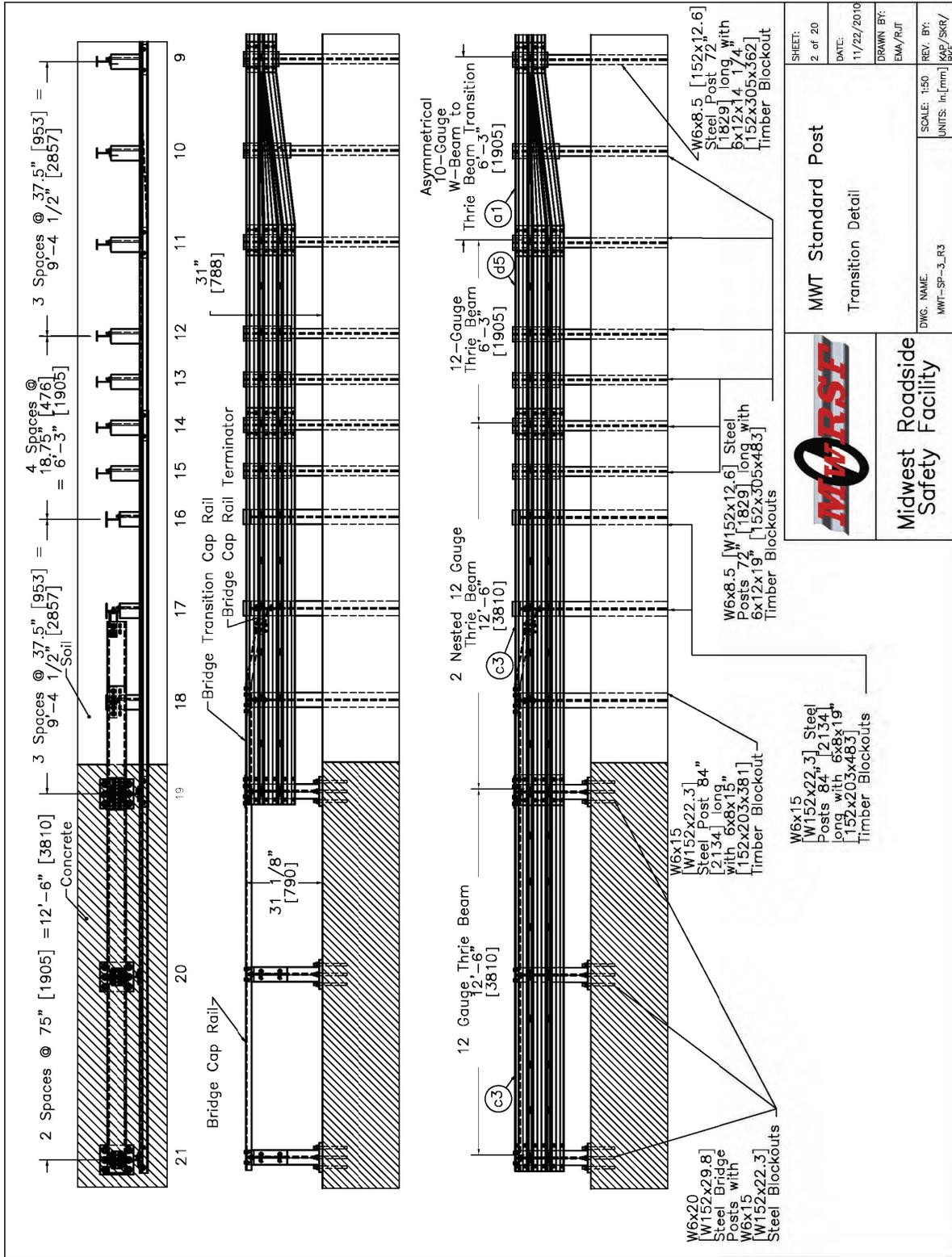
Figure 12. Downstream End System Layout, Test Nos. MWTSP-1 through 3
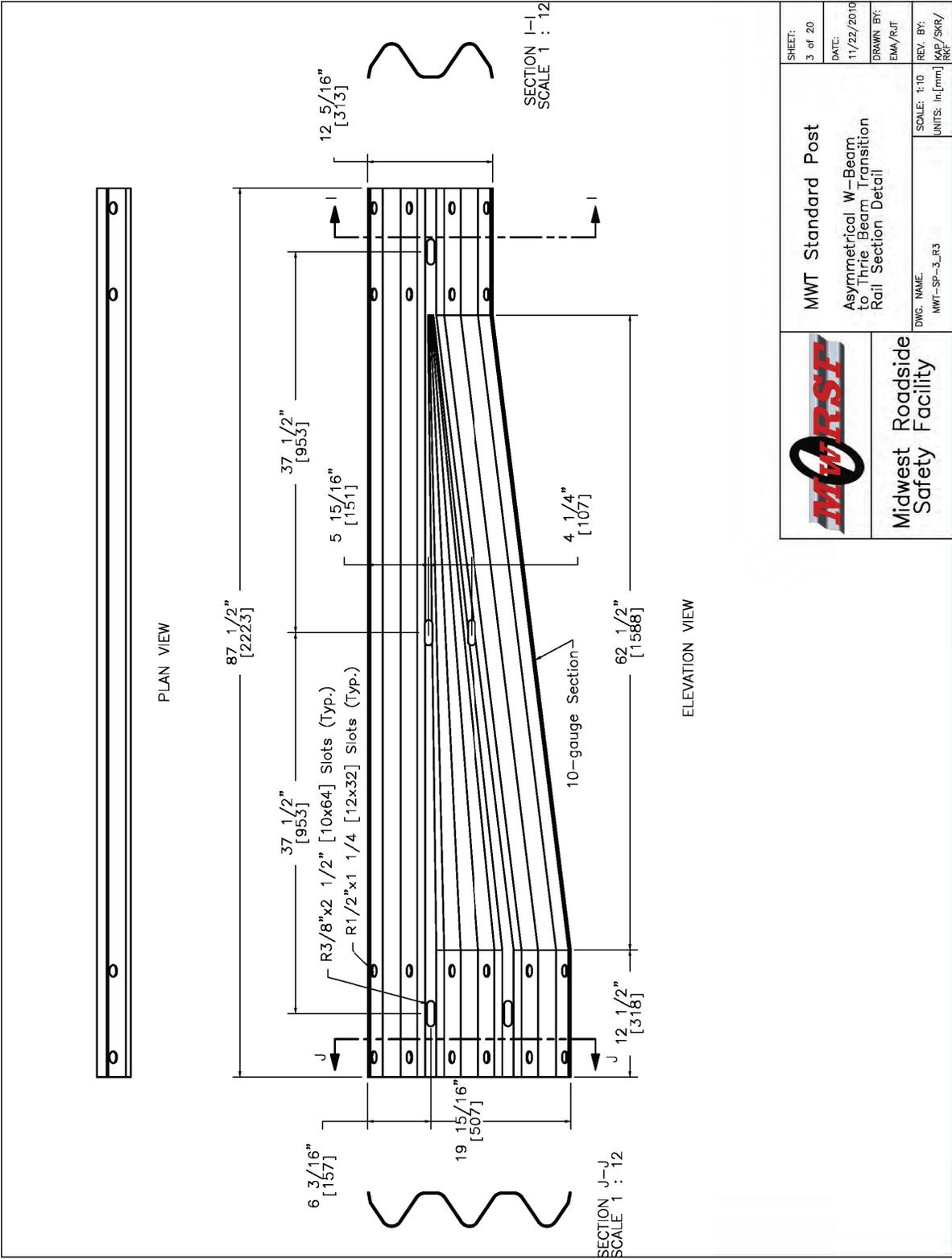
Figure 13. Asymmetrical W-Beam to Thrie Beam Element Details, Test Nos. MWTSP-1 through 3
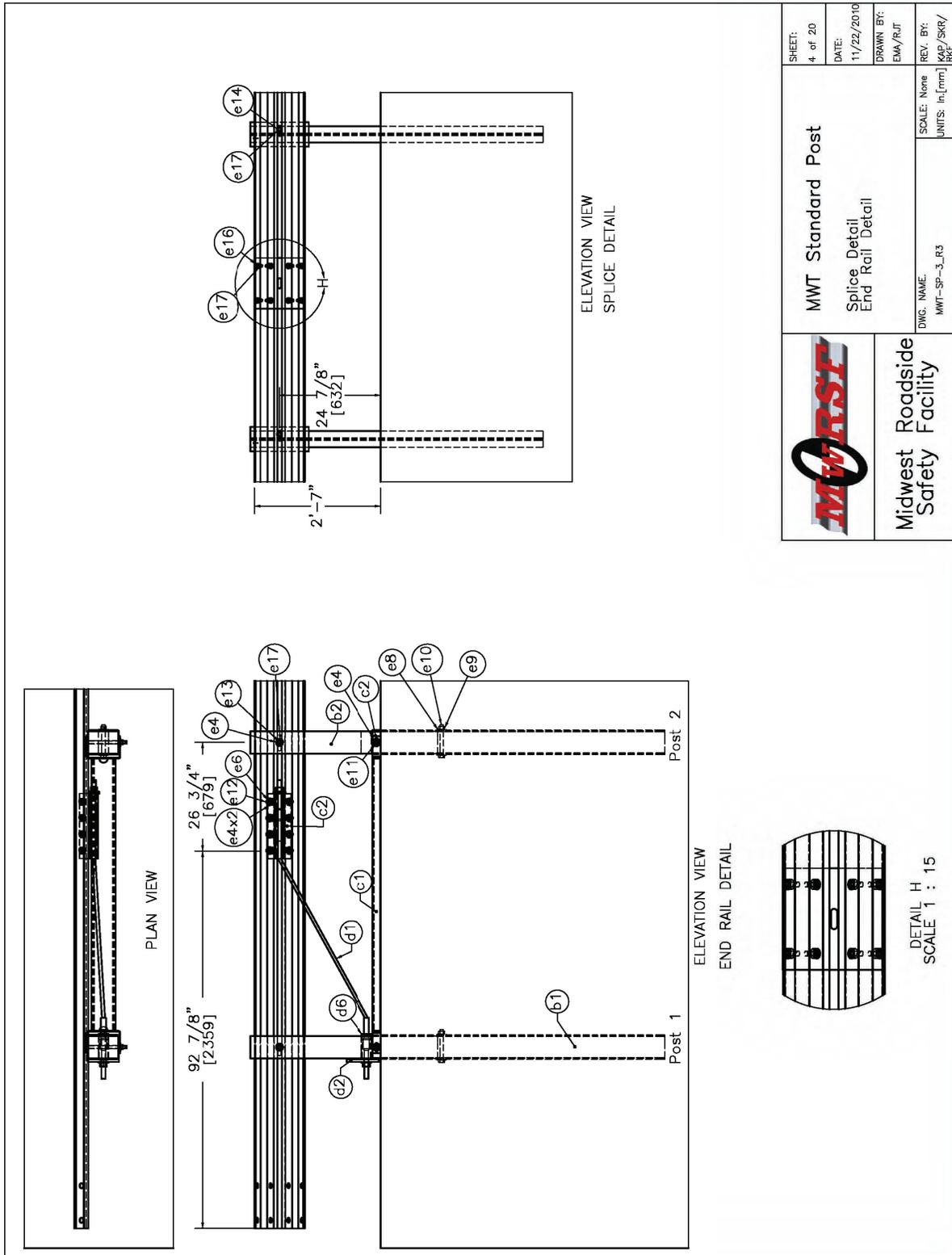
Figure 14. Splice and End Rail Details, Test Nos. MWTSP-1 through 3

Figure 15. Post Nos. 3 through 15 Details, Test Nos. MWTSP-1 through 3
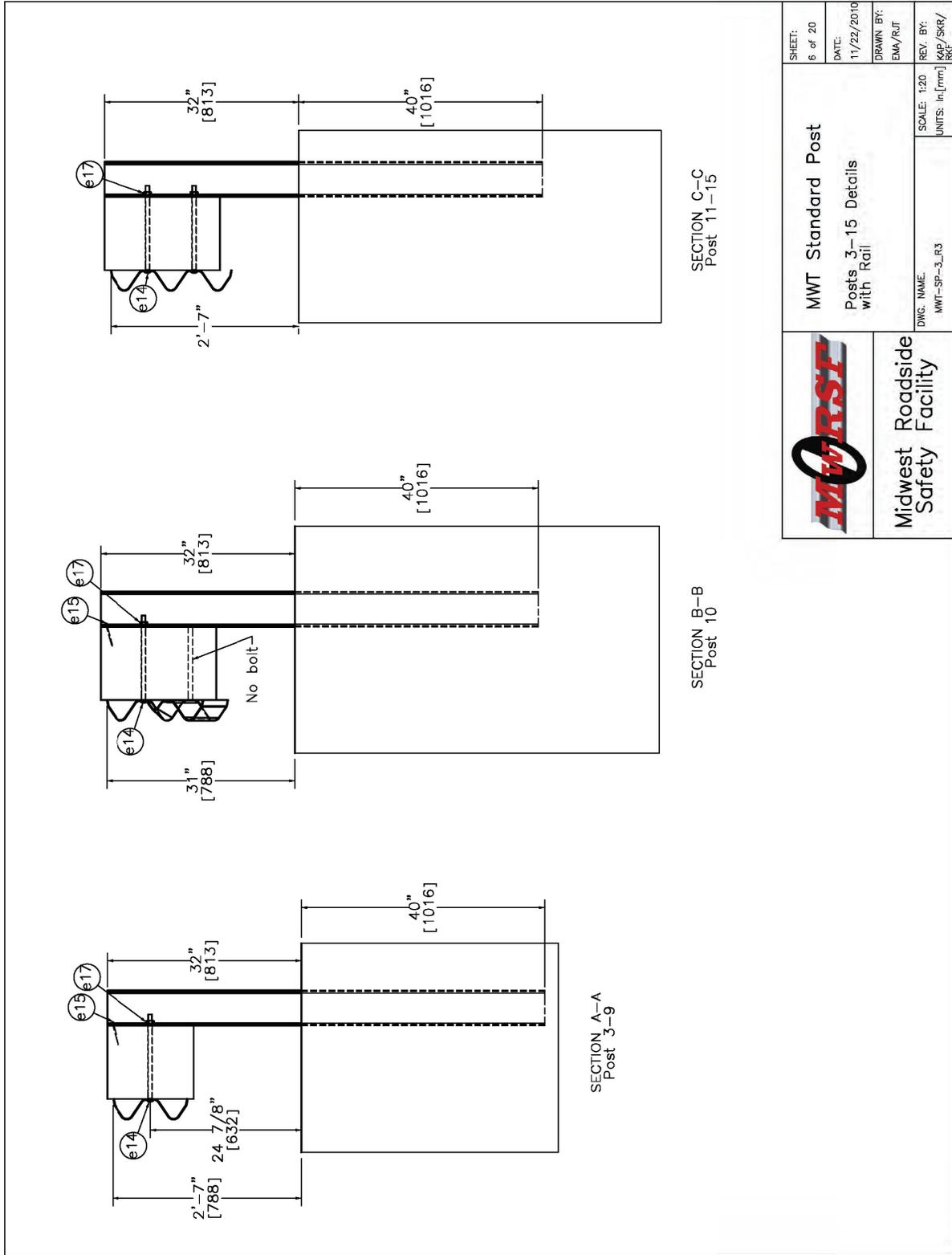
Figure 16. Post Nos. 3 through 15, Test Nos. MWTSP-1 through 3

Figure 17. Post Nos. 16 and 17 Details, Test Nos. MWTSP-1 through 3
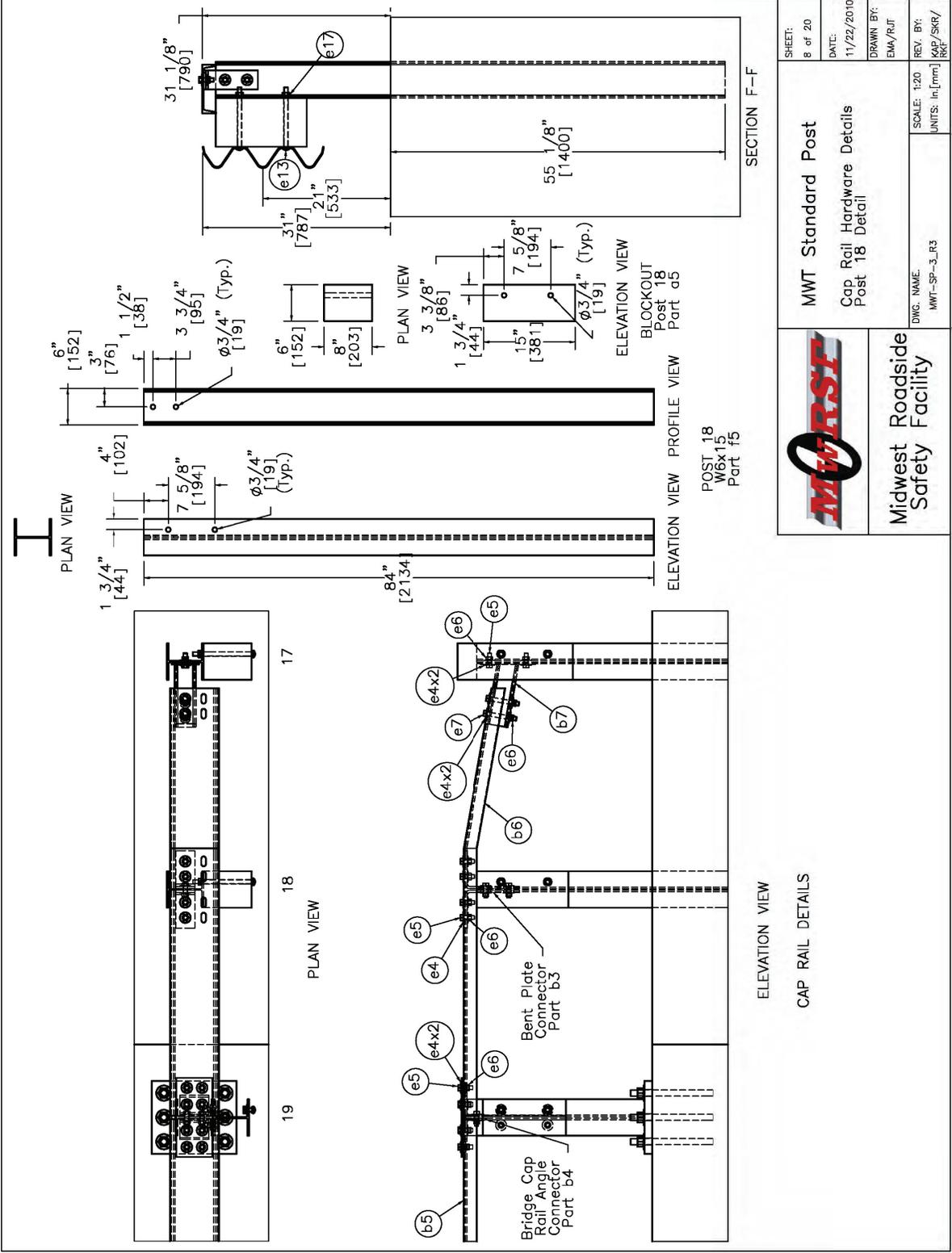
Figure 18. Cap Rail Hardware and Post No. 18 Details, Test Nos. MWTSP-1 through 3
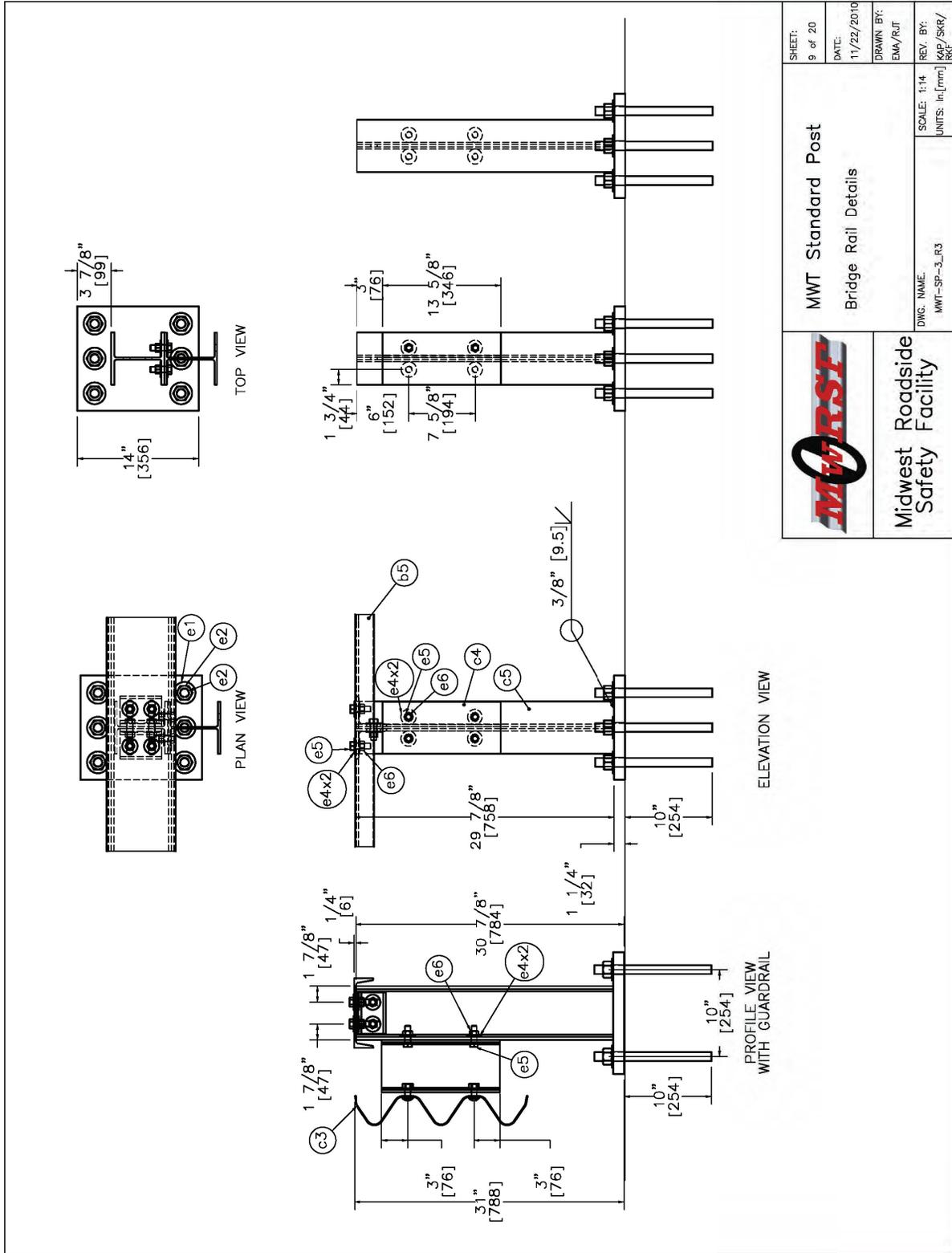
Figure 19. Bridge Rail Details, Test Nos. MWTSP-1 through 3

Figure 20. Bridge Rail Component Details, Test Nos. MWTSP-1 through 3
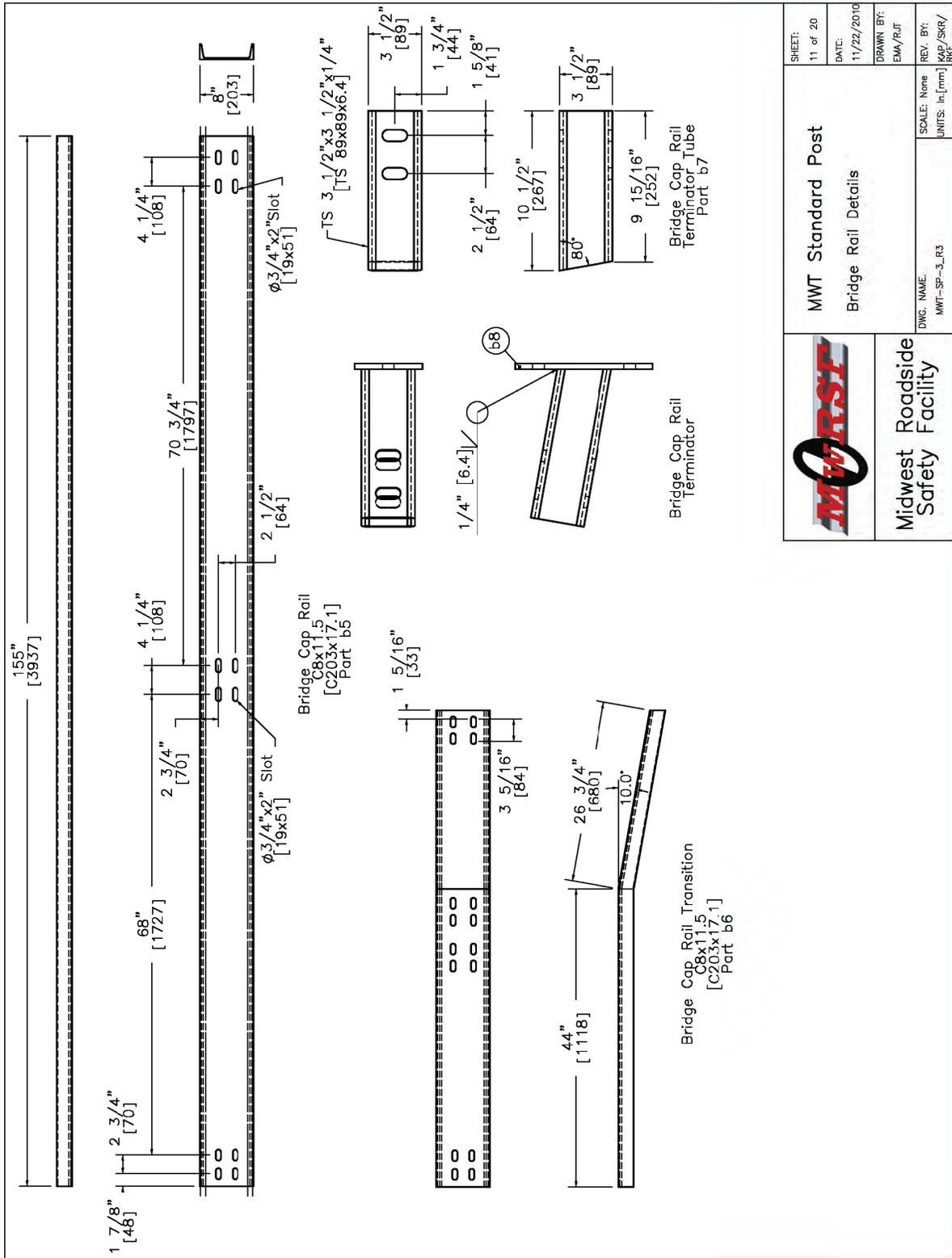
Figure 21. Bridge Rail Cap Details, Test Nos. MWTSP-1 through 3

Figure 22. Bridge Rail Cap Connection Details, Test Nos. MWTSP-1 through 3
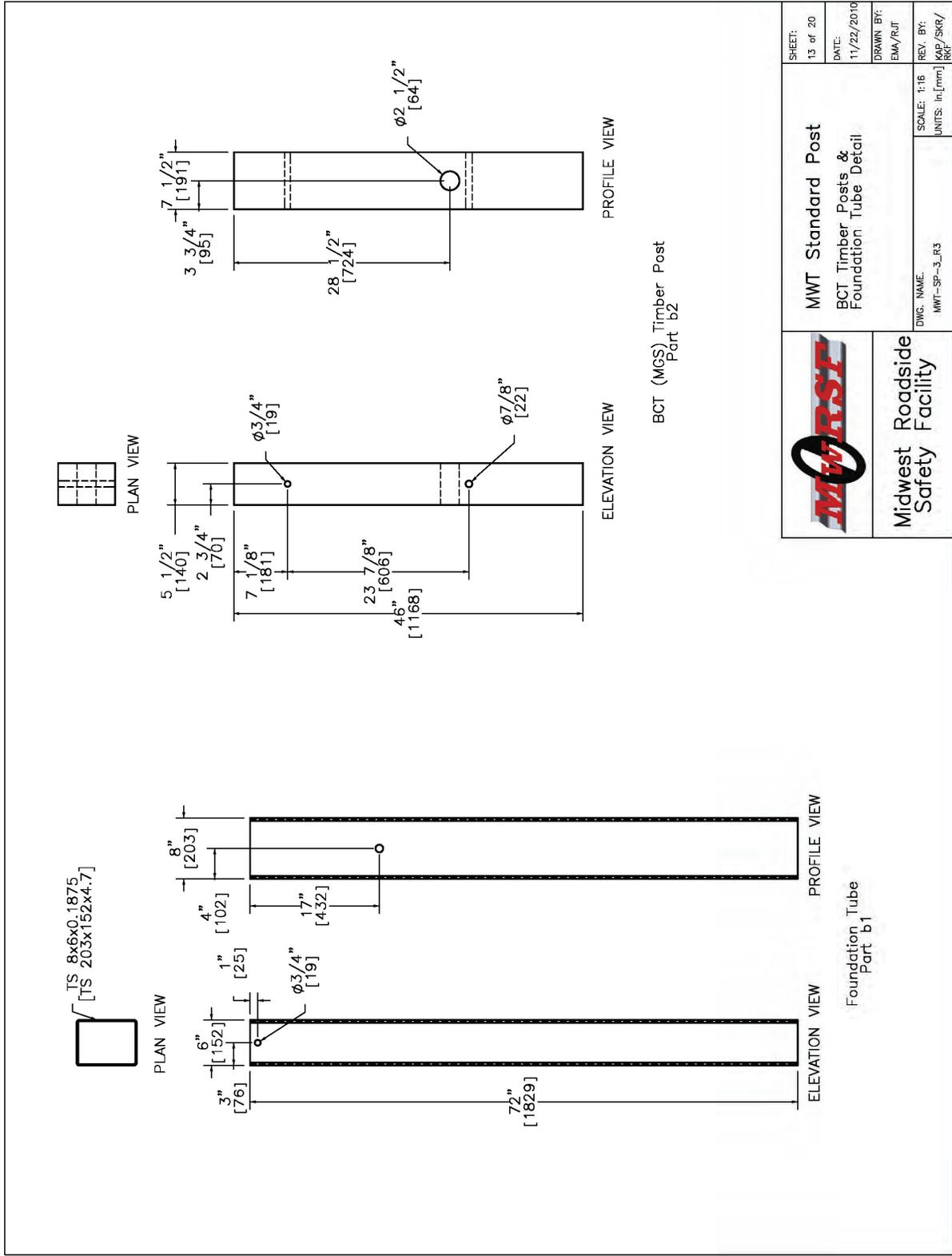
Figure 23. BCT Post and Foundation Tube Details, Test Nos. MWTSP-1 through 3
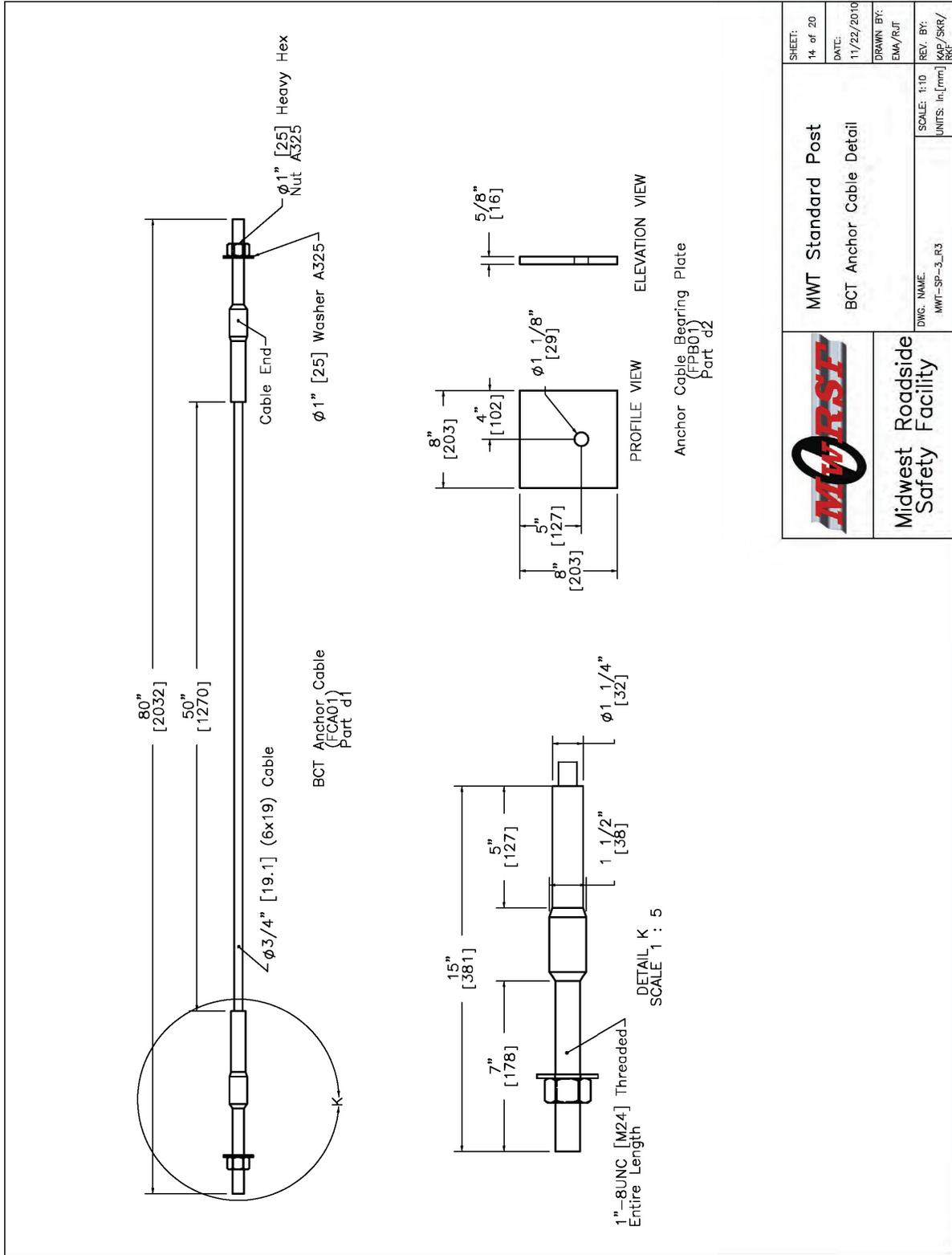
Figure 24. BCT Anchor Cable Details, Test Nos. MWTSP-1 through 3
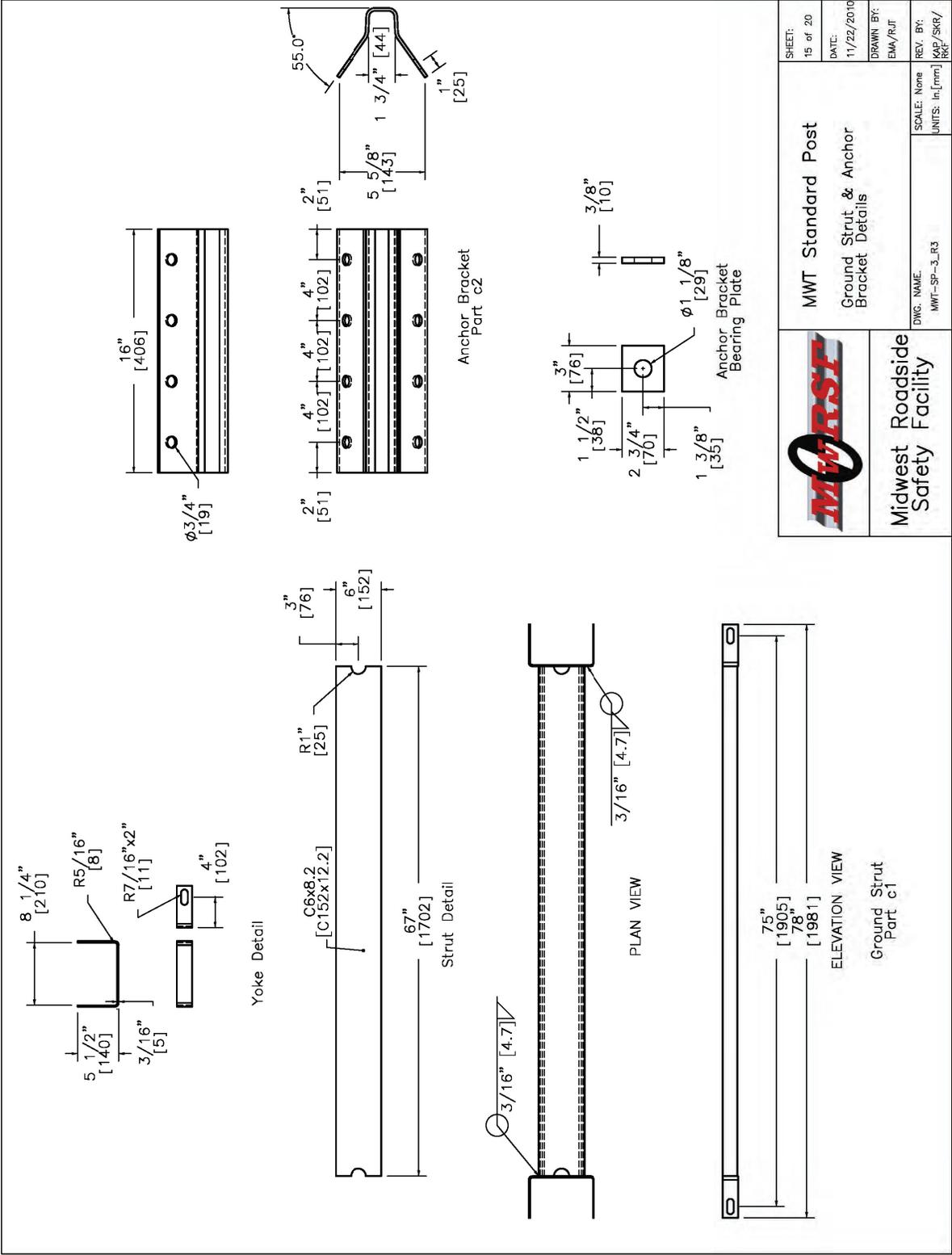
Figure 25. Ground Strut and Anchor Bracket Details, Test Nos. MWTSP-1 through 3

Figure 26. W-Beam Rail Section Details, Test Nos. MWTSP-1 through 3
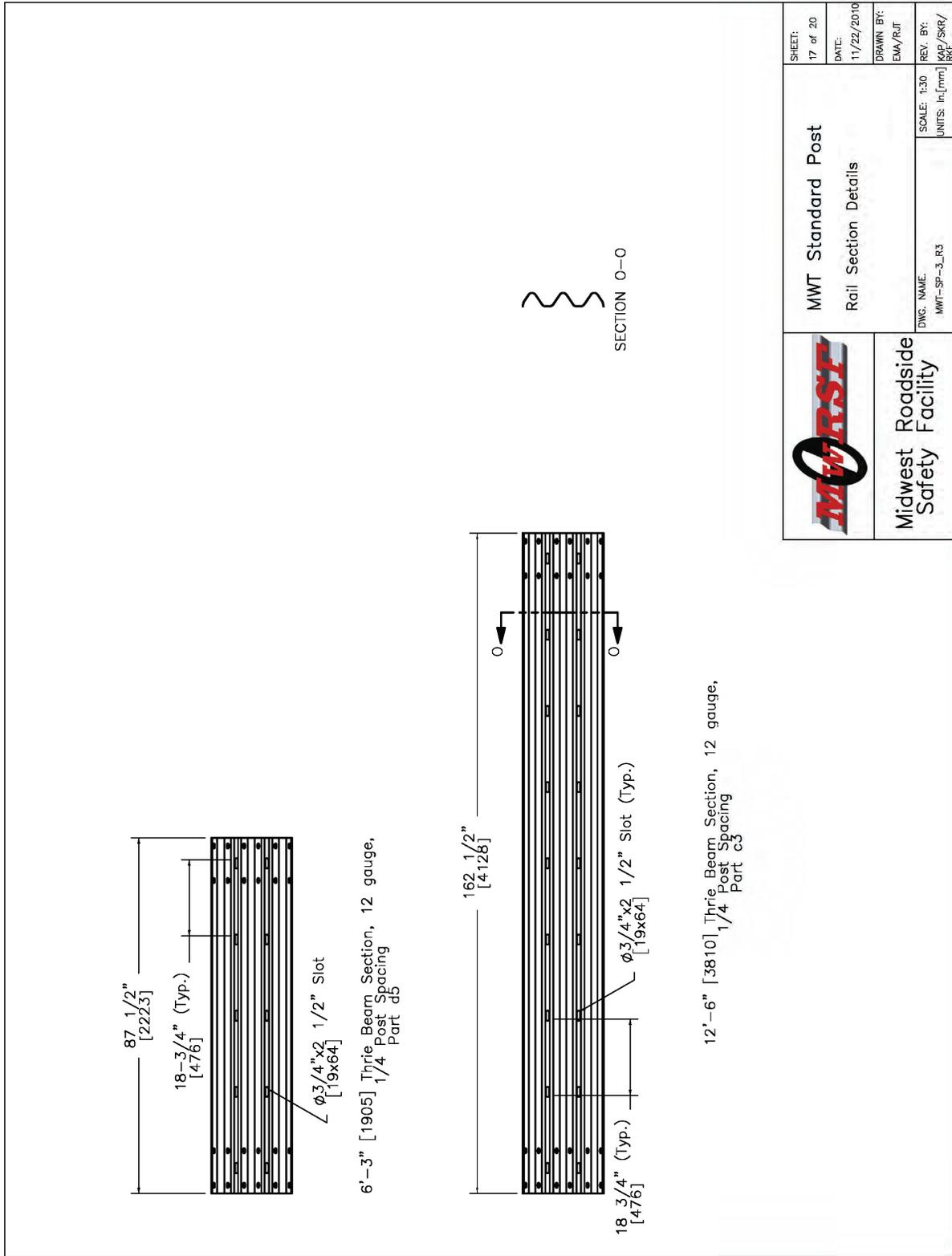
Figure 27. Thrie Beam Rail Section Details, Test Nos. MWTSP-1 through 3

Midwest Guardrail System with Standard Post Spacing

Item No.	QTY.	Description	Material Spec	Hardware Guide
a1	1	6'-3" [1905] W-Beam to Thrie-Beam Transition Section	10 gauge AASHTO M180	–
a2	7	6x12x14 1/4" [152x305x362] Blockout	SYP Grade No.1 or better	–
a3	6	6x12x19" [152x305x483] Blockout – Post 10-15	SYP Grade No.1 or better	–
a4	2	6x8x19" [152x305x483] Blockout – Post 16-17	SYP Grade No.1 or better	–
a5	1	6x8x15" [152x305x381] Blockout – Post 18	SYP Grade No.1 or better	–
b1	2	72" [1829] Foundation Tube	A500 Grade B	PTE05
b2	2	BCT Timber Post –MGS Height	SYP Grade No. 1 or better	PDF01
b3	2	Bridge Cap Rail Bent Plate Connector 6 1/4x9x3/8" [159x229x9.5]	A36 Steel	–
b4	6	Bridge Cap Rail Angle 3 1/2x3 1/2x5/16" [89x89x7.9]	A36 Steel	–
b5	1	Bridge Cap Rail C8x11.5 [C203x17.1]	A36 Steel	–
b6	1	Bridge Cap Rail C8x11.5 [C203x17.1]	A36 Steel	–
b7	1	Bridge Cap Rail Terminator Tube 3 1/2x3 1/2x1/4" [89x89x6.4]	A36 Steel	–
b8	1	Terminator Plate 9x4 1/2x3/8" [229x114x9.5]	A36 Steel	–
b9	1	Bridge Cap Rail Splice Plate 5 7/8x13x3/8" [149x330x9.5]	A36 Steel	–
c1	1	Strut and Yoke Assembly	A36 Steel	PFP01
c2	1	Anchor Bracket	A36 Steel	FPA01
c3	3	12'-6" [3810] Thrie Beam Section – 1/2 Post Spacing	12 gauge AASHTO M180	–
c4	3	W6x15 [W152x22.3] Steel Bridge Blockout	A36 Steel	–
c5	3	W6x20 [W152x29.8] Steel Bridge Post	A36 Steel	–
c6	3	12x14x1 1/4" [305x356x32] Bridge Cap Connector Plate	A36 Steel	–
d1	1	BCT Anchor Cable 6' [1829] Long	6x19 Cable	FCA01
d2	1	8x8x5/8" [203x203x15.9] Anchor Bearing Plate	A36 Steel	FPB01
d3	1	25' [7620] W-Beam MGS End Section	12 gauge AASHTO M180	–
d4	2	12'-6" [3810] W-Beam MGS Section	12 gauge AASHTO M180	–
d5	1	6'-3" [1905] Thrie Beam Section – 1/2 Post Spacing	12 gauge AASHTO M180	–
d6	1	2 3/8" [60] O.D.x 6" [152] long BCT Hole Insert	ASTM A53 Grade B Schedule 40	FMM02

Title Block:
MWT Standard Post
Bill of Materials
Midwest Roadside Safety Facility
DWG. NAME: MWT-SP-3_R3
SCALE: None
UNITS: In.[mm]
SHEET: 18 of 20
DATE: 11/22/2010
DRAWN BY: EMA/RJT
REV. BY: KAP/SKR/RKF

Figure 28. Bill of Materials, Test Nos. MWTSP-1 through 3

Midwest Guardrail System with Standard Post Spacing

Item No.	QTY.	Description	Material Spec	Hardware Guide
e1	20	1"Dia. [25] Flat Washer	Grade 5	FWC24a
e2	20	1"Dia. [25] Heavy Hex Nut	Grade 5	A325 or A449 Substitute
e3	18	1"Dia. [25] Threaded Rod	Grade A307	–
e4	116	5/8"Dia. [15.9] Flat Washer	Grade 5	–
e5	42	5/8"Dia. x 2" [M16x51] long Hex Head Bolt	Grade 5	FBX16a
e6	54	5/8"Dia. [15.9] Hex Nut	Grade 5	A325 or A449 Substitute
e7	2	5/8"Dia. x 5" [M16x127] long Hex Head Bolt	Grade 5	FBX16a
e8	4	7/8"Dia. [22.2] Flat Washer	Grade 5	FWC22a
e9	2	7/8"Dia. [22.2] Hex Nut	Grade 5	FBX22a
e10	2	7/8"Dia. x 7 1/2" [M22x191] long Hex Head Bolt	Grade 5	FBX22a
e11	2	5/8"Dia. x 10" [M16x254] long Hex Head Bolt	Grade 5	FBX16a
e12	8	5/8"Dia. x 1 1/2" [M16x38.1] long Hex Head Bolt	Grade 5	FBX16a
e13	8	5/8"Dia. x 10" [M16x254] long Guardrail Bolt	Grade A307	FBB03
e14	18	5/8"Dia. x 14" [M16x356] long Guardrail Bolt	Grade A307	FBB06
e15	8	16D Double Head Nail	–	–
e16	66	5/8"Dia. x 1 1/2" [M16x38] Guardrail Bolt	Grade A307	FBB01
e17	92	5/8"Dia. [15.9] Guardrail Nut	Grade 5	–
f1	7	W6x8.5 [W152x12.6] 72" [1829] long – Post Nos. 3-9	A36 Steel	–
f2	6	W6x8.5 [W152x12.6] 72" [1829] long – Post Nos. 10-15	A36 Steel	–
f3	1	W6x15 [W152x22.3] 84" [2134] long – Post No. 16	A36 Steel	–
f4	1	W6x15 [W152x22.3] 84" [2134] long – Post No. 17	A36 Steel	–
f5	1	W6x15 [W152x22.3] 84" [2134] long – Post No. 18	A36 Steel	–

Midwest Roadside Safety Facility

MWT Standard Post
Bill of Materials

SHEET:	19 of 20
DATE:	11/22/2010
DRAWN BY:	EMA/RJT
REV. BY:	KAP/SKR/ RKF
DWG. NAME.	MWT-SP-3_R3
SCALE: None	UNITS: In.[mm]

Figure 29. Bill of Materials, Test Nos. MWTSP-1 through 3

57
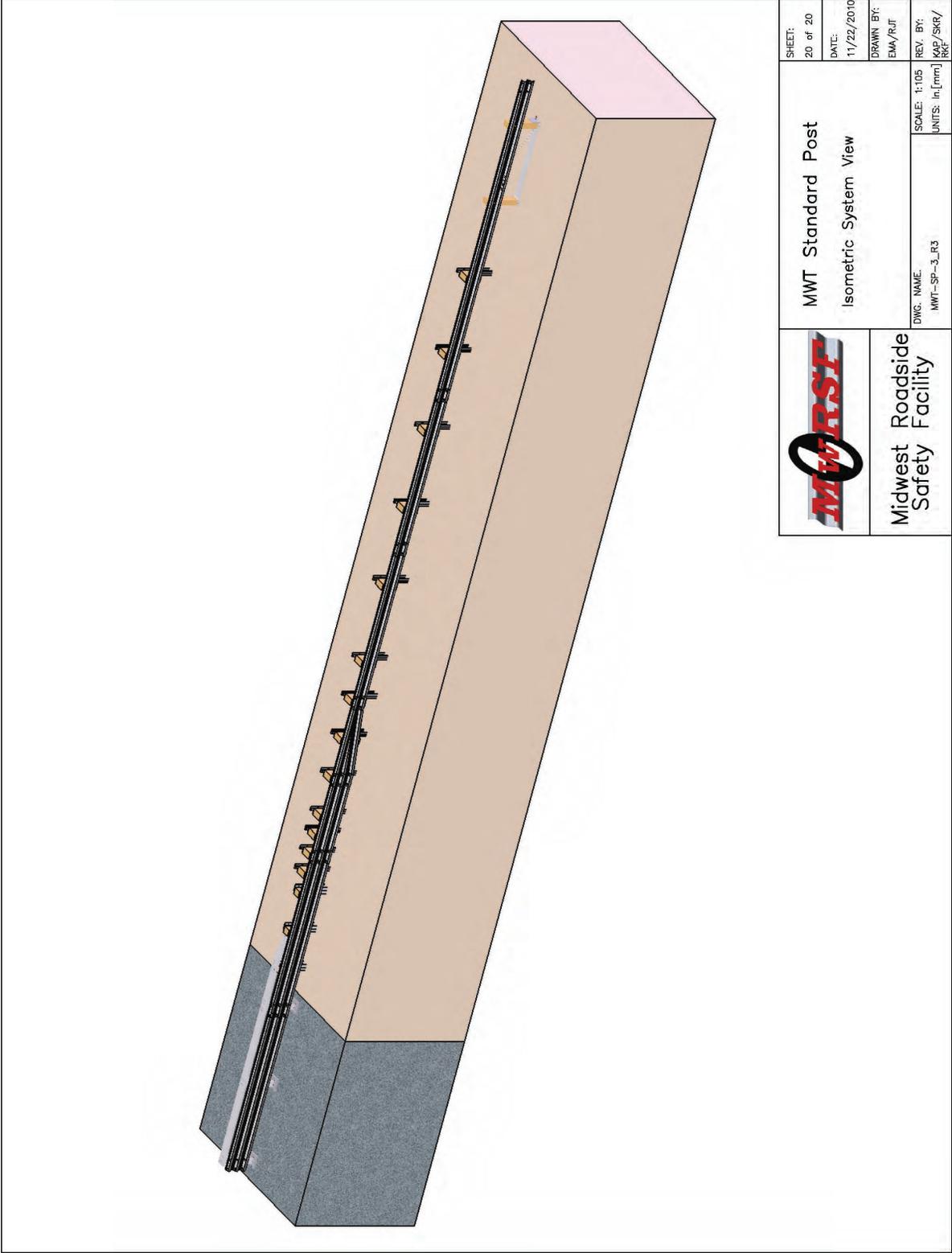
Figure 30. Isometric System View, Test Nos. MWTSP-1 through 3

Figure 31. System Photographs, Test No. MWTSP-1

Figure 32. System Photographs, Test No. MWTSP-1

Figure 33. Simulated Bridge Photographs, Test No. MWTSP-1

Figure 34. Transition Element Photographs, Test No. MWTSP-1

Figure 35. Anchor and Tarmac Connection, Test No. MWTSP-1

7 TEST REQUIREMENTS AND EVALUATION CRITERIA

7.1 Test Requirements

Longitudinal barriers, such as approach guardrail transitions, must satisfy impact safety standards in order to be accepted by the Federal Highway Administration (FHWA) for use on National Highway System (NHS) new construction projects or as a replacement for existing designs not meeting current safety standards. In recent years, these safety standards have consisted of the guidelines and procedures published in NCHRP Report No. 350 [8]. However, NCHRP Project 22-14(2) generated revised testing procedures and guidelines for use in the evaluation of roadside safety appurtenances and are provided in MASH [9]. According to Test Level 3 (TL-3) of MASH, longitudinal barrier systems must be subjected to two full-scale vehicle crash tests. The two full-scale crash tests are as follows:

1. Test Designation 3-20 consisting of a 2,425-lb (1,100-kg) small car impacting the W-beam to thrie beam transition system at a nominal speed and angle of 62 mph (100 km/h) and 25 degrees, respectively.

2. Test Designation 3-21 consisting of a 5,000-lb (2,268-kg) pickup truck impacting the W-beam to thrie beam transition system at a nominal speed and angle of 62 mph (100 km/h) and 25 degrees, respectively.

The test conditions of TL-3 longitudinal barriers are summarized in Table 5.

Table 5. MASH TL-3 Crash Test Conditions

| Test Article | Test Designation No. | Test Vehicle | Impact Conditions | | | Evaluation Criteria [1] |
| | | | Speed | | Angle (deg) | |
			mph	km/h		
Longitudinal Barrier Transition	3-20	1100C	62	100	25	A,D,F,H,I
	3-21	2270P	62	100	25	A,D,F,H,I

[1] Evaluation criteria explained in Table 6.

7.2 Evaluation Criteria

Evaluation criteria for full-scale vehicle crash testing are based on three appraisal areas: (1) structural adequacy; (2) occupant risk; and (3) vehicle trajectory after collision. Criteria for structural adequacy are intended to evaluate the ability of the guardrail transition to contain and redirect impacting vehicles. Occupant risk evaluates the degree of hazard to occupants in the impacting vehicle. Vehicle trajectory after collision is a measure of the potential for the post-impact trajectory of the vehicle to become involved in secondary collisions with other vehicles or fixed objects, thereby increasing the risk of injury to the occupant of the impacting vehicle and to other vehicles. These evaluation criteria are summarized in Table 6 and defined in greater detail in MASH. The full-scale vehicle crash tests were conducted and reported in accordance with the procedures provided in MASH.

In addition to the standard occupant risk measures, the Post-Impact Head Deceleration (PHD), the Theoretical Head Impact Velocity (THIV), and the Acceleration Severity Index (ASI) were determined and reported on the test summary sheet. Additional discussion on PHD, THIV and ASI is provided in Reference [9].

7.3 Soil Strength Requirements

In order to limit the variation of soil strength among testing agencies, foundation soil must satisfy the recommended performance characteristics set forth in Chapter 3 and Appendix B of MASH. Testing facilities must first subject the designated soil to a dynamic post test to demonstrate a minimum dynamic load of 7.5 kips (33.4 kN) at deflections between 5 and 20 in. (127 and 508 mm). If satisfactory results are observed, a static test is conducted using an identical test installation. The results of this static test become the baseline requirement for soil strength in future full-scale crash testing in which the designated soil is used. An additional post installed near the impact point is statically tested on the day of the full-scale crash test in the

same manner as used in the baseline test. The full-scale crash test can be conducted only if the

static test results show a soil resistance equal to or greater than 90 percent of the baseline test at

deflections of 5, 10, and 15 in. (127, 254, and 381 mm). Otherwise, testing must be postponed

until the soil demonstrates adequate strength.

Table 6. MASH Evaluation Criteria for Longitudinal Barriers, TL-3 Crash Testing

Structural Adequacy	A.	Test article should contain and redirect the vehicle or bring the vehicle to a controlled stop; the vehicle should not penetrate, underride, or override the installation although controlled lateral deflection of the test article is acceptable.		
Occupant Risk	D.	Detached elements, fragments or other debris from the test article should not penetrate or show potential for penetrating the occupant compartment, or present an undue hazard to other traffic, pedestrians, or personnel in a work zone. Deformations of, or intrusions into, the occupant compartment should not exceed limits set forth in Section 5.3 and Appendix E of MASH.		
	F.	The vehicle should remain upright during and after collision. The maximum roll and pitch angles are not to exceed 75 degrees.		
	H.	Occupant Impact Velocity (OIV) (see Appendix A, Section A5.3 of MASH for calculation procedure) should satisfy the following limits:		
		Occupant Impact Velocity Limits		
		Component	Preferred	Maximum
		Longitudinal and Lateral	30 ft/s (9.1 m/s)	40 ft/s (12.2 m/s)
	I.	The Occupant Ridedown Acceleration (ORA) (see Appendix A, Section A5.3 of MASH for calculation procedure) should satisfy the following limits:		
		Occupant Ridedown Acceleration Limits		
		Component	Preferred	Maximum
		Longitudinal and Lateral	15.0 g's	20.49 g's

8 TEST CONDITIONS

8.1 Test Facility

The testing facility is located at the Lincoln Air Park on the northwest side of the Lincoln Municipal Airport and is approximately 5 miles (8.0 km) northwest of the University of Nebraska-Lincoln.

8.2 Vehicle Tow and Guidance System

A reverse cable tow system with a 1:2 mechanical advantage was used to propel the test vehicles. The distance traveled and the speed of the tow vehicle were one-half that of the test vehicles. The test vehicle was released from the tow cable before impact with the barrier system. A digital speedometer on the tow vehicle increased the accuracy of the test vehicle impact speed.

A vehicle guidance system developed by Hinch [26] was used to steer the test vehicle. A guide flag, attached to the left-front wheel and the guide cable, was sheared off before impact with the barrier system. The ⅜-in. (10-mm) diameter guide cable was tensioned to approximately 3,500 lbf (15.6 kN) and supported both laterally and vertically every 100 ft (30.48 m) by hinged stanchions. The hinged stanchions stood upright while holding up the guide cable, but as the vehicle was towed down the line, the guide flag struck and knocked each stanchion to the ground.

8.3 Test Vehicles

For test no. MWTSP-1, a 2003 Dodge Ram 1500 Quad Cab pickup truck was used as the test vehicle. The test inertial and gross static weights were 5,009 lb (2,272 kg) and 5,169 lb (2,345 kg), respectively. Photographs of the test vehicle are shown in Figure 36, and vehicle dimensions are shown in Figure 37.

For test no. MWTSP-2, a 2002 Dodge Ram 1500 Quad Cab pickup truck was used as the test vehicle. The test inertial and gross static weights were 4,993 lb (2,265 kg) and 5,158 lb

(2,340 kg), respectively. Photographs of the test vehicle are shown in Figure 38, and vehicle dimension are shown in Figure 39.

For test no. MWTSP-3, a 2002 Kia Rio was used as the test vehicle. The test inertial and gross static weights were 2,394 lb (1,086 kg) and 2,591 lb (1,175 kg), respectively. Photographs of the test vehicle are shown in Figure 40, and vehicle dimension are shown in Figure 41.

The longitudinal component of the center of gravity (c.g.) for each vehicle was determined using the measured axle weights. The Suspension Method [27] was used to determine the vertical component of the c.g. for the pickup trucks. This method is based on the principle that the c.g. of any freely suspended body is in the vertical plane through the point of suspension. The vehicle was suspended successively in three positions, and the respective planes containing the c.g. were established. The intersection of these planes pinpointed the final c.g. location for the test inertial condition. The c.g. height of the 1100C vehicle was estimated based on historical c.g. height measurements. The locations of the final centers of gravity are shown in Figures 37, 39, and 41. Details on vehicle mass distributions are shown in Appendix D.

Square black and white-checkered targets were placed on the vehicles to aid in the analysis of the high-speed digital videos, as shown in Figures 42 through 44. Round, checkered targets were placed on the center of gravity, on the left-side door, on the right-side door, and on the roof of the vehicle. The remaining targets were located for references so that they could be viewed from the high-speed cameras for video analysis.

The front wheels of the test vehicles were aligned for camber, caster, and toe-in values of zero so that the vehicles would track properly along the guide cable. A 5B flash bulb was mounted under the left-side windshield wiper to pinpoint the time of impact with the barrier system on the high-speed digital videos. The flash bulb was fired by a pressure tape switch

68

mounted on the impact corner of the bumper. A remote controlled brake system was installed in

the test vehicles so that they could be brought safely to a stop after the tests.

Figure 36. Test Vehicle, Test No. MWTSP-1

Date:	1/28/2008	**Test Number:**	MWTSP-1	**Model:**	Ram 1500 Quad Cab	
Make:	Dodge	**Vehicle I.D.#:**	1D7HA18N03S139761			
Tire Size:	265/70 R17	**Year:**	2003	**Odometer:**	137921	

*(All Measurements Refer to Impacting Side)
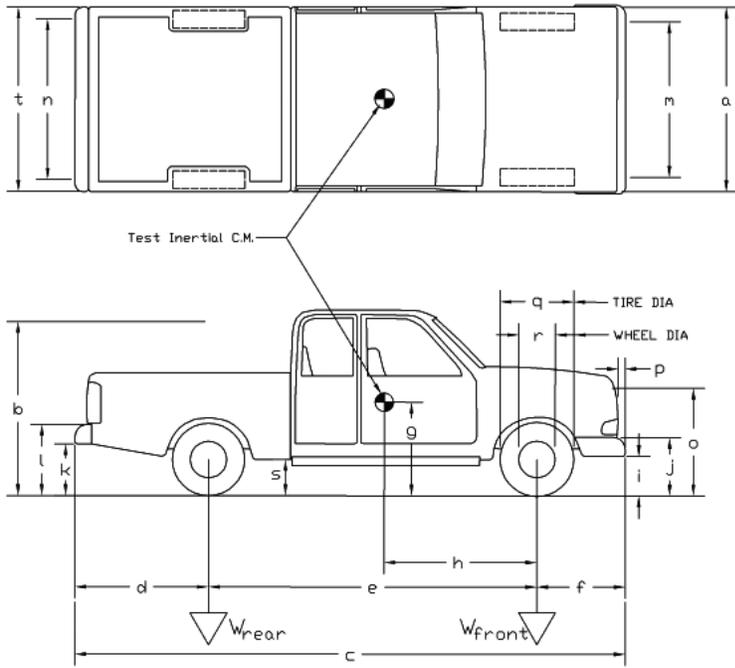
Vehicle Geometry -- in. (mm)

a	77 1/2 (1969)	b	74 1/2 (1892)
c	227 1/2 (5779)	d	47 1/4 (1200)
e	140 1/4 (3562)	f	40 (1016)
g	28 1/8 (714)	h	63 1/2 (1613)
i	14 1/2 (368)	j	24 3/4 (629)
k	21 (533)	l	29 1/4 (743)
m	68 1/4 (1734)	n	67 5/8 (1718)
o	43 (1092)	p	3 1/4 (83)
q	31 (787)	r	18 1/2 (470)
s	15 1/2 (394)	t	75 (1905)

Wheel Center Height Front 14 3/4 (375)
Wheel Center Height Rear 15 (381)
Wheel Well Clearance (FR) 34 3/4 (883)
Wheel Well Clearance (RR) 37 3/4 (959)
Frame Height (FR) 17 1/4 (438)
Frame Height (RR) 25 (635)
Engine Type 8 CYL. GAS
Engine Size 4.7L
Transmission Type: Automatic RWD

Weights lb(kg)	Curb	Test Inertial	Gross Static	
W-front	2860 (1297)	2785 (1263)	-	Front GVWR 3650
W-rear	2260 (1025)	2224 (1009)	-	Rear GVWR 3900
W-total	5121 (2323)	5009 (2272)	5179 (2349)	Total GVWR 6650

Dummy Weight 170 lb

Note any damage prior to test: none

Figure 37. Vehicle Dimensions, Test No. MWTSP-1

70

Figure 38. Test Vehicle, Test No. MWTSP-2

Date:	7/7/2008	Test Number:	MWTSP-2	Model:	Ram 1500 Quad Cab
Make:	Dodge	Vehicle I.D.#:	1D7HA18N925662937		
Tire Size:	265/70 R17	Year:	2002	Odometer:	86821

*(All Measurements Refer to Impacting Side)
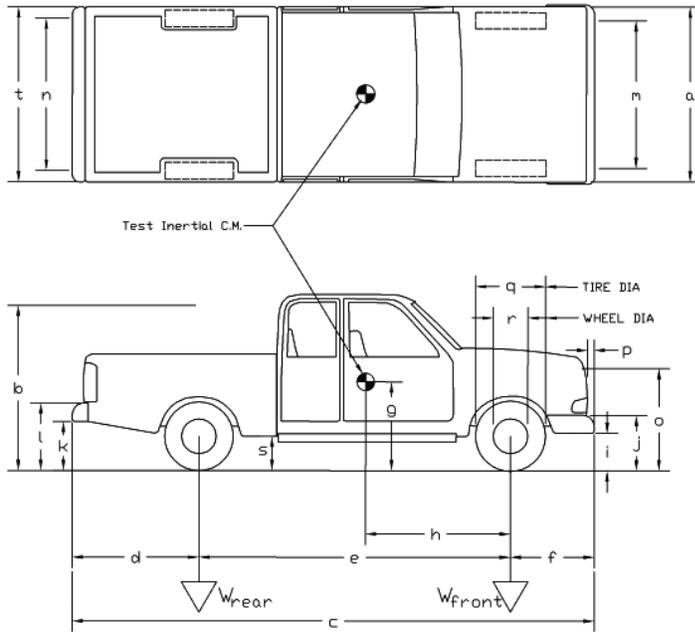
Vehicle Geometry -- in. (mm)

a	78	(1981)	b	75	(1905)
c	227 3/4	(5785)	d	46	(1168)
e	140 1/4	(3562)	f	36 1/2	(927)
g	28	(711)	h	62 3/8	(1584)
i	14	(356)	j	26 1/2	(673)
k	20 1/2	(521)	l	29	(737)
m	67 3/4	(1721)	n	67 1/2	(1715)
o	45	(1143)	p	3	(76)
q	31 1/2	(800)	r	18 1/2	(470)
s	15 1/2	(394)	t	75	(1905)

Wheel Center Height Front	15	(381)
Wheel Center Height Rear	15 1/4	(387)
Wheel Well Clearance (FR)	35	(889)
Wheel Well Clearance (RR)	37 3/4	(959)
Frame Height (FR)	18	(457)
Frame Height (RR)	25	(635)
Engine Type	8cyl. Gas	
Engine Size	4.7L	

Transmission Type:

Automatic

RWD

Weights lb (kg)	Curb	Test Inertial	Gross Static			
W-front	2865 (1300)	2767 (1255)	2868 (1301)	Front GVWR	3650
W-rear	2273 (1031)	2226 (1010)	2290 (1039)	Rear GVWR	3900
W-total	5138 (2331)	4993 (2265)	5158 (2340)	Total GVWR	6650

Dummy   170 lb

Note any damage prior to test: none

Figure 39. Vehicle Dimensions, Test No. MWTSP-2

Figure 40. Test Vehicle, Test No. MWTSP-3

Date:	10/9/2008	**Test Number:**	MWTSP-3	**Model:**		Rio Sedan
Make:	Kia	**Vehicle I.D.#:**		KNADC123226161906		
Tire Size:	P175/65R14	**Year:**	2002	**Odometer:**		80419

Tire Inflation Pressure: 30 psi

*(All Measurements Refer to Impacting Side)
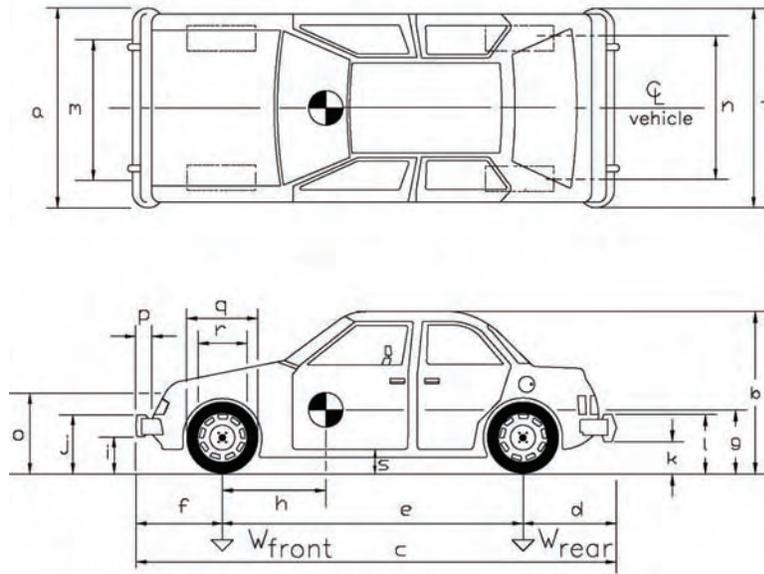
Vehicle Geometry -- in. (mm)

a	63 5/8	(1616)		b	54 1/2	(1384)
c	165 7/8	(4213)		d	37 3/4	(959)
e	95 1/4	(2419)		f	32 7/8	(835)
g	18	(457)		h	37	(940)
i	8	(203)		j	19 1/2	(495)
k	11	(279)		l	21	(533)
m	56 3/4	(1441)		n	56 7/8	(1445)
o	21 1/8	(537)		p	3	(76)
q	22 1/2	(572)		r	15 1/4	(387)
s	10 3/8	(264)		t	65 1/4	(1657)

Wheel Center Height Front	10 1/2	(267)
Wheel Center Height Rear	10 3/4	(273)
Wheel Well Clearance (FR)	24	(610)
Wheel Well Clearance (RR)	23 1/8	(587)
Frame Height (FR)	6 3/4	(171)
Frame Height (RR)	15 3/8	(391)
Engine Type	4 Cyl Gas	
Engine Size	1.4l	

Mass Distribution   lb (kg)

Gross Static	**LF**	785	(356)	**RF** 777	(352)
	LR	458	(208)	**RR** 571	(259)

Weights

lb (kg)	Curb	Test Inertial	Gross Static
W-front	1500 (680)	1460 (662)	1562 (709)
W-rear	899 (408)	934 (424)	1029 (467)
W-total	2399 (1088)	2394 (1086)	2591 (1175)

Transmition Type:

Automatic   Manual

FWD   RWD   4WD

GVWR Ratings

Front	1808
Rear	1742
Total	3315

Dummy Data

Type: Hybrid 2

Mass: 166 lb

Seat Position: Passenger

Note any damage prior to test: Rocker panel dents and fender dent repair on passenger side.

Figure 41. Vehicle Dimensions, Test No. MWTSP-3
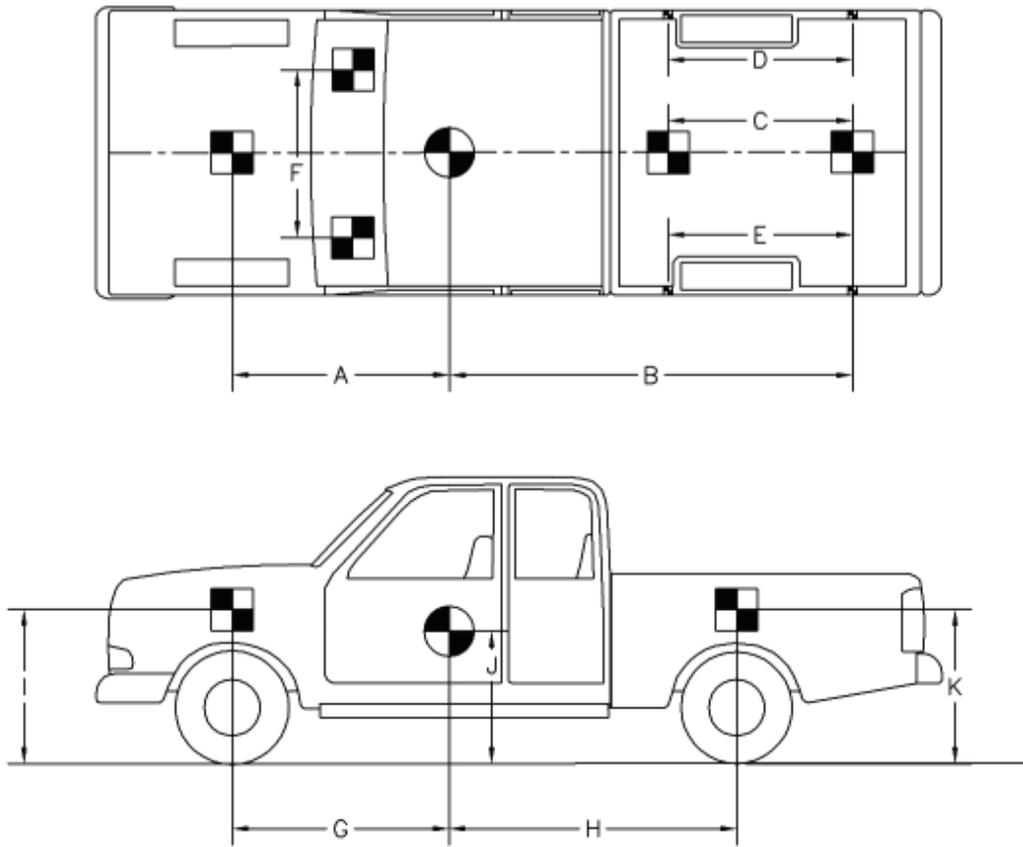
TEST #: MWTSP-1

TARGET GEOMETRY-- in. (mm)

A	75 3/8	(1915)	**E**	63 7/8	(1622)	**I**	39 1/8	(994)
B	109	(2769)	**F**	34 3/4	(883)	**J**	28 1/8	(714)
C	48 1/4	(1226)	**G**	63 1/2	(1613)	**K**	42	(1067)
D	63 7/8	(1622)	**H**	76 3/4	(1949)			

Figure 42. Target Geometry, Test No. MWTSP-1

75
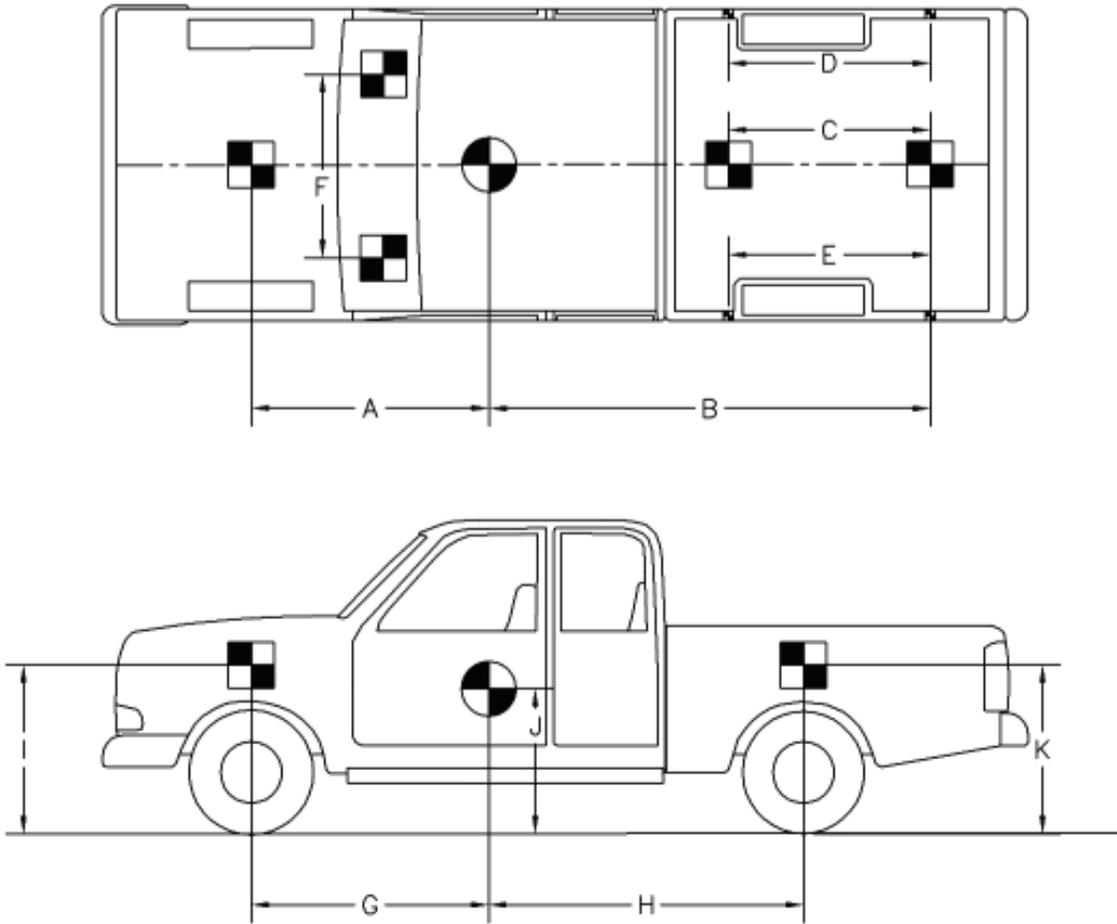
TEST #: MWTSP-2

TARGET GEOMETRY-- in. (mm)

A	67	(1702)	**E**	64	(1626)	**I**	39 1/4	(997)
B	113 1/2	(2883)	**F**	44	(1118)	**J**	28	(711)
C	48	(1219)	**G**	62 3/8	(1584)	**K**	42 1/4	(1073)
D	64	(1626)	**H**	78	(1981)			

Figure 43. Target Geometry, Test No. MWTSP-2
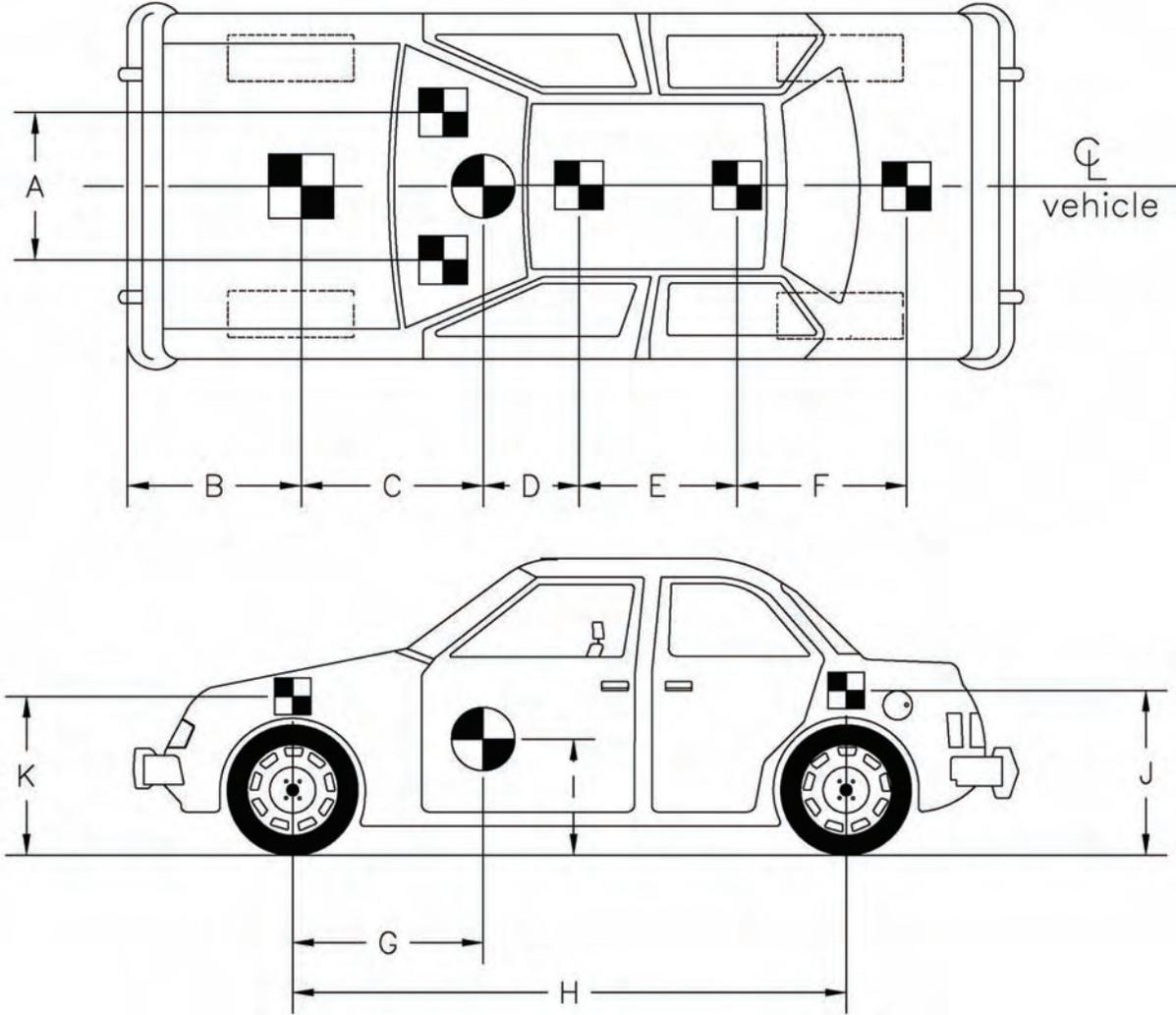
TEST #: MWTSP-3
TARGET GEOMETRY-- in. (mm)

A	35 1/4	(895)	**E**	30 7/8	(784)	**I**	18	(457)
B	30	(762)	**F**	44 3/4	(1137)	**J**	27 1/8	(689)
C	39 1/4	(997)	**G**	37	(940)	**K**	27 7/8	(708)
D	6 1/4	(159)	**H**	95 1/4	(2419)			

Figure 44. Vehicle Target Geometry, Test No. MWTSP-3

77

8.4 Simulated Occupant

For all tests, a Hybrid II 50th-Percentile, Adult Male Dummy was placed in the right-front seat of the test vehicle with the seat belt fastened. The dummy was equipped with clothing and footwear and had a final weight of 170 lb (77 kg). The dummy was manufactured by Android Systems of Carson California under model no. 572 and serial no. 451. As recommended by MASH, the dummy was not included in calculating the c.g. location.

8.5 Data Acquisition Systems

8.5.1 Accelerometers

Three environmental shock and vibration sensor/recorder systems were used to measure the accelerations in the longitudinal, lateral, and vertical directions. All of the accelerometers were mounted near the center of gravity of the test vehicles.

The first system was a two-Arm piezoresistive accelerometer system developed by Endevco of San Juan Capistrano, California. Three accelerometers were used to measure each of the longitudinal, lateral, and vertical accelerations independently at a sample rate of 10,000 Hz. Data was collected using a Sensor Input Module (SIM), Model TDAS3-SIM-16M, which was developed by Diversified Technical Systems, Inc. (DTS) of Seal Beach, California. The SIM was configured with 16 MB SRAM memory and 8 sensor input channels with 250 kB SRAM/channel. The SIM was mounted on a TDAS3-R4 module rack. The module rack was configured with isolated power/event/communications, 10BaseT Ethernet and RS232 communication, and an internal backup battery. Both the SIM and module rack are crashworthy. The computer software program "DTS TDAS Control" and a customized Microsoft Excel worksheet were used to analyze and plot the accelerometer data.

The second unit was a triaxial piezoresistive accelerometer system, developed by Instrumented Sensor Technology (IST) of Okemos, Michigan and includes three differential

channels as well as three single-ended channels. The EDR-4 6DOF-500/1200 was configured with 24 MB of RAM memory, a range of ±500 g's, a sample rate of 10,000 Hz, and a 1,677 Hz anti-aliasing filter. "EDR4COM" and "DynaMax Suite" computer software programs and a customized Microsoft Excel worksheet were used to analyze and plot the accelerometer data.

The third system, Model EDR-3, was a triaxial piezoresistive accelerometer system developed by Instrumented Sensor Technology (IST) of Okemos, Michigan. The EDR-3 was configured with 256 kB of RAM memory, a range of ±200 g's, a sample rate of 3,200 Hz, and a 1,120 Hz lowpass filter. The computer software program "DynaMax 1 (DM-1)" and a customized Microsoft Excel worksheet were used to analyzed and plot the accelerometer data.

8.5.2 Rate Transducers

An angle rate sensor, the ARS-1500, with a range of 1,500 degrees/sec in each of the three directions (roll, pitch, and yaw) was used to measure the rates of rotation of the test vehicles. The angular rate sensor was mounted on an aluminum block inside the test vehicle near the center of gravity and recorded data at 10,000 Hz to the SIM. The raw data measurements were then downloaded, converted to the proper Euler angles for analysis, and plotted. The computer software program "DTS TDAS Control" and a customized Microsoft Excel worksheet were used to analyze and plot the angular rate sensor data.

8.5.3 Pressure Tape Switches

For test nos. MWTSP-1 through MWTSP-3, five pressure-activated tape switches, spaced at approximately 6.56 ft (2 m) intervals, were used to determine the speed of the vehicle before impact. Each tape switch fired a strobe light which sent an electronic timing signal to the data acquisition system as the right-front tire of the test vehicle passed over it. Test vehicle speeds were determined from electronic timing mark data recorded using TestPoint and LabVIEW

79

computer software programs. Strobe lights and high-speed video analysis are used only as a backup in the event that vehicle speed cannot be determined from the electronic data.

8.5.4 High Speed Photography

Four high-speed AOS VITcam digital video cameras, one high-speed AOS X-PRI digital video camera, four JVC digital video cameras, and two Canon digital video cameras were utilized to record test no. MWTSP-1. Camera details, camera operating speeds, lens information, and a schematic of the camera locations relative to the system are shown in Figure 45.

For test nos. MWTSP-2 and MWTSP-3, three high-speed AOS VITcam digital video cameras, one high-speed AOS X-PRI digital video camera, five JVC digital video cameras, and two Canon digital video cameras were utilized to record the test. Camera details, camera operating speeds, lens information, and a schematic of the camera locations relative to the system are shown in Figures 46 and 47, respectively.

The high-speed videos were analyzed using ImageExpress MotionPlus and Redlake Motion Scope software. Actual camera speed and camera divergence factors were considered in the analysis of the high-speed videos.

No.	Type	Operating Speed (frames/sec)	Lens	Lens Setting
1	AOS Vitcam CTM	500	Fixed 12.5 mm	-
2	AOS Vitcam CTM	500	Sigma 24-70 mm	28
3	AOS Vitcam CTM	500	Fixed – Fujinon 50 mm	-
4	AOS Vitcam CTM	500	Sigma 70-200 mm	200
5	AOS X-PRI	500	Fixed - Sigma 50 mm	-
2	JVC – GZ-MG27u (Everio)	29.97		
3	JVC – GZ-MG27u (Everio)	29.97		
4	JVC – GZ-MG27u (Everio)	29.97		
5	JVC – GZ-MG27u (Everio)	29.97		
7	Canon ZR90	29.97		
8	Canon ZR10	29.97		

Figure 45. Camera Locations, Speeds, and Lens Settings, Test No. MWTSP-1

No.	Type	Operating Speed (frames/sec)	Lens	Lens Setting
High-Speed Video				
2	AOS Vitcam CTM	500	Fixed 12.5 mm	-
3	AOS Vitcam CTM	500	Fixed - Sigma 50 mm	-
4	AOS Vitcam CTM	500	Sigma 70-200 mm	135
5	AOS X-PRI	500	Sigma 24 – 70 mm	48
Digital Video				
1	JVC – GZ-MC500 (Everio)	29.97		
2	JVC – GZ-MG27u (Everio)	29.97		
3	JVC – GZ-MG27u (Everio)	29.97		
4	JVC – GZ-MG27u (Everio)	29.97		
5	JVC – GZ-MG27u (Everio) (Did not Record)	29.97		
7	Canon ZR90	29.97		
8	Canon ZR10	29.97		
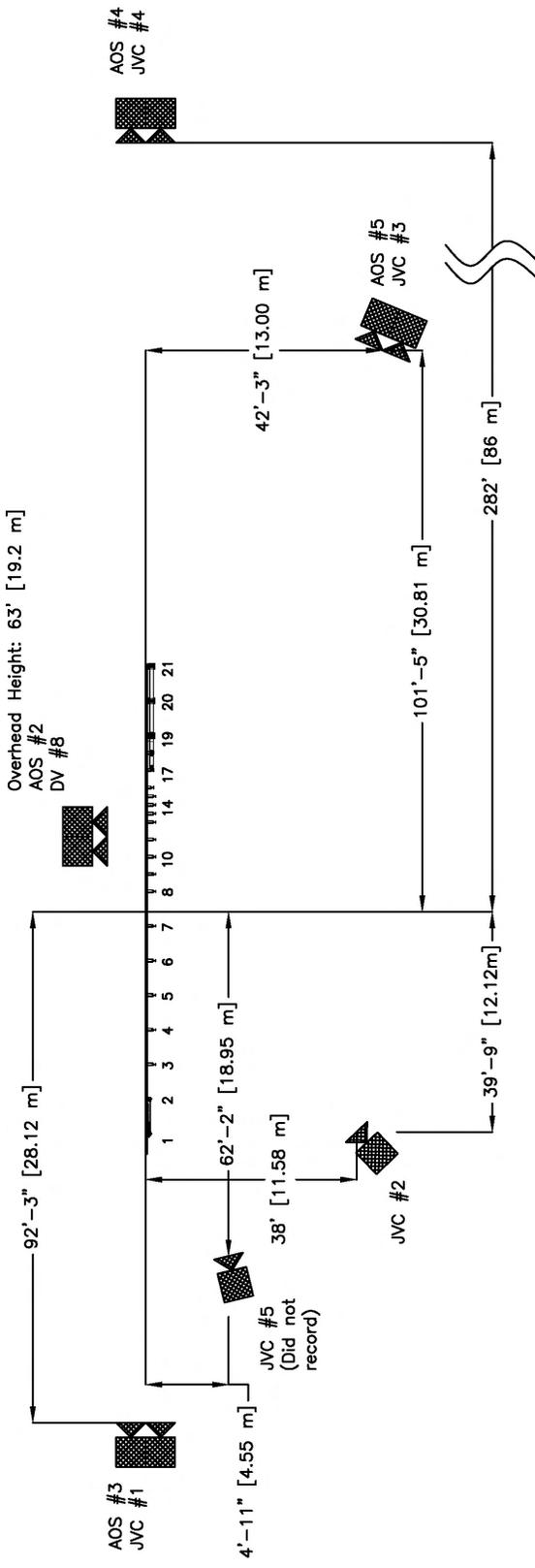
Figure 46. Camera Locations, Speeds, and Lens Settings, Test No. MWTSP-2

82

	No.	Type	Operating Speed (frames/sec)	Lens	Lens Setting
High-Speed Video	2	AOS Vitcam CTM	500	Fixed 12.5 mm	-
	3	AOS Vitcam CTM	500	Fixed - Sigma 50 mm	-
	4	AOS Vitcam CTM	500	Sigma 24-70 mm	70
	5	AOS X-PRI	500	Sigma 70 – 200 mm	200
Digital Video	1	JVC – GZ-MC500 (Everio)	29.97		
	2	JVC – GZ-MG27u (Everio)	29.97		
	3	JVC – GZ-MG27u (Everio)	29.97		
	4	JVC – GZ-MG27u (Everio)	29.97		
	5	JVC – GZ-MG27u (Everio)	29.97		
	7	Canon ZR90	29.97		
	8	Canon ZR10	29.97		

Figure 47. Camera Locations, Speeds, and Lens Settings, Test No. MWTSP-3

9 FULL SCALE CRASH TEST NO. MWTSP-1

9.1 Test No. MWTSP-1

The 5,169-lb (2,345-kg) pickup truck with a simulated occupant in the right-front seat impacted the MGS to thrie beam transition system at a speed and angle of 61.5 mph (99.0 km/h) and 24.7 degrees, respectively. A summary of the test results and sequential photographs are shown in Figure 48. Additional sequential photographs are shown in Figures 49 through 51. Documentary photographs of the crash test are shown in Figure 52.

9.2 Weather Conditions

Test no. MWTSP-1 was conducted on January 28, 2008 at approximately 2:30 pm. The weather conditions as per the National Oceanic and Atmospheric Administration (station 14939/LNK) were documented and are shown in Table 7.

Table 7. Weather Conditions, Test No. MWTSP-1

Temperature	56° F
Humidity	57%
Wind Speed	15 mph
Wind Direction	210° from True North
Sky Conditions	Sunny
Visibility	10 Statute Miles
Pavement Surface	Dry
Previous 3-Day Precipitation	0.00 in.
Previous 7-Day Precipitation	0.03 in.

9.3 Test Description

Initial vehicle impact was to occur 75 in. (1,905 mm) upstream of post no. 9, as shown in Figure 53, which was determined using the results from the BARRIER VII analysis discussed in Chapter 5. The actual point of impact was 4 in. (102 mm) downstream of the targeted impact point. A sequential description of the impact events is shown in Table 8. The vehicle came to rest

18 ft – 3 in. (5.6 m) downstream of impact and while in contact with the rail. The final position

of the vehicle is shown in Figure 54.

Table 8. Sequential Description of Impact Events, Test No. MWTSP-1

TIME (sec)	EVENT
0.000	The vehicle impacted the system 71 in. (1,803 mm) upstream of post no. 9.
0.014	Post nos. 7 through 9 deflected backward and slightly downstream as the right-front bumper corner crushed inward toward the engine compartment.
0.026	Posts nos. 3 through 6 rotated downstream and post no. 1 deflected downstream from the guardrail being pulled toward the impact region. Also, the engine hood jarred open.
0.040	Post nos. 6 and 10 deflected backward, and the vehicle began to redirect.
0.068	Post nos. 11 through 15 deflected backward.
0.084	The guardrail disengaged from post no. 10, and the vehicle pitched downward.
0.100	The guardrail disengaged from post no. 11, and the right headlight shattered.
0.134	The right-front tire contacted post no. 10, causing the wheel assembly to bend and the blockout to fracture.
0.144	Post no. 1 fractured near ground level, allowing the guardrail upstream of impact to be pulled downstream. Post nos. 3 through 7 continued to rotate downstream.
0.150	Post no. 2 fractured near ground level and split in half from the bolt pulling up and through the post.
0.156	The guardrail disengaged from post no. 12, and the vehicle pitched downward extensively.
0.164	The guardrail disengaged from post no. 5, and the vehicle contacted post no. 12. Also, both rear tires became airborne due to vehicle pitch.
0.170	The guardrail disengaged from post nos. 3-7 and 15-21 due to the guardrail shifting downstream.
0.192	The guardrail was disengaged from all posts.
0.200	The right side of the front bumper contacted post no. 13, pushing it downstream.
0.224	Post no. 13 contacted post no. 14, causing it to deflect downstream. The vehicle was rapidly decelerating as it continued to pitch downward.
0.232	The front bumper contacted the ground, causing the front bumper and hood to crush.
0.250	Post no. 14 contacted post no. 15, and further crushing of the right-front corner of the vehicle was observed. The vehicle was parallel with the system.
0.292	Post no. 15 contacted post no. 16 while still in contact with post no. 14.

0.406	The guardrail reached a maximum lateral deflection of 49.6 in. (1,260 mm).
0.948	The vehicle's maximum pitch was observed, and the rear of the vehicle began to descend.
1.724	The right-rear tire contacted the guardrail on its descent.
1.826	The rear tires contacted the ground.
2.0 – 5.0	The vehicle bounced on its rear tires before coming to rest while still in contact with the guardrail pocket.

9.4 System Damage

Damage to the barrier was moderate, as shown in Figures 55 through 61. System damage consisted of deformed guardrail and posts, fractured wooden posts, soil displacement, fractured wooden spacer blockouts, and contact marks on the guardrail. The length of vehicle contact on the barrier system was approximately 17 ft – 11 in. (5.46 m), which spanned from 71 in. (1,803 mm) upstream from the centerline of post no. 9 to the upstream end of the nested thrie beam guardrail segment near post no. 14.

The entire length of guardrail was detached from the posts due to all of the bolts pulling through the guardrail slots, as shown in Figure 55. Only three of the guardrail slots were found to have tears resulting from bolt pullout. Both slots on post no. 21 were torn ½ in. (13 mm) on the upstream side, and the lower slot on post no. 12 was torn 3½ in. (89 mm) on the upstream side. A severe kink, measuring nearly 90 degrees, was found just upstream of the nested thrie beam segment, as shown in Figure 57. A deformed guardrail pocket was found upstream of the major kink extending to post no. 9. Throughout this region contact marks, rail flattening, and minor buckling was observed on the guardrail segments, as shown in Figure 56.

Soil gaps were evident around post nos. 7 through 15. Post nos. 6 through 9 had deflected backward and downstream. The magnitude of these post deflections increased moving downstream from post no. 6, as shown in Figure 58. Also, post nos. 8 and 9 were twisted

approximately 45 degrees downstream. Post nos. 10 through 13 were deflected backward and downstream with the top of each post resting between 4½ in. (114 mm) and 14¼ in. (362 mm) above the ground surface. These posts were also twisted such that the front flanges all faced downstream, as shown in Figure 58. The 4-in. (102-mm) deep blockout at post no. 10 was disengaged and the 8-in. (203-mm) deep blockout was rotated 90 degrees. Post nos. 14 through 16 were bent downstream and came to rest against each other, as shown in Figure 59. Post nos. 17 and 18 were twisted to face downstream, and the webs of the W-shape blockouts of post nos. 19 through 21 were bent such that the front flanges were all facing downstream.

Both upstream, BCT wood anchor posts were fractured at ground level, as shown in Figure 60. Post no. 2 split in half from the bolt pulling up from the bottom through the top of the post and came to rest on its side downstream of its base. The upper portion of post no. 1 was still attached to the guardrail and came to rest 65 in. (1,651 mm) in front of the barrier system. A large knot was found on post no. 1 just below surface level where the post fractured, as shown in Figures 60 and 61. The upper 3 in. (76 mm) on the upstream side of the foundation tube for post no. 1 was deformed from the bearing plate pushing against it. No measureable soil gaps were found around either of the upstream foundation tubes.

The permanent set of the barrier system is shown in Figures 55 and 56. The maximum lateral permanent set rail and post deflections were 35¾ in. (908 mm) and 45¾ in. (1,143 mm), respectively, as measured in the field at post no. 11. The maximum lateral dynamic rail and post deflections were 49.6 in. (1,260 mm) near post no. 10 and 47.2 in. (1,198 mm) at post no. 11, respectively, as determined from high-speed digital video analysis.

9.5 Vehicle Damage

The damage to the vehicle was moderate, as shown in Figures 62 and 63, and was concentrated at the right-front corner and front of the vehicle. The right side of the front bumper and the frame horn were crushed in toward the engine compartment. The radiator and fender supports were also extensively crushed. The engine hood was unlatched and sustained crushing and buckling to the right-front corner. The right-front quarter panel was crushed, and a large dent was found spanning from the right-front wheel well to the front of the right-side door. The right-front wheel was disengaged, deflated, rotated outward 90 degrees, and crushed back into the firewall and wheel well. Both the upper and lower control arms on the right side were disengaged, and heavy damage was sustained to the spring assembly and vertical stabilizer bar.

Occupant compartment deformations to the right side and center floorboard were minor and judged insufficient to cause serious injury. Maximum longitudinal deflections of ½ in (13 mm) were located near the right-front corner of the floorboard. Maximum lateral deflections of ¼ in. (6 mm) were located near the front and center of the right-side floorboard. Maximum vertical deflections of ¼ in. (6 mm) were located along the right side of the floorboard. Complete occupant compartment deformations and the corresponding locations are provided in Appendix E.

9.6 Occupant Risk

The calculated occupant impact velocities (OIVs) and maximum 0.010-sec occupant ridedown accelerations (ORAs) in both the longitudinal and lateral directions are shown in Table 9. The calculated THIV, PHD, and ASI values are also shown in Table 9. The EDR-4 unit did not trigger during the test. Thus, no data was collected with this transducer. It was noted that the longitudinal ORA exceeded the limits provided in MASH. The results of the occupant risk

analysis, as determined from the accelerometer data, are also summarized in Figure 48. The recorded data from the accelerometers and the rate transducers are shown graphically in Appendix F.

Table 9. Summary of OIV, ORA, THIV, PHD, and ASI Values, Test No. MWTSP-1

Evaluation Criteria		Transducer			MASH Limit
		EDR-3	EDR-4	DTS	
OIV ft/s (m/s)	Longitudinal	-17.66 (-5.38)	NA	-18.62 (-5.68)	≤ 40 (12.2)
	Lateral	-16.32 (-4.97)	NA	-16.49 (-5.03)	≤ 40 (12.2)
ORA g's	Longitudinal	-24.77	NA	-24.82	≤ 20.49
	Lateral	-6.24	NA	-7.01	≤ 20.49
THIV ft/s (m/s)		-	NA	23.36 (7.12)	not required
PHD g's		-	NA	24.81	not required
ASI		1.33	NA	1.32	not required

9.7 Discussion

The analysis of the test results for test no. MWTSP-1 showed that the new simplified stiffness transition between MGS and a thrie beam approach guardrail transition system did not meet safety performance criteria established in MASH. The system adequately contained the vehicle, but it did not safely redirect it as the vehicle came to an abrupt stop inside the pocket of the barrier system. There were no detached elements nor fragments which showed potential for penetrating the occupant compartment nor presented undue hazard to other traffic. The deformation of, or intrusion into, the occupant compartment that could pose a threat to cause serious injury did not occur. The test vehicle did not penetrate nor ride over the barrier and

remained upright during and after the collision. Vehicle roll, pitch, and yaw angular displacements did not adversely influence occupant risk safety criteria nor cause rollover. Both the vehicle pitch and roll angular displacements remained below 75 degrees. Analysis of the accelerometer data showed that the longitudinal occupant ridedown accelerations exceeded the limit set in MASH. Therefore, test no. MWTSP-1 [test designation no. 3-21] was determined to be unacceptable according to the TL-3 safety performance criteria found in MASH due to the vehicle pocketing resulting in no redirection and excessive longitudinal decelerations.

0.000 sec   0.132 sec   0.200 sec   0.324 sec   0.984 sec
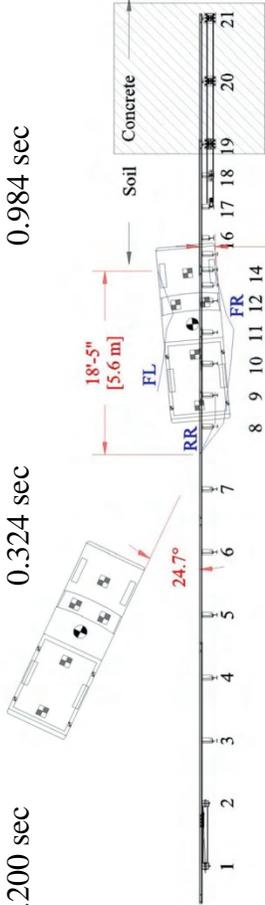
- Test Agency .... MwRSF
- Test Number MWTSP-1
- Date 1/28/08
- MASH Test Designation 3-21
- Test Article .... Stiffness Transition between MGS and Thrie Beam Transition
- Total Length .... 87 ft - 6 in. (26.7 m)
- Height to Top of Rail .... 31 in. (787 mm)
- Key Components – Steel W-Beam Guardrail
  - Thickness .... 12 gauge (2.66 mm)
- Key Components – Steel W-Beam to Thrie Beam Transition
  - Thickness .... 10 gauge (3.42 mm)
  - Segment Length .... 75 in. (1,905 mm)
- Key Components – Steel Thrie Beam
  - Thickness .... 12 gauge (2.66 mm)
- Key Components – Steel Posts
  - Post Nos. 3 - 15 .... 72 in. (1,829 mm) long, W6x9 (W152x13.4)
  - Post Nos. 16 - 18 .... 84 in. (2,134 mm) long, W6x15 (W152x22.3)
  - Post Nos. 19 - 21 .... 29⁵⁄₈ in. (752 mm) long, W6x20 (W152x29.8)
- Post Spacing
  - Post Nos. 1 - 8, 19 - 21 .... 75 in. (1,905 mm)
  - Post Nos. 8 - 12, 16 - 19 .... 37½ in. (953 mm)
  - Post Nos. 12 - 16 .... 18¾ in. (476 mm)
- Type of Soil .... Grading B – AASHTO M 147-65
- Vehicle
  - Make and Model .... 2003 Dodge Ram 1500 Quad Cab
  - Curb .... 5,121 lb (2,323 kg)
  - Test Inertial .... 5,009 lb (2,272 kg)
  - Gross Static .... 5,169 lb (2,345 kg)
- Impact Conditions
  - Speed .... 61.5 mph (99.0 km/h)
  - Angle .... 24.7 deg
  - Impact Location .... 75 in. (1,905 mm) US of Post No. 9
- Exit Conditions
  - Speed .... NA
  - Angle .... NA
- Vehicle Damage .... Moderate
  - VDS[28] 1-RFQ-5
  - CDC[29] 01-RFEW2
- Vehicle Stability .... Satisfactory
- Exit Box Criterion .... NA

- Vehicle Stopping Distance .... 18 ft -3 in. (5.6 m) DS of Impact
- Test Article Damage .... Moderate
- Test Article Deflections
  - Permanent Set .... 45¾ in. (1,162 mm)
  - Dynamic .... 49.6 in. (1,260 mm)
  - Working Width .... NA
- Maximum Angular Displacements
  - Roll .... 17.1° < 75°
  - Pitch .... 41.9° < 75°
  - Yaw .... 30.2°
- Impact Severity .... 114.1 kip-ft (154.7 kJ) < 106 kip-ft (144 kJ)
- Transducer Data

Evaluation Criteria		Transducer			MASH Limit
		EDR-3	EDR-4	DTS	
OIV ft/s (m/s)	Longitudinal	-17.66 (-5.38)	NA	-18.62 (-5.68)	≤40 (12.2)
	Lateral	-16.32 (-4.97)	NA	-16.49 (-5.03)	≤40 (12.2)
ORA g's	Longitudinal	-24.77	NA	-24.82	≤20.49
	Lateral	-6.24	NA	-7.01	≤20.49
THIV – ft/s (m/s)		-	NA	23.36 (7.12)	not required
PHD – g's		-	NA	24.81	not required
ASI		1.33	NA	1.32	not required

Figure 48. Summary of Test Results and Sequential Photographs, Test No. MWTSP-1

91

0.000 sec

0.164 sec

0.042 sec

0.192 sec

0.088 sec

0.306 sec

0.150 sec

0.640 sec

Figure 49. Additional Sequential Photographs, Test No. MWTSP-1

0.000 sec

0.208 sec

0.062 sec

0.292 sec

0.118 sec

0.450 sec

0.170 sec

0.878 sec

Figure 50. Additional Sequential Photographs, Test No. MWTSP-1

93
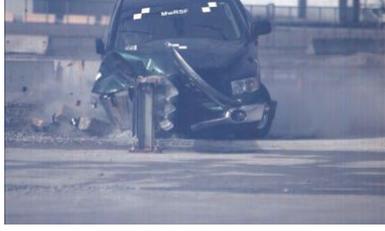
0.000 sec	0.000 sec
0.082 sec	0.092 sec
0.148 sec	0.128
0.252 sec	0.184 sec
0.930 sec	0.274 sec
1.834 sec	0.820 sec

Figure 51. Additional Sequential Photographs, Test No. MWTSP-1

94

Figure 52. Documentary Photographs, Test No. MWTSP-1

Figure 53. Impact Location, Test No. MWTSP-1

Figure 54. Vehicle Final Position, Test No. MWTSP-1

97

Figure 55. System Damage, Test No. MWTSP-1

98
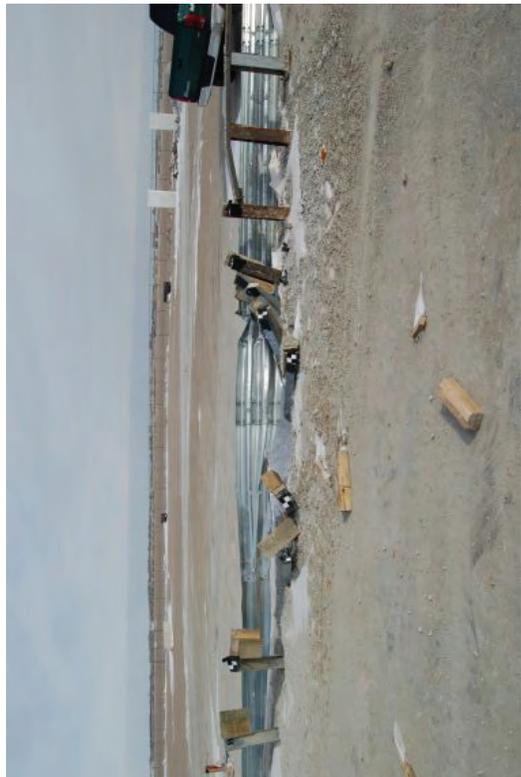
Figure 56. Rail Deformation, Test No. MWTSP-1

99
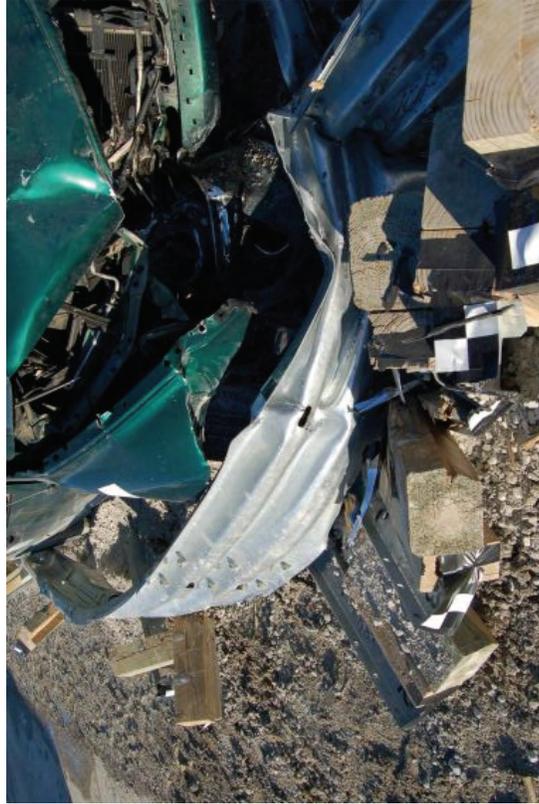
Figure 57. Rail Pocket, Test No. MWTSP-1

100
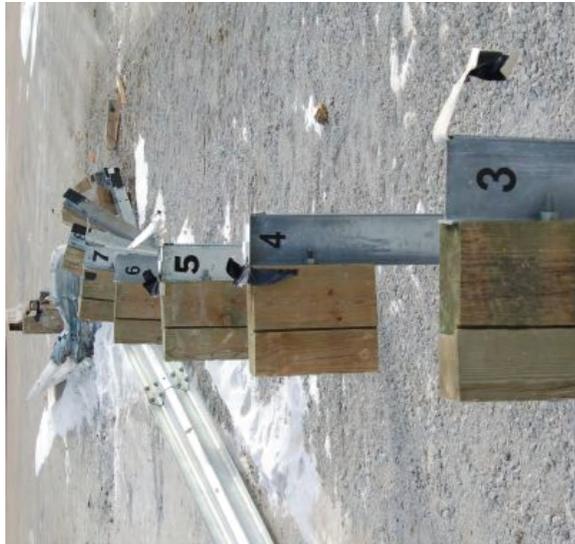
Figure 58. Post Deflections, Test No. MWTSP-1

101

Figure 59. Posts Nos. 13 through 16 Damage, Test No. MWTSP-1
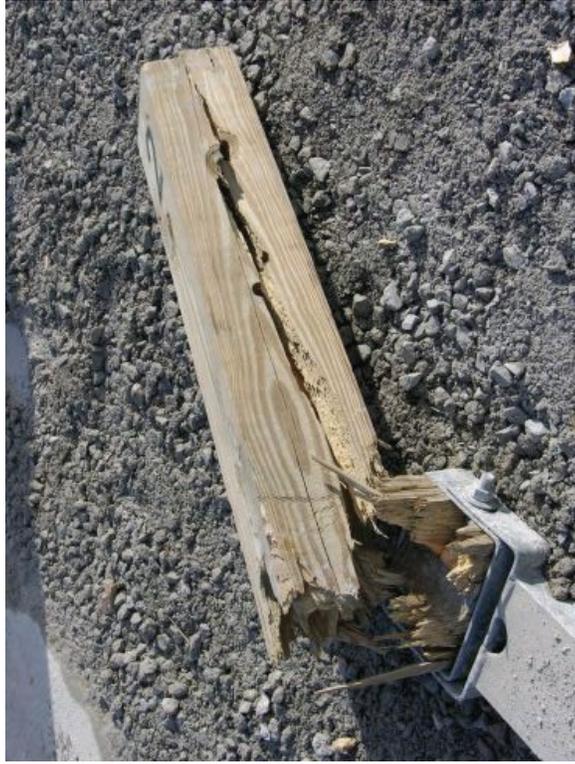
Figure 60. Upstream Anchorage Damage, Test No. MWTSP-1

103

Figure 61. Anchorage Post No. 1 Damage, Test No. MWTSP-1

Figure 62. Vehicle Damage, Test No. MWTSP-1
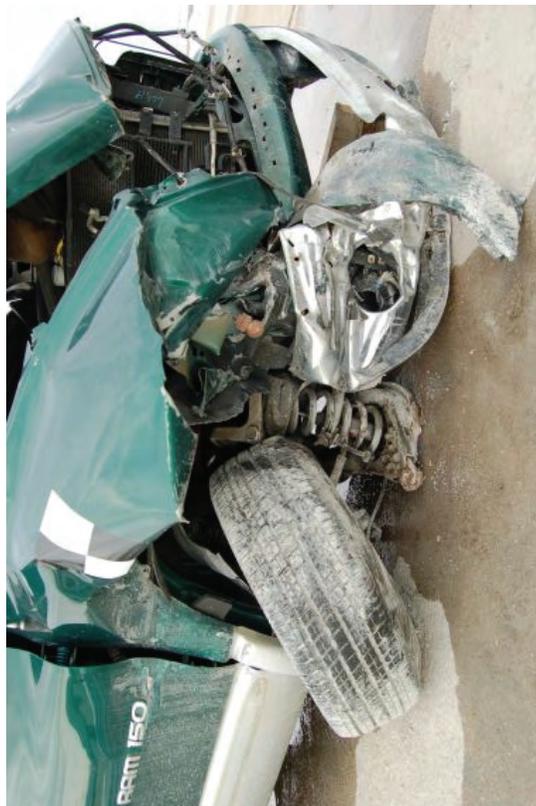
Figure 63. Right-Front Wheel Assembly Damage, Test No. MWTSP-1

10 ANALYSIS AND DISCUSSION OF TEST NO. MWTSP-1

Following a review of the high-speed videos and damaged barrier hardware from crash test no. MWTSP-1, several potential factors affecting the unsatisfactory outcome were identified. First, the BCT wood anchor post, post no. 1, was observed to release due to post fracture. A closer inspection of post no. 1 revealed significant checking through the wide faces of the post along with a critically placed knot on the upstream, back side corner of the post, just above the steel cable anchor plate, as shown in Figure 61. The upstream high-speed video showed that post no. 1 was pulled downstream and toward the traveled way as the W-beam rail was loaded. Thus, the highest stress was located on the upstream, back-side corner of the post. A corner section of the post was then fractured near the groundline extending up toward the knot. Upon review of the test results, it is believed that the BCT post was significantly weakened by the checks and a critically-placed knot, thus resulting in post fracture and contributing greatly to the test failure.

Second, the steel foundation tube supporting post no. 1 was not displaced during the test. Previous full-scale crash tests of W-beam guardrail systems utilizing the same end anchorage has demonstrated the ability of the anchor posts and foundation tubes to be displaced up to 5 in. (127 mm) longitudinally at the groundline [23,30-31]. The lack of anchorage movement in test no. MWTSP-1 could have been due to either inadequate load imparted to the foundation tube prior to wood post fracture or a stiffer than normal soil material compacted around the foundation tube. To estimate the magnitude of anchor loading and displacement during the crash test, BARRIER VII computer simulations were conducted using the Design K barrier model from Chapter 5 and a vehicle model created for the 2270P vehicle. The analysis indicated that the anchor loading should have been approximately 30.5 kips (135.7 kN) at the time of post fracture, 140 msec after impact, as estimated from high-speed videos. The maximum anchor load observed in the simulation was 36.8 kips (163.7 kN) at 185 msec. These loadings are below the

estimated anchor design load of 42 kips (187 kN). Under the 30.5-kip (135.7-kN) load at the time of post fracture, the soil around the foundation tube would have been expected to move approximately 3 in. (76 mm). However, soil gaps were not found adjacent to the anchor posts. Thus, the soil surrounding the foundation tube was likely stiffer than typically observed in standard guardrail testing. This added stiffness may have been the result of some subsurface frost or other soil anomaly. Although an overly stiff foundation tube could increase anchor loading, it is believed that this condition would have had only a minor contribution to the failed post and test, since much-higher anchor loadings have been observed during prior full-scale crash tests on the high flare rate MGS designs [30].

Another possible cause for the unsatisfactory test was the aggressive design selected for crash testing. Recall, Design K was the most aggressive system design described in Chapter 5 as it had an increased propensity for vehicle pocketing and a higher barrier deflection than the other designs. However, both MwRSF researchers and the Midwest States Pooled Fund representatives wanted to push the limits and selected the shortest transition design for full-scale crash testing.

Upon review of this information, it was believed the main cause of failure for test no. MWTSP-1 was the fracture of the weak, upstream BCT anchor posts. Further, MwRSF researchers remained confident that the stiffness transition between the MGS and the thrie beam approach guardrail transition system would have satisfactorily redirected the vehicle if the wood BCT anchor posts had adequate strength and had not fractured. After deliberations with the members of the Midwest States Pooled Fund Program, the decision was made to rerun the crash test under the same impact conditions and with the same system design. The only modification made to the previous system was that the wood BCT anchor posts were prescribed a more stringent inspection and evaluation with the intention of preventing premature post fracture. The wood posts could not contain defects near the critical section, or within 18 in. (457 mm) of the

groundline. Thus, the anchorage system for test no. MWTSP-2 was expected to develop its full capacity.

11 FULL SCALE CRASH TEST NO. MWTSP-2

11.1 Static Soil Test

Before full-scale test no. MWTSP-2 was conducted, the strength of the foundation soil was evaluated with a static test, as described by MASH. The static test results, as shown in Appendix G, demonstrated a soil resistance above the baseline test limits. Thus, the soil provided adequate strength, and the full-scale crash test on the barrier system could be conducted.

11.2 Test No. MWTSP-2

The 5,158-lb (2,340-kg) pickup truck with a simulated occupant in the right-front seat impacted the MGS to thrie beam transition system at a speed of 61.2 mph (98.5 km/h) and at an angle of 26.3 degrees. A summary of the test results and sequential photographs are shown in Figure 64. Additional sequential photographs are shown in Figures 65 and 66. Documentary photographs of the crash test are shown in Figure 67.

11.3 Weather Conditions

Test no. MWTSP-2 was conducted on July 7, 2008 at approximately 3:00 pm. The weather conditions as per the National Oceanic and Atmospheric Administration (station 14939/LNK) were documented and are shown in Table 10.

Table 10. Weather Conditions, Test No. MWTSP-2

Temperature	91° F
Humidity	49%
Wind Speed	9 mph
Wind Direction	230° from True North
Sky Conditions	Sunny
Visibility	10 Statute Miles
Pavement Surface	Dry
Previous 3-Day Precipitation	0.30 in.
Previous 7-Day Precipitation	0.30 in.

11.4 Test Description

Initial vehicle impact was to occur 75 in. (1,905 mm) upstream of post no. 9, as shown in Figure 68, which was determined using the results from the BARRIER VII analysis discussed in Chapter 5. The actual point of impact was ½ in. (13 mm) downstream of the targeted impact point. A sequential description of the impact events is shown in Table 11. The vehicle came to rest 263 ft (80.2 m) downstream of impact and 44 ft (13.4 m) laterally behind the system. The vehicle trajectory and final position are shown in Figure 69.

Table 11. Sequential Description of Impact Events, Test No. MWTSP-2

TIME (sec)	EVENT
0.000	The vehicle impacted the system 74½ in. (1,892 mm) upstream of post no. 9.
0.004	The guardrail bent at the impact point, and post nos. 7 through 9 began to deflect backward.
0.008	The right-front corner of the vehicle was crushed inward.
0.028	The vehicle hood crushed, and the grill contacted the top of the guardrail.
0.030	Post nos. 6 and 10 began to deflect backward.
0.044	Post no. 11 began to deflect, and the posts upstream of impact twisted to face downstream.
0.052	The vehicle yawed away from the system.
0.072	The rail disengaged from post no. 9. Post no. 12 began to deflect laterally, and a kink developed in the rail on the upstream side of post no. 12.
0.088	The right-front corner of the vehicle contacted the wooden blockout at post no. 10, causing it to split. The rail disengaged from post no. 10.
0.090	The rail buckled between post nos. 13 and 14.
0.118	The right-front tire contacted post no. 10, causing the post to bend downstream and the tire to disengage from the vehicle. The vehicle began to pitch downward.
0.132	The rail disengaged from the top bolt of post no. 11.
0.136	The front-right door became ajar at the top.
0.170	The left-rear tire became airborne.
0.214	The right-rear corner of the vehicle contacted the rail near post no. 8.
0.246	The vehicle was parallel to the system with a speed of 41.4 mph, and the vehicle began to roll toward the barrier.

0.360	The vehicle reached its maximum downward pitch as the vehicle continued to yaw away from the system.
0.448	The left-front tire became airborne.
0.454	The right-front axle contacted the ground.
0.506	The vehicle exited the system at a speed and angle of 37.3 mph and 16.5 degrees, respectively.
0.590	The vehicle reached its maximum roll toward the barrier.
1.110	The left-side tires contacted to the ground.

11.5 System Damage

Damage to the barrier was moderate, as shown in Figures 70 through 74. System damage consisted of deformed guardrail and posts, soil displacement, fractured wooden spacer blockouts, and contact marks on the guardrail. The length of vehicle contact on the barrier system was approximately 18 ft – 8 in. (5.7 m), which spanned from 37 in. (940 mm) upstream from the centerline of post no. 8 to the centerline of post no. 14.

Post nos. 3 through 9 were twisted such that the front of each post was facing slightly downstream. Soil gaps measuring ½ in. (13 mm) and 1 in. (25 mm) were found at the front side of post nos. 6 and 7, respectively. Localized soil failures left craters measuring 10 in. (254 mm) and 12 in. (305 mm) in diameter around the bases of post nos. 8 and 9, respectively, as shown in Figure 72. Post no. 9 rotated laterally, bent longitudinally downstream, and twisted to face downstream. The bolt at post no. 9 also pulled through the rail slot. Buckling was found along the top of the W-beam rail at the centerline of post no. 7 and 18 in. (457 mm) upstream of post no. 8. The bottom of the W-beam rail was folded under at post nos. 8 and 9.

Post no. 10 bent both backward and downstream, and contact marks were found on the upstream side of the post. The wooden blockout at post no. 10 was fractured into several pieces. Post no. 11 deflected backward and slightly downstream. Localized soil failures resulted in craters measuring 20 in. (508 mm) and 16 in. (406 mm) in diameter in front of post nos. 10 and

11, respectively. The W-beam to thrie beam transition element encountered only contact marks and minor deformations, as shown in Figure 73. Similar to the W-beam rail just upstream, the bottom of the transition piece was bent upward. Minor buckling of the rail occurred at post no. 10. Both bolts at post no. 10 and the top bolt at post no. 11 pulled through the rail slots.

Post nos. 12 through 16 deflected backward, and post no. 12 also deflected downstream. Soil gaps were found at the front of post nos. 12 through 16 measuring 5 in., 3 in., 2 in., 1 in., and ½ in. (127 mm, 76 mm, 51 mm, 25 mm, and 13 mm), respectively. Soil gaps of 1 in. (25 mm) were also located behind post nos. 12 through 14. The thrie beam rail spanning between post nos. 11 and 14 sustained minor folds and buckling, as shown in Figure 74. The bottom of the thrie beam rail folded backward, and the middle hump between post nos. 12 and 13 was flattened. Localized deformations were found around both bolt heads at post no. 13. The top and bottom of the thrie beam rail just upstream of the splice at post no. 14 buckled, and the top of the nested thrie beam at post no. 15 buckled slightly. Both bolts at post no. 12 pulled through the rail.

The two wood BCT anchor posts on the upstream end of the system were pulled and rotated downstream, as shown in Figure 71. Soil gaps were found on the upstream side of post nos. 1 and 2 measuring 1 in. (25 mm) and ¾ in. (19 mm), respectively.

The permanent set of the barrier is shown in Figure 70. The maximum lateral permanent set rail and post deflections were 21⅞ in. (556 mm) at the centerline of post no. 11 and 25¾ in. (654 mm) at post no. 11, respectively, as measured in the field. The maximum lateral dynamic rail and post deflections were 30.7 in. (779 mm) at the centerline of post no. 10 and 32.8 in. (833 mm) at post no. 11, respectively, as determined from high-speed digital video analysis. The working width of the system was found to be 51.6 in. (1,310 mm).

113

11.6 Vehicle Damage

Damage to the vehicle was moderate, as shown in Figures 75 through 78. Vehicle damage was concentrated on the right-front corner of the pickup truck. The right-front corner of the vehicle, including the bumper and quarter panel, was crushed inward, and the right headlight was fractured. As a result of this crushing, the center of the front bumper protruded outward, and the engine hood was jarred upward. Minor windshield cracking occurred near the base of the right side of the windshield.

The right-front tire was disengaged, as shown in Figure 76. The upper control arm and the steering arm pin were both bent. The right side of the vehicle was crushed from the right-front wheel well to the right-front door. The bottom of the right-front door was crushed inward 4 in. (102 mm), causing the top of the door to become ajar. Gouges were found on the bottom of the right side of the vehicle from the front door to the rear bumper. The bottom of the right-rear quarter panel deformed inward, and scrapes and contact marks were located on the right-rear tire, as shown in Figure 77. The right-side shock absorber bracket on the rear axle was bent inward, and the right side of the rear bumper was bent and folded.

Occupant compartment deformations to the floorboard, as shown in Figure 78, were judged insufficient to cause serious injury to the vehicle occupants. Maximum longitudinal and lateral deformations of 1 in. (25 mm) and 1¼ in. (32 mm), respectively, were both located at the right-front corner of the floorboard. A maximum vertical deformation of 1 in. (25 mm) was located near the front of the floorboard on the passenger side of the vehicle. Deformations were recorded from two separate reference points before and after the test. Complete occupant compartment deformations and the corresponding locations are provided in Appendix E.

11.7 Occupant Risk

The calculated occupant impact velocities (OIVs) and maximum 0.010-sec occupant ridedown accelerations (ORAs) in both the longitudinal and lateral directions are shown in Table 12. The calculated THIV, PHD, and ASI values are also shown in Table 12. The DTS and EDR-4 units experienced technical difficulties during the test. Thus, no data was collected with these transducers. It was noted that the occupant risk limits provided in MASH were all satisfied. The results of the occupant risk analysis, as determined from the accelerometer data, are also summarized in Figure 64. The recorded data from the accelerometers and the rate transducers are shown graphically in Appendix H.

Table 12. Summary of OIV, ORA, THIV, PHD, and ASI Values, Test No. MWTSP-2

Evaluation Criteria		Transducer			MASH Limit
		EDR-3	EDR-4	DTS	
OIV ft/s (m/s)	Longitudinal	-21.21 (-6.46)	NA	NA	≤ 40 (12.2)
	Lateral	-16.91 (-5.15)	NA	NA	≤ 40 (12.2)
ORA g's	Longitudinal	-12.03	NA	NA	≤ 20.49
	Lateral	-9.87	NA	NA	≤ 20.49
THIV ft/s (m/s)		-	NA	NA	not required
PHD g's		-	NA	NA	not required
ASI		0.91	NA	NA	not required

11.8 Discussion

The analysis of the test results for test no. MWTSP-2 showed that the new simplified stiffness transition between MGS and a thrie beam approach guardrail transition system

adequately contained and redirected the vehicle without significant permanent displacements of the barrier. There were no detached elements or fragments which showed potential for penetrating the occupant compartment or presented undue hazard to other traffic. The deformation of, or intrusion into, the occupant compartment was minimal and did not pose a threat to cause serious injury. The test vehicle did not penetrate nor override the barrier and remained upright during and after the collision. Vehicle roll, pitch, and yaw angular displacements did not adversely influence occupant risk safety criteria nor cause rollover. Both the vehicle pitch and roll angular displacements remained below 75 degrees. After impact, the vehicle exited the barrier at an angle of 22 degrees and did not intrude into adjacent traffic lanes. Analysis of the accelerometer data showed that both the occupant ridedown decelerations and the occupant impact velocities satisfied the limits set in MASH. Therefore, test no. MWTSP-2 [test designation no. 3-21] was determined to be acceptable according to the TL-3 safety performance criteria found in MASH.

0.000 sec 0.072 sec 0.184 sec 0.246 sec 0.506 sec

- Test Agency .... MwRSF
- Test Number MWTSP-2
- Date 7/7/08
- MASH Test Designation 3–21
- Test Article .... Stiffness Transition between MGS and
  Thrie Beam Transition
- Total Length .... 87 ft – 6 in. (26.7 m)
- Height to Top of Rail .... 31 in. (787 mm)
- Key Components – Steel W-Beam Guardrail
  Thickness .... 12 gauge (2.66 mm)
- Key Components – Steel W-Beam to Thrie Beam Transition
  Thickness .... 10 gauge (3.42 mm)
  Segment Length .... 75 in. (1,905 mm)
- Key Components – Steel Thrie Beam
  Thickness .... 12 gauge (2.66 mm)
- Key Components – Steel Posts
  Post Nos. 3 - 15 .... 72 in. (1,829 mm) long, W6x9 (W152x13.4)
  Post Nos. 16 - 18 .... 84 in. (2,134 mm) long, W6x15 (W152x22.3)
  Post Nos. 19 - 21 .... 29⁵⁄₈ in. (752 mm) long, W6x20 (W152x29.8)
- Post Spacing
  Post Nos. 1 - 8, 19 - 21 .... 75 in. (1,905 mm)
  Post Nos. 8 - 12, 16 - 19 .... 37¹⁄₂ in. (953 mm)
  Post Nos. 12 - 16 .... 18¾ in. (476 mm)
- Type of Soil .... Grading B – AASHTO M 147-65
- Vehicle
  Make and Model .... 2002 Dodge Ram 1500 Quad Cab
  Curb .... 5,138 lb (2,331 kg)
  Test Inertial .... 4,993 lb (2,265 kg)
  Gross Static .... 5,158 lb (2,340 kg)
- Impact Conditions
  Speed .... 61.2 mph (98.5 km/h)
  Angle .... 26.3 deg
  Impact Location .... 75 in. (1,905 mm) US of Post No. 9
- Exit Conditions
  Speed .... 37.3 mph (60.0 km/h)
  Angle .... 22.0 deg
- Vehicle Stability .... Satisfactory
- Exit Box Criteria .... Passed
- Vehicle Damage .... Moderate
  VDS[28] 1-RFQ-5
  CDC[29] 01-RFEW2
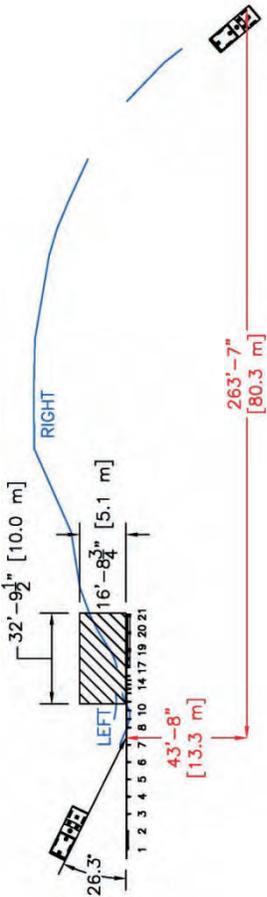
- Vehicle Stopping Distance .... 263 ft (80.2 m) DS of Impact
  43.7 ft (13.3 m) Laterally Behind the System
- Test Article Damage .... Moderate
- Test Article Deflections
  Permanent Set .... 25¾ in. (654 mm)
  Dynamic .... 32.8 in. (833 mm)
  Working Width .... 51.6 in. (1,310 mm)
- Maximum Angular Displacements
  Roll .... 13° <75°
  Pitch .... 10° <75°
  Yaw .... 51°
- Impact Severity .... 126.8 kip-ft (171.9 kJ) > 106 kip-ft (144 kJ)
- Transducer Data

Evaluation Criteria			Transducer			MASH Limit
		EDR-3	EDR-4	DTS	
OIV ft/s (m/s)	Longitudinal	-21.21 (-6.46)	NA	NA	≤40 (12.2)
	Lateral	-16.91 (-5.15)	NA	NA	≤40 (12.2)
ORA g's	Longitudinal	-12.03	NA	NA	≤20.49
	Lateral	-9.87	NA	NA	≤20.49
THIV – ft/s (m/s)		-	NA	NA	not required
PHD – g's		-	NA	NA	not required
ASI		0.91	NA	NA	not required

Figure 64. Summary of Test Results and Sequential Photographs, Test No. MWTSP-2

0.000 sec

0.000 sec

0.060 sec

0.084 sec

0.128 sec

0.142 sec

0.244 sec

0.204 sec

0.336 sec

0.314 sec

0.454 sec

0.502 sec

Figure 65. Additional Sequential Photographs, Test No. MWTSP-2

118
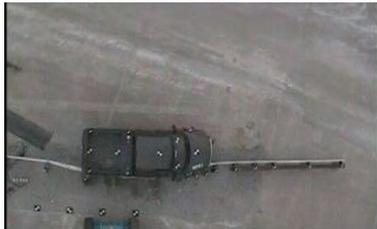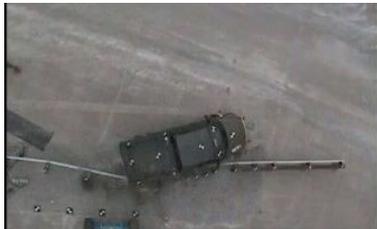
0.000 sec	0.000 sec
0.092 sec	0.067 sec
0.170 sec	0.167 sec
0.244 sec	0.234 sec
0.448 sec	0.334 sec
0.796 sec	0.501 sec

Figure 66. Additional Sequential Photographs, Test No. MWTSP-2

Figure 67. Documentary Photographs, Test No. MWTSP-2

120
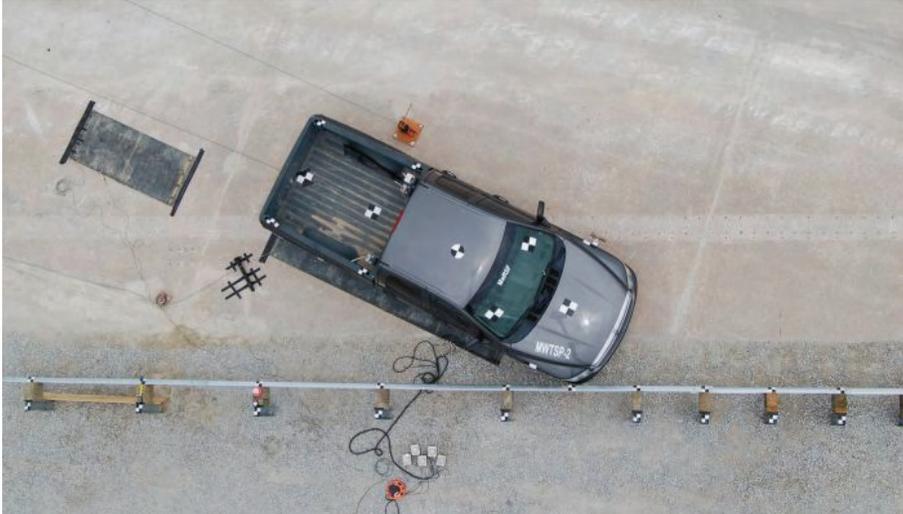
Figure 68. Impact Location, Test No. MWTSP-2

121

Figure 69. Vehicle Trajectory and Final Position, Test No. MWTSP-2
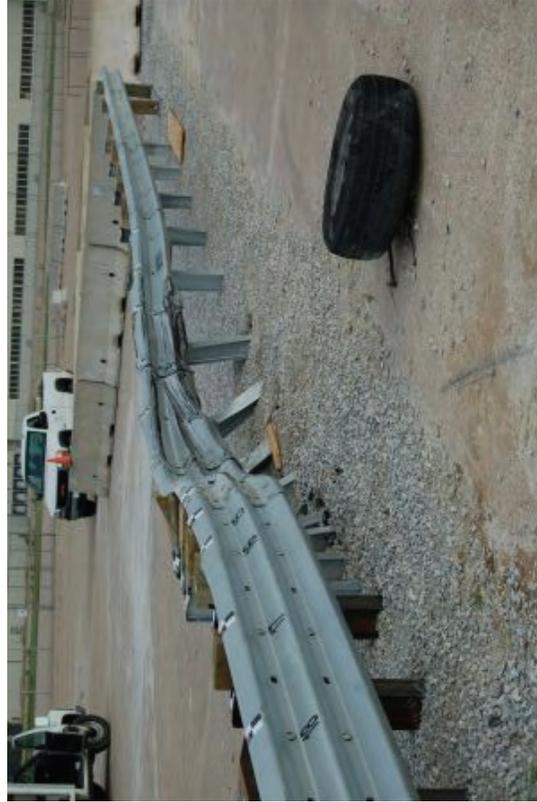
Figure 70. System Damage, Test No. MWTSP-2

Figure 71. Upstream Anchorage Damage, Test No. MWTSP-2

Figure 72. Post Nos. 7 through 9 Damage, Test No. MWTSP-2

125

Figure 73. Post Nos. 10 and 11 Damage, Test No. MWTSP-2

Figure 74. Post Nos. 12 through 14 Damage, Test No. MWTSP-2

Figure 75. Vehicle Damage, Test No. MWTSP-2
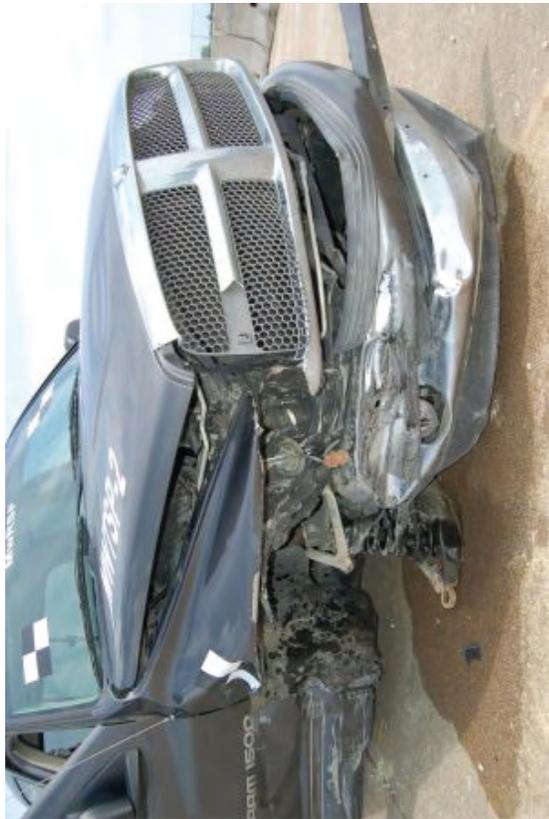
Figure 76. Vehicle Damage, Test No. MWTSP-2

Figure 77. Vehicle Damage, Test No. MWTSP-2

Figure 78. Occupant Compartment Damage, Test No. MWTSP-2

12 FULL SCALE CRASH TEST NO. MWTSP-3

12.1 Static Soil Test

Before full-scale test no. MWTSP-3 was conducted, the strength of the foundation soil was evaluated with a static test, as described by MASH. The static test results, as shown in Appendix G, demonstrated a soil resistance above the baseline test limits. Thus, the soil provided adequate strength, and the full-scale crash test on the barrier system could be conducted.

12.2 Test No. MWTSP-3

The 2,591-lb (1,175-kg) small car, with a simulated occupant in the right-front seat, impacted the MGS to thrie beam transition system at a speed of 61.0 mph (98.2 km/h) and at an angle of 25.7 degrees. A summary of the test results and sequential photographs are shown in Figure 79. Additional sequential photographs are shown in Figures 80 and 81. Documentary photographs of the crash test are shown in Figure 82.

12.3 Weather Conditions

Test no. MWTSP-3 was conducted on October 9, 2008 at approximately 2:00 pm. The weather conditions as per the National Oceanic and Atmospheric Administration (station 14939/LNK) were documented and are shown in Table 16.

Table 13. Weather Conditions, Test No. MWTSP-3

Temperature	71° F
Humidity	26%
Wind Speed	15 mph
Wind Direction	130° from True North
Sky Conditions	Sunny
Visibility	10 Statute Miles
Pavement Surface	Dry
Previous 3-Day Precipitation	0.20 in.
Previous 7-Day Precipitation	0.20 in.

12.4 Test Description

The CIP for test no. MWTSP-3 was selected to maximize pocketing as well as the probability of the vehicle wedging under the asymmetrical W-beam to thrie beam transition element. A BARRIER VII analysis was conducted utilizing the previous system model and an 1100C vehicle model. The impact point in BARRIER VII was moved longitudinally until a maximum pocketing angle on the W-beam to thrie beam transition element was achieved. Based on this analysis, initial vehicle impact occurred at the targeted impact point 93¾ in. (2,381 mm) upstream of post no. 9, as shown in Figure 83. A sequential description of the impact events is shown in Table 14. The vehicle came to rest directly in front of post no. 12. The vehicle trajectory and final position are shown in Figure 84.

Table 14. Sequential Description of Impact Events, Test No. MWTSP-3

TIME (sec)	EVENT
0.000	The vehicle impacted the system 93¾ in. (2.3 m) upstream of post no. 9.
0.008	The rail deflected backward near the impact point, and the vehicle bumper crushed inward.
0.036	Post nos. 8 and 9 deflected backward, and the posts upstream of impact twisted to face downstream.
0.040	The engine hood jarred open as the vehicle began to redirect.
0.046	The right-front corner of the bumper contacted post no. 8, and the vehicle pitched downward.
0.058	The right-front tire contacted post no. 8, and post no. 10 began to deflect backward.
0.066	The rail disengaged from post no. 8.
0.072	The right-front corner of the bumper contacted post no. 9, and post no. 11 began to deflect backward.
0.078	The vehicle rolled away from the barrier.
0.080	The rail disengaged from post no. 9.
0.088	The wood blockout disengaged from post no. 9, and the front-right door contacted the rail between post nos. 7 and 8.
0.102	The right-rear tire became airborne.

0.110	The right-front window shattered as the dummy's head was ejected out the vehicle's side window.
0.118	The left-front bumper corner contacted the ground, causing the bumper to detach from the vehicle.
0.124	The right-front tire contacted post no. 10, separating the wood blockout from the post. The vehicle began to pitch upward.
0.164	The right-front tire contacted the wood blockout at post no. 11.
0.182	The blockout disengaged from post no. 11.
0.192	The rail reached its maximum deflection between post nos. 9 and 10.
0.210	The vehicle stopped yawing and began skidding laterally. However, the right-front corner of the vehicle remained in contact with the rail.
0.278	The vehicle yawed rapidly toward the rail as the front of the vehicle approached post no. 12.
0.382	The right-rear tire contacted the ground as the vehicle continued to yaw with the front of the vehicle facing post no. 12.
0.628	The vehicle exited the system at a speed and angle of 6 mph and 71 degrees, respectively, while continuing to yaw about its front tire.
1.120	The vehicle ceased to yaw.
1.648	The vehicle came to its final resting position just in front of post no. 12.

12.5 System Damage

Damage to the barrier was moderate, as shown in Figures 85 through 88. System damage consisted of deformed guardrail and posts, soil displacement, fractured wooden spacer blockouts, and contact marks on the guardrail. The length of vehicle contact on the barrier system was approximately 17 ft – 2 in. (5.24 m), which spanned from 93¾ in. (2,381 mm) upstream of post no. 9 to the centerline of post no. 12.

Post nos. 8 and 9 bent backward and downstream to the extent that they laid nearly flat on the ground, as shown in Figure 86. Only small soil gaps were present on the front and upstream sides of these posts. The rail disengaged from both post nos. 8 and 9, and the wood blockout had disengaged from post no. 9. Contact marks were found on both corrugations of the W-beam rail between post nos. 8 and 9, and the lower edge of the guardrail was folded back and up from contact with the vehicle bumper. The rail buckled at post no. 7.

134

Post no. 10 bent downstream and slightly forward to the extent that it was nearly flat on the ground, while post no. 11 bent about 45 degrees downstream and backward. The rail disengaged from post nos. 10 and 11, as shown in Figure 87. The blockout disengaged from post no. 10. The blockout at post no. 11 remained attached, but was fractured and partially removed. The asymmetrical transition rail element was deformed backward and bent upward, as shown in Figure 85, and encountered contact marks along its top corrugation and pinching deformations to the bottom corrugation.

Post no. 12 bent a few inches downstream. The guardrail disengaged from both bolts at post no. 12, as shown in Figure 88. All downstream posts remained intact without permanent deformations. Significant buckling of the thrie beam guardrail was found at post no. 12, and minor buckling occurred along the top of the thrie beam between post nos. 13 and 14.

The permanent set of the barrier is shown in Figure 85. The maximum lateral permanent set rail deflection was 18 in. (457 mm) at the centerline of post no. 10, as measured in the field, and the maximum lateral permanent set post deflection was 27.6 in. (686 mm) at post no. 8, as determined from high-speed digital video analysis. The maximum lateral dynamic rail and post deflections were 25.9 in. (658 mm) at the midpoint between post nos. 9 and 10 and 34.8 in. (883 mm) at post no. 8, respectively, as determined from high-speed digital video analysis. The working width of the system was found to be 56.0 in. (1,422 mm).

It should be noted that the permanent and dynamic post deflection for test no. MWTSP-3 was found to be larger than the deflections found in MWTSP-2, despite the lower mass of the vehicle used in MWTSP-3. This occurred because the right-front tire of the 1100C vehicle in test no. MWTSP-3 rode up the face of post no. 8, which caused the post to be pushed to the ground and rotate backward in the soil. Researchers believed that this excess in permanent and dynamic deflections misrepresented the behavior of the system, as post no. 8 was detached from the

system before being pushed to the ground. Thus, the maximum permanent and dynamic deflection of post no. 8 were neglected. The second largest lateral permanent and dynamic post deflections were 15.6 in. (396 mm) and 18.5 in. (470 mm) at post no. 11, as determined from high-speed digital video analysis. The working width corresponding to this point was 39.8 in. (1,011 mm).

12.6 Vehicle Damage

Damage to the vehicle was moderate, as shown in Figures 89 through 91. Vehicle damage was concentrated on the front and right-front corner of the vehicle. The right-front corner of the vehicle, including the quarter panel and portions of the frame, was crushed inward, and both headlights were fractured. The coolant reservoir and fan were crushed and deformed. The alternator and the engine block were both displaced backward. Both the windshield wiper fluid reservoir and the radiator were crushed and displaced toward the engine block. The right-side mirror and the front bumper disengaged. The right-front window was broken out as a result of the dummy's head being ejected from the vehicle during redirection. The right-front corner of the engine hood was crushed inward, and the middle of the hood buckled upward. The engine hood deformations caused many cracks in the windshield. However, the windshield remained intact, and the occupant compartment was not penetrated.

Significant damage was found on the right-front wheel, as shown in Figure 90. The right-front tire was flat, and a gash measuring 4 in. (102 mm) long was found on the outside face of the tire. A steel piece, measuring 6 in. (152 mm) long, fractured off the inside of the right-front wheel rim. The right-front suspension was bent, and the lower control arm was twisted as the tire was pushed backward and into the wheel well.

Occupant compartment deformations to the floorboard, as shown in Figure 91, were judged insufficient to cause serious injury to the vehicle occupants. A maximum longitudinal

deformation of 1¾ in. (44 mm) was located near the front of the floorboard on the passenger side of the vehicle. A maximum lateral deformation of 1¾ in. (44 mm) was located near the middle of the passenger-side floorboard, and a maximum vertical deformation of 1¾ in. (44 mm) was located near the left-front corner of the floorboard on the passenger side. Also, a dent was found on the right side of the vehicle's roof, and the front-passenger side door was buckled outward slightly. Complete occupant compartment deformations and the corresponding locations are provided in Appendix E.

12.7 Occupant Risk

The calculated occupant impact velocities (OIVs) and maximum 0.010-sec occupant ridedown accelerations (ORAs) in both the longitudinal and lateral directions are shown in Table 15. The calculated THIV, PHD, and ASI values are also shown in Table 15. The EDR-4 unit experienced technical difficulties during the test, thus, no data was collected with this transducer. It was noted that the occupant risk limits provided in MASH were all satisfied. The results of the occupant risk analysis, as determined from the accelerometer data, are also summarized in Figure 79. The recorded data from the accelerometers and the rate transducers are shown graphically in Appendix I.

12.8 Discussion

The analysis of the test results for test no. MWTSP-3 showed that the new simplified stiffness transition between the MGS and a thrie beam approach guardrail transition system adequately contained the vehicle without significant permanent displacements of the barrier. There were no detached elements or fragments which showed potential for penetrating the occupant compartment or presented undue hazard to other traffic. The deformation of, or intrusion into, the occupant compartment was minimal and did not pose a threat to cause serious injury. The test vehicle did not penetrate nor ride over the barrier and remained upright during

137

Table 15. Summary of OIV, ORA, THIV, PHD, and ASI Values, Test No. MWTSP-3

Evaluation Criteria		Transducer			MASH Limit
		EDR-3	EDR-4	DTS	
OIV ft/s (m/s)	Longitudinal	-27.55 (-8.40)	NA	-25.62 (-7.81)	≤ 40 (12.2)
	Lateral	-17.05 (-5.20)	NA	-18.61 (-5.67)	≤ 40 (12.2)
ORA g's	Longitudinal	-14.70	NA	-13.70	≤ 20.49
	Lateral	-5.76	NA	-6.74	≤ 20.49
THIV ft/s (m/s)		-	NA	30.12 (9.18)	not required
PHD g's		-	NA	14.25	not required
ASI		1.11	NA	1.12	not required

and after the collision. Vehicle roll, pitch, and yaw angular displacements did not adversely influence occupant risk safety criteria nor cause rollover. Both the vehicle pitch and roll angular displacements remained below 75 degrees. After impact, the vehicle came to a stop adjacent to the barrier and did not intrude into adjacent traffic lanes. The vehicle did encounter wheel snagging on the guardrail posts, but analysis of the accelerometer data showed that both the occupant ridedown accelerations and the occupant impact velocities satisfied the limits set in MASH. Therefore, test no. MWTSP-3 [test designation no. 3-20] was determined to be acceptable according to the TL-3 safety performance criteria found in MASH.

0.000 sec   0.066 sec   0.112 sec   0.240 sec   0.330 sec
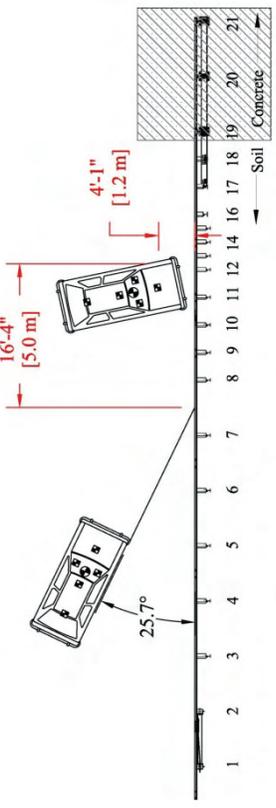
- Test Agency .... MwRSF
- Test Number MWTSP-3
- Date 10/9/08
- MASH Test Designation 3-20
- Test Article .... Stiffness Transition between MGS and Thrie Beam Transition
- Total Length .... 87 ft - 6 in. (26.7 m)
- Height to Top of Rail .... 31 in. (787 mm)
- Key Components – Steel W-Beam Guardrail
  Thickness .... 12 gauge (2.66 mm)
- Key Components – Steel W-Beam to Thrie Beam Transition
  Thickness .... 10 gauge (3.42 mm)
  Segment Length .... 75 in. (1,905 mm)
- Key Components – Steel Thrie Beam
  Thickness .... 12 gauge (2.66 mm)
- Key Components – Steel Posts
  Post Nos. 3 - 15 .... 72 in. (1,829 mm) long W6x9 (W152x13.4)
  Post Nos. 16 - 18 .... 84 in. (2,134 mm) long W6x15 (W152x22.3)
  Post Nos. 19 - 21 .... 29$^5/_8$ in. (752 mm) long W6x20 (W152x29.8)
- Post Spacing
  Post Nos. 1 - 8, 19 - 21 .... 75 in. (1,905 mm)
  Post Nos. 8 - 12, 16 - 19 .... 37$^1/_2$ in. (953 mm)
  Post Nos. 12 - 16 .... 18$^3/_4$ in. (476 mm)
- Type of Soil .... Grading B – AASHTO M 147-65
- Vehicle
  Make and Model .... 2002 Kia Rio
  Curb .... 2,399 lb (1,088 kg)
  Test Inertial .... 2,394 lb (1,086 kg)
  Gross Static .... 2,591 lb (1,175 kg)
- Impact Conditions
  Speed .... 61.0 mph (98.2 km/h)
  Angle .... 25.7 deg
  Impact Location .... 93¾ in. (2,381 mm) US of Post No. 9
- Exit Conditions
  Speed .... 5.8 mph (9.4 km/h)
  Angle .... 68.7 deg
- Vehicle Stability .... Satisfactory
- Exit Box Criterion .... NA
- Vehicle Damage .... Moderate
  VDS[28] 1-RFQ-5
  CDC[29] 01-RFEW2

- Vehicle Stopping Distance .... 16 ft (4.9 m) DS of Impact
  4.1 ft (1.2 m) in front of the system
- Test Article Damage .... Moderate
- Test Article Deflections
  Permanent Set .... 15.6 in. (396 mm)
  Dynamic .... 18.5 in. (470 mm)
  Working Width .... 39.8 in. (1,011 mm)
- Maximum Angular Displacements
  Roll .... 6.9° <75°
  Pitch .... -4.2° <75°
  Yaw .... 60.7°
- Impact Severity .... 60.6 kip-ft (82.2 kJ) > 51.0 kip-ft (69.7 kJ)
- Transducer Data

Evaluation Criteria		Transducer			MASH
---	---	EDR-3	EDR-4	DTS	Limit
OIV ft/s (m/s)	Longitudinal	-27.55 (-8.40)	NA	-25.62 (-7.81)	≤40 (12.2)
	Lateral	-17.05 (-5.20)	NA	-18.61 (-5.67)	≤40 (12.2)
ORA g's	Longitudinal	-14.70	NA	-13.70	≤20.49
	Lateral	-5.76	NA	-6.74	≤20.49
THIV – ft/s (m/s)		-	NA	30.12 (9.18)	not required
PHD – g's		-	NA	14.25	not required
ASI		1.11	NA	1.13	not required

Figure 79. Summary of Test Results and Sequential Photographs, Test No. MWTSP-3

139

0.000 sec

0.000 sec

0.060 sec

0.067 sec

0.124 sec

0.167 sec

0.220 sec

0.267 sec

0.390 sec

0.434 sec

0.520 sec

0.968 sec

Figure 80. Additional Sequential Photographs, Test No. MWTSP-3

0.000 sec	0.000 sec
0.058 sec	0.078 sec
0.120 sec	0.118 sec
0.164 sec	0.192 sec
0.192 sec	0.350 sec
0.382 sec	0.536 sec

Figure 81. Additional Sequential Photographs, Test No. MWTSP-3

141

Figure 82. Documentary Photographs, Test No. MWTSP-3

Figure 83. Impact Location. Test No. MWTSP-3

Figure 84. Vehicle Trajectory and Final Position, Test No. MWTSP-3

Figure 85. System Damage, Test No. MWTSP-3

145

Figure 86. Posts Nos. 7 through 9 Damage, Test No. MWTSP-3

146

Figure 87. Posts Nos. 10 and 11 Damage, Test No. MWTSP-3

147

Figure 88. Post Nos. 12 through 14 Damage, Test No. MWTSP-3

148
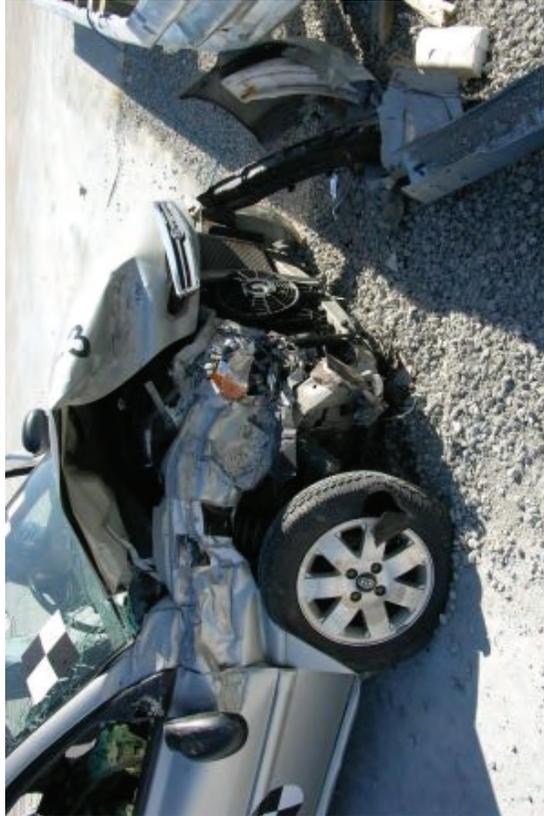
Figure 89. Vehicle Damage, Test No. MWTSP-3

149

Figure 90. Vehicle Damage, Test No. MWTSP-3
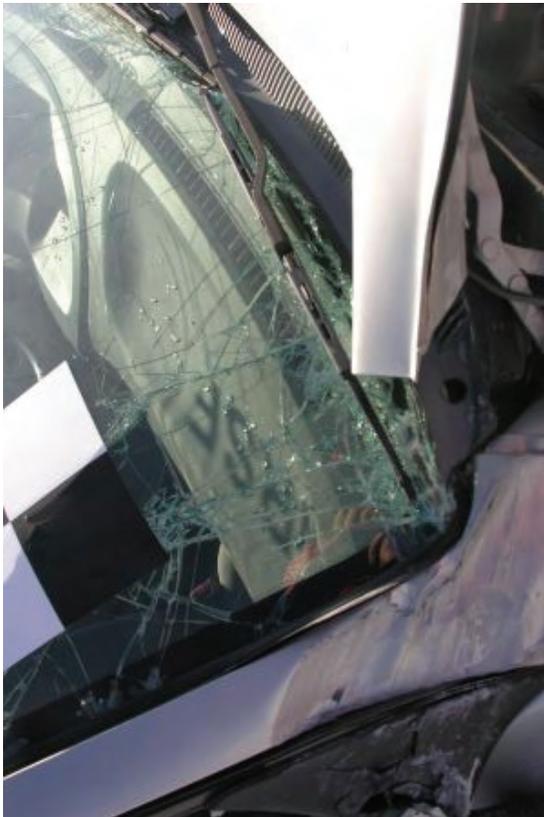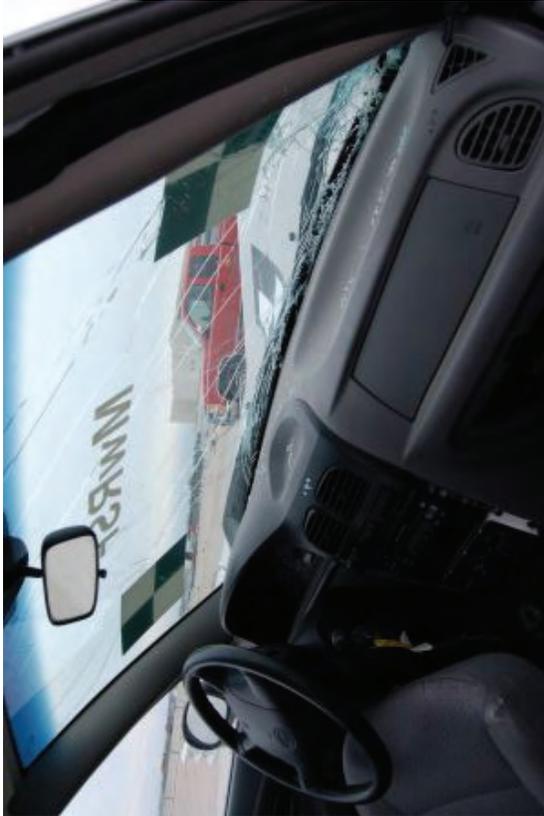
Figure 91. Occupant Compartment Deformation and Windshield Damage, Test No. MWTSP-3

13 SUMMARY, CONCLUSIONS, AND GENERAL RECOMMENDATIONS

This study set out to develop a new, simplified stiffness transition between the MGS and a previously-accepted thrie beam approach guardrail transition. The simplified stiffness transition incorporated an asymmetrical W-beam to thrie beam transition element, standard MGS and thrie beam guardrail, and standard steel W6x9 (W152x13.4) posts. The system was crash tested and evaluated using the TL-3 safety performance criteria set forth by MASH.

Multiple stiffness transition configurations were created by varying (1) the number of posts, (2) the spacings between posts, (3) the length of MGS and thrie beam guardrail, and (4) the longitudinal position of the asymmetrical W-beam to thrie beam transition element. BARRIER VII computer simulations were utilized to evaluate the different configurations under the TL-3 impact conditions found in NCHRP Report No. 350. Barrier displacement as well as the propensity for vehicle pocketing and wheel snag were evaluated and recorded for multiple impact points on each transition configuration. After comparing the BARRIER VII results, Design K was identified as the shortest stiffness transition system that limited both excessive vehicle pocketing and wheel snag. Thus, Design K was selected for evaluation through the use of a full-scale crash testing program.

Three full-scale crash tests were conducted on the simplified stiffness transition according to the TL-3 safety performance criteria presented in MASH. A summary of the safety performance evaluation for all three tests is provided in Table 16. The initial crash test, test no. MWTSP-1, was performed according to test designation no. 3-21 of MASH with a ½–ton Quad Cab pickup truck. During the test, the upstream BCT wood anchor posts failed prematurely, causing a loss of tension in the rail which allowed the vehicle to pocket excessively. As a result, the longitudinal occupant ridedown decelerations exceeded the recommended safety limits

152

established by MASH. Upon inspection, it was determined that a knot located in the critical section of the first BCT wood anchor post led to the premature post failure.

The second full-scale crash test, test no. MWTSP-2, repeated the impact scenario of test no. MWTSP-1, except that additional attention was given to the quality of the BCT wood anchor posts to ensure that they provided adequate strength. The pickup truck was safely contained and redirected with moderate damage to the barrier. There was minimal damage to the vehicle, and the test did not pose any significant risk to the occupants of the vehicle. Therefore, test no. MWTSP-2 was determined to be acceptable according to test designation no. 3-21 of MASH.

The third full-scale crash test, test no. MWTSP-3, was performed with a small car. The vehicle was safely contained and redirected with moderate damage to the barrier. The vehicle did not intrude into adjacent lanes and came to a stop adjacent to the barrier system due to moderate wheel snag on several steel posts. There was moderate damage to the vehicle, but analysis of the test data did not reveal any decelerations that would pose a significant risk to the occupants of the vehicle. Therefore, test no. MWTSP-3 was determined to be acceptable according to test designation no. 3-20 of MASH.

Upon the successful completion of the MASH TL-3 crash testing matrix, the new, simplified stiffness transition between the MGS and an accepted thrie beam approach guardrail transition was found to meet current impact safety standards. The simplified stiffness transition consists of standard steel posts and an asymmetric W-beam-to-thrie beam transition element. Since a very stiff thrie beam guardrail transition was used in the full-scale crash testing program, the upstream stiffness transition developed herein should be applicable to most other thrie beam approach guardrail transition designs. Details for attaching the approach guardrail transition to other thrie beam transition systems are presented in Chapter 14.

153

The stiffness transition to a thrie beam approach guardrail transition was 28 ft – 1½ in. (8.57 m) in length (as measured from the beginning of the series of reduced post spacings to the first bridge post) and had 43 ft – 9 in. (13.3 m) of standard MGS between the stiffness transition and the upstream BCT wood anchor post. Thus, the length of W-beam rail between the upstream end of the asymmetrical W-beam to thrie beam section and the first terminal post was 46 ft – 10½ in. (14.3 m) for Design K. For this installation length, the barrier system met the current MASH impact safety standards. Guardrail end terminals are designed, crash tested, and evaluated for use when directly attached to semi-rigid W-beam guardrail systems instead of the stiff approach guardrail transitions. However, the placement of the upstream end anchorage too close to the stiffness transition may negatively affect system performance, thus potentially resulting in excessive barrier deflections, vehicle pocketing, wheel snagging on posts, vehicle-to-barrier override, or other vehicle instabilities. Thus, the following implementation guidelines should be followed:

1. A recommended minimum length of 12 ft – 6 in. (3.8 m) for standard MGS is to be installed between the upstream end of the asymmetrical W-beam to thrie beam transition section and the interior end of an acceptable TL-3 guardrail end terminal. This segment includes one half-post spacing for Design K and three half-post spacings for Design L.

2. A recommended minimum barrier length of 46 ft – 10½ in. (13.3 m) is to be installed beyond the upstream end of the asymmetrical W-beam to thrie beam transition section, which includes standard MGS, a crashworthy guardrail end terminal, and an acceptable anchorage system. This segment includes one half-post spacing for Design K and three half-post spacings for Design L.

3. For flared guardrail applications, a minimum length of 25 ft (7.6 m) is recommended between the upstream end of the asymmetrical W-beam to thrie beam transition section and the start of the flared section (i.e. bend between flare and tangent sections). This segment includes one half-post spacing for Design K and three half-post spacings for Design L.

Recall, Design K was selected over Design L by the members of the Midwest States Pooled Fund Program and for use in the full-scale crash testing program. Design K utilizes one

less post than Design L. However, BARRIER VII analysis was conducted on all design configurations and revealed that Design L significantly reduced lateral deflections as well as the propensity for wheel snag and vehicle pocketing. For these reasons, MwRSF researchers have confidence that Design L would also perform in an acceptable manner and meet the TL-3 safety criteria. Therefore, it is our opinion that either Design K or Design L could be implemented.

As discussed previously, the MGS has been used within the design of the new, simplified stiffness transition. As such, some additional discussion is warranted regarding the potential issues arising from the use of the MGS. First, it is unknown as to whether a non-blocked version of the MGS will perform in an acceptable manner when installed adjacent to the new stiffness transition. The safety performance of the non-blocked MGS in conjunction with the new stiffness transition can only be verified through the use of full-scale crash testing. As such, it is recommended that a minimum of 25 ft (7.6 m) of standard MGS with spacer blocks be placed adjacent to the new stiffness transition prior to transitioning to other non-blocked, 31-in. (787-mm) tall, W-beam guardrail systems. Second, several design problems were identified during the development and testing of a new stiffness transition between the MGS and a thrie beam approach guardrail transition, as described herein. In addition, it would seem reasonable that similar design problems would also be identified when adapting the stiffness transition to other existing transition designs. Therefore, all approach guardrail transitions should be examined and/or evaluated to assess the risk of degraded performance for vehicular impacts occurring upstream from the current, crashworthy approach guardrail transition systems.

The new simplified stiffness transition was successfully crash tested and evaluated for use with a thrie beam approach guardrail transition where all posts were installed in level terrain. Therefore, this stiffness transition should be implemented with a minimum of 2 ft (0.61 m) of

level or gently-sloped fill placed behind the posts, unless special design provisions are made to

account for decreased post-soil resistence.

Table 16. Summary of Safety Performance Evaluation Results

Evaluation Factors	Evaluation Criteria	Test No. MWTSP-1 (2270P Test)	Test No. MWTSP-2 (2270P Test)	Test No. MWTSP-3 (1100C Test)
Structural Adequacy	A. Test article should contain and redirect the vehicle or bring the vehicle to a controlled stop; the vehicle should not penetrate, underride, or override the installation although controlled lateral deflection of the test article is acceptable.	U	S	S
	D. Detached elements, fragments or other debris from the test article should not penetrate or show potential for penetrating the occupant compartment, or present an undue hazard to other traffic, pedestrians, or personnel in a work zone. Deformations of, or intrusions into, the occupant compartment should not exceed limits set forth in Section 5.3 and Appendix E of MASH.	S	S	S
	F. The vehicle should remain upright during and after collision. The maximum roll and pitch angles are not to exceed 75 degrees.	S	S	S
Occupant Risk	H. Occupant Impact Velocity (OIV) (see Appendix A, Section A5.3 of MASH for calculation procedure) should satisfy the following limits:	S	S	S

Occupant Impact Velocity Limits

Component	Preferred	Maximum
Longitudinal and Lateral	30 ft/s (9.1 m/s)	40 ft/s (12.2 m/s)

Evaluation Factors	Evaluation Criteria	Test No. MWTSP-1 (2270P Test)	Test No. MWTSP-2 (2270P Test)	Test No. MWTSP-3 (1100C Test)
	I. The Occupant Ridedown Acceleration (ORA) (see Appendix A, Section A5.3 of MASH for calculation procedure) should satisfy the following limits:	U	S	S

Occupant Ridedown Acceleration Limits

Component	Preferred	Maximum
Longitudinal and Lateral	15.0 g's	20.49 g's

S – Satisfactory   U – Unsatisfactory   NA - Not Applicable

14 STIFFNESS TRANSITION ADAPTATION RECOMMENDATIONS

14.1 Attachment to Crashworthy, Thrie Beam, Steel Post Transition Systems

The upstream stiffness transition developed within this study was full-scale crash tested while attached to a thrie beam approach guardrail transition for Missouri's thrie beam and channel bridge rail. However, it is believed that this stiffness transition can be adapted to other steel post, thrie beam approach guardrail transitions to mitigate concerns for vehicle pocketing and vehicle instabilities. Thus, several examples of adapting the new stiffness transition to other approach guardrail transitions are provided below. It should be noted that the original approach guardrail transitions should only be used in conjunction with the bridge rail types for which they were designed, tested, or approved.

14.1.1 Missouri Transition to Thrie Beam Bridge Rail

The Missouri approach guardrail transition to thrie beam bridge rail system formed the foundation for the development of the new stiffness transition between the MGS and a thrie beam approach guardrail transition [5-7]. The original approach guardrail transition was 25 ft (7.6 m) long [10-11], while the adapted stiffness transition is configured to be 28 ft – 1½ in. (8.6 m) long, as measured from the centerline of the first post at half-post spacing to the centerline of the splice between the thrie beam and the bridge rail, as shown in Figure 92. The 12-gauge (2.66-mm thick) symmetrical W-beam to thrie beam transition piece has been replaced with a 10-gauge (3.42-mm thick) asymmetrical transition element. This change would allow for a 31-in. (787-mm) tall, MGS to be used as the approach guardrail. The two upstream 84-in. (2,134-mm) long, W6x15 (W152x22.3) steel posts at half-post spacing are replaced with four 72-in. (1,829-mm) long, W6x9 (W152x13.4) steel posts at quarter-post spacing. Also, one 72-in. (1,829-mm) long, W6x9 (W152x13.4) steel post are added to the system upstream of the asymmetrical transition element at half-post spacing.

14.1.2 Missouri Transition to Single Slope Median Barrier

The Missouri approach guardrail transition to a single slope concrete median barrier, the adapted stiffness transition, and the successfully tested stiffness transition evaluated herein, are shown in Figure 93. The original approach guardrail transition was 18 ft – 9 in. (5.7 m) long [32-33], and the adapted stiffness transition is configured to be 28 ft – 1½ in. (8.6 m) long, as measured from the centerline of the first post at half-post spacing to the centerline of the splice between the thrie beam and the bridge rail. The 12-gauge (2.66-mm thick) asymmetrical W-beam to thrie beam transition element has been replaced with a 10-gauge (3.42-mm thick) asymmetrical transition element in order to accommodate for 31-in. (787-mm) tall, MGS approach guardrail. A 75-in. (1,905-mm) long, 12-gauge (2.66-mm thick) thrie beam section and four 72-in. (1,829-mm) long, W6x9 (W152x13.4) steel posts at quarter-post spacing were added upstream from the 12-ft 6-in. (3.8-m) long thrie beam section and downstream of the asymmetrical transition element. Finally, a 72-in. (1,829-mm) long, W6x9 (W152x13.4) steel post was incorporated upstream from the asymmetrical transition at a half-post spacing.

14.1.3 Nebraska Transition to Vertical Face Concrete Parapet

The Nebraska approach guardrail transition for vertical-face concrete parapets, an adapted stiffness transition, and the successfully-tested stiffness transition, are shown in Figure 94. The original approach guardrail transition was 25 ft (7.6 m) long, as measured from the first W6x15 (W152x22.3) post to the centerline of the splice between the thrie beam and the concrete parapet [34-35], and the adapted system is configured to be 34 ft – 4½ in. (10.5 m) long, as measured from the centerline of the first post at half-post spacing to the centerline of the splice between the thrie beam and the concrete parapet. The original transition system used two 8-ft 6-in. (2.6-m) long, W6x25 (W152x37.2) steel posts and three 84-in. (2,134-mm) long, W6x15 (W152x22.3) steel posts between the approach guardrail and the thrie beam rail, followed by one

84-in. (2,134-mm) long, W6x15 (W152x22.3) steel post at full-post spacing upstream of the symmetrical w-beam to thrie beam transition element. For the adapted system, the 12-gauge (2.66-mm thick) asymmetrical W-beam to thrie beam transition element has been replaced with a 10-gauge (3.42-mm thick) asymmetrical transition element in order to accommodate the 31-in. (787-mm) tall, MGS approach guardrail. The adapted system includes another 12-ft 6-in. (3.8-m) section of 12-gauge (2.66-mm thick) thrie beam immediately downstream of the asymmetrical stiffness transition element and upstream of the nested 12-gauge (2.66-mm thick) thrie beam. The adapted system retains the two W6x25 (W152x37.2) steel posts, the two W6x15 (W152x22.3) steel posts, as well as the simulated post with tubular structure. Upstream from these posts, four 72-in. (1,829-mm) long, W6x9 (W152x13.4) steel posts are installed at a quarter-post spacing. Four 72-in. (1,829-mm) long, W6x9 (W152x13.4) steel posts at half-post spacing are placed upstream from the posts installed at quarter-post spacing. These posts are placed such that the first post at half-post spacing occurs 37½ in. (953 mm) upstream of the centerline of the splice between the MGS guardrail and the asymmetrical stiffness transition element.

14.1.4 Transition to Thrie Beam and Tube Bridge Rail

The approach guardrail transition to the thrie beam and tube bridge rail, the adapted stiffness transition, and the successfully tested stiffness transition evaluated herein, are shown in Figure 95. The original approach guardrail transition was 18 ft – 9 in. (5.7 m) long [17-20], while the adapted system is configured to be 28 ft – 1½ in. (8.6 m) long, as measured from the centerline of the first post at half-post spacing to the centerline of the splice between the thrie beam and the bridge rail. The 12-gauge (2.66-mm thick) asymmetrical W-beam to thrie beam transition element has been replaced with the 10-gauge (3.42-mm thick) asymmetrical transition element in order to accommodate the 31-in. (787-mm) tall, MGS approach guardrail. A 75-in.

160

(1,905-mm) long, 12-gauge (2.66-mm thick) thrie beam section are used between the asymmetrical stiffness transition element and the 10-gauge (3.42-mm thick) thrie beam section. Four out of the five 84-in. (2,134-mm) long, W6x15 (W152x22.3) steel posts are retained. Upstream from these four posts, four 72-in. (1,829-mm) long, W6x9 (W152x13.4) steel posts are installed at quarter-post spacing. Next. four 72-in. (1,829-mm) long, W6x9 (W152x13.4) steel posts are installed at half-post spacing, such that the first upstream post at half-post spacing is located 37½ in. (953 mm) upstream of the centerline of the splice between the MGS approach guardrail and the asymmetrical stiffness transition element.

14.1.5 Iowa Transition to New Jersey Safety Shape Concrete Parapet

The Iowa approach guardrail transition to New Jersey safety shape concrete parapet, the adapted stiffness transition, and the successfully tested stiffness transition evaluated herein, are shown in Figure 96. The original approach guardrail transition was 18 ft – 9 in. (5.7 m) long [36-39], while the adapted stiffness transition system is configured to be 28 ft – 1½ in. (8.6 m) long, as measured from the centerline of the first post at half-post spacing to the centerline of the splice between the thrie beam and the concrete parapet. The upstream 78-in. (1,981-mm) long, W6x9 (W152x13.4) steel post was removed. Four 72-in. (1,829-mm) long, W6x9 (W152x13.4) steel posts were placed at a quarter-post spacing and upstream from the 78-in. (1,981-mm) long, W6x9 (W152x13.4) steel posts. Upstream from these posts, four 72-in. (1,829-mm) long, W6x9 (W152x13.4) steel posts were placed at a half-post spacing. The first post at half-post spacing was located 37½ in. (953-mm) upstream of the centerline of the splice between the MGS and the asymmetrical stiffness transition element.

14.1.6 Adaptations to Other Thrie Beam Transitions

Although not specifically shown, the new stiffness transition described herein can be adapted to other thrie beam approach guardrail transitions. Small adjustments in rail height for

161

upstream stiffness transition may be necessary to match previously-approved approach guardrail transitions, such as those with heights of 31⅝ in. (804 mm).

14.2 Wood Post Systems

Future research will extend this project to develop an equivalent, simplified, stiffness transition using wood posts. Further bogie testing of both wooden and steel posts will provide a method for determining the required size, post length, and embedment depth for wood posts to match the force vs. deflection properties of the W6x9 (W152x13.4) and W6x15 (W152x22.3) steel posts. BARRIER VII simulations will also be utilized to illustrate that the wood-post stiffness transition will provide similar safety performance to that observed for the simplified steel post system. Upon completion of this equivalent wood post system, the State DOTs should have the option for using either steel or wood posts throughout the length of the new stiffness transition as well as in the prior crashworthy approach guardrail transition systems.
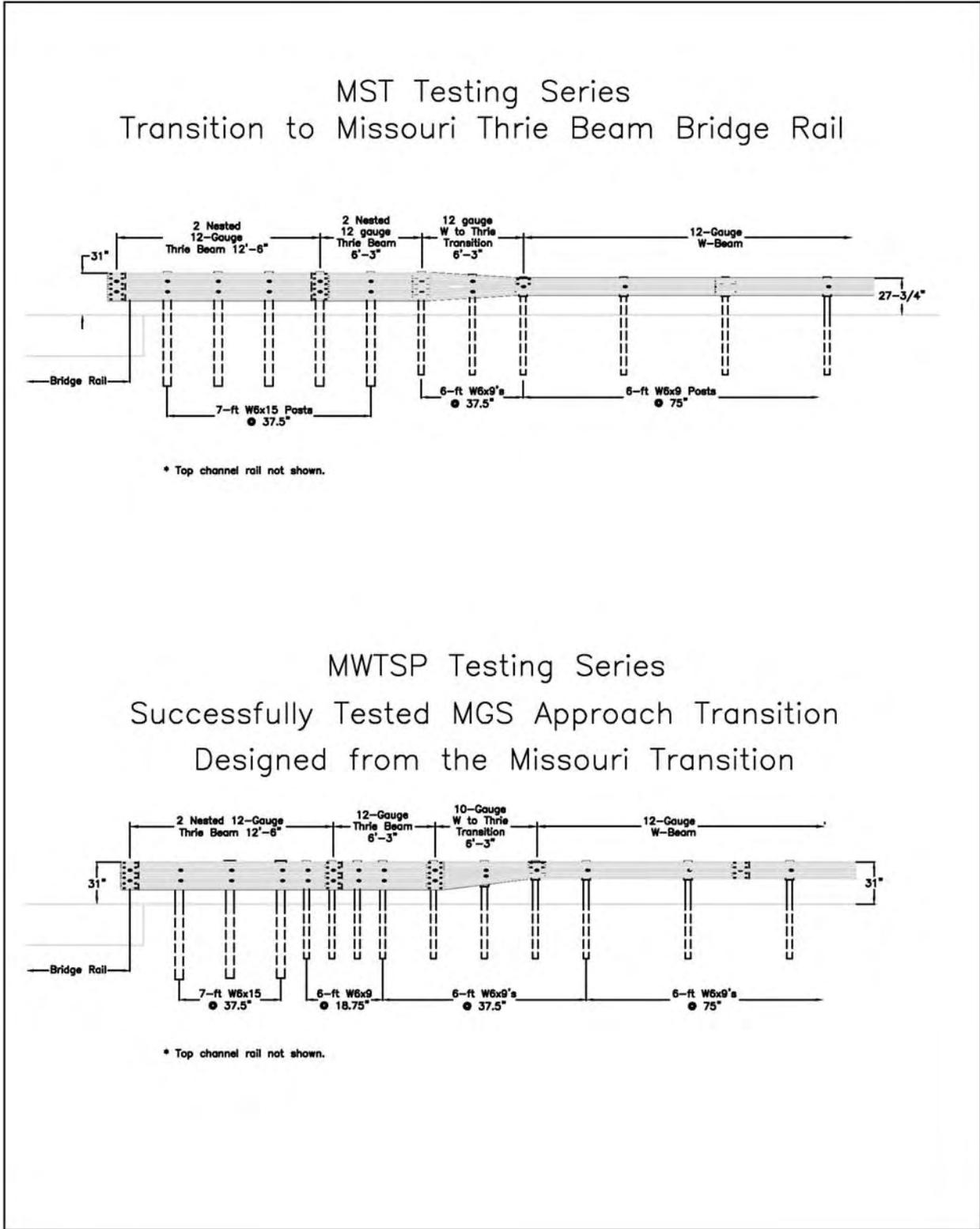
Figure 92. Attachment to Missouri Transition to Thrie Beam Bridge Rail, MST Testing Series [10-11]
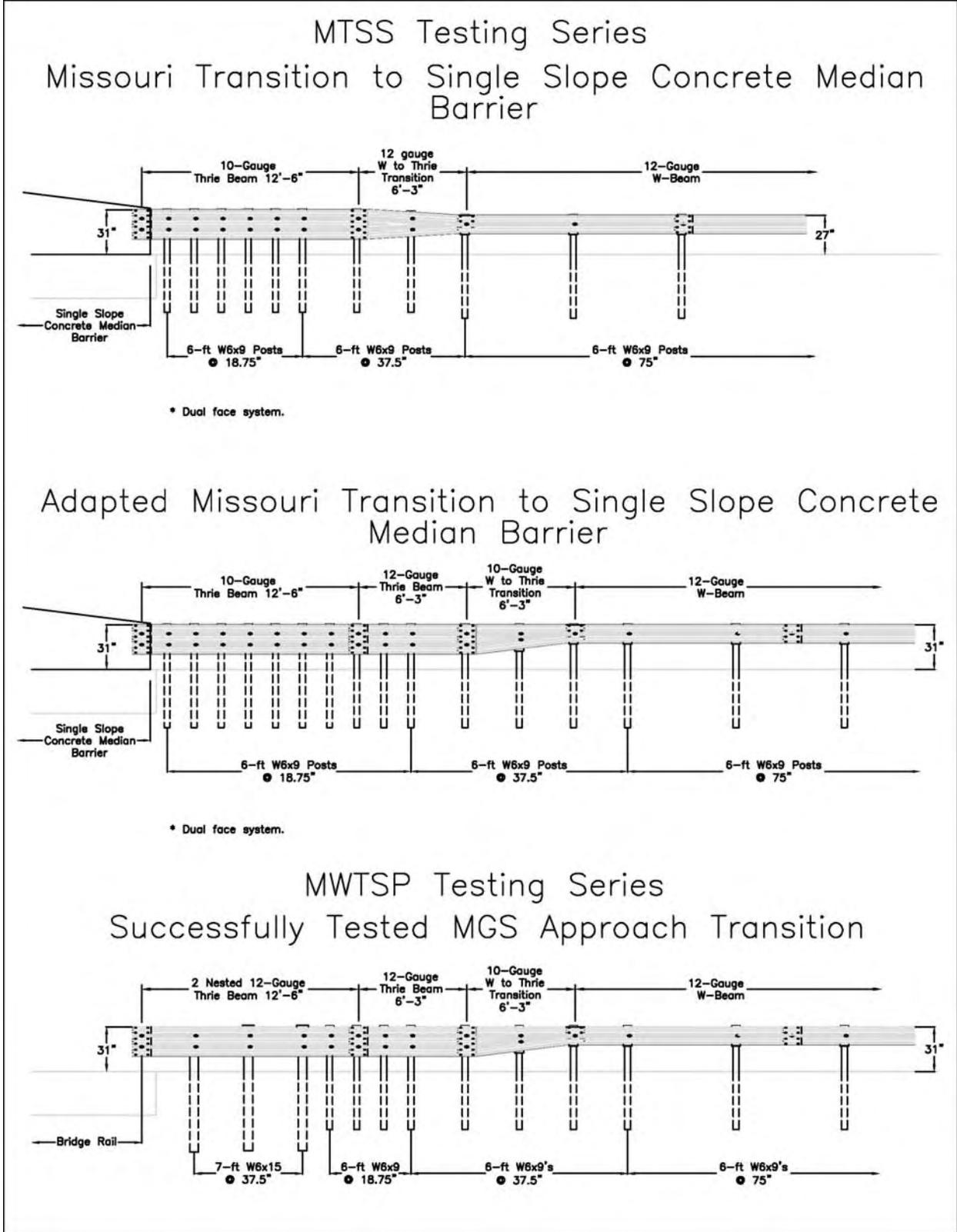
Figure 93. Attachment to Missouri Transition to Single Slope Parapet, MTSS Testing Series [32-33]
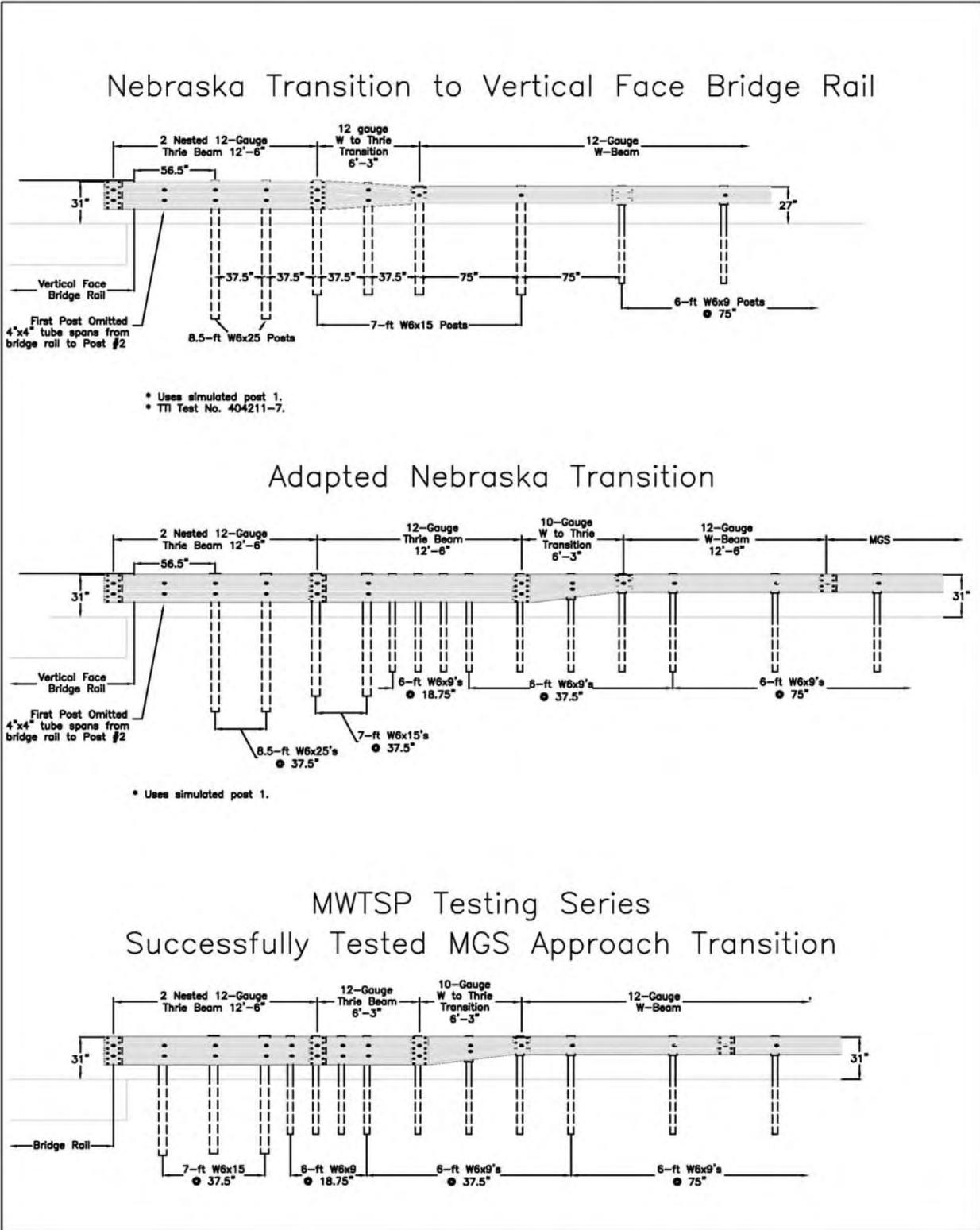
Figure 94. Attachment to Nebraska Transition to Vertical Face Concrete Parapet [34-35]
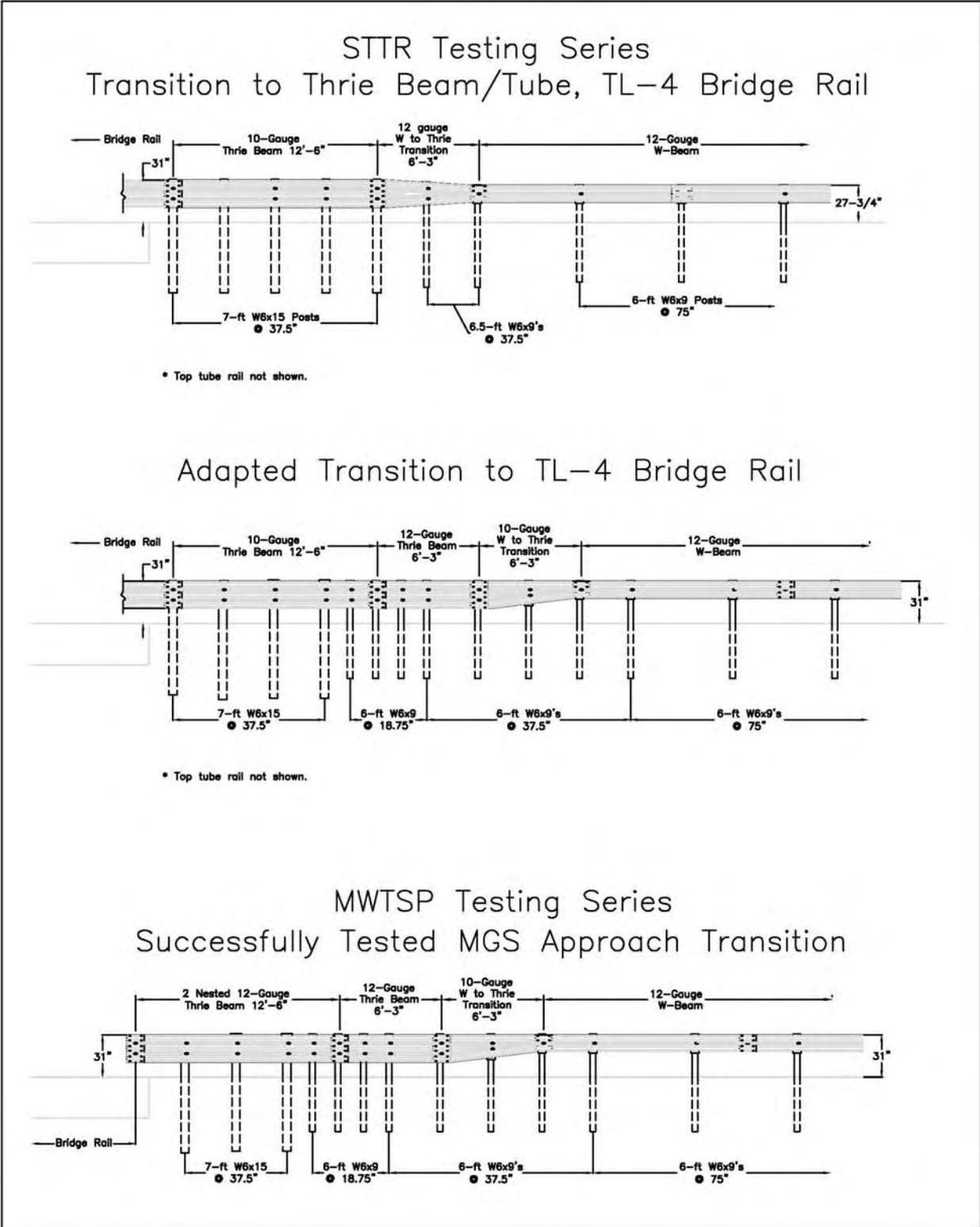
Figure 95. Attachment to Transition to Thrie Beam & Tube Bridge Rail, STTR Testing Series [17-20]

ITNJ Testing Series
Iowa Transition to NJ Shape Concrete Bridge Rail

Adapted Iowa Transition

* Embedment of 6-ft Posts = 40" (MGS)
** Embedment of 6.5-ft Posts = 49" (As Per Test No. ITNJ-2).
   As a consequence, tops of posts are 2" shorter than the thrie beam rail.
   6.5-ft posts utilize tapered tube blockouts (see Refs. 33-36 for description)
All Posts are W6x9's

MWTSP Testing Series
Successfully Tested MGS Approach Transition

Figure 96. Attachment to Iowa Transition to NJ Shape Concrete Parapet, ITNJ Testing Series [36-39]

15 REFERENCES

1. Bryden, J.E. and Phillips, R.G., *Performance of a Thrie Beam Steel-Post Bridge-Rail System*, Report No. FHWA/NY/RR-85/118, Submitted to the Office of Research, Development, and Technology, Federal Highway Administration, Performed by New York State Department of Transportation, February 1985.

2. Bryden, J.E. and Phillips, R.G., *Performance of a Thrie Beam Steel-Post Bridge-Rail System*, Transportation Research Record No. 1024, Transportation Research Board, Washington, D.C., 1985.

3. Mak, K.K. and Menges, W.L., *Testing and Evaluation of the W-beam Transition (on Steel Posts with Timber Blockouts) to the Vertical Flared-Back Concrete Bridge Parapet*, Turner-Fairbank Highway Research Center, Texas Transportation Institute, 1997.

4. Polivka, K.A., Faller, R.K., Sicking, D.L., Reid, J.D., Rohde, J.R., and Holloway, J.C., *Crash Testing of Missouri's W-Beam to Thrie beam Transition Element*, Final Report to the Midwest States Regional Pooled Fund Program, Transportation Research Report No. TRP-03-94-00, Project No. SPR-3(017)-Year 9, Midwest Roadside Safety Facility, University of Nebraska-Lincoln, Lincoln, NE, September 12, 2000.

5. Polivka, K.A., Eller, C.M., Faller, R.K., Sicking, D.S., Rohde, J.R., Reid, J.D., Bielenberg, B.W., Allison, E.M., *Development of the Midwest Guardrail System (MGS) W-Beam to Thrie Beam Transition Element*, Final Report to the Midwest States Regional Pooled Fund Program, Transportation Research Report No. TRP-03-167-07, Project No. SPR-3(017)-Year 16, Midwest Roadside Safety Facility, University of Nebraska-Lincoln, Lincoln, NE, November 26, 2007.

6. Polivka, K.A., Coon, B.A., Sicking, D.L., Faller, R.K., Bielenberg, R.W., Rohde, J.R., and Reid, J.D., *Midwest Guardrail System (MGS) W-Beam to Thrie Beam Transition*, Transportation Research Record No. 2025, Transportation Research Board, Washington, D.C., August 31, 2007, pp 45-50.

7. Nicol, D.A., *FHWA NCHRP Report No. 350 Approval Letter B-187 of the Transition from MGS to Asymmetrical Thrie Beam*, To R. K. Faller, Midwest Roadside Safety Facility, February 13, 2009.

8. Ross, H.E., Sicking, D.L., Zimmer, R.A., and Michie, J.D., *Recommended Procedures for the Safety Performance Evaluation of Highway Features*, National Cooperative Highway Research Program (NCHRP) Report No. 350, Transportation Research Board, Washington, D.C., 1993.

9. *Manual for Assessing Safety Hardware,* American Association of State Highway and Transportation Officials (AASHTO), Washington, D.C., 2009.

10. Polivka, K.A., Faller, R.K., Reid, J.D., Sicking, D.L., Rohde, J.R., and Keller, E.A., and Holloway, J.C., *Development of an Approach Guardrail Transition Attached to a Thrie Beam and Channel Bridge Railing*, Transportation Report No. TRP-03-91-99, Midwest Roadside Safety Facility, University of Nebraska-Lincoln, March 21, 2000.

11. Horne, D.A., *FHWA NCHRP Report No. 350 Approval Letter of the W-Beam Transition to Thrie Beam and Channel*, To R. K. Faller, Midwest Roadside Safety Facility, June 4, 1999.

12. Michie, J.D., *Recommended Procedures for the Safety Performance Evaluation of Highway Appurtenances*, National Cooperative Highway Research Program (NCHRP) Report No. 230, Transportation Research Board, Washington, D.C., March 1981.

13. *Standard Specifications for Transportation Materials and Methods of Sampling and Testing*, Seventeenth Edition, Part I Specifications, American Association of State Highway and Transportation Officials (AASHTO), Washington, D.C., 1995.

14. Speer, D., Peter, R., Jewell, J., Clark, N., *Vehicular Crash Tests of a Nested Thrie Beam Transition Barrier*, Report No. FHWA/CA/TL-2001/09, Materials Engineering and Testing Services, California Department of Transportation, Sacramento, CA, May, 2002.

15. Society of Automotive Engineers (SAE), *Instrumentation for Impact Test - Part I – Electronic Instrumentation – SAE J211/1 MAR95*, New York City, NY, 1999.

16. Powell, G.H., *Barrier VII: A Computer Program For Evaluation of Automobile Barrier Systems*, Prepared for: Federal Highway Administration, Report No. FHWA RD-73-51, April 1973.

17. Polivka, K.A., Faller, R.K., Rosson, B.T., Ritter, M.A., Fowler, M.D., and Keller, E.A., *Two Test Level 4 Bridge Railing and Transition Systems for Transverse Glue-Laminated Timber Decks*, Transportation Research No. TRP-03-71-01, Midwest Roadside Safety Facility, University of Nebraska - Lincoln, January 30, 2002.

18. Faller, R.K., Ritter, M.A., Rosson, B.T., Fowler, M.D., and Duwadi, S.R., *Two Test Level 4 Bridge Railing and Transition Systems for Transverse Timber Deck Bridges*, Transportation Research Record No. 1696, Transportation Research Board, Washington, D.C., 2000, pp 334-351.

19. Fowler, M.D., *Design and Testing of a Test Level 4 Bridge Railing for Transverse Glulam Timber Deck Bridges*, M.S. Thesis, University of Nebraska-Lincoln, May 1997.

20. Baxter, J.R., *FHWA NCHRP Report No. 350 Approval Letter B-138 of TL-2 and TL-4 Railings and Transitions for Timber Bridge Decks*, To R. K. Faller, Midwest Roadside Safety Facility, August 4, 2005.

21.   Dey, G., Faller, R.K., Hascall, J.A., Bielenberg, R.W., Polivka, K.A., and Molacek, K., *Dynamic Impact Testing of W152x13.4 (W6x9) Steel Posts on a 2:1 Slope,* Final Report to the Midwest States Regional Pooled Regional Pooled Fund Program, Transportation Research Report No. TRP-03-165-07, Midwest Roadside Safety Facility, University of Nebraska - Lincoln, March 23, 2007.

22.   Kuipers, B.D. and Reid, J.D., *Testing of W152x23.8 (W6x16) Steel Posts - Soil Embedment Depth Study for the Midwest Guardrail System (Non-Proprietary Guardrail System)*, Final Report to the Midwest States Regional Pooled Fund Program, Transportation Research Report No. TRP-03-136-03, Midwest Roadside Safety Facility, University of Nebraska - Lincoln, June 12, 2003.

23.   Polivka, K.A., Faller, R.K., Sicking, D.L., Reid, J.D., Rohde, J.R., Holloway, J.C., Bielenberg, R.W., Kuipers, B.D., *Development of the Midwest Guardrail System (MGS) for Standard and Reduced Post Spacing and in Combination with Curbs*, Final Report to the Midwest States Regional Pooled Fund Program, Transportation Research Report No. TRP-03-139-04, Midwest Roadside Safety Facility, University of Nebraska - Lincoln, September 2004.

24.   Polivka, K.A., Faller, R.K., Sicking, D.L., Rohde, J.R., Bielenberg, R.W., Reid, J.D., *Performance Evaluation of the Midwest Guardrail System – Update to NCHRP 350 Test No. 3-11 with 28" C.G. Height (2214MG-2)*, Transportation Research Report No. TRP-03-171-06, Midwest Roadside Safety Facility, University of Nebraska - Lincoln, October 11, 2006.

25.   Reid, J.D., Sicking, D.L., and Bligh, R., *Critical Impact Point for Longitudinal Barriers*, Journal of Transportation Engineering, Vol. 124, No. 1, January / February 1998.

26.   Hinch, J., Yang, T.L., and Owings, R., *Guidance Systems for Vehicle Testing,* ENSCO, Inc., Springfield, VA, 1986.

27.   *Center of Gravity Test Code - SAE J874 March 1981,* SAE Handbook Vol. 4, Society of Automotive Engineers, Inc., Warrendale, Pennsylvania, 1986.

28.   *Vehicle Damage Scale for Traffic Investigators*, Second Edition, Technical Bulletin No. 1, Traffic Accident Data (TAD) Project, National Safety Council, Chicago, Illinois, 1971.

29.   *Collision Deformation Classification – Recommended Practice J224 March 1980*, Handbook Volume 4, Society of Automotive Engineers (SAE), Warrendale, Pennsylvania, 1985.

30.   Stolle, C.S., Polivka, K.A., Faller, R.K., Sicking, D.L., Rohde, J.R., Bielenberg, R.W., Reid, J.D., *Evaluation of the Critical Flare Rates for the Midwest Guardrail System (MGS)*, Transportation Research Report No. TRP-03-191-08, Midwest Roadside Safety Facility, University of Nebraska - Lincoln, July 2008.

31.   Bielenberg, R.W., Faller, R.K., Sicking, D.L., Rohde, J.R., Reid, J.D., Holloway, J.C., Allison, E.A., Polivka, K.,A., *Midwest Guardrail System for Long-Span Culvert Applications*, Transportation Research Report No. TRP-03-187-07, Midwest Roadside Safety Facility, University of Nebraska - Lincoln, November, 2007.

32.   Soyland, K., Faller, R.K., Sicking, D.L., and Holloway, J.C., *Development and Testing of an Approach Guardrail Transition to a Single Slope Concrete Median Barrier*, Final Report to the Missouri Highway and Transportation Department, Project SPR‑3(017), Transportation Report No. TRP‑03‑47‑95, Midwest Roadside Safety Facility, University of Nebraska ‑ Lincoln, November 1995.

33.   Faller, R.K., Soyland, K., and Sicking, D.L., *Approach Guardrail Transition for Single Slope Concrete Barriers*, Transportation Research Record No. 1528, Transportation Research Board, Washington, D.C., September 1996, pp 97-108.

34.   Jacoby, C.H., *FHWA NCHRP Report No. 350 Approval Letter B-105 of Nebraska Thrie Beam Transition*, To P. TenHulzen, Nebraska Department of Roads, September 5, 2002.

35.   Menges, W.L., Williams, W.F., Buth, C.E., and Schoeneman, S.K., *NCHRP Report 350 Test 3-21 of the Nebraska Thrie Beam Transition*, Texas Transportation Institute, Texas A&M University, College Station, Texas, May 2000.

36.   Faller, R.K., Reid, J.D., Rohde, J.R., Sicking, D.L., and Keller, E.A., *Two Approach Guardrail Transitions for Concrete Safety Shape Barriers*, Final Report to the Midwest States Regional Pooled Fund Program, Transportation Research Report No. TRP‑03‑69‑98, Project No. SPR‑3(017)‑Year 6, Midwest Roadside Safety Facility, University of Nebraska ‑ Lincoln, May 15, 1998.

37.   Faller, R.K., Reid, J.D., and Rohde, J.R., *Approach Guardrail Transition for Concrete Safety Shape Barriers*, Transportation Research Record No. 1647, Transportation Research Board, Washington, D.C., November 1998, pp 111-121.

38.   Horne, D.A., *FHWA NCHRP Report No. 350 Approval Letter B-47 of Steel Post and Wood Post Thrie Beam Transitions to Concrete Parapets*, To R. K. Faller, Midwest Roadside Safety Facility, March 6, 1998.

39.   Horne, D.A., *FHWA NCHRP Report No. 350 Approval Letter B-47A of Conditional Acceptance of Steel Post and Wood Post Thrie Beam Transitions to Vertical Wall*, To D. L. Sicking, Midwest Roadside Safety Facility, May 28, 1999.

16 APPENDICES

Appendix A. Bogie Test Results

The results of the recorded data from each transducer and both dynamic bogie tests are provided in the summary sheets found in this appendix. Summary sheets include acceleration, velocity, and displacement versus time plots as well as force and energy versus displacement plots.

MIDWEST ROADSIDE SAFETY FACILITY

Bogie Test Summary

Test Information — Bogie-Post Test

Test Number:	MGSATB-1
Test Date:	4-Oct-2007
Failure Type:	Rotation Through Soil

Post Properties

Post Type:	Steel	
Post Size:	W6x15	W152x22.3
Post Length:	84 in.	213.4 cm
Embedment Depth:	54 in.	137.2 cm
Orientation:	Strong Axis	

Soil Properties

Gradation:	350 Strong Soil
Moisture Content:	NA
Compaction Method:	nuematic tamper
Soil Density, γd:	NA

Bogie Properties

Impact Velocity:	19.22 mph (28.2 fps)	8.59 m/s
Impact Height:	24.875 in.	63.2 cm
Bogie Mass:	1810 lbs	821 kg

Data Acquired

Acceleration Data:	EDR-3
Camera Data:	AOS-1 Perpendicular - 17'

Test Results Summary

Max. Deflection:	19.5 in.
Peak Force:	20.1 k
Initial Linear Stiffness:	10.0 k/in.
Total Energy:	268.5 k-in.

Figure A-1. Results of Test No. MGSATB-1 (EDR-3)

MIDWEST ROADSIDE SAFETY FACILITY

Bogie Test Summary

Test Information	Bogie-Post Test
Test Number:	MGSATB-1
Test Date:	4-Oct-2007
Failure Type:	Rotation Through Soil

Post Properties		
Post Type:	Steel	
Post Size:	W6x15	W152x22.3
Post Length:	84 in.	213.4 cm
Embedment Depth:	54 in.	137.2 cm
Orientation:	Strong Axis	

Soil Properties	
Gradation:	350 Strong Soil
Moisture Content:	NA
Compaction Method:	nuematic tamper
Soil Density, γd:	NA

Bogie Properties		
Impact Velocity:	19.22 mph (28.2 fps)	8.59 m/s
Impact Height:	24.875 in.	63.2 cm
Bogie Mass:	1810 lbs	821 kg

Data Acquired	
Acceleration Data:	EDR-4 M6
Camera Data:	AOS-1 Perpendicular - 17'

Test Results Summary	
Max. Deflection:	22.6 in.
Peak Force:	17.1 k
Initial Linear Stiffness:	8.7 k/in.
Total Energy:	267.9 k-in.

Figure A-2. Results of Test No. MGSATB-1 (EDR-4)

MIDWEST ROADSIDE SAFETY FACILITY

Bogie Test Summary

Test Information	Bogie - Post		Test Results Summary	
Test Number:	MGSATB-1		Max. Deflection:	20.0 in.
Test Date:	4-Oct-2009		Peak Force:	19.7 k
Failure Type:	Rotation Through Soil		Initial Linear Stiffness:	10.3 k/in.
			Total Energy:	268.0 k-in.

Post Properties

Post Type:	Steel	
Post Size:	W6x15	W152x22.3
Post Length:	84 in.	213.4 cm
Embedment Depth:	54 in.	137.2 cm
Orientation:	Strong Axis - Centered On Post	

Soil Properties

Gradation:	350 Strong Soil
Moisture Content:	NA
Compaction Method:	pneumatic tamper
Soil Density, γd:	NA

Bogie Properties

Impact Velocity:	19.22 mph (28.2 fps)	8.59 m/s
Impact Height:	24.875 in.	63.2 cm
Bogie Mass:	1810 lbs	821 kg

Data Acquired

Acceleration Data:	DTS
Camera Data:	AOS-1 Perpendicular - 17'

Figure A-3. Results of Test No. MGSATB-1 (DTS)

MIDWEST ROADSIDE SAFETY FACILITY

Bogie Test Summary

Test Information   Bogie-Post Test

Test Number:	MGSATB-2
Test Date:	4-Oct-2007
Failure Type:	Rotation Through Soil

Test Results Summary

Max. Deflection:	19.3 in.
Peak Force:	19.9 k
Initial Linear Stiffness:	9.4 k/in.
Total Energy:	282.8 k-in.

Post Properties

Post Type:	Steel	
Post Size:	W6x15	W152x22.3
Post Length:	84 in.	213.4 cm
Embedment Depth:	54 in.	137.2 cm
Orientation:	Strong Axis	

Soil Properties

Gradation:	350 Strong Soil
Moisture Content:	NA
Compaction Method:	nuematic tamper
Soil Density, γd:	NA

Bogie Properties

Impact Velocity:	19.71 mph (28.9 fps)	8.81 m/s
Impact Height:	24.875 in.	63.2 cm
Bogie Mass:	1810 lbs	821 kg

Data Acquired

| Acceleration Data: | EDR-3 |
| Camera Data: | AOS-1 Perpendicular - 17' |

Figure A-4. Results of Test No. MGSATB-2 (EDR-3)

MIDWEST ROADSIDE SAFETY FACILITY

Bogie Test Summary

Test Information — Bogie-Post Test

Test Number:	MGSATB-2
Test Date:	4-Oct-2007
Failure Type:	Rotation Through Soil

Post Properties

Post Type:	Steel	
Post Size:	W6x15	W152x22.3
Post Length:	84 in.	213.4 cm
Embedment Depth:	54 in.	137.2 cm
Orientation:	Strong Axis	

Soil Properties

Gradation:	350 Strong Soil
Moisture Content:	NA
Compaction Method:	nuematic tamper
Soil Density, γd:	NA

Bogie Properties

Impact Velocity:	19.71 mph (28.9 fps)	8.81 m/s
Impact Height:	24.875 in.	63.2 cm
Bogie Mass:	1810 lbs	821 kg

Data Acquired

Acceleration Data:	EDR-4 M6
Camera Data:	AOS-1 Perpendicular - 17'

Test Results Summary

Max. Deflection:	21.5 in.
Peak Force:	17.4 k
Initial Linear Stiffness:	8.7 k/in.
Total Energy:	282.1 k-in.

Figure A-5. Results of Test No. MGSATB-2 (EDR-4)

MIDWEST ROADSIDE SAFETY FACILITY

Bogie Test Summary

Test Information	Bogie - Post		Test Results Summary	
Test Number:	MGSATB-2		Max. Deflection:	19.3 in.
Test Date:	4-Oct-2009		Peak Force:	19.7 k
Failure Type:	Rotation Through Soil		Initial Linear Stiffness:	10.9 k/in.
			Total Energy:	282.1 k-in.

Post Properties

Post Type:	Steel	
Post Size:	W6x15	W152x22.3
Post Length:	84 in.	213.4 cm
Embedment Depth:	54 in.	137.2 cm
Orientation:	Strong Axis - Centered On Post	

Soil Properties

Gradation:	350 Strong Soil
Moisture Content:	NA
Compaction Method:	pneumatic tamper
Soil Density, γd:	NA

Bogie Properties

Impact Velocity:	19.71 mph (28.9 fps)	8.81 m/s
Impact Height:	24.875 in.	63.2 cm
Bogie Mass:	1810 lbs	821 kg

Data Acquired

Acceleration Data:	DTS
Camera Data:	AOS-1 Perpendicular - 17'

Figure A-6. Results of Test No. MGSATB-2 (DTS)

Appendix B.   BARRIER VII Computer Model Design Configurations

An example BARRIER VII input data file (for Design Configuration D) is shown on the following pages. The BARRIER VII input files for the remaining designs were similar with the only differences being the locations of posts and rail elements. The input file is followed by a layout drawing for each of the seven design configurations analyzed using BARRIER VII.

Example Input file for Design Configuration D

```
MGST (12 gauge W-Beam to Thrie Beam Transition) - MGST-D.b7
165     2       1       195     19      2       0
0.0001  0.0001  0.750   3000    0       1.0     1
10      10      50      10      500     10
1       0.00    0.0     0.0
165     1537.50 0.0     0.0
1       165     163     1
1       165     0.45

165 164 163 162 161 160 159 158 157 156
155 154 153 152 151 150 149 148 147 146
145 144 143 142 141 140 139 138 137 136
135 134 133 132 131 130 129 128 127 126
125 124 123 122 121 120 119 118 117 116
115 114 113 112 111 110 109 108 107 106
105 104 103 102 101 100  99  98  97  96
 95  94  93  92  91  90  89  88  87  86
 85  84  83  82  81  80  79  78  77  76
 75  74  73  72  71  70  69  68  67  66
 65  64  63  62  61  60  59  58  57  56
 55  54  53  52  51  50  49  48  47  46
 45  44  43  42  41  40  39  38  37  36
 35  34  33  32  31  30  29  28  27  26
 25  24  23  22  21  20  19  18  17  16
 15  14  13  12  11  10   9   8   7   6
  5   4   3   2   1
100  11

1    2.29   1.99  9.375  30000.0   6.92   99.5   68.5  0.05  12-GAUGE W-BEAM
2    3.114  2.650 9.375  30000.0   9.216  132.5  91.25 0.05  10-GAUGE W TO THRIE BEAM
3    3.341  2.830 9.375  30000.0   9.847  141.5  97.75 0.05  10-GAUGE W TO THRIE BEAM
4    3.569  3.010 9.375  30000.0  10.478  150.5  104.25 0.05  10-GAUGE W TO THRIE BEAM
5    3.796  3.190 9.375  30000.0  11.109  159.5  110.75 0.05  10-GAUGE W TO THRIE BEAM
6    4.024  3.370 9.375  30000.0  11.741  168.5  117.25 0.05  10-GAUGE W TO THRIE BEAM
7    4.251  3.550 9.375  30000.0  12.372  177.5  123.75 0.05  10-GAUGE W TO THRIE BEAM
8    4.479  3.730 9.375  30000.0  13.003  186.5  130.25 0.05  10-GAUGE W TO THRIE BEAM
9    4.706  3.910 9.375  30000.0  13.634  195.5  136.75 0.05  10-GAUGE W TO THRIE BEAM
10   3.76   3.10  9.375  30000.0  10.81   155.0  109.5  0.05  12-GAUGE THRIE BEAM
11   7.52   6.20  9.375  30000.0  21.62   310.0  219.0  0.05  12-GAUGE NESTED THRIE
300  5
1    24.875 0.00  6.0    6.0      100.0   675.0  675.0  0.05
```

```
100.0    100.0    15.0    15.0    15.0    100.0                    Simulated Strong Anchor Post
2   24.875   50.0   0.00   15.0    3.0     3.0    150.0   225.00 0.05
         50.0    50.0    15.0    15.0            100.0             Second BCT Post
3   24.875   15.0   0.0    16.0    3.00    2.60    92.88   143.65 0.05
          6.0    16.0    16.0     3.0             54.0             W6x9 by 6-ft Long (40.125" Embedment Depth)
4   24.875   15.0   0.0    18.0    3.40    9.00   105.0    171.00 0.05
         15.0    35.0    18.0    18.0            105.0             W6x15 by 7-ft Long (54" Embedment Depth)
5   24.875   35.0   0.0            129.0   200.0  612.5    362.90 804.60 0.05
         20.0    45.0     4.0     4.0                               W6x20 STEEL BRIDGE POST
1      1     2            4.0     4.0     0.0    0.0    0.0    0.0
93    93    94    92    101     0.0     0.0    0.0    0.0    0.0
94    94    95           102     0.0     0.0    0.0    0.0    0.0
95    95    96           103     0.0     0.0    0.0    0.0    0.0
96    96    97           104     0.0     0.0    0.0    0.0    0.0
97    97    98           105     0.0     0.0    0.0    0.0    0.0
98    98    99           106     0.0     0.0    0.0    0.0    0.0
99    99   100           107     0.0     0.0    0.0    0.0    0.0
100  100   101           108     0.0     0.0    0.0    0.0    0.0
101  101   112   116     109     0.0     0.0    0.0    0.0    0.0
117  117   118   132     110     0.0     0.0    0.0    0.0    0.0
133  133   134   164     110     0.0     0.0    0.0    0.0    0.0
165    1           301     6      4      0      0.0    0.0    0.0
166    9           302
167   17           303   174      8
175   81           303   181      4
182  109           303   187      2
188  121           304   190      4
191  133           305   195      8
4409.25  47400.0    6      20      4      0
1   0.055    0.12    6     6.00    17.0     1
2   0.057    0.15    7     7.00    18.0
3   0.062    0.18   10    10.00    12.0
4   0.110    0.35   12    12.00     6.0
5   0.35     0.45    6     6.00     5.0
6   1.45     1.50   15    15.00     1.0
1   90.0    13.25    1     1       12.0     1     0     0     0
2   90.0    25.25    1     1       12.0     1     0     0     0
3   90.0    37.25    2     2       12.0     1     0     0     0
4   78.0    37.25    2     2       12.0     1     0     0     0
5   66.0    37.25    2     2       12.0     1     0     0     0
6   54.0    37.25    2     2       12.0     1     0     0     0
```

182

7	42.0	37.25	2	12.0	1	0	0	0	
8	30.0	37.25	2	12.0	1	0	0	0	
9	18.0	37.25	2	12.0	1	0	0	0	
10	6.0	37.25	2	12.0	1	0	0	0	
11	-28.0	37.25	3	12.0	1	0	0	0	
12	-48.0	37.25	3	12.0	1	0	0	0	
13	-68.0	37.25	3	12.0	1	0	0	0	
14	-88.0	37.25	3	12.0	1	0	0	0	
15	-108.0	37.25	3	12.0	1	0	0	0	
16	-128.0	37.25	4	12.0	1	0	0	0	
17	-128.0	-37.25	4	12.0	0	0	0	0	
18	90.0	-37.25	1	12.0	0	0	0	0	
19	55.0	36.125	5	1.0	1	0	0	0	
20	-76.5	36.125	6	1.0	1	0	0	0	
1	55.0	31.375		0.0	639.3				
2	55.0	-31.375		0.0	639.3				
3	-75.5	31.375		0.0	463.0				
4	-75.5	-31.375		0.0	463.0				
1	0.00	0.00		25.0	62.14	0.0	0.0	1.0	
3	675.00	0.0							

Figure B-1. Layout Drawing of Design Configuration MGST-D

Figure B-1. Layout Drawing of Design Configuration MGST-D (Continued)

Figure B-2. Layout Drawing of Design Configuration MGST-F

Figure B-2. Layout Drawing of Design Configuration MGST-F (Continued)

MGST-G

| Actual Post Type | BCT Post 1 | BCT Post 2 | V6x9 6-ft (40.125") | V6x9 6-ft (40.125") | V6x9 6-ft (40.125") | V6x9 6-ft (40.125") | V6x9 6-ft (40.125") | V6x9 6-ft (40.125") | V6x9 6-ft (40.125") | V6x9 6-ft (40.125") |

Post Member Type: 1, 2, 3, 3, 3, 3, 3, 3, 3, 3

Post Member Numbers: 65, 66, 67, 68, 69, 70, 71, 72, 73, 74

Actual Post Numbers: 1, 2, 3, 4, 5, 6, 7, 8, 9, 10

Beam Member Numbers

Beam Member Type

Node Numbers
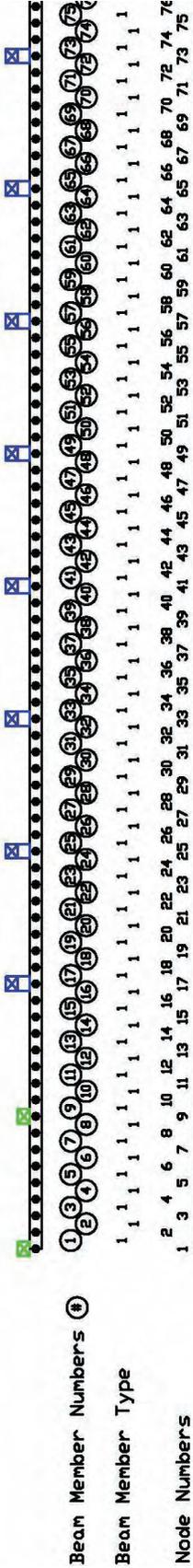
Post Location (in.): 0, 75, 150, 225, 300, 375, 450, 525, 600, 675

IMPACT @ 600

12-Gauge W-Beam 25'

12-Gauge W-Beam 25'

Figure B-3. Layout Drawing of Design Configuration MGST-G

188

Figure B-3. Layout Drawing of Design Configuration MGST-G (Continued)

189

Figure B-4. Layout Drawing of Design Configuration MGST-H

Figure B-4. Layout Drawing of Design Configuration MGST-H (Continued)

Figure B-5. Layout Drawing of Design Configuration MGST-J

Figure B-5. Layout Drawing of Design Configuration MGST-J (Continued)

Figure B-6. Layout Drawing of Design Configuration MGST-K

194

Figure B-6. Layout Drawing of Design Configuration MGST-K (Continued)

Figure B-7. Layout Drawing of Design Configuration MGST-L

Figure B-7. Layout Drawing of Design Configuration MGST-L (Continued)

Appendix C. BARRIER VII Simulation Results for Design Configurations D – L

Table C-1. BARRIER VII Results for Design Configuration D

Impact At Node (No.)	Impact Distance Upstream of Bridge Post (in.)	Maximum Pocket Angle (deg.)	@ Node	Maximum Force (kips)	@ Node	Maximum Deflection (in.)	@ Node	Worst Case Snag Points on Posts Post #	Snag (in.)	Post #	Snag (in.)	Post #	Snag (in.)	Vehicle Parallel Time (sec)
49	787.500	26.1	81	54.61	56	47.87	68	-	-	-	-	-	-	0.386
50	778.125	28.5	81	55.60	53	48.08	69	-	-	-	-	-	-	0.386
51	768.750	29.8	81	54.86	57	48.22	70	-	-	-	-	-	-	0.387
52	759.375	29.6	81	54.08	59	49.08	72	-	-	-	-	-	-	0.391
53	750.000	29.5	85	54.38	60	49.45	72	-	-	-	-	-	-	0.395
54	740.625	31.2	85	54.10	54	49.76	73	-	-	-	-	-	-	0.401
55	731.250	31.1	85	53.98	49	49.46	74	-	-	-	-	-	-	0.402
56	721.875	30.2	85	53.85	61	48.48	75	-	-	-	-	-	-	0.397
57	712.500	30.2	89	57.79	62	48.05	75	-	-	-	-	-	-	0.399
58	703.125	28.8	85	59.78	57	45.65	76	-	-	-	-	-	-	0.381
59	693.750	29.3	89	58.70	57	45.71	77	-	-	-	-	-	-	0.381
60	684.375	31.3	89	58.61	57	46.33	78	-	-	-	-	-	-	0.389
61	675.000	30.8	89	58.54	57	46.42	80	-	-	-	-	-	-	0.396
62	665.625	29.0	89	57.73	68	46.50	80	-	-	-	-	-	-	0.401
63	656.250	26.3	93	59.40	57	46.14	81	-	-	-	-	-	-	0.404
64	646.875	25.6	93	59.59	65	44.27	82	-	-	-	-	-	-	0.399
65	637.500	24.8	89	62.03	65	42.56	82	-	-	-	-	-	-	0.392
66	628.125	24.7	93	60.19	65	42.49	83	-	-	-	-	-	-	0.390
67	618.750	24.8	93	60.46	65	42.70	84	-	-	-	-	-	-	0.394
68	609.375	23.6	91	61.59	65	43.18	85	-	-	-	-	-	-	0.402
69	600.000	23.7	97	61.35	65	43.46	86	-	-	-	-	-	-	0.409
70	590.625	24.0	97	60.49	65	43.03	87	16	0.06	-	-	-	-	0.409
71	581.250	23.1	97	59.36	65	41.22	88	16	1.21	-	-	-	-	0.402
72	571.875	21.6	97	62.43	73	38.73	88	-	-	-	-	-	-	0.391
73	562.500	22.2	97	64.14	81	39.04	89	-	-	-	-	-	-	0.395
74	553.125	22.0	97	67.59	85	39.10	90	-	-	-	-	-	-	0.395
75	543.750	21.5	89	66.65	87	39.30	91	-	-	-	-	-	-	0.396
76	534.375	21.6	101	66.97	90	39.62	93	-	-	-	-	-	-	0.396
77	525.000	22.6	101	64.47	73	39.63	93	17	1.41	-	-	-	-	0.394
78	515.625	22.7	101	69.28	89	39.03	94	-	-	-	-	-	-	0.390
79	506.250	21.7	101	65.48	89	37.61	95	-	-	-	-	-	-	0.382
80	496.875	21.1	101	69.06	94	35.75	95	-	-	-	-	-	-	0.368
81	487.500	21.5	105	68.93	91	36.09	96	-	-	-	-	-	-	0.372
82	478.125	22.4	105	72.96	93	35.28	97	-	-	-	-	-	-	0.369
83	468.750	20.5	105	73.92	93	32.58	97	-	-	-	-	-	-	0.350
84	459.375	21.6	106	74.24	93	32.44	98	-	-	-	-	-	-	0.345
85	450.000	22.9	106	72.16	91	32.64	99	18	1.22	-	-	-	-	0.345
86	440.625	21.2	106	78.33	97	30..50	99	18	0.6	-	-	-	-	0.333
87	431.250	21.9	107	75.96	92	30.46	100	18	2.09	-	-	-	-	0.329
88	421.875	22.2	107	76.40	97	30.45	101	19	0.35	-	-	-	-	0.326
89	412.500	22.5	109	75.26	97	30.59	102	19	1.94	-	-	-	-	0.327

199

Table C-1. BARRIER VII Results for Design Configuration D (Continued)

Impact At Node (No.)	Impact Distance Upstream of Bridge Post (in.)	Maximum Pocket Angle (deg.)	@ Node	Maximum Force (kips)	@ Node	Maximum Deflection (in.)	@ Node	Worst Case Snag Points on Posts Post #	Snag (in.)	Post #	Snag (in.)	Post #	Snag (in.)	Post #	Snag (in.)	Vehicle Parallel Time (sec)
90	403.125	21.6	107	78.89	101	29.08	103	19	2.01	-	-	-	-	-	-	0.320
91	393.750	21.9	107	80.03	94	29.13	104	20	0.03	-	-	-	-	-	-	0.322
92	384.375	22.2	110	76.98	101	28.80	104	20	1.76	-	-	-	-	-	-	0.321
93	375.000	23.1	112	76.00	102	28.98	106	20	3.31	-	-	-	-	-	-	0.326
94	365.625	22.2	111	79.99	102	27.75	106	20	3.41	21	0.35	-	-	-	-	0.322
95	356.250	22.3	112	81.88	104	27.50	107	21	1.88	-	-	-	-	-	-	0.325
96	346.875	22.2	111	80.22	98	27.20	107	21	3.27	-	-	-	-	-	-	0.329
97	337.500	22.7	111	84.08	106	27.30	108	22	1.4	-	-	-	-	-	-	0.339
98	328.125	21.7	113	84.97	107	25.85	109	22	2.02	-	-	-	-	-	-	0.331
99	318.750	21.9	113	84.80	101	25.82	110	22	3.5	-	-	-	-	-	-	0.333
100	309.375	21.9	113	91.56	106	25.43	111	22	4.68	23	1.44	24	0.54	-	-	0.338
101	300.000	20.6	113	88.27	107	24.11	112	22	4.76	23	2.15	24	1.94	-	-	0.332
102	290.625	20.2	114	83.92	105	23.79	112	18	0.54	23	3.25	24	3.44	-	-	0.331
103	281.250	20.8	117	85.51	105	23.29	114	19	2.11	23	4.2	24	5.13	-	-	0.334
104	271.875	21.2	117	84.70	105	23.09	114	19	0.67	20	3.22	24	5.97	-	-	0.338
105	262.500	20.1	117	83.54	109	21.99	115	20	2.1	23	4.65	24	6.15	-	-	0.328
106	253.125	19.6	117	86.52	109	21.78	116	20	0.54	21	2.99	24	6.71	-	-	0.328
107	243.750	18.4	117	84.93	111	20.86	116	21	1.87	22	3.67	24	6.7	-	-	0.324
108	234.375	16.9	117	84.13	115	19.71	117	22	3.02	23	3.9	24	6.9	-	-	0.319
109	225.000	16.0	118	87.31	113	19.01	118	23	3.56	24	7.2	25	3.7	-	-	0.318
110	215.625	14.7	118	92.98	115	17.73	119	23	3.08	24	7.3	25	4.8	-	-	0.313
111	206.250	13.3	119	87.26	117	16.40	119	23	2.3	24	7.1	25	5.6	-	-	0.306
112	196.875	12.5	122	89.87	119	15.54	120	23	1.32	24	6.7	25	6.1	-	-	0.295
113	187.500	12.2	122	91.43	119	15.00	120	24	5.7	25	6.4	-	-	-	-	0.296
114	178.125	11.7	123	91.37	119	14.48	122	24	4.6	25	6.7	-	-	-	-	0.291
115	168.750	11.7	125	91.98	121	14.36	123	25	6.3	26	4.3	-	-	-	-	0.280
116	159.375	12.0	126	88.73	122	13.89	124	25	5.8	26	4.8	-	-	-	-	0.273
117	150.000	13.0	128	94.10	121	13.29	124	25	5.2	26	5.7	-	-	-	-	0.271
118	140.625	15.0	129	96.07	122	12.96	126	25	4.2	26	6.2	-	-	-	-	0.260
119	131.250	16.9	129	99.73	125	13.19	127	25	2.9	26	6.3	-	-	-	-	0.266
120	121.875	17.6	129	104.34	125	12.86	127	26	6.15	-	-	-	-	-	-	0.274

Table C-2. BARRIER VII Results for Design Configuration F

Impact At Node (No.)	Impact Distance Upstream of Bridge Post (in.)	Maximum Pocket Angle		Maximum Force		Maximum Deflection		Worst Case Snag Points on Posts						Vehicle Parallel Time (sec)
		(deg.)	@ Node	(kips)	@ Node	(in.)	@ Node	Post #	Snag (in.)	Post #	Snag (in.)	Post #	Snag (in.)	
57	862.500	18.2	85.0	58.10	58	46.35	76	-	-	-	-	-	-	0.384
58	853.125	18.7	85.0	58.40	57	46.77	78	-	-	-	-	-	-	0.384
59	843.750	19.0	85.0	59.46	57	47.18	78	-	-	-	-	-	-	0.384
60	834.375	19.3	92.0	57.00	65	47.72	79	-	-	-	-	-	-	0.382
61	825.000	20.6	93.0	57.14	57	48.24	80	-	-	-	-	-	-	0.382
62	815.625	22.3	93.0	57.05	73	48.61	82	-	-	-	-	-	-	0.386
63	806.250	21.9	93.0	57.72	59	48.24	84	-	-	-	-	-	-	0.389
64	796.875	21.8	93.0	57.94	73	47.25	85	-	-	-	-	-	-	0.385
65	787.500	21.2	93.0	61.14	67	44.73	84	-	-	-	-	-	-	0.366
66	778.125	20.9	94.0	60.98	74	45.35	85	-	-	-	-	-	-	0.370
67	768.750	21.9	94.0	62.24	65	45.82	85	-	-	-	-	-	-	0.370
68	759.375	22.7	95.0	62.85	65	46.09	85	-	-	-	-	-	-	0.372
69	750.000	23.4	95.0	62.76	65	46.67	88	-	-	-	-	-	-	0.375
70	740.625	23.0	98.0	63.28	65	47.11	88	-	-	-	-	-	-	0.382
71	731.250	22.9	98.0	61.24	65	46.77	89	-	-	-	-	-	-	0.386
72	721.875	22.0	98.0	62.02	82	44.62	89	-	-	-	-	-	-	0.373
73	712.500	21.3	98.0	64.46	82	42.76	90	-	-	-	-	-	-	0.361
74	703.125	21.6	99.0	63.83	73	43.01	90	-	-	-	-	-	-	0.361
75	693.750	22.4	100.0	64.82	73	43.45	92	-	-	-	-	-	-	0.364
76	684.375	21.7	98.0	63.73	84	43.78	93	-	-	-	-	-	-	0.367
77	675.000	21.9	102.0	65.99	86	44.09	94	-	-	-	-	-	-	0.373
78	665.625	21.9	102.0	65.31	85	44.17	96	-	-	-	-	-	-	0.375
79	656.250	21.5	103.0	64.10	86	43.33	96	-	-	-	-	-	-	0.375
80	646.875	20.9	103.0	63.44	84	42.15	96	-	-	-	-	-	-	0.374
81	637.500	20.2	104.0	66.19	93	40.17	97	-	-	-	-	-	-	0.366
82	628.125	20.0	99.0	67.91	93	40.54	98	-	-	-	-	-	-	0.370
83	618.750	19.7	106.0	65.48	94	40.51	99	-	-	-	-	-	-	0.371
84	609.375	19.7	107.0	67.25	97	40.55	100	-	-	-	-	-	-	0.372
85	600.000	19.6	101.0	65.64	97	40.52	101	-	-	-	-	-	-	0.377
86	590.625	19.4	111.0	67.46	97	40.09	102	-	-	-	-	-	-	0.378
87	581.250	19.8	112.0	67.96	97	39.78	103	-	-	-	-	-	-	0.379
88	571.875	19.8	113.0	67.29	92	38.79	103	18	0.1	-	-	-	-	0.376
89	562.500	18.3	113.0	70.66	97	36.51	104	-	-	-	-	-	-	0.366
90	553.125	19.2	113.0	71.35	97	36.57	106	18	1.02	-	-	-	-	0.365
91	543.750	18.9	113.0	72.39	101	36.89	106	-	-	-	-	-	-	0.369
92	534.375	18.5	111.0	71.33	97	37.17	107	-	-	-	-	-	-	0.369
93	525.000	18.6	117.0	71.27	95	37.18	108	19	0.05	-	-	-	-	0.370
94	515.625	19.0	117.0	72.37	101	36.81	110	-	-	-	-	-	-	0.370
95	506.250	18.3	113.0	69.53	103	36.08	110	-	-	-	-	-	-	0.364
96	496.875	18.2	113.0	71.88	104	35.46	111	-	-	-	-	-	-	0.357
97	487.500	17.7	113.0	73.51	97	33.79	112	-	-	-	-	-	-	0.349

Table C-2. BARRIER VII Results for Design Configuration F (Continued)

Impact At Node (No.)	Impact Distance Upstream of Bridge Post (in.)	Maximum Pocket Angle (deg.)	@ Node	Maximum Force (kips)	@ Node	Maximum Deflection (in.)	@ Node	Post #	Snag (in.)	Post #	Snag (in.)	Post #	Snag (in.)	Vehicle Parallel Time (sec)
98	478.125	17.6	113.0	72.18	97	33.23	112	-	-	-	-	-	-	0.345
99	468.750	18.1	121.0	72.86	97	32.60	113	-	-	-	-	-	-	0.340
100	459.375	17.7	121.0	75.99	106	31.14	114	-	-	-	-	-	-	0.331
101	450.000	18.2	121.0	75.37	101	30.98	114	20	0.87	-	-	-	-	0.330
102	440.625	18.4	121.0	72.66	101	30.20	115	20	1.8	-	-	-	-	0.327
103	431.250	18.0	122.0	75.75	105	29.21	117	-	-	-	-	-	-	0.323
104	421.875	18.3	122.0	80.32	108	29.39	117	-	-	-	-	-	-	0.323
105	412.500	18.9	125.0	79.37	105	29.20	118	-	-	-	-	-	-	0.323
106	403.125	18.7	126.0	79.82	109	28.14	119	-	-	-	-	-	-	0.318
107	393.750	19.9	126.0	82.81	110	28.30	120	21	0.41	-	-	-	-	0.313
108	384.375	20.7	127.0	81.99	109	28.45	121	21	1.83	-	-	-	-	0.310
109	375.000	21.2	127.0	83.57	109	28.61	122	21	2.92	-	-	-	-	0.310
110	365.625	20.7	127.0	86.52	113	27.40	122	22	0.35	-	-	-	-	0.306
111	356.250	21.1	127.0	84.76	113	27.45	123	22	1.76	-	-	-	-	0.309
112	346.875	21.5	129.0	85.67	113	27.55	124	22	3.02	-	-	-	-	0.312
113	337.500	22.0	129.0	83.26	113	27.32	125	23	1.65	-	-	-	-	0.315
114	328.125	21.6	129.0	87.34	117	26.35	126	23	2.1	-	-	-	-	0.313
115	318.750	21.9	129.0	89.19	117	26.18	126	23	3.64	24	0.23	-	-	0.316
116	309.375	21.9	129.0	87.13	117	26.10	127	24	1.83	-	-	-	-	0.321
117	300.000	21.4	130.0	89.70	117	25.36	128	24	3.14	25	3	-	-	0.323
118	290.625	20.7	133.0	88.97	121	24.35	129	24	3.69	25	3.94	-	-	0.321
119	281.250	21.2	133.0	86.54	121	24.08	130	24	4.6	25	5.5	-	-	0.332
120	271.875	21.5	133.0	88.93	121	23.62	130	21	3.26	25	6.68	-	-	0.335
121	262.500	20.5	133.0	90.68	125	22.51	132	21	2.3	25	7.11	-	-	0.330
122	253.125	19.9	133.0	88.15	126	22.40	132	21	0.72	22	3.58	26	1.15	0.334
123	243.750	19.2	133.0	88.66	131	22.11	133	22	2.43	26	2.87	-	-	0.335
124	234.375	18.2	134.0	85.50	129	21.68	133	22	1.05	26	4.47	-	-	0.336
125	225.000	17.1	134.0	94.03	129	20.46	134	23	2.57	26	5.14	-	-	0.334
126	215.625	15.7	135.0	91.92	131	19.46	135	23	1.09	26	6.02	-	-	0.335
127	206.250	14.0	138.0	86.45	131	18.22	135	24	2.52	26	6.47	-	-	0.318
128	196.875	13.6	138.0	88.60	133	17.09	136	24	1.42	26	6.69	-	-	0.309
129	187.500	12.9	139.0	88.05	135	15.70	136	24	0.02	26	6.75	-	-	0.303
130	178.125	12.2	139.0	88.67	135	15.00	139	26	6.72	-	-	-	-	0.295
131	168.750	12.0	142.0	83.10	137	14.66	139	26	6.28	-	-	-	-	0.283
132	159.375	12.4	143.0	82.48	137	14.09	140	26	5.87	-	-	-	-	0.275
133	150.000	13.8	145.0	85.24	137	13.41	141	27	5.77	-	-	-	-	0.272
134	140.625	16.2	145.0	85.76	137	13.19	142	27	6.12	-	-	-	-	0.258
135	131.250	17.9	145.0	97.26	141	13.40	143	27	6.36	-	-	-	-	0.265
136	121.875	18.6	145.0	99.62	141	13.28	144	27	6	-	-	-	-	0.277
137	112.500	17.9	145.0	96.81	141	12.85	146	27	5.55	-	-	-	-	0.297

202

Table C-3. BARRIER VII Results for Design Configuration G

Impact At Node (No.)	Impact Distance Upstream of Bridge Post (in.)	Maximum Pocket Angle (deg.)	@ Node	Maximum Force (kips)	@ Node	Maximum Deflection (in.)	@ Node	Worst Case Snag Points on Posts Post #	Snag (in.)	Post #	Snag (in.)	Post #	Snag (in.)	Vehicle Parallel Time (sec)
57	712.500	20.0	85	57.16	62	49.25	77	-	-	-	-	-	-	0.400
58	703.125	18.7	85	57.53	62	46.84	77	-	-	-	-	-	-	0.385
59	693.750	19.0	85	58.10	57	47.20	78	-	-	-	-	-	-	0.384
60	684.375	19.1	85	57.31	66	47.79	79	-	-	-	-	-	-	0.382
61	675.000	20.4	93	57.24	57	48.20	81	-	-	-	-	-	-	0.382
62	665.625	22.1	93	57.93	57	48.49	82	-	-	-	-	-	-	0.385
63	656.250	22.2	93	57.24	60	48.50	84	-	-	-	-	-	-	0.390
64	646.875	22.0	94	57.36	73	47.02	85	-	-	-	-	-	-	0.384
65	637.500	21.2	93	61.25	65	44.62	84	-	-	-	-	-	-	0.366
66	628.125	21.4	94	61.13	65	45.36	85	-	-	-	-	-	-	0.369
67	618.750	22.3	94	61.47	65	45.78	85	-	-	-	-	-	-	0.370
68	609.375	24.0	97	62.49	65	45.97	85	-	-	-	-	-	-	0.371
69	600.000	24.9	97	63.22	65	46.85	88	-	-	-	-	-	-	0.376
70	590.625	23.9	98	62.59	65	47.09	88	-	-	-	-	-	-	0.381
71	581.250	23.5	98	60.50	81	46.82	89	-	-	-	-	-	-	0.385
72	571.875	22.4	98	62.26	82	44.69	89	-	-	-	-	-	-	0.372
73	562.500	21.9	98	64.47	83	42.89	90	-	-	-	-	-	-	0.361
74	553.125	22.1	101	64.35	73	42.93	90	-	-	-	-	-	-	0.359
75	543.750	23.1	101	63.57	73	43.41	92	-	-	-	-	-	-	0.363
76	534.375	22.6	102	64.08	86	43.95	93	-	-	-	-	-	-	0.367
77	525.000	23.3	103	66.68	86	44.05	94	-	-	-	-	-	-	0.370
78	515.625	23.9	105	65.53	85	44.23	95	-	-	-	-	-	-	0.373
79	506.250	23.7	105	63.60	86	43.41	96	16	0.96	-	-	-	-	0.371
80	496.875	23.5	105	62.86	73	42.02	96	-	-	-	-	-	-	0.367
81	487.500	22.5	105	66.13	81	40.12	97	16	1.3	-	-	-	-	0.359
82	478.125	23.0	105	66.67	93	40.11	97	-	-	-	-	-	-	0.361
83	468.750	22.8	108	66.78	97	40.32	98	-	-	-	-	-	-	0.363
84	459.375	24.1	109	68.73	97	39.81	98	-	-	-	-	-	-	0.363
85	450.000	25.8	110	66.94	81	39.60	101	-	-	-	-	-	-	0.365
86	440.625	26.6	110	71.19	101	39.45	102	17	1.36	-	-	-	-	0.366
87	431.250	27.3	111	69.30	97	38.84	103	17	2.89	-	-	-	-	0.363
88	421.875	28.1	112	70.12	97	38.35	104	18	0.16	-	-	-	-	0.366
89	412.500	26.0	113	73.52	97	35.96	104	17	3.66	-	-	-	-	0.353
90	403.125	27.3	113	72.47	97	35.95	105	18	1.19	-	-	-	-	0.353
91	393.750	28.7	113	71.19	103	35.92	105	18	2.98	-	-	-	-	0.353
92	384.375	28.4	113	72.94	101	35.92	106	19	0.76	-	-	-	-	0.360
93	375.000	28.8	113	73.74	101	35.67	107	19	2.42	-	-	-	-	0.362
94	365.625	28.9	113	73.41	97	35.24	108	19	4.02	-	-	-	-	0.365
95	356.250	28.6	113	73.71	103	34.74	109	19	4.84	20	0.39	-	-	0.369
96	346.875	28.7	117	71.71	104	34.03	109	20	1.51	-	-	-	-	0.369
97	337.500	27.3	117	74.25	106	32.21	110	20	1.42	-	-	-	-	0.360

Table C-3. BARRIER VII Results for Design Configuration G (Continued)

Impact At Node (No.)	Impact Distance Upstream of Bridge Post (in.)	Maximum Pocket Angle		Maximum Force		Maximum Deflection		Worst Case Snag Points on Posts								Vehicle Parallel Time (sec)
		(deg.)	@ Node	(kips)	@ Node	(in.)	@ Node	Post #	Snag (in.)	Post #	Snag (in.)	Post #	Snag (in.)	Post #	Snag (in.)	
98	328.125	26.8	117	78.21	107	31.29	110	20	3.04	-	-	-	-	-	-	0.361
99	318.750	25.1	113	81.49	109	29.24	111	20	2.72	-	-	-	-	-	-	0.352
100	309.375	25.0	117	80.00	110	28.73	112	20	4.15	21	3.6	-	-	-	-	0.357
101	300.000	25.3	117	77.73	107	28.21	112	20	4.97	21	4.83	-	-	-	-	0.370
102	290.625	23.3	117	83.17	108	25.95	113	20	4.87	21	5.4	-	-	-	-	0.352
103	281.250	23.6	117	83.46	106	25.72	114	20	5.56	21	6.57	-	-	-	-	0.362
104	271.875	23.4	117	77.47	105	25.29	115	17	3.31	21	7.57	-	-	-	-	0.365
105	262.500	22.1	117	83.95	109	23.98	116	17	2.24	21	7.87	-	-	-	-	0.354
106	253.125	21.5	117	85.14	111	23.75	116	17	0.69	18	3.62	22	2.04	-	-	0.357
107	243.750	20.7	117	77.82	109	23.53	117	18	2.42	22	3.87	-	-	-	-	0.359
108	234.375	19.8	118	77.89	109	23.03	117	18	0.96	22	5.6	-	-	-	-	0.363
109	225.000	18.4	118	80.91	113	21.70	118	19	2.61	22	5.92	-	-	-	-	0.356
110	215.625	17.3	119	83.60	113	20.97	119	19	1.03	22	6.75	-	-	-	-	0.350
111	206.250	15.2	120	82.65	115	19.14	119	20	2.48	21	7.6	22	6.7	-	-	0.327
112	196.875	14.0	122	81.11	117	17.59	120	20	1.4	21	6.8	22	6.9	-	-	0.316
113	187.500	13.3	122	84.93	119	16.06	120	21	5.8	22	6.9	-	-	-	-	0.306
114	178.125	12.7	123	78.74	119	15.33	122	21	4.5	22	6.9	-	-	-	-	0.297
115	168.750	12.5	126	83.19	121	14.95	123	22	6.5	23	4.6	-	-	-	-	0.284
116	159.375	12.5	127	82.97	121	14.32	124	22	5.9	23	5.3	-	-	-	-	0.276
117	150.000	13.8	128	82.14	121	13.64	124	22	5.2	23	6	-	-	-	-	0.273
118	140.625	16.4	129	92.50	125	13.46	126	22	4.1	23	6.2	-	-	-	-	0.260
119	131.250	18.0	129	100.00	125	13.65	127	22	3	23	6.3	-	-	-	-	0.267
120	121.875	18.5	129	96.77	125	13.51	128	23	6.03	-	-	-	-	-	-	0.281
121	112.500	18.5	129	92.69	125	13.38	130	23	5.5	-	-	-	-	-	-	0.299

Table C-4. BARRIER VII Results for Design Configuration H

Impact At Node (No.)	Impact Distance Upstream of Bridge Post (in.)	Maximum Pocket Angle		Maximum Force		Maximum Deflection		Worst Case Snag Points on Posts						Vehicle Parallel Time (sec)
		(deg.)	@ Node	(kips)	@ Node	(in.)	@ Node	Post #	Snag (in.)	Post #	Snag (in.)	Post #	Snag (in.)	
53	750.000	24.1	84	53.83	57	49.96	73	-	-	-	-	-	-	0.394
54	740.625	24.0	83	53.26	65	50.48	74	-	-	-	-	-	-	0.397
55	731.250	24.8	85	53.39	53	50.34	75	-	-	-	-	-	-	0.401
56	721.875	24.4	86	53.41	62	49.16	76	-	-	-	-	-	-	0.398
57	712.500	24.6	86	57.19	65	48.79	76	-	-	-	-	-	-	0.392
58	703.125	23.0	86	57.77	59	46.36	77	-	-	-	-	-	-	0.374
59	693.750	23.5	87	59.04	57	46.64	78	-	-	-	-	-	-	0.375
60	684.375	24.3	87	58.46	68	47.00	79	-	-	-	-	-	-	0.376
61	675.000	24.2	87	58.25	68	47.54	80	-	-	-	-	-	-	0.381
62	665.625	24.8	90	58.68	57	47.63	81	-	-	-	-	-	-	0.383
63	656.250	24.9	90	57.85	68	47.56	82	-	-	-	-	-	-	0.387
64	646.875	23.8	90	57.70	65	45.70	82	-	-	-	-	-	-	0.378
65	637.500	23.0	90	60.58	71	43.74	82	-	-	-	-	-	-	0.368
66	628.125	23.0	91	60.63	69	43.81	85	14	0.33	-	-	-	-	0.366
67	618.750	23.4	91	61.34	65	44.60	85	-	-	-	-	-	-	0.372
68	609.375	23.1	94	61.31	65	45.16	85	-	-	-	-	-	-	0.378
69	600.000	23.3	95	60.78	74	45.02	85	-	-	-	-	-	-	0.382
70	590.625	24.0	97	62.66	65	45.44	88	-	-	-	-	-	-	0.388
71	581.250	23.4	96	61.82	84	44.64	88	-	-	-	-	-	-	0.388
72	571.875	22.6	96	64.82	86	43.22	89	-	-	-	-	-	-	0.388
73	562.500	22.3	97	66.95	73	41.34	89	-	-	-	-	-	-	0.380
74	553.125	21.4	95	63.12	73	41.66	90	-	-	-	-	-	-	0.385
75	543.750	21.4	94	66.63	86	41.88	91	-	-	-	-	-	-	0.388
76	534.375	21.5	94	64.03	83	42.27	92	-	-	-	-	-	-	0.393
77	525.000	21.3	102	63.29	89	42.20	94	-	-	-	-	-	-	0.395
78	515.625	22.0	105	63.08	84	42.09	94	-	-	-	-	-	-	0.397
79	506.250	21.4	105	61.62	89	40.14	95	-	-	-	-	-	-	0.385
80	496.875	19.9	103	68.16	89	37.57	96	-	-	-	-	-	-	0.372
81	487.500	20.6	105	66.01	90	37.80	96	17	0.35	-	-	-	-	0.373
82	478.125	21.5	105	66.70	94	37.91	97	17	1.94	-	-	-	-	0.371
83	468.750	22.2	105	66.67	93	38.01	98	-	-	-	-	-	-	0.372
84	459.375	21.8	109	67.36	93	37.74	98	-	-	-	-	-	-	0.369
85	450.000	23.4	109	67.40	98	37.31	101	-	-	-	-	-	-	0.367
86	440.625	24.4	110	69.66	93	36.90	101	18	0.63	-	-	-	-	0.362
87	431.250	25.2	110	67.09	99	36.18	102	18	1.87	-	-	-	-	0.357
88	421.875	25.7	111	68.90	98	35.90	103	18	2.72	-	-	-	-	0.353
89	412.500	24.1	111	72.22	98	33.83	104	18	2.37	-	-	-	-	0.343
90	403.125	24.5	111	72.29	101	33.47	104	-	-	-	-	-	-	0.343
91	393.750	25.2	113	71.73	105	32.73	105	19	0.73	-	-	-	-	0.337
92	384.375	24.1	113	76.94	103	31.22	106	19	0.84	-	-	-	-	0.327

205

Table C-4. BARRIER VII Results for Design Configuration H (Continued)

Impact At Node (No.)	Impact Distance Upstream of Bridge Post (in.)	Maximum Pocket Angle		Maximum Force		Maximum Deflection		Worst Case Snag Points on Posts						Vehicle Parallel Time (sec)
		(deg.)	@ Node	(kips)	@ Node	(in.)	@ Node	Post #	Snag (in.)	Post #	Snag (in.)	Post #	Snag (in.)	
93	375.000	24.4	113	77.76	105	31.07	106	19	1.98	-	-	-	-	0.327
94	365.625	22.5	111	80.34	103	28.90	107	19	1.99	-	-	-	-	0.316
95	356.250	23.2	113	79.02	103	29.01	107	19	2.95	-	-	-	-	0.322
96	346.875	23.8	113	76.94	105	28.97	108	20	1.28	-	-	-	-	0.328
97	337.500	24.1	113	75.94	105	28.80	109	20	3.05	-	-	-	-	0.327
98	328.125	23.3	113	82.86	109	27.52	110	20	3.4	-	-	-	-	0.323
99	318.750	23.6	113	84.77	109	27.45	111	20	4.65	21	1.33	22	0.45	0.332
100	309.375	23.7	113	85.22	106	27.26	111	21	2.68	22	2.29	-	-	0.337
101	300.000	23.4	117	80.20	104	26.84	112	21	3.85	22	3.84	-	-	0.344
102	290.625	22.3	117	86.73	107	25.30	113	21	4.32	22	4.45	-	-	0.338
103	281.250	22.9	117	88.15	105	25.19	114	22	6.07	-	-	-	-	0.354
104	271.875	22.6	117	80.83	105	24.66	115	22	7.33	-	-	-	-	0.352
105	262.500	21.7	117	85.89	109	23.53	116	18	2.2	22	7.62	-	-	0.346
106	253.125	21.1	117	86.78	109	23.34	116	18	0.73	23	1.75	-	-	0.350
107	243.750	20.2	117	80.52	109	23.08	117	19	2.45	23	3.5	-	-	0.350
108	234.375	19.3	118	78.55	109	22.65	117	19	0.98	20	3.65	23	4.88	0.353
109	225.000	18.0	118	86.61	113	21.28	118	20	2.54	23	5.79	-	-	0.348
110	215.625	16.5	119	87.92	115	20.09	119	20	1.04	23	6.5	-	-	0.345
111	206.250	14.8	119	84.29	115	18.88	119	21	2.48	22	7.5	23	6.7	0.325
112	196.875	14.0	122	83.13	117	17.55	120	21	1.39	22	6.8	23	6.7	0.316
113	187.500	13.1	122	86.76	119	15.89	120	22	5.8	23	6.9	-	-	0.304
114	178.125	12.5	123	82.84	119	15.17	122	22	4.6	23	6.9	-	-	0.296
115	168.750	12.3	126	84.06	121	14.80	123	23	6.4	24	4.6	-	-	0.283
116	159.375	12.4	127	84.03	121	14.23	124	23	5.9	24	5.2	-	-	0.276
117	150.000	13.8	128	82.88	121	13.58	124	23	5.1	24	5.9	-	-	0.273
118	140.625	16.4	129	91.71	125	13.40	126	23	4.2	24	6.2	-	-	0.259
119	131.250	18.0	129	101.12	125	13.60	127	23	3	24	6.2	-	-	0.267
120	121.875	18.6	129	98.29	125	13.33	128	24	5.99	-	-	-	-	0.278
121	112.500	18.4	129	94.81	125	13.30	130	24	5.5	-	-	-	-	0.298

Table C-5. BARRIER VII Results for Design Configuration J

Impact At Node (No.)	Impact Distance Upstream of Bridge Post (in.)	Maximum Pocket Angle (deg.)	@ Node	Maximum Force (kips)	@ Node	Maximum Deflection (in.)	@ Node	Post #	Snag (in.)	Post #	Snag (in.)	Post #	Snag (in.)	Vehicle Parallel Time (sec)
49	862.500	18.7	77	54.48	57	48.02	69	-	-	-	-	-	-	0.401
50	853.125	18.9	77	54.91	79	48.42	70	-	-	-	-	-	-	0.401
51	843.750	18.7	77	54.34	49	48.94	71	-	-	-	-	-	-	0.400
52	834.375	18.8	78	53.08	50	49.77	73	-	-	-	-	-	-	0.401
53	825.000	18.5	69	53.67	49	50.22	74	-	-	-	-	-	-	0.404
54	815.625	18.9	85	53.14	57	50.47	76	-	-	-	-	-	-	0.405
55	806.250	19.3	85	54.14	49	50.91	77	-	-	-	-	-	-	0.408
56	796.875	19.0	85	53.05	49	49.58	77	-	-	-	-	-	-	0.404
57	787.500	17.8	85	57.54	57	47.07	77	-	-	-	-	-	-	0.388
58	778.125	18.4	85	57.50	57	47.53	77	-	-	-	-	-	-	0.389
59	768.750	18.8	86	59.28	57	47.53	77	-	-	-	-	-	-	0.388
60	759.375	19.2	91	58.30	65	48.43	79	-	-	-	-	-	-	0.388
61	750.000	20.3	92	57.65	57	48.83	80	-	-	-	-	-	-	0.388
62	740.625	22.2	93	58.56	57	49.21	81	-	-	-	-	-	-	0.392
63	731.250	21.7	93	57.27	57	48.97	82	-	-	-	-	-	-	0.398
64	721.875	21.4	94	58.89	74	47.37	83	-	-	-	-	-	-	0.391
65	712.500	21.0	93	61.00	65	44.97	83	14	0.97	-	-	-	-	0.370
66	703.125	20.7	94	60.17	65	45.31	84	-	-	-	-	-	-	0.371
67	693.750	21.6	94	59.75	65	45.60	85	-	-	-	-	-	-	0.371
68	684.375	22.7	95	60.99	65	46.24	87	15	0.81	-	-	-	-	0.371
69	675.000	23.3	95	61.43	70	46.79	88	-	-	-	-	-	-	0.373
70	665.625	23.2	98	61.48	76	47.02	88	-	-	-	-	-	-	0.376
71	656.250	23.1	98	60.99	65	46.44	88	-	-	-	-	-	-	0.375
72	646.875	21.4	98	63.47	78	42.63	90	-	-	-	-	-	-	0.355
73	637.500	21.7	99	63.18	76	42.90	90	16	1.06	-	-	-	-	0.355
74	628.125	21.7	99	63.18	76	42.90	90	-	-	-	-	-	-	0.355
75	618.750	22.2	100	62.56	84	43.00	92	-	-	-	-	-	-	0.357
76	609.375	21.7	102	63.26	85	43.31	93	-	-	-	-	-	-	0.361
77	600.000	22.0	103	62.81	85	43.31	94	-	-	-	-	-	-	0.364
78	590.625	22.2	105	62.68	83	43.22	95	17	1.25	-	-	-	-	0.364
79	581.250	22.5	105	63.78	73	42.99	96	-	-	-	-	-	-	0.365
80	571.875	21.6	103	62.73	73	42.59	97	-	-	-	-	-	-	0.369
81	562.500	21.3	102	62.77	92	42.41	98	-	-	-	-	-	-	0.375
82	553.125	20.9	102	64.14	73	42.15	98	18	0.65	-	-	-	-	0.377
83	543.750	20.1	102	65.49	91	40.57	99	-	-	-	-	-	-	0.370
84	534.375	20.4	109	68.92	97	40.54	100	18	1.94	-	-	-	-	0.370
85	525.000	20.0	103	66.18	97	40.52	101	-	-	-	-	-	-	0.374
86	515.625	20.3	111	68.22	96	40.21	102	-	-	-	-	-	-	0.375
87	506.250	20.7	113	67.75	97	39.85	103	19	0.96	-	-	-	-	0.374
88	496.875	20.7	113	67.10	87	38.97	103	19	2.45	-	-	-	-	0.371
89	487.500	20.7	113	69.77	85	38.30	104	19	3.25	-	-	-	-	0.369

Table C-5. BARRIER VII Results for Design Configuration J (Continued)

Impact At Node (No.)	Impact Distance Upstream of Bridge Post (in.)	Maximum Pocket Angle (deg.)	@ Node	Maximum Force (kips)	@ Node	Maximum Deflection (in.)	@ Node	Post #	Snag (in.)	Post #	Snag (in.)	Post #	Snag (in.)	Vehicle Parallel Time (sec)
90	478.125	20.0	113	71.13	97	36.59	105	14	1.26	19	3.25	-	-	0.360
91	468.750	20.8	113	70.65	99	36.65	106	-	-	-	-	-	-	0.361
92	459.375	20.8	113	72.07	96	36.68	106	-	-	-	-	-	-	0.361
93	450.000	21.8	117	71.25	105	36.30	107	20	0.51	-	-	-	-	0.359
94	440.625	23.0	117	72.32	99	36.07	109	15	1.13	20	2.25	-	-	0.356
95	431.250	23.5	118	70.29	105	35.25	109	20	3.55	-	-	-	-	0.350
96	421.875	23.9	118	72.32	105	34.67	110	20	4.63	-	-	-	-	0.346
97	412.500	23.0	118	75.54	97	32.99	112	20	4.36	-	-	-	-	0.338
98	403.125	23.2	119	75.27	100	32.52	112	16	1.28	21	1.54	-	-	0.337
99	393.750	23.6	119	74.51	109	31.70	112	21	2.35	-	-	-	-	0.331
100	384.375	22.8	119	79.28	102	30.53	113	21	2.65	-	-	-	-	0.323
101	375.000	23.2	121	88.10	109	30.32	114	21	4.08	-	-	-	-	0.321
102	365.625	21.9	119	82.98	107	28.41	114	17	1.12	21	3.98	-	-	0.313
103	356.250	22.3	119	81.19	105	28.45	115	21	5.18	22	1.8	-	-	0.316
104	346.875	22.9	121	79.25	111	28.51	116	22	3.62	-	-	-	-	0.322
105	337.500	23.2	121	79.37	107	28.23	117	22	5.31	23	1.07	-	-	0.323
106	328.125	22.7	121	80.08	109	26.93	118	22	6.3	23	2.83	-	-	0.320
107	318.750	23.0	121	86.94	111	26.93	119	22	6.94	23	3.81	-	-	0.326
108	309.375	23.0	121	85.98	109	26.81	119	23	5.22	24	4.95	-	-	0.330
109	300.000	22.5	121	84.10	109	26.17	120	19	3.2	23	6.58	24	6.8	0.334
110	290.625	21.6	125	86.60	113	24.84	121	19	1.55	23	6.98	24	7.66	0.329
111	281.250	22.3	125	87.27	113	24.88	122	23	7.64	24	8.96	-	-	0.347
112	271.875	22.2	125	83.45	113	24.34	122	20	5.27	24	9.92	-	-	0.346
113	262.500	21.2	125	84.98	117	23.12	124	20	3.96	25	2.12	-	-	0.339
114	253.125	20.6	125	85.51	117	22.97	124	21	2.29	21	5.78	25	4.24	0.343
115	243.750	19.9	125	82.24	118	22.81	125	21	4.37	22	6.81	25	6.09	0.345
116	234.375	18.8	126	81.16	123	22.24	125	21	2.77	22	5.86	25	7.97	0.345
117	225.000	17.6	126	86.37	121	21.05	126	22	4.53	23	6.55	25	8.41	0.342
118	215.625	16.2	127	90.98	123	19.79	127	22	2.84	23	5.6	25	9.07	0.340
119	206.250	14.7	127	84.69	123	18.63	127	23	4.43	24	9.8	25	9.2	0.322
120	196.875	13.8	130	85.42	125	17.32	128	23	3.15	24	9	25	9.4	0.313
121	187.500	13.0	130	86.61	127	15.86	128	24	7.8	25	9.3	26	4.9	0.304
122	178.125	12.5	131	85.28	127	15.14	130	24	6.5	25	9.1	26	6.3	0.296
123	168.750	12.3	134	83.83	129	14.75	131	24	5	25	8.7	26	7.3	0.284
124	159.375	12.4	135	83.56	129	14.19	132	24	3.3	25	8	26	7.7	0.275
125	150.000	13.8	136	82.81	129	13.49	132	25	7.14	26	8.33	-	-	0.272
126	140.625	16.3	137	90.81	133	13.30	134	25	5.94	26	8.51	-	-	0.259
127	131.250	18.0	137	100.45	133	13.52	135	25	4.71	26	8.58	-	-	0.266
128	121.875	18.6	137	98.46	133	13.28	136	25	3.22	26	8.03	-	-	0.278
129	112.500	18.2	139	95.43	133	13.09	138	26	7.41	-	-	-	-	0.298

Table C-6. BARRIER VII Results for Design Configuration K

Impact At Node (No.)	Impact Distance Upstream of Bridge Post (in.)	Maximum Pocket Angle		Maximum Force		Maximum Deflection		Worst Case Snag Points on Posts						Vehicle Parallel Time (sec)
		(deg.)	@ Node	(kips)	@ Node	(in.)	@ Node	Post #	Snag (in.)	Post #	Snag (in.)	Post #	Snag (in.)	
57	712.500	18.8	93	58.29	57	46.50	76	-	-	-	-	-	-	0.386
58	703.125	20.8	93	58.18	57	47.14	78	-	-	-	-	-	-	0.387
59	693.750	22.2	93	58.28	57	47.40	79	-	-	-	-	-	-	0.386
60	684.375	23.1	93	57.96	65	48.03	79	-	-	-	-	-	-	0.384
61	675.000	24.0	93	57.81	57	48.60	81	-	-	-	-	-	-	0.384
62	665.625	26.2	93	58.71	57	48.76	82	13	1.52	-	-	-	-	0.386
63	656.250	27.5	93	57.81	60	48.73	83	-	-	-	-	-	-	0.389
64	646.875	24.9	94	58.04	73	47.03	83	-	-	-	-	-	-	0.382
65	637.500	25.0	93	62.05	67	44.97	83	-	-	-	-	-	-	0.365
66	628.125	24.1	94	61.49	65	45.03	84	-	-	-	-	-	-	0.365
67	618.750	26.2	97	62.34	65	45.33	85	-	-	-	-	-	-	0.365
68	609.375	28.5	97	62.96	65	45.80	86	14	2.05	-	-	-	-	0.367
69	600.000	29.0	97	62.77	65	46.19	88	-	-	-	-	-	-	0.370
70	590.625	26.5	97	62.73	65	46.43	89	-	-	-	-	-	-	0.375
71	581.250	25.9	98	60.75	65	45.95	89	15	0.2	-	-	-	-	0.377
72	571.875	24.8	101	61.46	82	44.25	90	15	0.85	-	-	-	-	0.368
73	562.500	23.9	98	64.15	83	42.48	90	-	-	-	-	-	-	0.357
74	553.125	24.3	101	64.05	75	42.56	91	15	2.34	-	-	-	-	0.358
75	543.750	24.7	101	63.45	73	43.07	92	-	-	-	-	-	-	0.362
76	534.375	23.8	103	63.70	73	43.48	93	-	-	-	-	-	-	0.366
77	525.000	24.1	105	64.49	86	43.57	94	16	0.37	-	-	-	-	0.370
78	515.625	24.6	105	63.81	93	43.59	96	16	1.89	-	-	-	-	0.372
79	506.250	24.5	105	64.65	78	43.16	96	-	-	-	-	-	-	0.374
80	496.875	23.6	105	65.27	94	41.29	97	-	-	-	-	-	-	0.369
81	487.500	23.0	105	65.35	87	39.87	97	-	-	-	-	-	-	0.362
82	478.125	23.2	105	65.57	93	40.04	98	-	-	-	-	-	-	0.365
83	468.750	23.0	107	69.50	94	40.39	99	-	-	-	-	-	-	0.368
84	459.375	24.8	109	71.80	97	40.51	100	17	0.6	-	-	-	-	0.373
85	450.000	26.7	110	71.45	98	40.56	101	17	2.72	-	-	-	-	0.374
86	440.625	27.3	110	67.90	81	40.32	102	17	4.41	-	-	-	-	0.376
87	431.250	26.7	111	69.56	97	38.47	103	17	5.83	18	0.41	-	-	0.369
88	421.875	25.1	110	73.49	98	36.35	103	17	5.15	-	-	-	-	0.360
89	412.500	26.3	111	74.58	97	36.62	104	18	2.74	-	-	-	-	0.362
90	403.125	28.1	113	74.13	92	36.75	105	13	1.67	18	4.65	-	-	0.363
91	393.750	29.6	113	73.34	102	36.62	105	18	6.53	19	1.78	-	-	0.362
92	384.375	29.3	113	72.24	103	36.76	106	19	4.18	-	-	-	-	0.373
93	375.000	29.6	113	72.64	103	36.44	107	19	5.89	-	-	-	-	0.377
94	365.625	29.3	113	72.56	105	35.62	108	14	1.6	19	7.35	-	-	0.375
95	356.250	28.6	113	74.42	105	34.68	109	20	3.22	-	-	-	-	0.374
96	346.875	27.1	113	76.54	97	32.68	109	20	3.13	-	-	-	-	0.361

Table C-6. BARRIER VII Results for Design Configuration K (Continued)

Impact At Node (No.)	Impact Distance Upstream of Bridge Post (in.)	Maximum Pocket Angle		Maximum Force		Maximum Deflection		Worst Case Snag Points on Posts						Vehicle Parallel Time (sec)
		(deg.)	@ Node	(kips)	@ Node	(in.)	@ Node	Post #	Snag (in.)	Post #	Snag (in.)	Post #	Snag (in.)	
97	337.500	27.7	117	76.37	109	32.47	110	20	5.07	-	-	-	-	0.367
98	328.125	27.4	117	78.49	110	31.55	110	15	1.19	20	6.04	-	-	0.367
99	318.750	25.4	113	81.04	109	29.39	111	20	5.88	-	-	-	-	0.356
100	309.375	25.0	117	81.22	110	28.70	112	20	7.07	21	6.77	-	-	0.355
101	300.000	25.1	117	78.60	103	27.99	112	16	3.16	20	8.05	21	8.54	0.367
102	290.625	23.7	117	82.67	111	26.37	113	16	1.48	20	7.69	21	8.61	0.358
103	281.250	24.0	117	82.50	108	26.10	114	21	9.68	-	-	-	-	0.367
104	271.875	23.6	117	76.75	105	25.53	115	17	5.38	21	10.72	-	-	0.368
105	262.500	23.1	117	79.48	111	24.93	116	17	3.97	18	6.88	22	3.71	0.367
106	253.125	21.8	117	85.32	111	23.98	116	17	2.31	18	5.8	22	5.1	0.360
107	243.750	21.0	117	77.68	109	23.79	117	17	0.38	18	4.41	22	6.99	0.364
108	234.375	20.0	118	76.71	109	23.19	117	18	2.82	20	7.49	22	8.91	0.369
109	225.000	18.4	118	80.99	113	21.73	118	20	6.69	21	11.2	22	9.3	0.357
110	215.625	17.4	119	80.39	113	21.10	119	20	5.67	21	10.6	22	9.8	0.357
111	206.250	15.2	120	82.37	115	19.26	119	21	9.9	22	9.6	23	2.2	0.329
112	196.875	14.1	122	81.46	117	17.71	120	21	9.1	22	9.5	23	3.7	0.317
113	187.500	13.3	122	84.61	119	16.07	120	21	7.9	22	9.4	23	5.2	0.306
114	178.125	12.8	123	78.54	119	15.36	123	21	6.4	22	9.2	23	6.6	0.297
115	168.750	12.5	126	81.75	121	14.99	123	21	5	22	8.7	23	7.2	0.284
116	159.375	12.6	127	82.89	121	14.33	124	22	8	23	7.9	-	-	0.276
117	150.000	13.8	128	81.51	121	13.65	124	22	7.1	23	8.4	-	-	0.273
118	140.625	16.5	129	92.72	125	13.51	126	22	6	23	8.5	-	-	0.260
119	131.250	18.0	129	97.28	125	13.68	127	22	4.7	23	8.6	-	-	0.268
120	121.875	18.9	129	93.99	125	13.50	128	22	3.2	23	8.1	-	-	0.281
121	112.500	18.4	129	92.12	125	13.34	130	23	7.37	-	-	-	-	0.299

Table C-7. BARRIER VII Results for Design Configuration L

Impact At Node (No.)	Impact Distance Upstream of Bridge Post (in.)	Maximum Pocket Angle (deg.)	@ Node	Maximum Force (kips)	@ Node	Maximum Deflection (in.)	@ Node	Post #	Snag (in.)	Post #	Snag (in.)	Post #	Snag (in.)	Vehicle Parallel Time (sec)
57	787.500	18.6	92	59.03	57	46.63	76	-	-	-	-	-	-	0.386
58	778.125	20.6	93	59.13	57	46.92	78	-	-	-	-	-	-	0.387
59	768.750	21.9	93	60.30	57	47.54	79	-	-	-	-	-	-	0.386
60	759.375	22.9	93	58.46	61	48.16	80	-	-	-	-	-	-	0.385
61	750.000	23.9	93	59.55	57	48.73	81	-	-	-	-	-	-	0.385
62	740.625	26.0	93	58.91	57	49.05	82	14	1.34	-	-	-	-	0.387
63	731.250	24.6	94	58.40	57	48.86	83	-	-	-	-	-	-	0.391
64	721.875	24.1	94	58.52	68	47.10	83	-	-	-	-	-	-	0.384
65	712.500	24.7	94	61.36	73	47.23	84	-	-	-	-	-	-	0.382
66	703.125	23.2	94	61.85	65	45.17	84	-	-	-	-	-	-	0.367
67	693.750	25.2	97	62.65	65	45.58	85	15	0.13	-	-	-	-	0.367
68	684.375	26.9	97	62.97	65	45.91	87	15	2.14	-	-	-	-	0.368
69	675.000	27.0	97	62.69	65	46.29	88	-	-	-	-	-	-	0.371
70	665.625	25.9	101	63.42	65	46.74	89	-	-	-	-	-	-	0.378
71	656.250	27.8	101	62.45	65	46.47	90	16	0.49	-	-	-	-	0.380
72	646.875	26.6	101	61.23	82	44.77	90	16	1.39	-	-	-	-	0.370
73	637.500	25.6	101	63.92	83	42.71	90	16	0.44	-	-	-	-	0.358
74	628.125	25.6	101	63.34	73	42.81	91	16	2.58	-	-	-	-	0.358
75	618.750	25.8	101	62.93	76	43.22	92	-	-	-	-	-	-	0.361
76	609.375	26.0	105	63.99	73	43.53	93	-	-	-	-	-	-	0.365
77	600.000	27.6	105	64.60	86	43.86	94	17	1.06	-	-	-	-	0.370
78	590.625	26.7	105	64.17	73	43.82	96	17	2.97	-	-	-	-	0.373
79	581.250	25.8	105	64.60	94	43.58	97	-	-	-	-	-	-	0.377
80	571.875	24.2	105	64.57	94	41.50	97	-	-	-	-	-	-	0.372
81	562.500	24.0	105	66.69	88	39.99	97	-	-	-	-	-	-	0.364
82	553.125	22.6	109	65.76	90	40.39	98	-	-	-	-	-	-	0.369
83	543.750	23.1	109	68.90	94	40.60	99	18	1.57	-	-	-	-	0.373
84	534.375	23.0	109	68.06	98	41.10	100	18	3.18	-	-	-	-	0.380
85	525.000	21.8	108	67.80	97	40.97	102	-	-	-	-	-	-	0.383
86	515.625	21.1	111	69.09	93	40.48	102	-	-	-	-	-	-	0.384
87	506.250	20.5	101	67.29	93	38.77	103	19	0.23	-	-	-	-	0.379
88	496.875	19.8	101	71.48	98	36.71	104	-	-	-	-	-	-	0.370
89	487.500	19.8	105	71.62	99	36.85	104	19	1.97	-	-	-	-	0.371
90	478.125	20.4	113	71.51	98	37.16	105	14	1.56	19	3.62	-	-	0.370
91	468.750	20.8	113	72.13	105	37.29	106	-	-	-	-	-	-	0.372
92	459.375	20.4	115	72.50	105	37.34	108	-	-	-	-	-	-	0.371
93	450.000	21.7	116	74.22	105	37.49	109	20	0.75	-	-	-	-	0.373
94	440.625	22.2	117	75.31	103	36.64	109	15	1.53	20	2.64	-	-	0.366
95	431.250	21.8	117	72.18	92	35.27	110	20	3.34	-	-	-	-	0.358
96	421.875	21.1	117	75.17	99	33.81	111	20	3.04	-	-	-	-	0.348

Table C-7. BARRIER VII Results for Design Configuration L (Continued)

Impact At Node (No.)	Impact Distance Upstream of Bridge Post (in.)	Maximum Pocket Angle (deg.)	@ Node	Maximum Force (kips)	@ Node	Maximum Deflection (in.)	@ Node	Post #	Snag (in.)	Post #	Snag (in.)	Post #	Snag (in.)	Vehicle Parallel Time (sec)
97	412.500	22.1	118	77.67	109	34.04	112	20	4.5	-	-	-	-	0.350
98	403.125	20.5	118	76.80	101	31.18	112	16	1.32	20	3.97	-	-	0.335
99	393.750	21.1	118	75.70	101	31.31	112	20	5.14	21	1.1	-	-	0.334
100	384.375	21.3	118	78.70	106	30.83	113	21	3.06	-	-	-	-	0.330
101	375.000	21.6	121	78.24	113	30.80	114	17	3.11	21	4.44	-	-	0.329
102	365.625	20.5	120	82.07	105	28.95	115	17	1.55	21	4.43	-	-	0.321
103	356.250	21.4	121	80.51	105	29.04	116	21	5.42	22	2.13	-	-	0.320
104	346.875	22.0	121	78.84	113	28.85	116	22	4.07	-	-	-	-	0.319
105	337.500	22.8	123	80.60	105	28.74	117	18	3.07	22	5.55	-	-	0.320
106	328.125	22.5	123	82.99	117	27.43	118	18	1.38	22	6.02	-	-	0.315
107	318.750	23.9	125	84.80	110	27.39	118	22	6.83	23	3.93	-	-	0.319
108	309.375	23.9	125	83.96	110	27.13	119	23	5.54	24	5.45	-	-	0.323
109	300.000	23.4	125	82.64	109	26.62	120	19	3.29	23	6.8	24	7.33	0.328
110	290.625	22.8	125	83.76	118	25.61	121	19	1.44	23	7.04	24	7.67	0.329
111	281.250	23.4	125	82.94	113	25.43	122	23	7.76	24	9.13	-	-	0.336
112	271.875	23.6	125	81.81	121	25.00	123	20	5.11	24	10.21	-	-	0.342
113	262.500	23.2	125	82.53	122	24.35	124	20	3.83	21	6.52	24	10.9	0.345
114	253.125	22.2	125	83.50	117	23.45	124	20	2.08	21	5.4	24	11.1	0.343
115	243.750	21.4	125	85.96	117	22.96	125	21	4.01	22	6.47	25	7.91	0.347
116	234.375	20.1	127	81.97	117	22.37	126	21	2.5	22	5.55	25	9.3	0.360
117	225.000	19.3	129	85.90	123	21.13	127	23	6.69	24	10.9	25	9.6	0.354
118	215.625	18.7	129	89.87	121	20.55	127	23	5.69	24	10.5	25	10.1	0.343
119	206.250	17.5	129	86.99	123	19.48	128	24	9.7	25	9.8	26	4.8	0.333
120	196.875	16.6	132	81.40	126	17.92	128	24	8.9	25	9.7	26	5.4	0.321
121	187.500	16.5	132	84.69	127	16.41	131	24	7.8	25	9.8	26	6.7	0.313
122	178.125	15.8	133	90.45	129	16.15	131	24	6.7	25	9.8	26	7.8	0.305
123	168.750	15.2	134	95.25	129	15.83	132	25	9.2	26	8.4	-	-	0.297
124	159.375	15.6	136	90.63	129	15.65	132	25	8.3	26	8.6	-	-	0.291
125	150.000	17.7	137	87.51	129	14.62	132	25	7.4	26	9.1	-	-	0.281
126	140.625	19.2	137	88.61	133	14.48	135	26	6.3	26	9.2	-	-	0.274
127	131.250	20.2	137	95.52	133	14.35	136	25	4.7	26	9.1	-	-	0.283
128	121.875	21.1	137	96.66	133	15.20	139	25	2.8	26	8.4	-	-	0.305
129	112.500	20.4	138	98.09	133	16.25	139	26	7.6	-	-	-	-	0.326

Appendix D. Vehicle Center of Gravity Determination

MWTSP-1			Vehicle:	2003 Dodge Ram 1500QC			
				Vehicle CG Determination			
VEHICLE	Equipment	Weight	Long CG	Vert CG		HOR M	Vert M
+	Unbalasted Truck	5065	62.5	28.3		316562.5	143339.5
+	Brake receivers/wires	5	116	51		580	255
+	Brake Frame	5	34	31		170	155
+	Brake Cylinder	22	74	29		1628	638
+	Strobe Battery	6	74	30		444	180
+	Hub	27	0	14.875		0	401.625
+	CG Plate (EDRs)	8	54	32		432	256
-	Battery	-43	-7	45		301	-1935
-	Oil	-8	8	19		-64	-152
-	Interior	-56	44	24		-2464	-1344
-	Fuel	-140	111	20		-15540	-2800
-	Coolant	-17	-18	35		306	-595
-	Washer fluid	-9	-15	35		135	-315
BALLAST	Water	130	111	20		14430	2600
	Misc. (DTS equip)	20	74	27		1480	540
	Misc.		0	0		0	0
						318400.5	141224.1
	TOTAL WEIGHT	5015				63.48963	28.16034

wheel base 140.25

NCHRP 350 Targets		CURRENT	Difference
Test Inertial Weight	5000	5015	15.0
Long CG	62	63.49	1.48963
Vert CG	28	28.16	0.16034

Note, Long. CG is measured from front axle of test vehicle

Curb Weight				Actual test inertial weight		
	Left	Right			Left	Right
Front	1467	1366		Front	1408	1377
Rear	1106	1126		Rear	1104	1120
FRONT	2833			FRONT	2785	
REAR	2232			REAR	2224	
TOTAL	5065			TOTAL	5009	

Figure D-1. Vehicle Mass Distribution, Test No. MWTSP-1

MWTSP-2			Vehicle:	2002 Dodge Ram 1500QC		
			Vehicle CG Determination			
VEHICLE	Equipment	Weight	Long CG	Vert CG	HOR M	Vert M
+	Unbalasted Truck	5138	61.875	28.08	317913.8	144275
+	Brake receivers/wires	5	116	51	580	255
+	Brake Frame	5	34	31	170	155
+	Brake Cylinder	22	74	29	1628	638
+	Strobe Battery	6	74	30	444	180
+	Hub	27	0	14.875	0	401.625
+	CG Plate (EDRs)	8	54	32	432	256
-	Battery	-47	-7	45	329	-2115
-	Oil	-8	8	19	-64	-152
-	Interior	-79	44	24	-3476	-1896
-	Fuel	-149	111	20	-16539	-2980
-	Coolant	-19	-18	35	342	-665
-	Washer fluid	-3	-15	35	45	-105
BALLAST	Water	80	111	20	8880	1600
	Misc. (DTS equip)	20	74	27	1480	540
	Misc.		0	0	0	0
					312164.8	140387.7
	TOTAL WEIGHT	5006			62.35812	28.04388

wheel base   140.25

NCHRP 350 Targets		CURRENT	Difference
Test Inertial Weight	5000	5006	6.0
Long CG	62	62.36	0.35812
Vert CG	28	28.04	0.04388

Note, Long. CG is measured from front axle of test vehicle

Curb Weight		
	Left	Right
Front	1452	1413
Rear	1134	1139
FRONT	2865	
REAR	2273	
TOTAL	5138	

Actual test inertial weight		
	Left	Right
Front	1411	1357
Rear	1088	1137
FRONT	2768	
REAR	2225	
TOTAL	4993	

Figure D-2. Vehicle Mass Distribution, Test No. MWTSP-2

MWTSP-3			Vehicle:	2002 Kia Rio	
			Vehicle CG Determination		
VEHICLE	Equipment	Weight	Long CG		HOR M
+	Unbalasted Car	2399	35.69		85629.75
+	Brake receivers/wire:	5	130.5		652.5
+	Brake Frame	10	29.5		295
+	Brake Cylinder	22	65		1430
+	Strobe Battery	6	65.5		393
+	Hub	17	0		0
+	CG Plate (EDRs)	8	35		280
-	Battery	-29	-9		261
-	Oil	-5	8		-40
-	Interior	-40	44		-1760
-	Fuel	-26	78		-2028
-	Coolant	-5	-18		90
-	Washer fluid	-3	0		0
BALLAST	Water	40	78		3120
	Misc.		0		0
	DTS	20	65		1300
					89623.25
	TOTAL WEIGHT	2419			37.04971

wheel base 95.25

NCHRP 350 Targets		CURRENT	Difference
Test Inertial Weight	2420 (+/-)55	2419	-1.0
Long CG	39 (+/-)4	37.05	-1.95029

Note, Long. CG is measured from front axle of test vehicle

Dummy = 166lbs.

Curb Weight		
	Left	Right
Front	741	759
Rear	463	436
FRONT	1500	
REAR	899	
TOTAL	2399	

Actual test inertial weight		
	Left	Right
Front	699	761
Rear	436	498
FRONT	1460	
REAR	934	
TOTAL	2394	

Figure D-3. Vehicle Mass Distribution, Test No. MWTSP-3

Appendix E.   Vehicle Deformation Records

VEHICLE PRE/POST CRUSH INFO
Set-1

TEST: MWTSP-1
VEHICLE: 2003 Dodge Ram

Note: If impact is on driver side need to enter negative number for Y

POINT	X	Y	Z	X'	Y'	Z'	DEL X	DEL Y	DEL Z
1	27 1/2	12 1/2	1 1/4	27 1/2	12 3/4	1 1/4	0	1/4	0
2	30	18	- 1/4	30	17 3/4	- 1/4	0	- 1/4	0
3	31	24 1/2	-1	31 1/2	24 1/2	-1	1/2	0	0
4	29	30 1/2	- 1/2	28 1/2	30 1/2	- 1/2	- 1/2	0	0
5	22 1/2	10 3/4	- 1/2	22 1/2	10 3/4	- 3/4	0	0	- 1/4
6	24 1/2	16 3/4	-4	24 1/2	16 3/4	-4	0	0	0
7	26	24 1/2	-5 1/2	26	24	-5 1/2	0	- 1/2	0
8	25 3/4	30 1/2	-5 3/4	25 1/2	30	-5 3/4	- 1/4	- 1/2	0
9	15	1 1/4	-1 1/4	15	1 1/4	-1 1/2	0	0	- 1/4
10	17 3/4	10	-3	17 3/4	10	-3	0	0	0
11	19 1/2	15 3/4	-7 1/4	19 1/2	16	-7	0	1/4	1/4
12	20 1/4	23 1/2	-8 3/4	20	24	-8 1/2	- 1/4	1/2	1/4
13	20 1/4	30 1/2	-9	20 1/4	30 1/2	-9	0	0	0
14	10	1 1/2	-2 1/4	10	1 1/2	-2 1/2	0	0	- 1/4
15	14	9 1/4	-4 1/4	13 1/2	9	-4 1/4	- 1/2	- 1/4	0
16	14 3/4	16 1/4	-9	14 3/4	16 1/4	-9	0	0	0
17	15	24 1/2	-9	15	24 1/2	-9	0	0	0
18	15	30 1/2	-9 1/2	14 3/4	30 1/2	-9 1/2	- 1/4	0	0
19	5 1/2	3/4	-2 1/4	5 1/4	3/4	-2 1/2	- 1/4	0	- 1/4
20	8 1/2	9 1/4	-5 1/4	8 1/2	9 1/4	-5	0	0	1/4
21	10 1/2	16	-9	10 1/2	16	-8 3/4	0	0	1/4
22	10 1/2	23 3/4	-8 3/4	10 1/2	24	-8 3/4	0	1/4	0
23	9 3/4	30 1/2	-8 3/4	9 3/4	30 1/2	-8 3/4	0	0	0
24	1	1 1/4	-2 1/4	1 1/4	1	-2 1/4	1/4	- 1/4	0
25	1	6 1/2	-2 1/4	1	6 1/2	-2 1/4	0	0	0
26	1	12 1/4	-5	1	12 1/4	-5	0	0	0
27	1	19 1/2	-5	1	19 1/2	-5	0	0	0
28	1	27 1/2	-4 1/2	1	27 1/4	-4 3/4	0	- 1/4	- 1/4
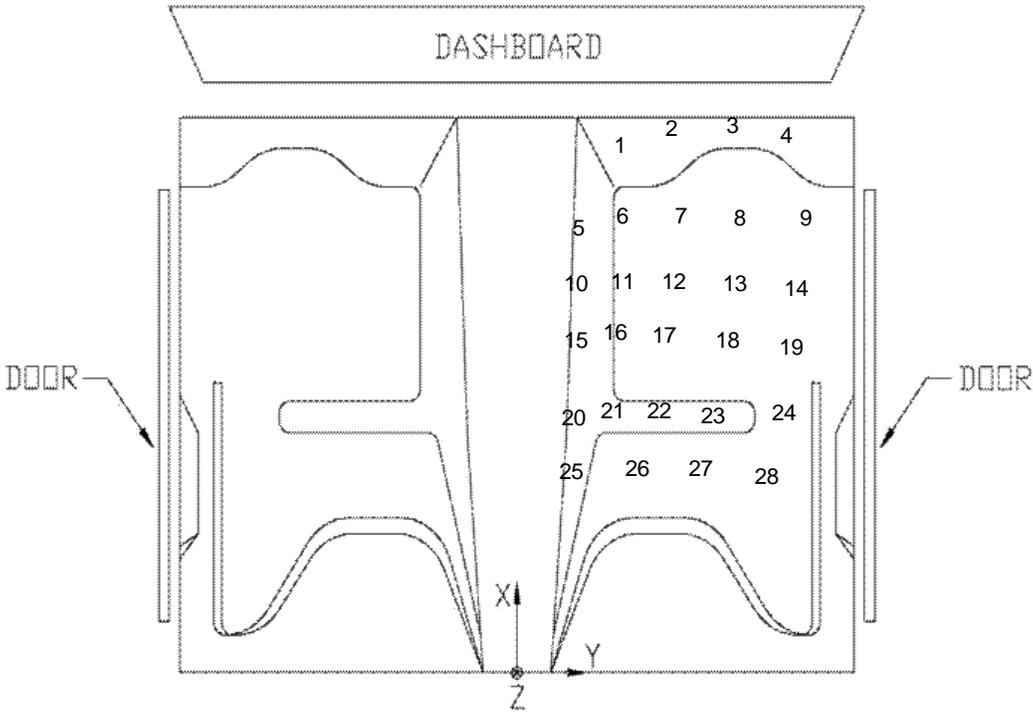
Figure E-1. Floor Board Deformation Data – Set 1, Test No. MWTSP-1

218

TEST: MWTSP-1
VEHICLE: 2003 Dodge Ram

POINT	X	Y	Z	X'	Y'	Z'	DEL X	DEL Y	DEL Z
1	50 1/2	14 3/4	1/2	50 1/2	15	1/2	0	1/4	0
2	53	20 1/4	-1 1/2	53	20	-1 1/4	0	- 1/4	1/4
3	54	26 3/4	-2	54 1/2	26 3/4	-2	1/2	0	0
4	52	32 3/4	-1	51 1/2	32 3/4	-1 1/4	- 1/2	0	- 1/4
5	45 1/2	13	-1 1/2	45 1/2	13	-1 3/4	0	0	- 1/4
6	47 1/2	19	-4 3/4	47 1/2	19	-4 3/4	0	0	0
7	49	26 3/4	-6 1/4	49	26 1/4	-6 1/2	0	- 1/2	- 1/4
8	48 3/4	32 3/4	-6	48 1/2	32 1/4	-6 1/2	- 1/4	- 1/2	- 1/2
9	38	3 1/2	-2 1/4	38	3 1/2	-2 1/2	0	0	- 1/4
10	40 3/4	12 1/4	-3 1/2	40 3/4	12 1/4	-3 3/4	0	0	- 1/4
11	42 1/2	18	-7 3/4	42 1/2	18 1/4	-8	0	1/4	- 1/4
12	43 1/4	25 3/4	-9 1/4	43	26 1/4	-9 1/2	- 1/4	1/2	- 1/4
13	43 1/4	32 3/4	-9 1/4	43 1/4	32 3/4	-9 1/2	0	0	- 1/4
14	33	3 3/4	-3	33	3 3/4	-3 1/2	0	0	- 1/2
15	37	11 1/2	-4 3/4	36 1/2	11 1/4	-5	- 1/2	- 1/4	- 1/4
16	37 3/4	18 1/2	-9 1/2	37 3/4	18 1/2	-9 3/4	0	0	- 1/4
17	38	26 3/4	-9 1/2	38	26 3/4	-9 1/2	0	0	0
18	38	32 3/4	-9 3/4	37 3/4	32 3/4	-10	- 1/4	0	- 1/4
19	28 1/2	3	-3	28 1/4	3	-3 1/2	- 1/4	0	- 1/2
20	31 1/2	11 1/2	-5 3/4	31 1/2	11 1/2	-6	0	0	- 1/4
21	33 1/2	18 1/4	-9	33 1/2	18 1/4	-9 1/4	0	0	- 1/4
22	33 1/2	26	-9	33 1/2	26 1/4	-9 1/4	0	1/4	- 1/4
23	32 3/4	32 3/4	-9	32 3/4	32 3/4	-9 1/4	0	0	- 1/4
24	24	3 1/2	-2 3/4	24 1/4	3 1/4	-3	1/4	- 1/4	- 1/4
25	24	8 3/4	-2 1/2	24	8 3/4	-2 1/4	0	0	1/4
26	24	14 1/2	-5 1/4	24	14 1/2	-5 1/2	0	0	- 1/4
27	24	21 3/4	-5	24	21 3/4	-5 1/4	0	0	- 1/4
28	24	29 3/4	-4 1/2	24	29 1/2	-5	0	- 1/4	- 1/2

Figure E-2. Floor Board Deformation Data – Set 2, Test No. MWTSP-1

Vehicle Type: 2003 Dodge Ram

OCDI = XXABCDEFGHI

XX = location of occupant compartment deformation

A = distance between the dashboard and a reference point at the rear of the occupant compartment, such as the top of the rear seat or the rear of the cab on a pickup

B = distance between the roof and the floor panel

C = distance between a reference point at the rear of the occupant compartment and the motor panel

D = distance between the lower dashboard and the floor panel

E = interior width

F = distance between the lower edge of right window and the upper edge of left window

G = distance between the lower edge of left window and the upper edge of right window

H= distance between bottom front corner and top rear corner of the passenger side window

I= distance between bottom front corner and top rear corner of the driver side window

Severity Indices

0 - if the reduction is less than 3%
1 - if the reduction is greater than 3% and less than or equal to 10 %
2 - if the reduction is greater than 10% and less than or equal to 20 %
3 - if the reduction is greater than 20% and less than or equal to 30 %
4 - if the reduction is greater than 30% and less than or equal to 40 %

where,
1 = Passenger Side
2 = Middle
3 = Driver Side

Location:

Measurement	Pre-Test (in.)	Post-Test (in.)	Change (in.)	% Difference	Severity Index
A1	55.50	55.50	0.00	0.00	0
A2	54.00	54.00	0.00	0.00	0
A3	56.25	56.25	0.00	0.00	0
B1	48.00	47.50	-0.50	-1.04	0
B2	42.50	42.50	0.00	0.00	0
B3	47.50	47.50	0.00	0.00	0
C1	64.00	64.25	0.25	0.39	0
C2	47.00	46.50	-0.50	-1.06	0
C3	67.00	66.75	-0.25	-0.37	0
D1	22.50	22.50	0.00	0.00	0
D2	13.00	13.25	0.25	1.92	0
D3	22.50	22.50	0.00	0.00	0
E1	65.50	65.50	0.00	0.00	0
E3	65.00	64.75	-0.25	-0.38	0
F	55.50	55.25	-0.25	-0.45	0
G	58.00	58.00	0.00	0.00	0
H	38.50	38.75	0.25	0.65	0
I	39.00	39.00	0.00	0.00	0

Note: Maximum severity index for each variable (A-I) is used for determination of final OCDI value

	XX	A	B	C	D	E	F	G	H	I
Final OCDI:	RF	0	0	0	0	0	0	0	0	0

Figure E-3. Occupant Compartment Deformation Index, Test No. MWTSP-1

Date:	1/28/2008	Test Number:	MWTSP-1		
Make:	Dodge	Model:	Ram 1500 Q.C.	Year:	2003

			in.	(mm)
Distance from C.G. to reference line - L_{REF}:			104	(2642)
Width of contact and induced crush - Field L:			48.75	(1238)
Crush measurement spacing interval (L/5) - I:			9.75	(248)
Distance from center of vehicle to center of Field L - D_{FL}:			14.375	(365)
Width of Contact Damage:			30.75	(781)
Distance from center of vehicle to center of contect damage - D_C:			25.375	(645)

	Crush Measurement		Lateral Location		Original Profile Measurement		Dist. Between Ref. Lines		Actual	Crush
	in.	(mm)	in.	(mm)	in.	(mm)	in.	(mm)	in.	(mm)
C_1	8	(203)	-10	-(254)	10.75	(273)	-9.25	-(235)	6.5	(165)
C_2	15	(381)	-0.25	-(6)	10.25	(260)			14	(356)
C_3	24.75	(629)	9.5	(241)	10.688	(271)			23.3125	(592)
C_4	18.5	(470)	19.25	(489)	12.359	(314)			15.3906	(391)
C_5	37.25	(946)	29	(737)	15.688	(398)			30.8125	(783)
C_6	33.25	(845)	38.75	(984)	29	(737)			13.5	(343)
C_{MAX}	24.75	(629)	9.5	(241)	10.688	(271)			23.3125	(592)

Figure E-4. Exterior Vehicle Crush (NASS) - Front, Test No. MWTSP-1

Date: __1/28/2008__   Test Number: __MWTSP-1__

Make: __Dodge__   Model: __Ram 1500 Q.C.__   Year: __2003__

	in.	(mm)
Distance from centerline to reference line - L_{REF}:	51.25	(1302)
Width of contact and induced crush - Field L:	63.5	(1613)
Crush measurement spacing interval (L/5) - I:	12.7	(323)
Distance from vehicle c.g. to center of Field L - D_{FL}:	71.75	(1822)
Width of Contact Damage:	63.5	(1613)
Distance from vehicle c.g. to center of contect damage - D_C:	71.75	(1822)

	Crush Measurement		Longitudinal Location		Original Profile Measurement		Dist. Between Ref. Lines		Actual Crush	
	in.	(mm)	in.	(mm)	in.	(mm)	in.	(mm)	in.	(mm)
C_1	10.5	(267)	40	(1016)	11.25	(286)	1.25	(32)	-2	-(51)
C_2	12.75	(324)	52.7	(1339)	10.5	(267)			1	(25)
C_3	6.5	(165)	65.4	(1661)	10.5	(267)			-5.25	-(133)
C_4	NA	NA	78.1	(1984)	0	()			-	-
C_5	30.5	(775)	90.8	(2306)	13.125	(333)			16.125	(410)
C_6	NA	NA	103.5	(2629)	37	(940)			-	-
C_{MAX}	30.5	(775)	90.8	(2306)	13.125	(333)			16.125	(410)

Figure E-5. Exterior Vehicle Crush (NASS) - Side, Test No. MWTSP-1

VEHICLE PRE/POST CRUSH INFO
Set-1

TEST: MWTSP-2   Note: If impact is on driver side need to
VEHICLE: 2002 Dodge Ram   enter negative number for Y

POINT	X	Y	Z	X'	Y'	Z'	DEL X	DEL Y	DEL Z
1	24 3/4	11	0	24 3/4	11	0	0	0	0
2	27 3/4	16 1/2	-1 3/4	27 1/2	16 1/2	-1 1/4	- 1/4	0	1/2
3	31	22 3/4	-3 1/4	31	22 1/2	-3	0	- 1/4	1/4
4	28 1/2	29 1/4	- 3/4	27 1/2	28	- 1/4	-1	-1 1/4	1/2
5	21	9 1/2	-1 1/2	21	10	-1	0	1/2	1/2
6	21 3/4	15 1/4	-4	21 1/2	15 3/4	-4	- 1/4	1/2	0
7	23	23	-7	23 1/4	22 1/2	-7	1/4	- 1/2	0
8	24 1/2	30 1/2	-5 3/4	24 1/4	30	-5 3/4	- 1/4	- 1/2	0
9	14 1/2	1	-3	14 1/2	1	-3	0	0	0
10	16	9	-3	16 1/4	8 3/4	-3	0	- 1/4	0
11	18 1/2	15 1/2	-7 3/4	18 1/2	15 1/2	-7 3/4	0	0	0
12	20	23	-8 1/4	20 1/4	23	-8 3/4	1/4	0	- 1/2
13	19 3/4	31 1/2	-8	20	31 1/4	-8 1/4	1/4	- 1/4	- 1/4
14	10 1/2	1/4	-3 1/2	10 1/2	1/4	-3 1/2	0	0	0
15	10 1/2	7 1/2	-3	10 3/4	7 1/2	-2 3/4	1/4	0	1/4
16	13	12	-9 1/4	13 1/4	12 1/4	-9 1/4	1/4	1/4	0
17	13 3/4	21	-8 1/2	14	20 1/2	-8 1/2	1/4	- 1/2	0
18	15	30 1/4	-7 3/4	15	29 3/4	-7 1/2	0	- 1/2	1/4
19	6	1 1/4	-3 1/2	6 1/4	1 1/4	-3 1/4	1/4	0	1/4
20	6 1/4	7 1/2	-3 1/4	6 1/4	7 3/4	-3	0	1/4	1/4
21	8 3/4	13 1/2	-9	8 3/4	12 1/2	-9	0	-1	0
22	9	21 3/4	-8	9	21 1/4	-8	0	- 1/2	0
23	8 3/4	30 1/2	-7 1/4	8 3/4	30 1/4	-7	0	- 1/4	1/4
24	1 1/2	1	-3	1 1/2	1	-2 3/4	0	0	1/4
25	1 1/2	7 1/2	-2 1/2	1 1/2	7 1/2	-2 1/4	0	0	1/4
26	1	13 1/4	-4 1/2	1	13 1/2	-4 1/2	0	1/4	0
27	1	21 1/2	-3 3/4	1	21 1/4	-3 1/2	0	- 1/4	1/4
28	1	28 3/4	-3	1	28 3/4	-2 3/4	0	0	1/4
29							0	0	0
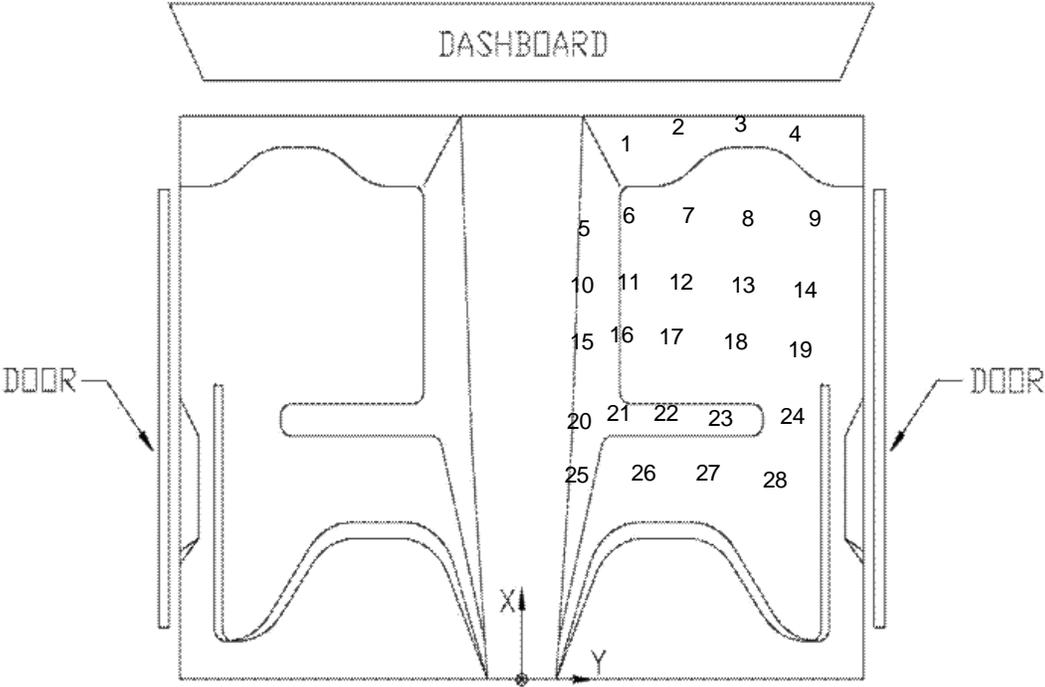
Figure E-6. Floor Board Deformation Data – Set 1, Test No. MWTSP-2

VEHICLE PRE/POST CRUSH INFO
Set-2

TEST: MWTSP-2
VEHICLE: 2002 Dodge Ram

Note: If impact is on driver side need to
enter negative number for Y

| POINT	X	Y	Z	X'	Y'	Z'	DEL X	DEL Y	DEL Z
1	47 3/4	12 1/4	0	47 3/4	12 1/4	1/4	0	0	1/4
2	50 3/4	17 3/4	-2	50 1/2	17 3/4	-1 1/4	- 1/4	0	3/4
3	54	24	-3 1/2	54	23 3/4	-3 1/4	0	- 1/4	1/4
4	51 1/2	30 1/2	-1 1/2	50 1/2	29 1/4	- 1/2	-1	-1 1/4	1
5	44	10 3/4	-1 1/2	44	11 1/4	- 3/4	0	1/2	3/4
6	44 3/4	16 1/2	-4 1/4	44 1/2	17	-3 3/4	- 1/4	1/2	1/2
7	46	24 1/4	-7 1/2	46 1/4	23 3/4	-7	1/4	- 1/2	1/2
8	47 1/2	31 3/4	-6 1/2	47 1/4	31 1/4	-6	- 1/4	- 1/2	1/2
9	37 1/2	2 1/4	-2 3/4	37 1/2	2 1/4	-2 1/4	0	0	1/2
10	39	10 1/4	-3	39 1/4	10	-2 1/2	0	- 1/4	1/2
11	41 1/2	16 3/4	-8	41 1/2	16 3/4	-7 3/4	0	0	1/4
12	43	24 1/4	-9	43 1/4	24 1/4	-8 3/4	1/4	0	1/4
13	42 3/4	32 3/4	-9	43	32 1/2	-8 1/2	1/4	- 1/4	1/2
14	33 1/2	1 1/2	-3	33 1/2	1 1/2	-3	0	0	0
15	33 1/2	8 3/4	-2 3/4	33 3/4	8 3/4	-2 1/2	1/4	0	1/4
16	36	13 1/4	-9 1/2	36 1/4	13 1/2	-9 1/4	1/4	1/4	1/4
17	36 3/4	22 1/4	-9	37	21 3/4	-9	1/4	- 1/2	0
18	38	31 1/2	-8 1/2	38	31	-8	0	- 1/2	1/2
19	29	2 1/2	-3	29 1/4	2 1/2	-2 3/4	1/4	0	1/4
20	29 1/4	8 3/4	-3	29 1/4	9	-3	0	1/4	0
21	31 3/4	14 3/4	-9	31 3/4	13 3/4	-9	0	-1	0
22	32	23	-8 1/2	32	22 1/2	-8 1/2	0	- 1/2	0
23	31 3/4	31 3/4	-8	31 3/4	31 1/2	-7 3/4	0	- 1/4	1/4
24	24 1/2	2 1/4	-2 1/2	24 1/2	2 1/4	-2 1/4	0	0	1/4
25	24 1/2	8 3/4	-2 1/4	24 1/2	8 3/4	-2	0	0	1/4
26	24	14 1/2	-4 1/2	24	14 3/4	-4 1/2	0	1/4	0
27	24	22 3/4	-4 1/4	24	22 1/2	-4 1/4	0	- 1/4	0
28	24	30	-4	24	30	-3 1/2	0	0	1/2
29							0	0	0

Figure E-7. Floor Board Deformation Data – Set 2, Test No. MWTSP-2

224

Occupant Compartment Deformation Index (OCDI)

Test No.   MWTSP-2
Vehicle Type: 2002 Dodge Ram

OCDI = XXABCDEFGHI

XX = location of occupant compartment deformation

A = distance between the dashboard and a reference point at the rear of the occupant compartment, such as the top of the rear seat or the rear of the cab on a pickup

B = distance between the roof and the floor panel

C = distance between a reference point at the rear of the occupant compartment and the motor panel

D = distance between the lower dashboard and the floor panel

E = interior width

F = distance between the lower edge of right window and the upper edge of left window

G = distance between the lower edge of left window and the upper edge of right window

H= distance between bottom front corner and top rear corner of the passenger side window

I= distance between bottom front corner and top rear corner of the driver side window

Severity Indices

0 - if the reduction is less than 3%
1 - if the reduction is greater than 3% and less than or equal to 10 %
2 - if the reduction is greater than 10% and less than or equal to 20 %
3 - if the reduction is greater than 20% and less than or equal to 30 %
4 - if the reduction is greater than 30% and less than or equal to 40 %

where,
1 = Passenger Side
2 = Middle
3 = Driver Side

Location:

Measurement	Pre-Test (in.)	Post-Test (in.)	Change (in.)	% Difference	Severity Index
A1	57.00	57.00	0.00	0.00	0
A2	50.25	50.25	0.00	0.00	0
A3	57.00	57.00	0.00	0.00	0
B1	47.00	47.00	0.00	0.00	0
B2	42.25	42.25	0.00	0.00	0
B3	47.25	47.25	0.00	0.00	0
C1	68.50	68.50	0.00	0.00	0
C2	47.50	47.50	0.00	0.00	0
C3	66.75	66.50	-0.25	-0.37	0
D1	23.50	23.00	-0.50	-2.13	0
D2	13.50	13.25	-0.25	-1.85	0
D3	22.75	23.00	0.25	1.10	0
E1	65.25	63.25	-2.00	-3.07	1
E3	64.00	64.00	0.00	0.00	0
F	58.50	58.50	0.00	0.00	0
G	59.00	59.00	0.00	0.00	0
H	37.00	37.25	0.25	0.68	0
I	36.75	37.00	0.25	0.68	0

Note: Maximum severity index for each variable (A-I) is used for determination of final OCDI value

```
             XX A B C D E F G H I
Final OCDI:  RF  0 0 0 0 1 0 0 0 0
```

Figure E-8. Occupant Compartment Deformation Index, Test No. MWTSP-2

Date: 7/7/2008   **Test Number:** MWTSP-2

Make: Dodge   **Model:** Ram 1500 Q.C.   **Year:** 2002

	in.	(mm)
Distance from C.G. to reference line - L_{REF}:	111	(2819)
Width of contact and induced crush - Field L:	48	(1219)
Crush measurement spacing interval (L/5) - I:	9.6	(244)
Distance from center of vehicle to center of Field L - D_{FL}:	15	(381)
Width of Contact Damage:	25	(635)
Distance from center of vehicle to center of contect damage - D_C:	26.5	(673)

	Crush Measurement		Lateral Location		Original Profile Measurement		Dist. Between Ref. Lines		Actual Crush	
	in.	(mm)	in.	(mm)	in.	(mm)	in.	(mm)	in.	(mm)
C_1	9.25	(235)	-9	-(229)	10.625	(270)	-1.125	-(29)	-0.25	-(6)
C_2	8.5	(216)	0.6	(15)	10.25	(260)			-0.625	-(16)
C_3	15	(381)	10.2	(259)	10.75	(273)			5.375	(137)
C_4	19	(483)	19.8	(503)	12.453	(316)			7.6719	(195)
C_5	NA	NA	29.4	(747)	15.797	(401)			-	-
C_6	NA	NA	39	(991)	29	(737)			-	-
C_{MAX}	35	(889)	26	(660)	14.5	(368)			21.625	(549)

Figure E-9. Exterior Vehicle Crush (NASS) - Front, Test No. MWTSP-2

Date: _____7/7/2008_____   Test Number: _____MWTSP-2_____

Make: ___Dodge___   Model: ___Ram 1500 Q.C.___   Year: ____2002____

		in.	(mm)
Distance from centerline to reference line - L_{REF}:		50.5	(1283)
Width of contact and induced crush - Field L:		227.75	(5785)
Crush measurement spacing interval (L/5) - I:		45.55	(1157)
Distance from vehicle c.g. to center of Field L - D_{FL}:		-15.13	-(384)
Width of Contact Damage:		227.75	(5785)
Distance from vehicle c.g. to center of contect damage - D_C:		-13.5	-(343)

|	Crush Measurement		Longitudinal Location		Original Profile Measurement		Dist. Between Ref. Lines		Actual Crush	
	in.	(mm)	in.	(mm)	in.	(mm)	in.	(mm)	in.	(mm)
C_1	17	(432)	-129	-(3277)	16	(406)	0.5	(13)	0.5	(13)
C_2	13	(330)	-83.45	-(2120)	10.5	(267)			2	(51)
C_3	14	(356)	-37.9	-(963)	11.604	(295)			1.8958	(48)
C_4	12	(305)	7.65	(194)	11.25	(286)			0.25	(6)
C_5	na	na	53.2	(1351)	10.5	(267)			-	-
C_6	44	(1118)	98.75	(2508)	36.125	(918)			7.375	(187)
C_{MAX}	36	(914)	90.5	(2299)	16.375	(416)			19.125	(486)

Figure E-10. Exterior Vehicle Crush (NASS) - Side, Test No. MWTSP-2

VEHICLE PRE/POST CRUSH INFO

TEST: MWTSP-3
VEHICLE: 2002 Kia Rio Sedan

Note: If impact is on driver side need to enter negative number for Y

POINT	X	Y	Z	X'	Y'	Z'	DEL X	DEL Y	DEL Z
1	28.5	5.5	-0.75	28.25	5	-2.5	-0.25	-0.5	-1.75
2	30	10	-3	29.5	10.25	-2.25	-0.5	0.25	0.75
3	30	16	-2.75	28.25	15	-2.25	-1.75	-1	0.5
4	24.5	24.25	-2	23.75	23.75	-2	-0.75	-0.5	0
5	24.25	4	-5.25	24	4	-5.25	-0.25	0	0
6	26.75	10	-6	26.5	9.5	-5.5	-0.25	-0.5	0.5
7	26	16.25	-6.25	26	15.75	-6.25	0	-0.5	0
8	23	24	-5.5	23	24.25	-5.5	0	0.25	0
9	19.75	4	-8	19.5	4.25	-8	-0.25	0.25	0
10	20.25	11	-8.5	20	10.5	-8.5	-0.25	-0.5	0
11	20	17.5	-7.5	20	16.25	-7.5	0	-1.25	0
12	20	24.25	-6.75	20	23.5	-7	0	-0.75	-0.25
13	15.75	4.5	-0.25	15.75	5	-0.5	0	0.5	-0.25
14	15.75	12	-8.25	15.75	12	-8.5	0	0	-0.25
15	15.5	17.25	-7.5	15.5	17	-7.5	0	-0.25	0
16	16	24.5	-7	16	24.5	-7	0	0	0
17	9.75	0.75	-4	9.75	0.75	-4	0	0	0
18	11	6	-8.5	11	6.25	-8.5	0	0.25	0
19	11.25	12	-8	11	11.5	-8.25	-0.25	-0.5	-0.25
20	11.5	18	-7.5	11.5	17.75	-7.75	0	-0.25	-0.25
21	11.25	24.5	-6	11.25	24.25	-6.75	0	-0.25	-0.75
22	5.5	2	-4	5.5	2	-4	0	0	0
23	7.5	6.75	-8.25	7.5	7	-8.25	0	0.25	0
24	7.5	13.25	-7.5	7.5	13	-7.5	0	-0.25	0
25	8.5	20.25	-7	8.5	20	-7	0	-0.25	0
26	0.5	1	-3	0.5	1	-3	0	0	0
27	1.25	7	-4.75	1.25	7.25	-4.75	0	0.25	0
28	1.25	13.75	-4.75	1.25	13.75	-5	0	0	-0.25
29	1.25	22.75	-3.25	1.25	23	-3.5	0	0.25	-0.25
30									

Figure E-11. Floor Board Deformation Data, Test No. MWTSP-3

Occupant Compartment Deformation Index (OCDI)

Test No.   MWTSP-3
Vehicle Type: 2002 Kia Rio Sedan

OCDI = XXABCDEFGHI

XX = location of occupant compartment deformation

A = distance between the dashboard and a reference point at the rear of the occupant compartment, such as the top of the rear seat or the rear of the cab on a pickup

B = distance between the roof and the floor panel

C = distance between a reference point at the rear of the occupant compartment and the motor panel

D = distance between the lower dashboard and the floor panel

E = interior width

F = distance between the lower edge of right window and the upper edge of left window

G = distance between the lower edge of left window and the upper edge of right window

H= distance between bottom front corner and top rear corner of the passenger side window

I= distance between bottom front corner and top rear corner of the driver side window

Severity Indices

0 - if the reduction is less than 3%
1 - if the reduction is greater than 3% and less than or equal to 10 %
2 - if the reduction is greater than 10% and less than or equal to 20 %
3 - if the reduction is greater than 20% and less than or equal to 30 %
4 - if the reduction is greater than 30% and less than or equal to 40 %

where,
1 = Passenger Side
2 = Middle
3 = Driver Side

Location:

Measurement	Pre-Test (in.)	Post-Test (in.)	Change (in.)	% Difference	Severity Index
A1	48.25	48.50	0.25	0.52	0
A2	47.50	47.25	-0.25	-0.53	0
A3	50.00	49.50	-0.50	-1.00	0
B1	41.50	41.50	0.00	0.00	0
B2	38.25	38.50	0.25	0.65	0
B3	38.50	39.00	0.50	1.30	0
C1	56.50	56.50	0.00	0.00	0
C2	43.00	43.25	0.25	0.58	0
C3	61.25	59.00	-2.25	-3.67	1
C4	25.25	22.50	-2.75	-10.89	2
D1	21.50	21.75	0.25	1.16	0
D2	19.25	19.25	0.00	0.00	0
D3	22.00	22.00	0.00	0.00	0
E1	52.75	52.50	-0.25	-0.47	0
E3	53.75	53.75	0.00	0.00	0
F	47.50	45.75	-1.75	-3.68	1
G	47.00	47.00	0.00	0.00	0
H	39.75	39.75	0.00	0.00	0
I	39.50	39.25	-0.25	-0.63	0

Note: Maximum severity index for each variable (A-I) is used for determination of final OCDI value

C4 Extra point measured from firewall/floorboard to seat bolt on the far right passenger side. (Max. crush area)

XX A B C D E F G H I
Final OCDI: RF 0 0 2 0 0 1 0 0 0

Figure E-12. Occupant Compartment Deformation Index, Test No. MWTSP-3

Date:	10/9/2008		Test Number:	MWTSP-3			
Make:	Kia		Model:	Rio Sedan		Year:	2002

		in.	(mm)
Distance from C.G. to reference line - L_{REF}:		82	(2083)
Width of contact and induced crush - Field L:		63.625	(1616)
Crush measurement spacing interval (L/5) - I:		12.725	(323)
Distance from center of vehicle to center of Field L - D_{FL}:		0.0125	()
Width of Contact Damage:		28	(711)
Distance from center of vehicle to center of contect damage - D_C:		16	(406)

	Crush Measurement		Lateral Location		Original Profile Measurement		Dist. Between Ref. Lines		Actual Crush	
	in.	(mm)	in.	(mm)	in.	(mm)	in.	(mm)	in.	(mm)
C_1	31.5	(800)	-31.8	-(808)	30.625	(778)	2.25	(57)	-1.375	-(35)
C_2	20	(508)	-19.08	-(485)	10.016	(254)			7.7344	(196)
C_3	24	(610)	-6.35	-(161)	7.75	(197)			14	(356)
C_4	24.5	(622)	6.375	(162)	7.75	(197)			14.5	(368)
C_5	29	(737)	19.1	(485)	9.9375	(252)			16.813	(427)
C_6	30	(762)	31.825	(808)	29.422	(747)			-1.672	-(42)
C_{MAX}	30	(762)	31.8	(808)	29.422	(747)			-1.672	-(42)

Figure E-13. Exterior Vehicle Crush (NASS) - Front, Test No. MWTSP-3

Date:	10/9/2008		Test Number:	MWTSP-3		
Make:	Kia		Model:	Rio Sedan	Year:	2002

	in.	(mm)
Distance from centerline to reference line - L_{REF}:	48	(1219)
Width of contact and induced crush - Field L:	35	(889)
Crush measurement spacing interval (L/5) - I:	7	(178)
Distance from vehicle c.g. to center of Field L - D_{FL}:	38.5	(978)
Width of Contact Damage:	36	(914)
Distance from vehicle c.g. to center of contect damage - D_C:	28.5	(724)

	Crush Measurement		Longitudinal Location		Original Profile Measurement		Dist. Between Ref. Lines		Actual Crush	
	in.	(mm)	in.	(mm)	in.	(mm)	in.	(mm)	in.	(mm)
C_1	16	(406)	21	(533)	4.5	(114)	12	(305)	-0.5	-(13)
C_2	17.5	(445)	28	(711)	7.625	(194)			-2.125	-(54)
C_3	17.5	(445)	35	(889)	17	(432)			-11.5	-(292)
C_4	17	(432)	42	(1067)	25.5	(648)			-20.5	-(521)
C_5	27	(686)	49	(1245)	25.5	(648)			-10.5	-(267)
C_6	22	(559)	56	(1422)	25.5	(648)			-15.5	-(394)
C_{MAX}	27.5	(699)	46	(1168)	25.5	(648)			-10	-(254)

Figure E-14. Exterior Vehicle Crush (NASS) - Side, Test No. MWTSP-3

**Appendix F.   Accelerometer and Rate Transducer Data Plots, Test No. MWSTP-1**

Figure F-1. 10-ms Average Longitudinal Deceleration (DTS), Test No. MWTSP-1

Figure F-2. Longitudinal Change in Velocity (DTS), Test No. MWTSP-1

234
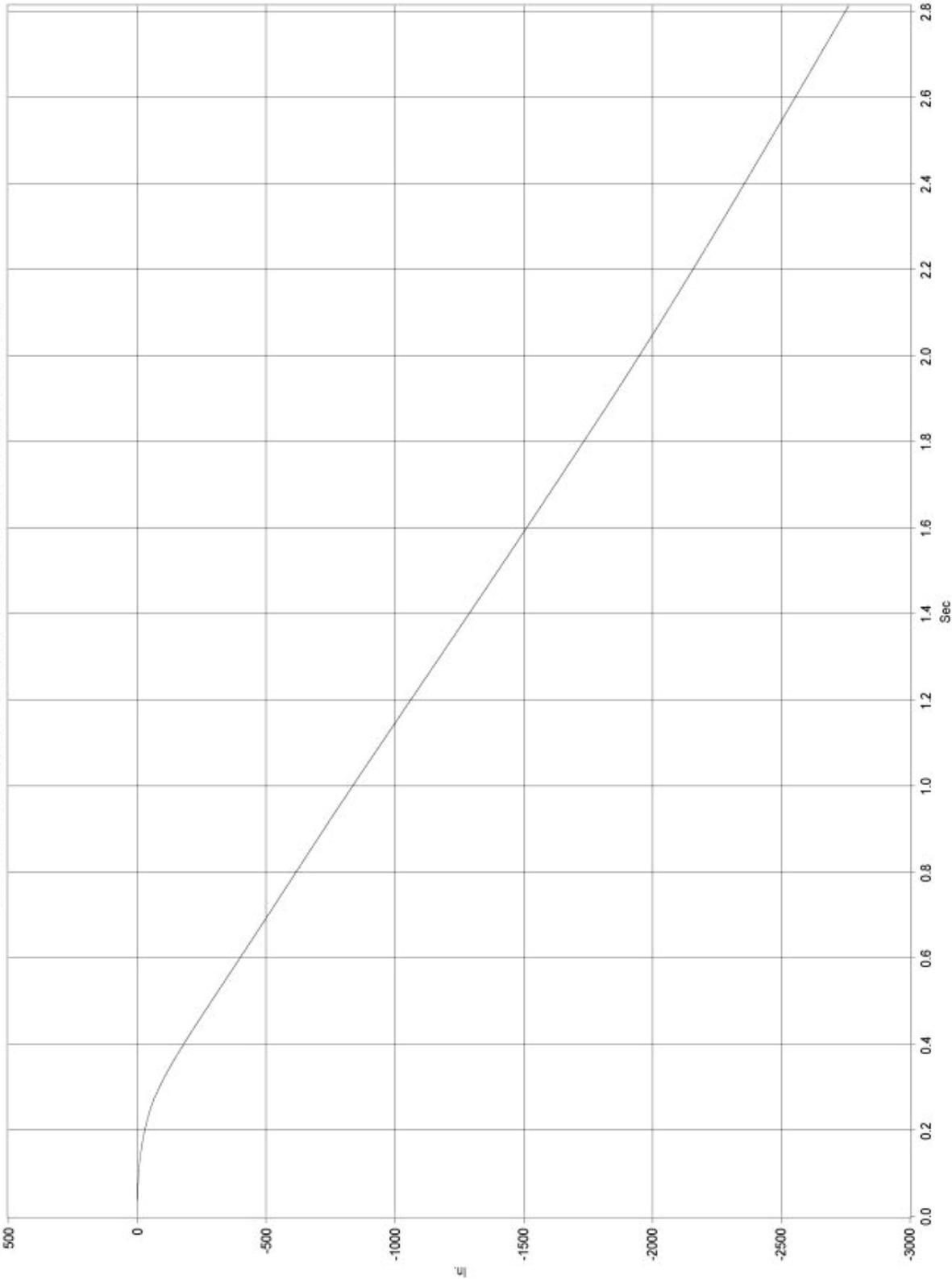
Figure F-3. Longitudinal Occupant Displacement (DTS), Test No. MWTSP-1
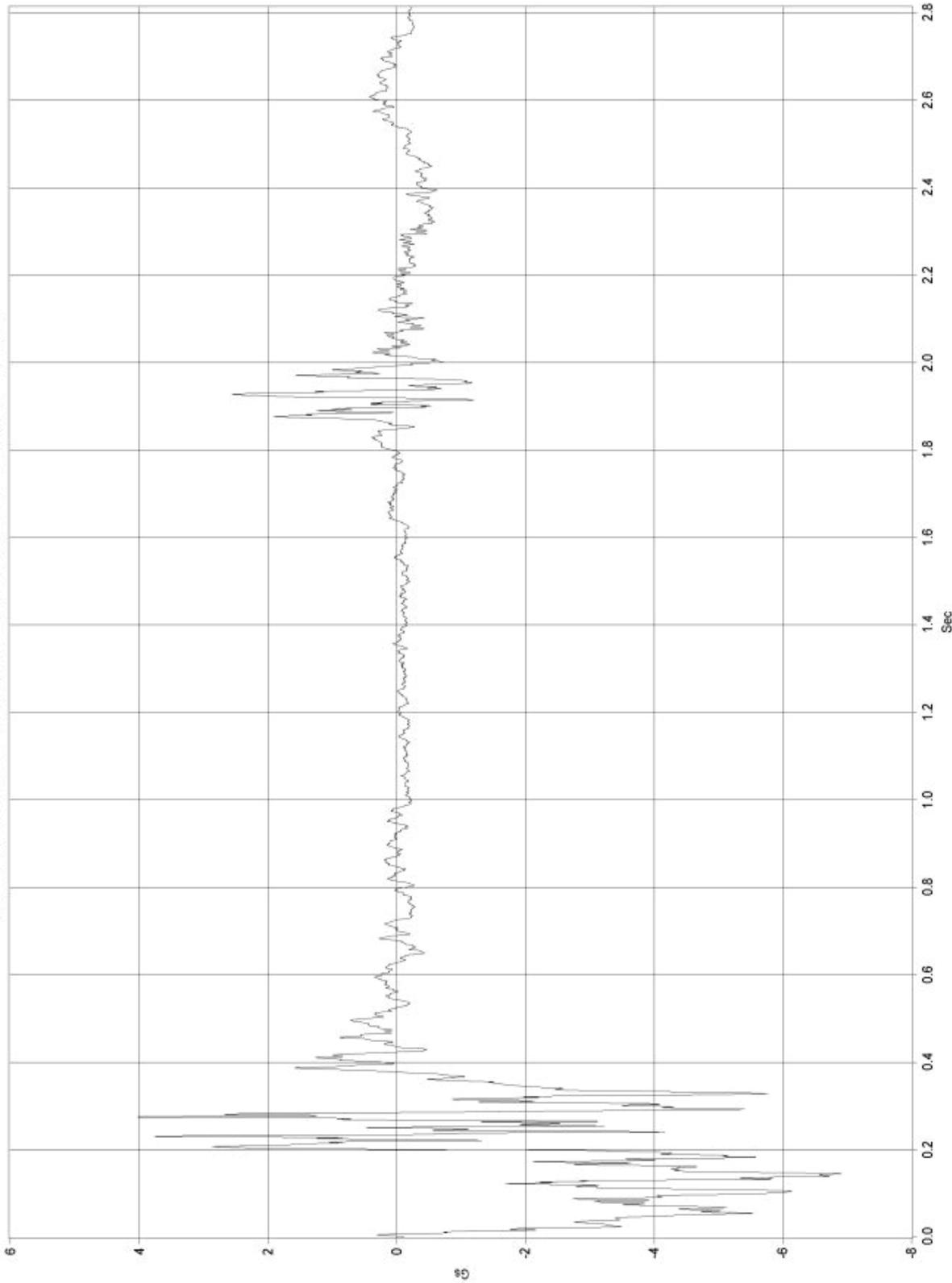
Figure F-4. 10-ms Average Lateral Deceleration (DTS), Test No. MWTSP-1
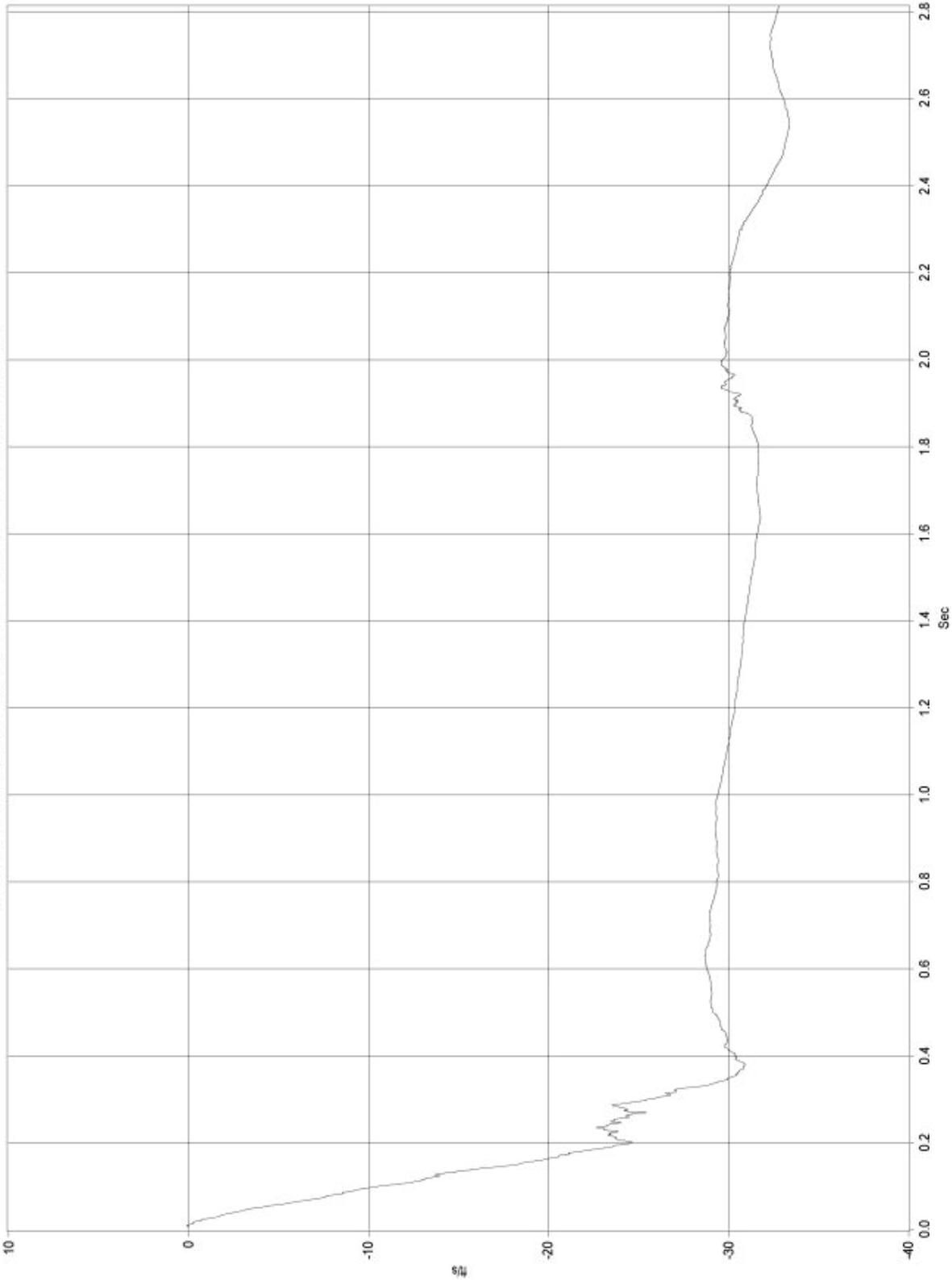
Figure F-5. Lateral Occupant Impact Velocity (DTS), Test No. MWTSP-1
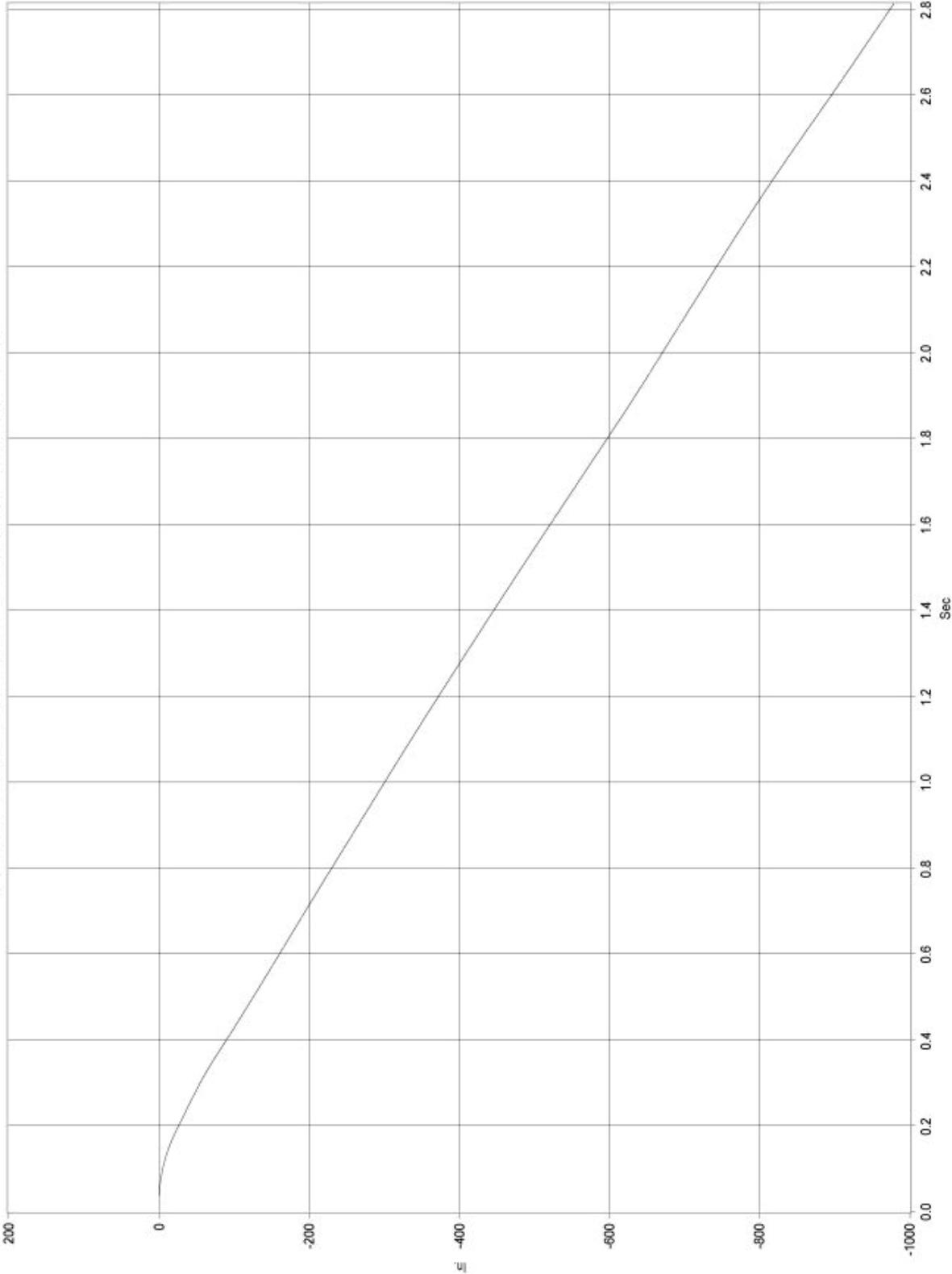
Figure F-6. Lateral Occupant Displacement (DTS), Test No. MWTSP-1
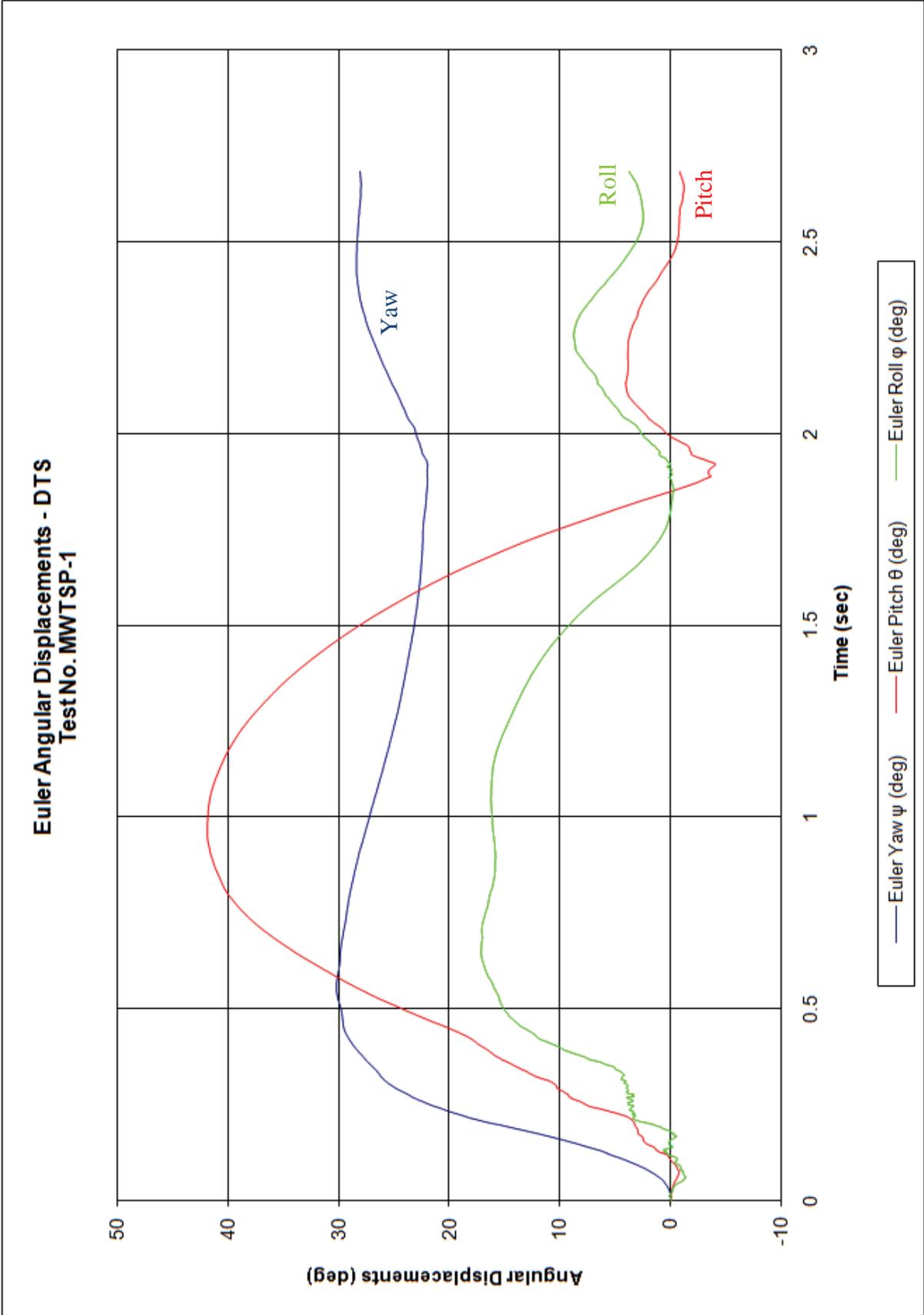
Figure F-7. Vehicle Angular Displacements (DTS), Test No. MWTSP-1
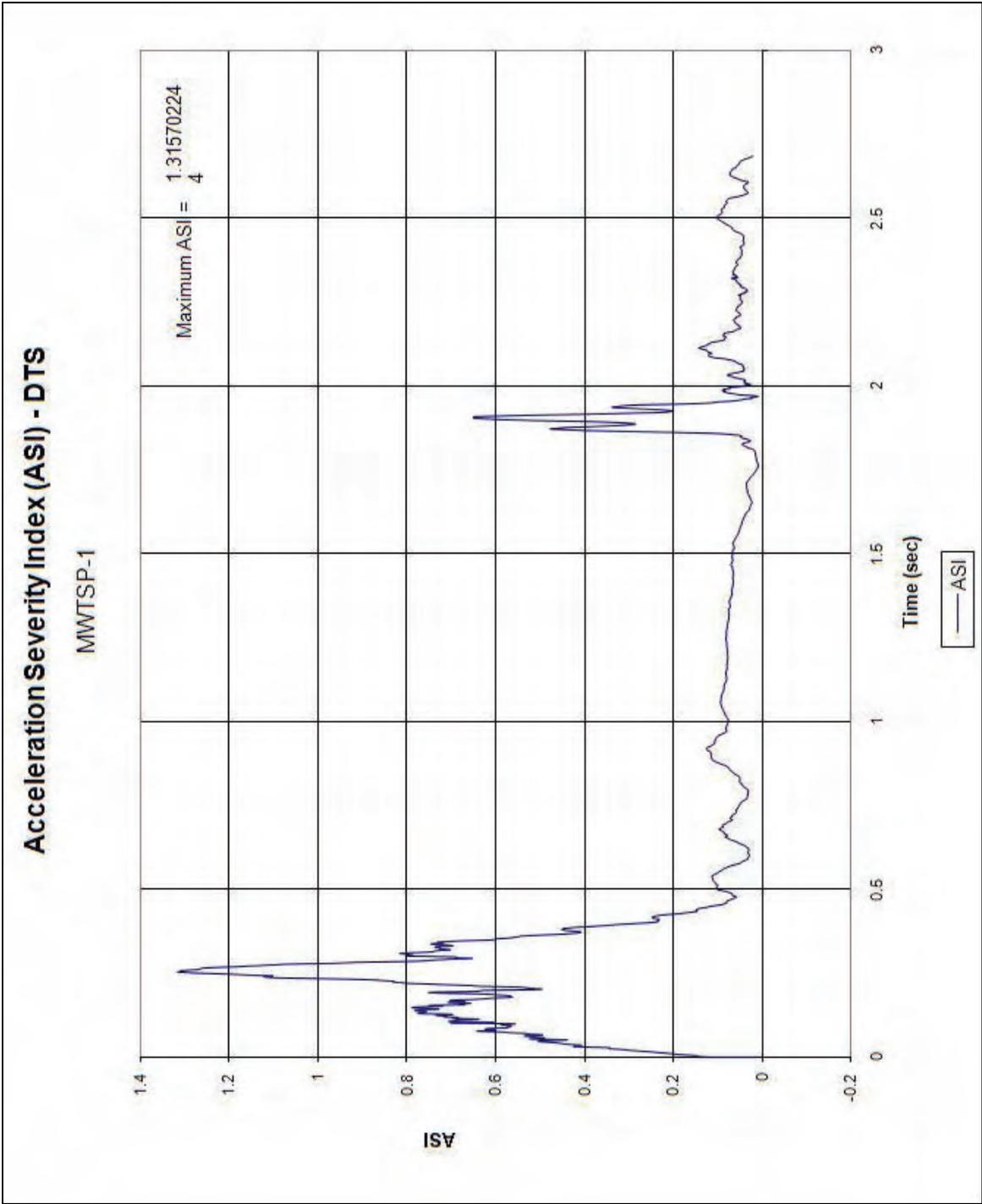
Figure F-8. Accident Severity Index (ASI) [DTS], Test No. MWTSP-1
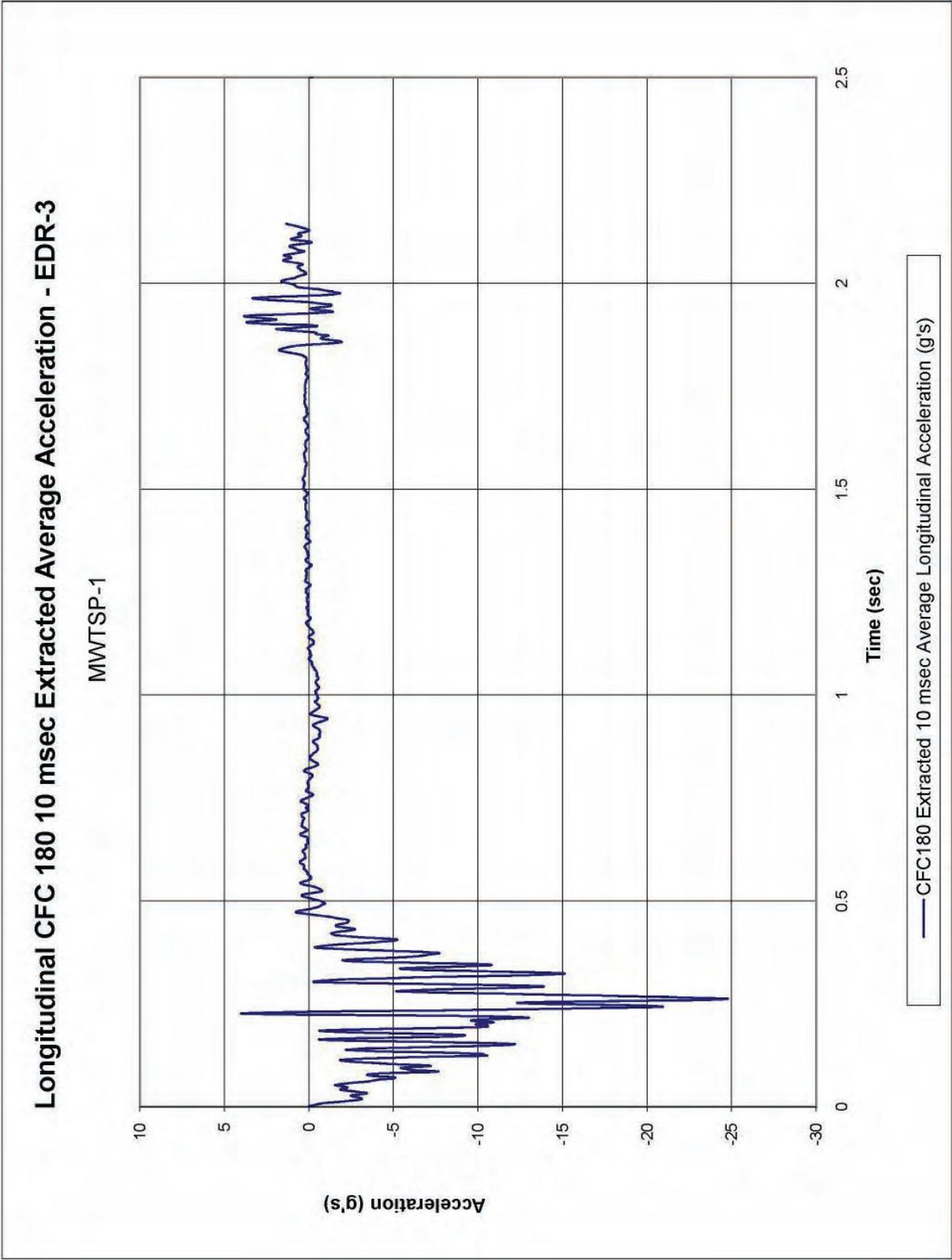
Figure F-9. 10-ms Average Longitudinal Deceleration (EDR-3), Test No. MWTSP-1
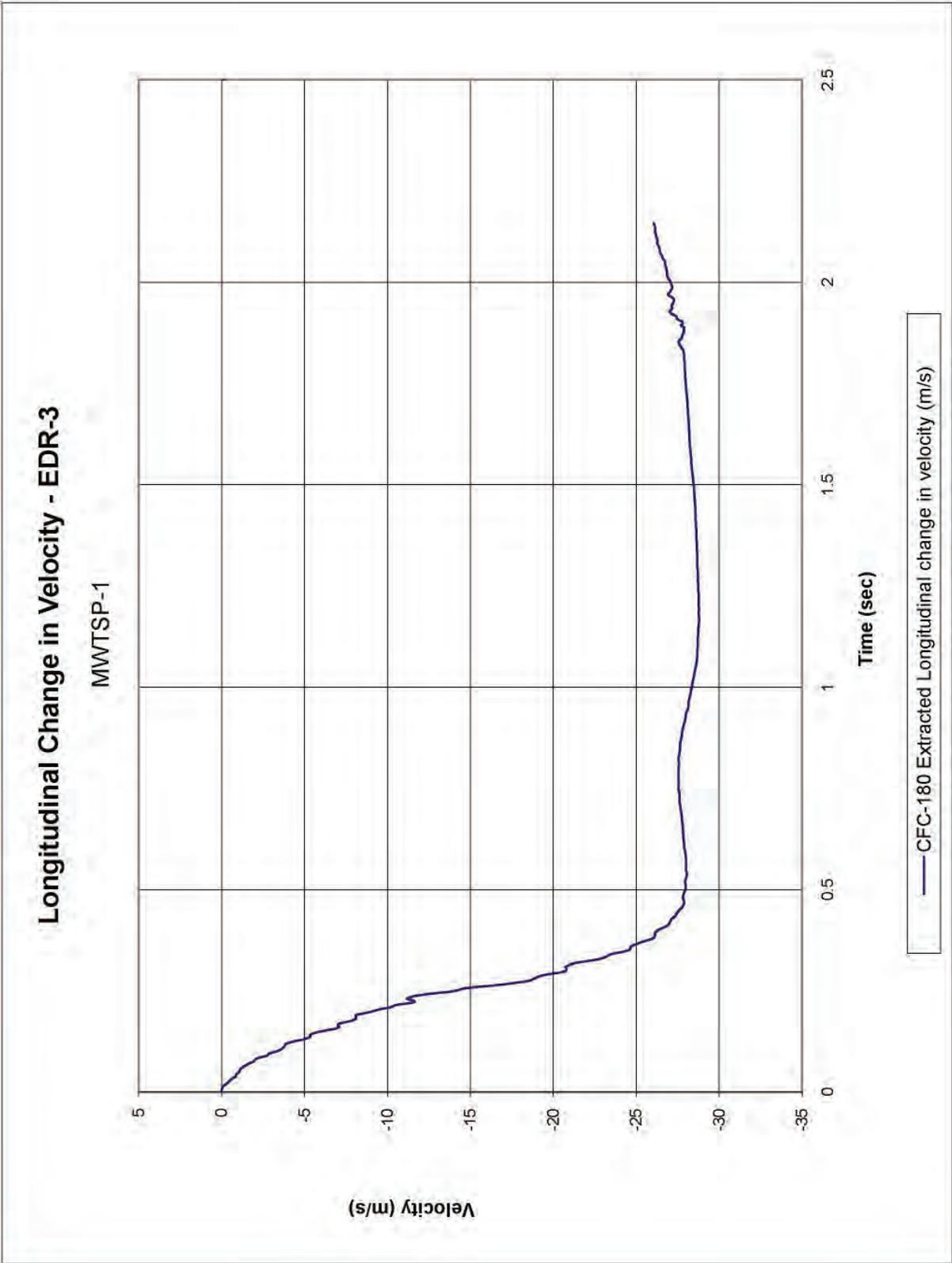
Figure F-10. Longitudinal Change in Velocity (EDR-3), Test No. MWTSP-1
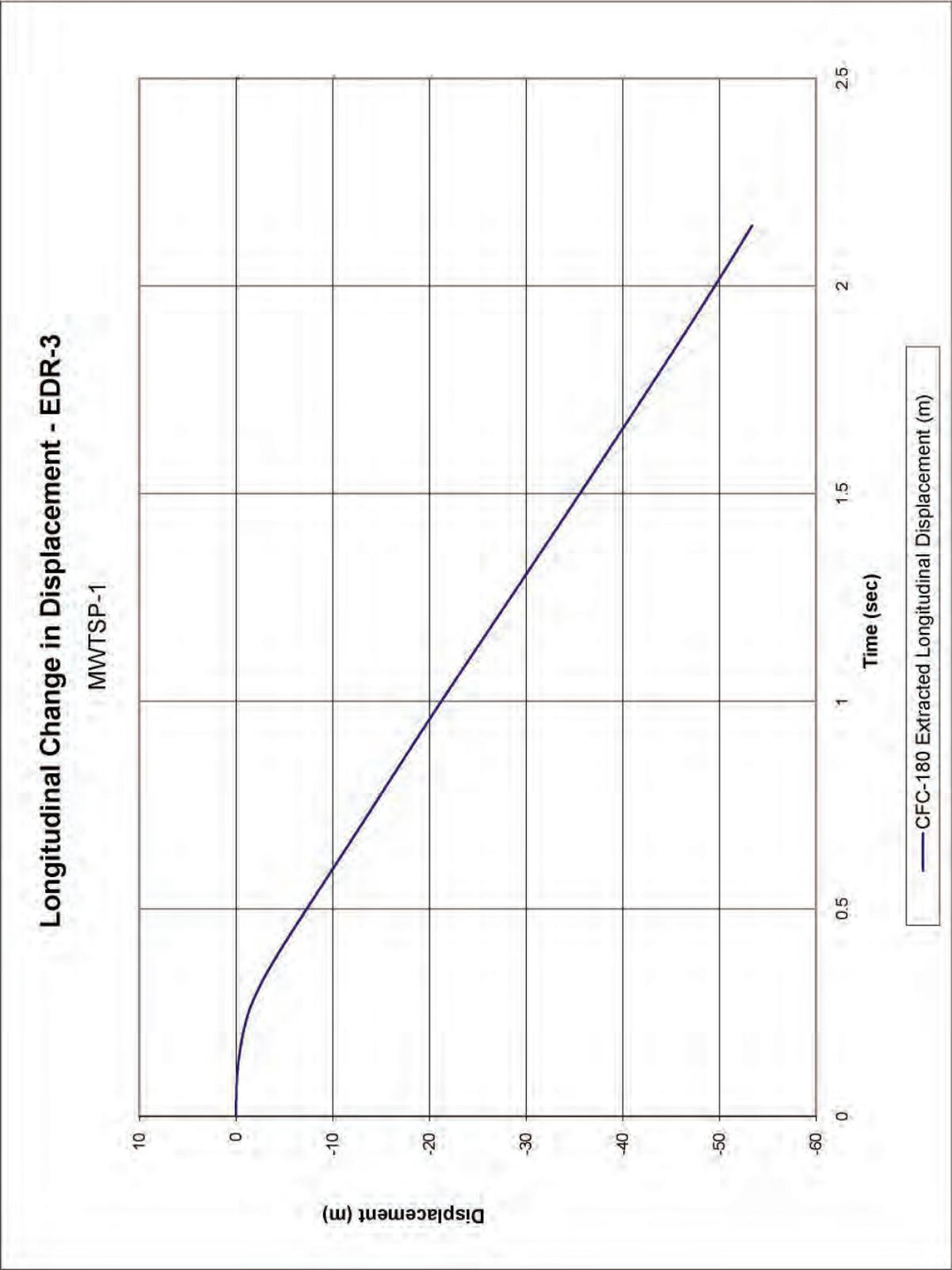
Figure F-11. Longitudinal Occupant Displacement (EDR-3), Test No. MWTSP-1
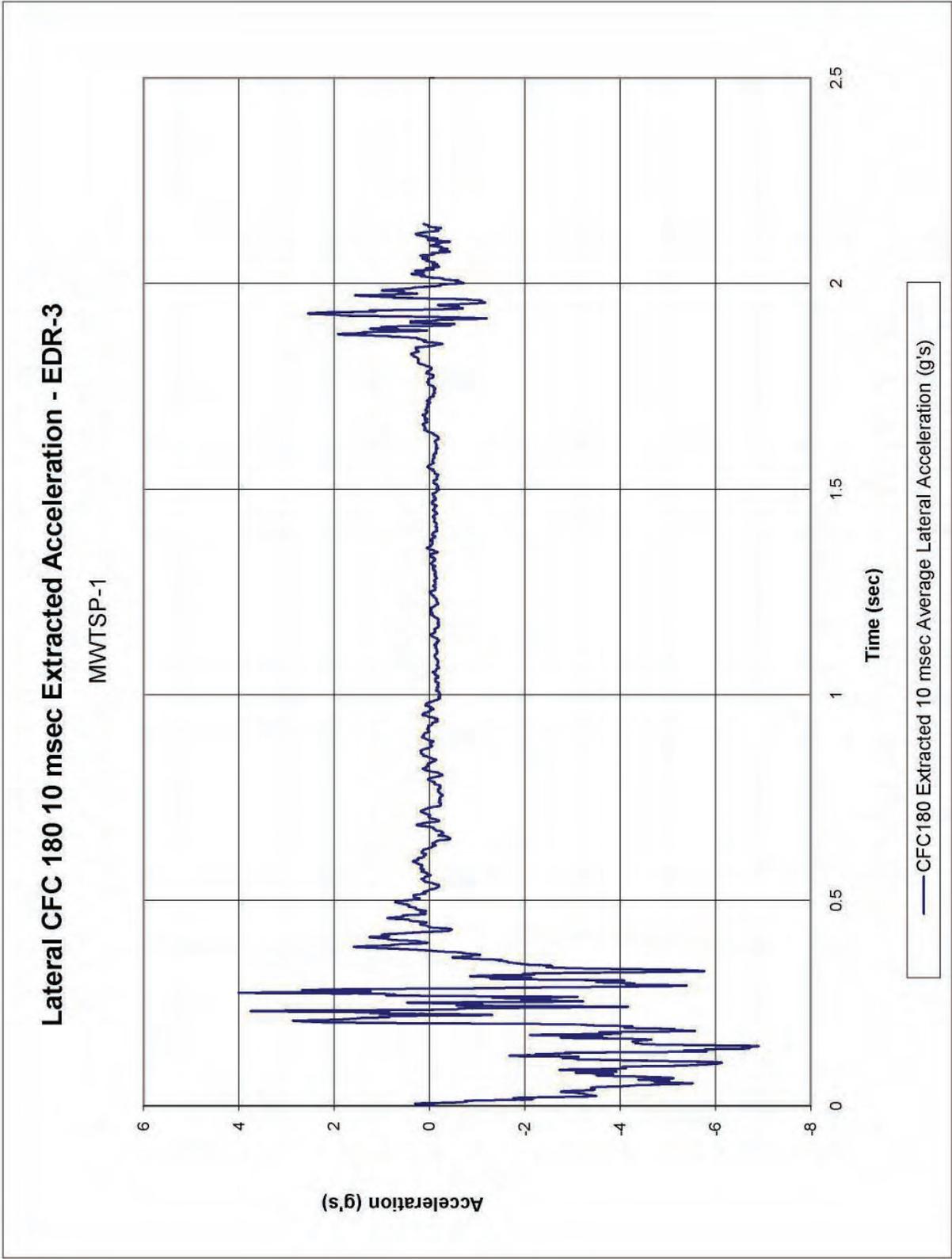
Figure F-12. 10-ms Average Lateral Deceleration (EDR-3), Test No. MWTSP-1
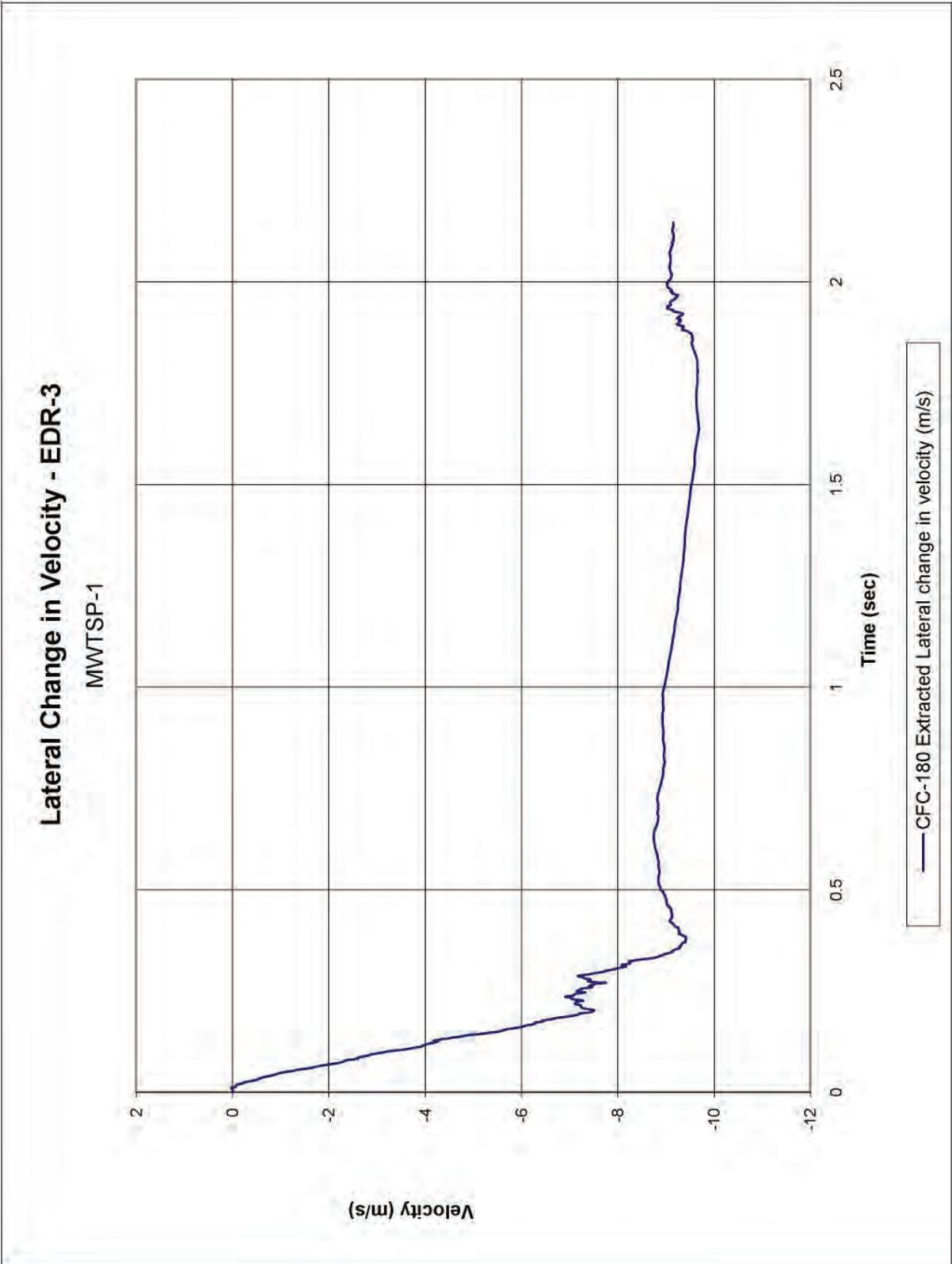
Figure F-13. Lateral Occupant Impact Velocity (EDR-3), Test No. MWTSP-1
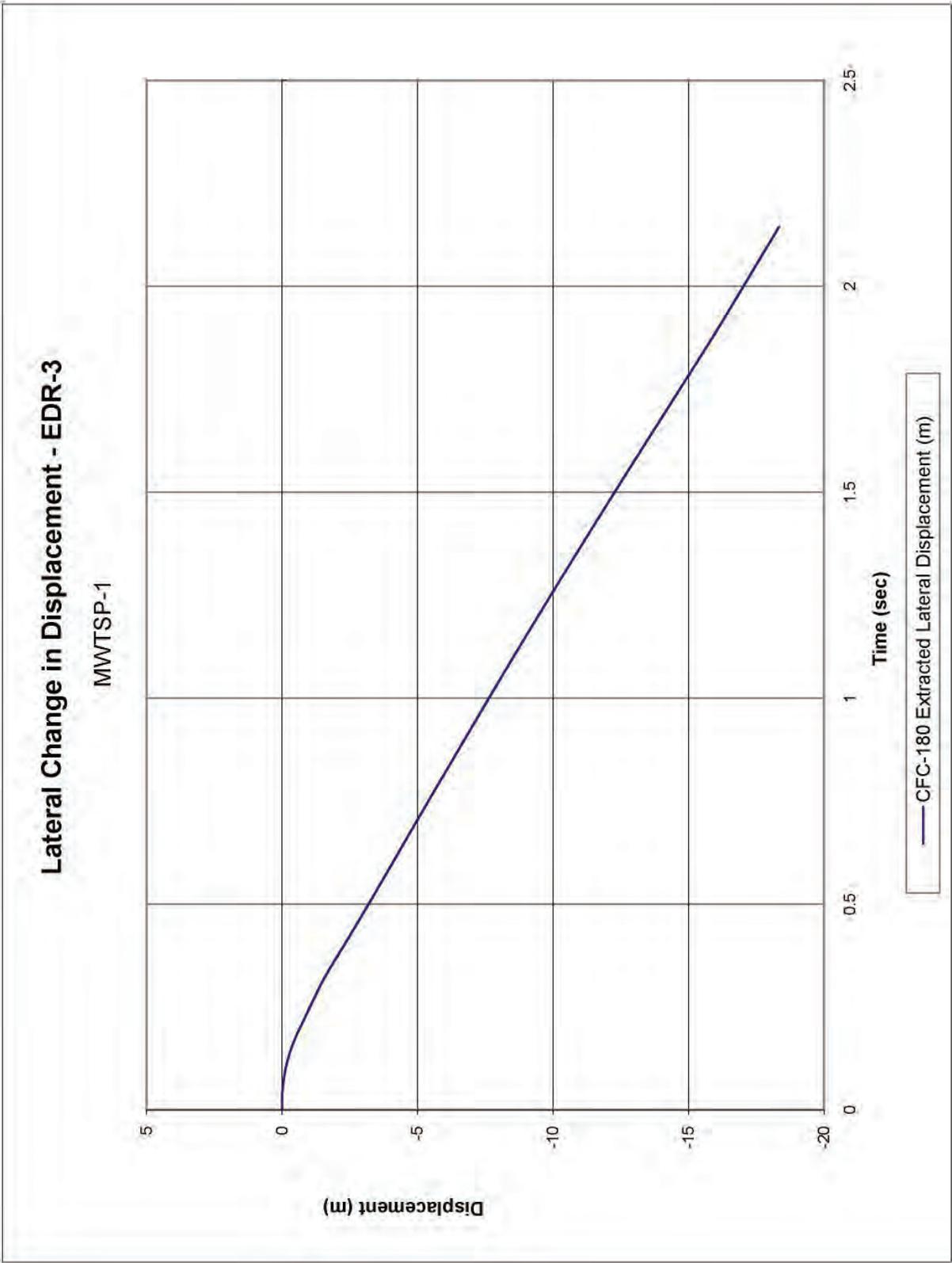
Figure F-14. Lateral Occupant Displacement (EDR-3), Test No. MWTSP-1
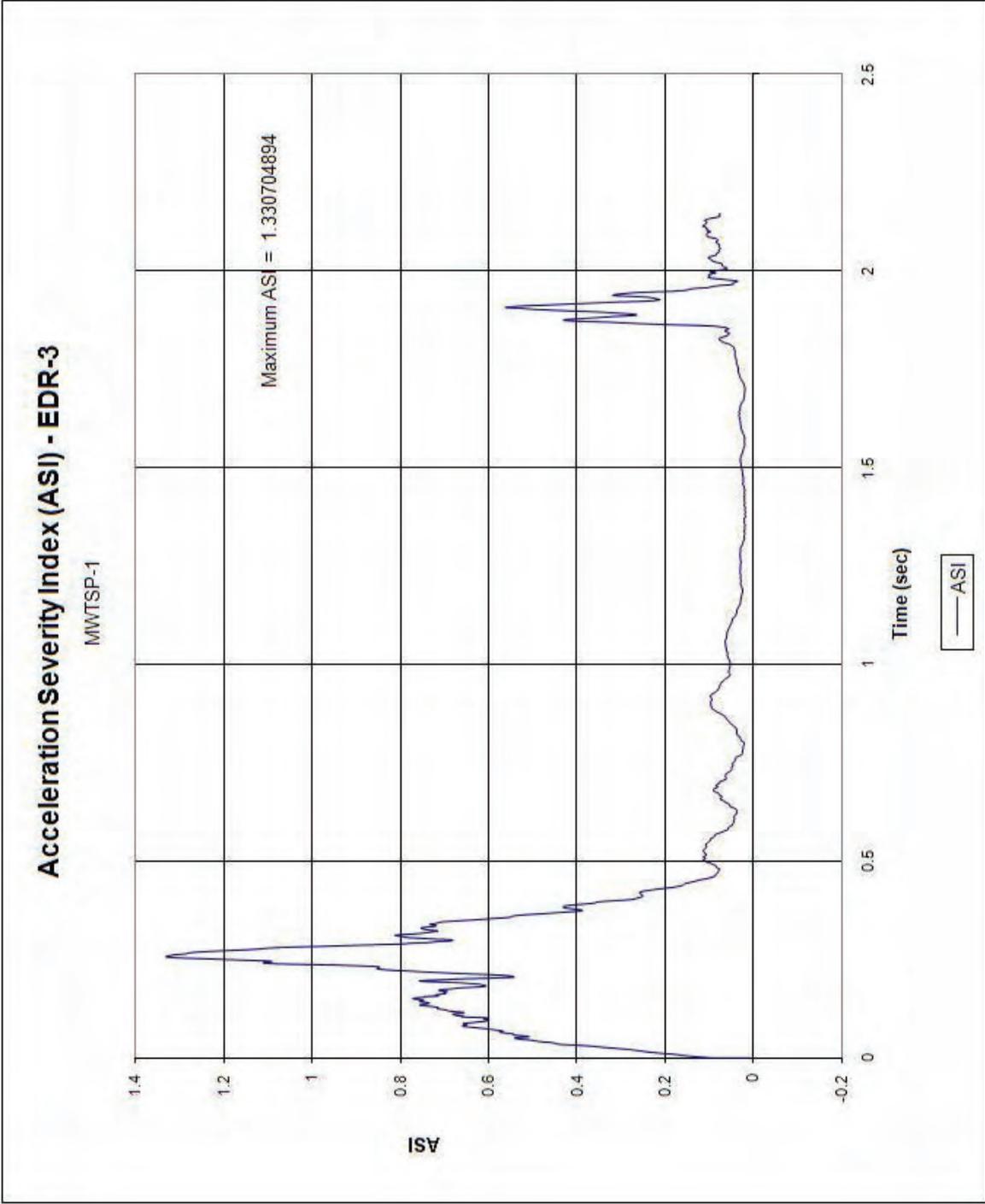
Figure F-15. Accident Severity Index (ASI) [EDR-3], Test No. MWTSP-1

Appendix G. Static Soil Tests
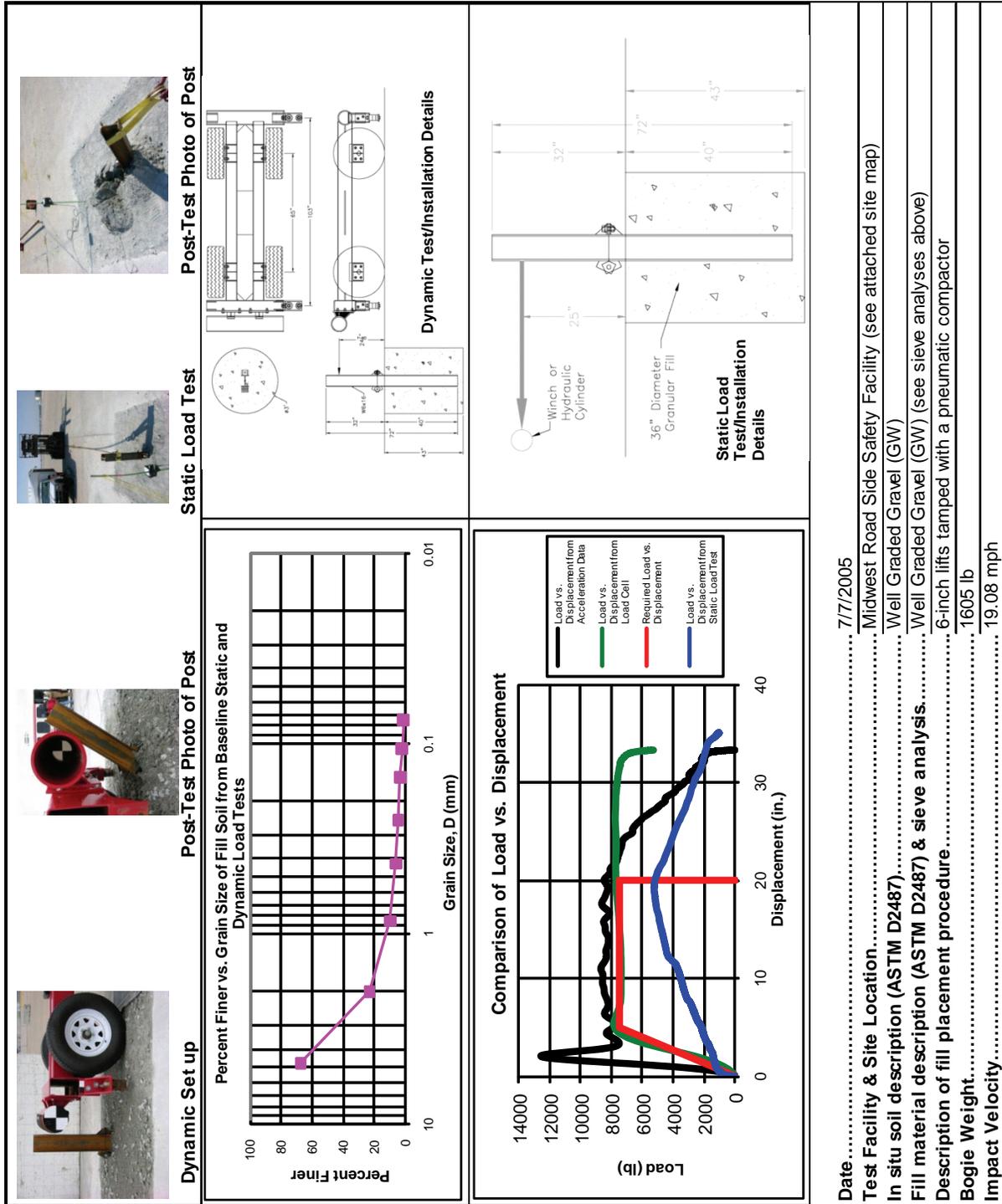
Figure G-1. Soil Strength, Initial Calibration Tests
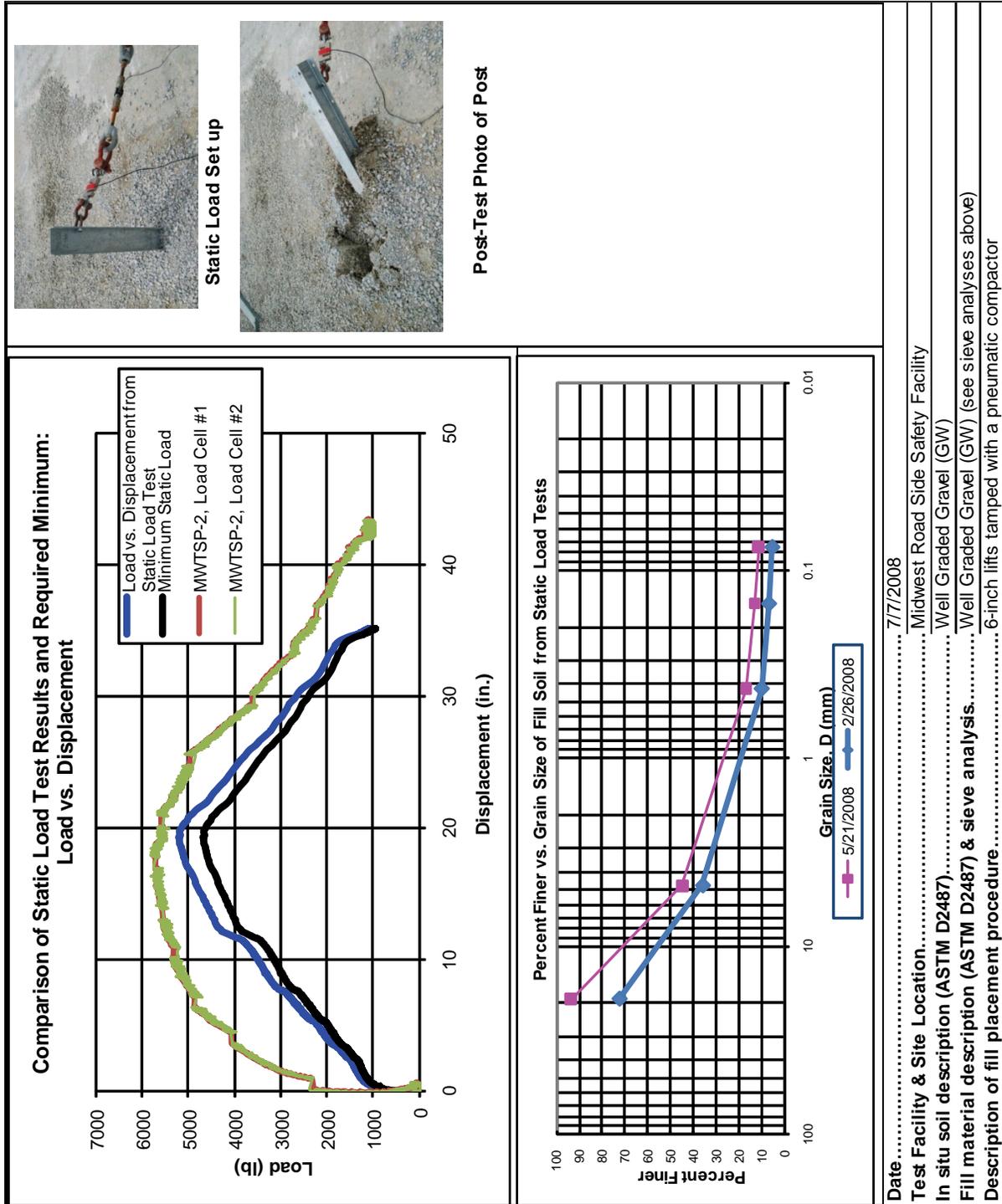
Figure G-2. Static Soil Test, Test No. MWTSP-2
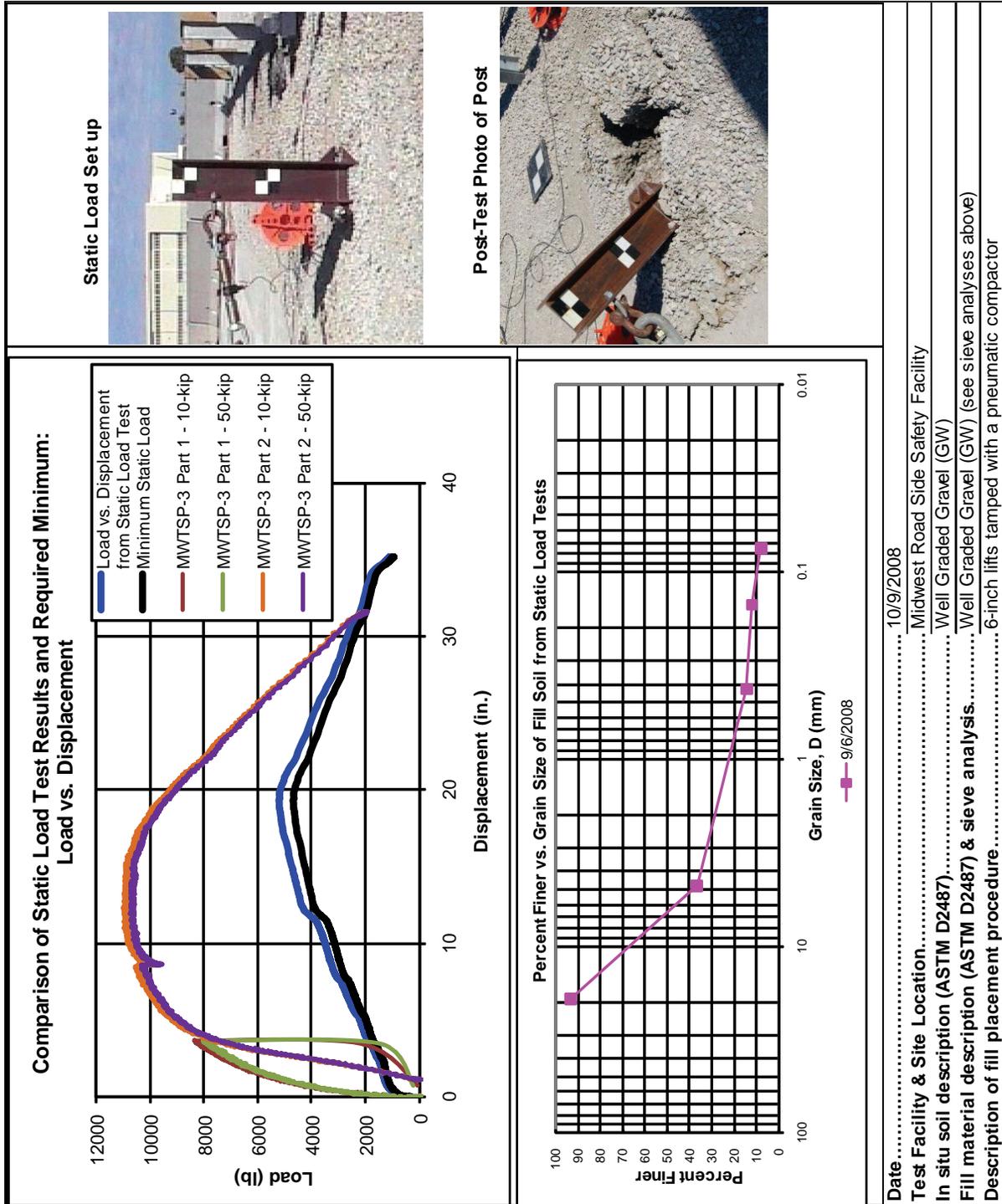
Figure G-3. Static Soil Test, Test No. MWSTP-3

**Appendix H. Accelerometer and Rate Transducer Data Plots, Test No. MWSTP-2**
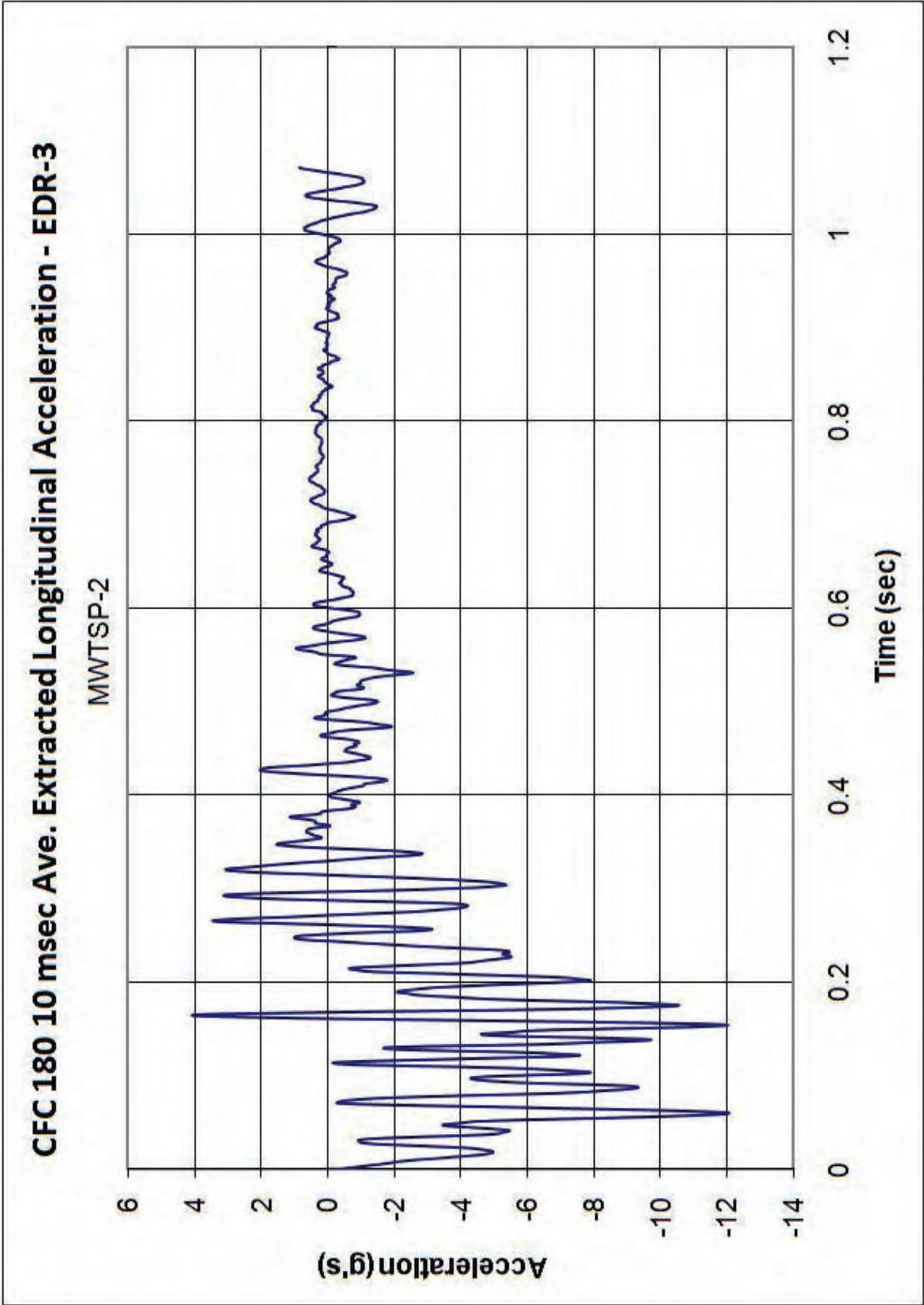
Figure H-1. 10-ms Average Longitudinal Deceleration (EDR-3), Test No. MWTSP-2
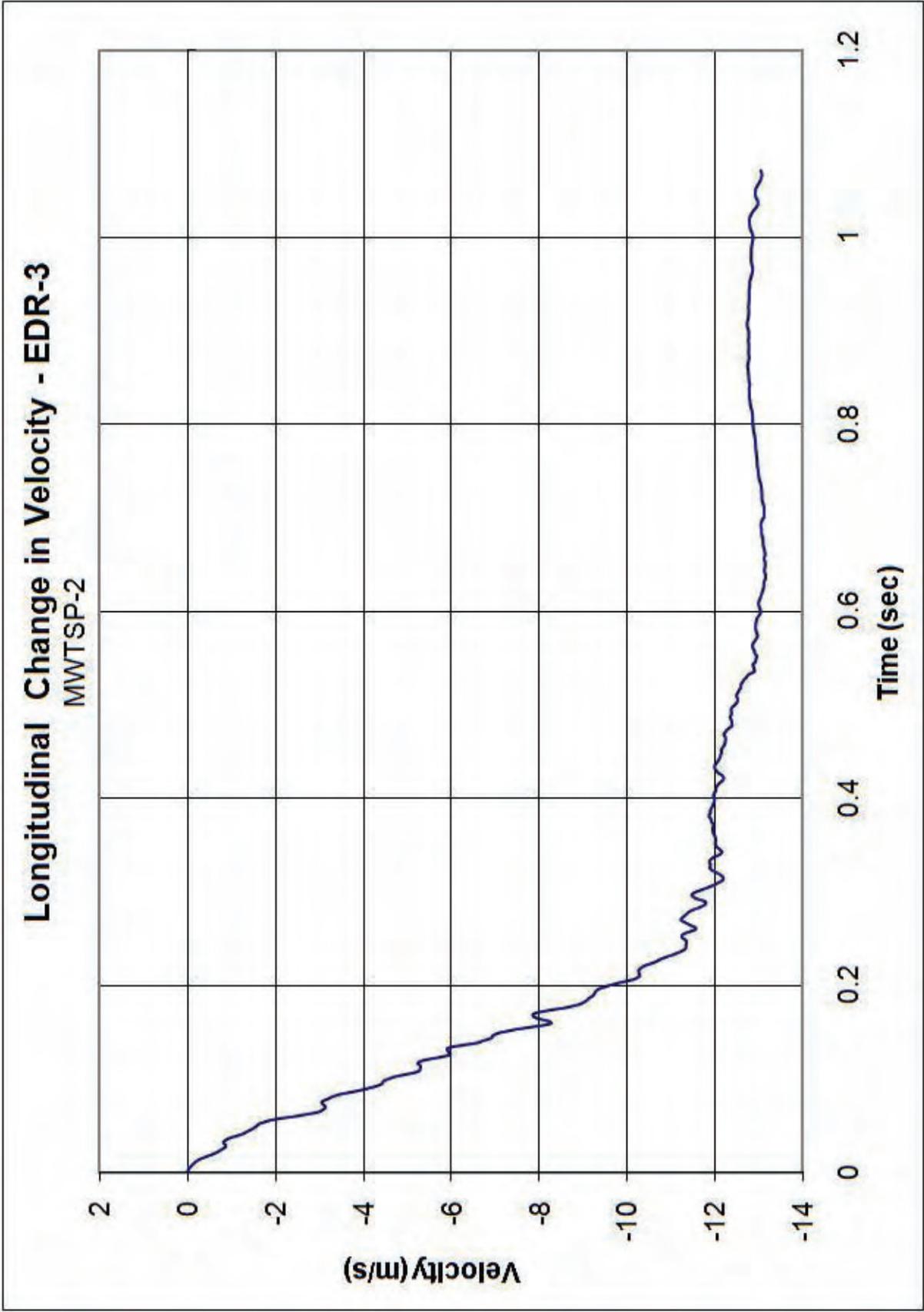
Figure H-2. Longitudinal Change in Velocity (EDR-3), Test No. MWTSP-2
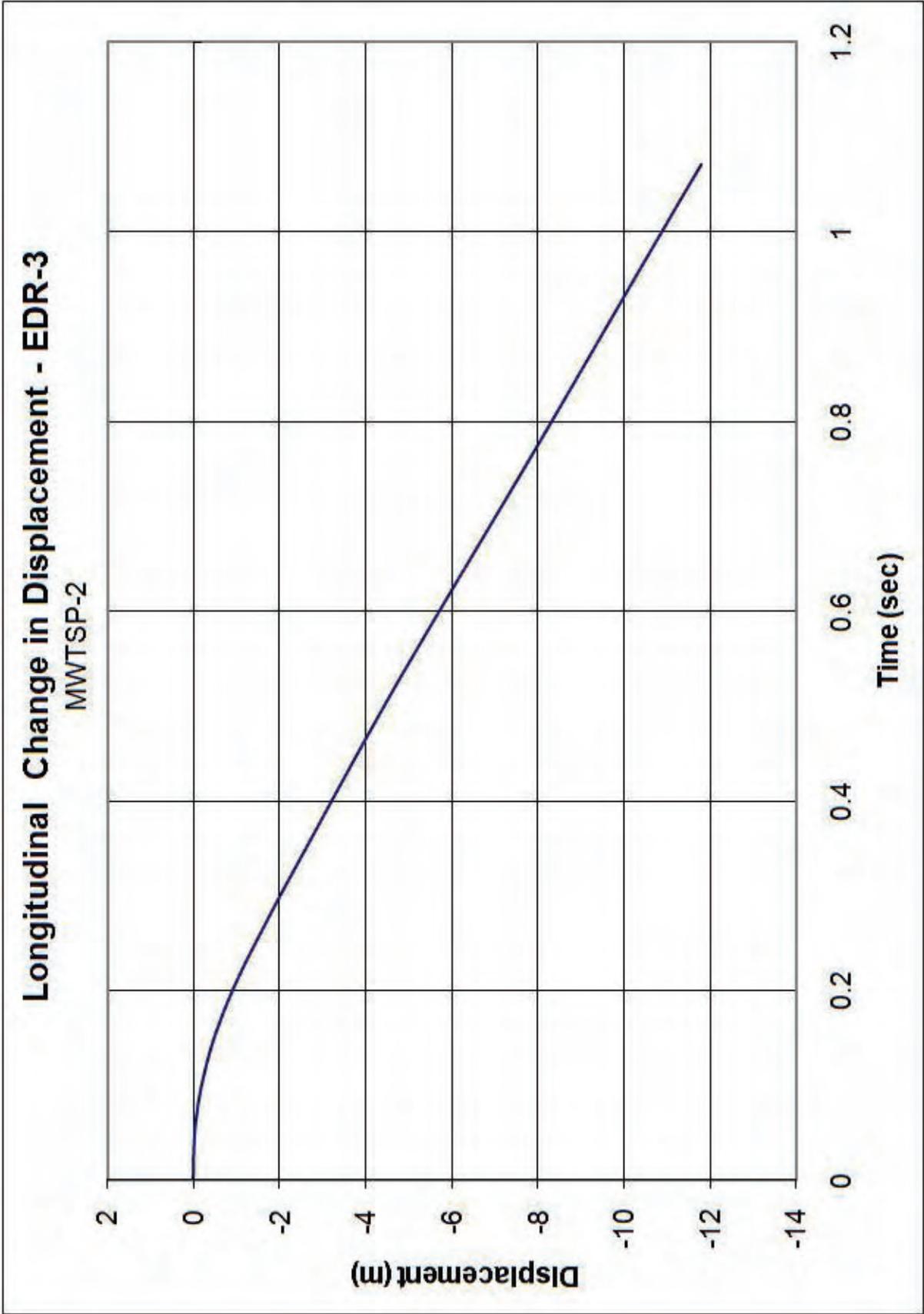
Figure H-3. Longitudinal Occupant Displacement (EDR-3), Test No. MWTSP-2
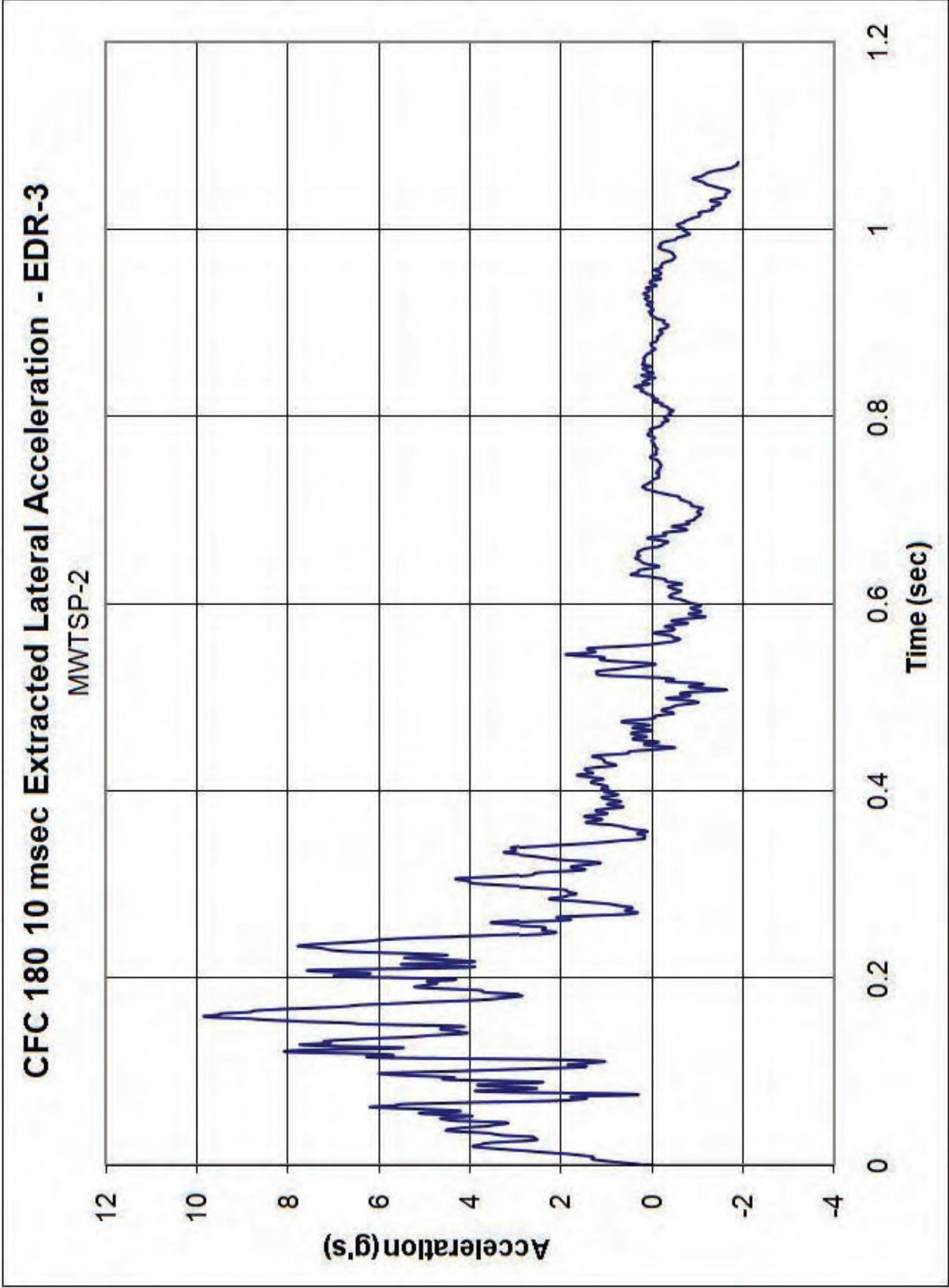
Figure H-4. 10-ms Average Lateral Deceleration (EDR-3), Test No. MWTSP-2
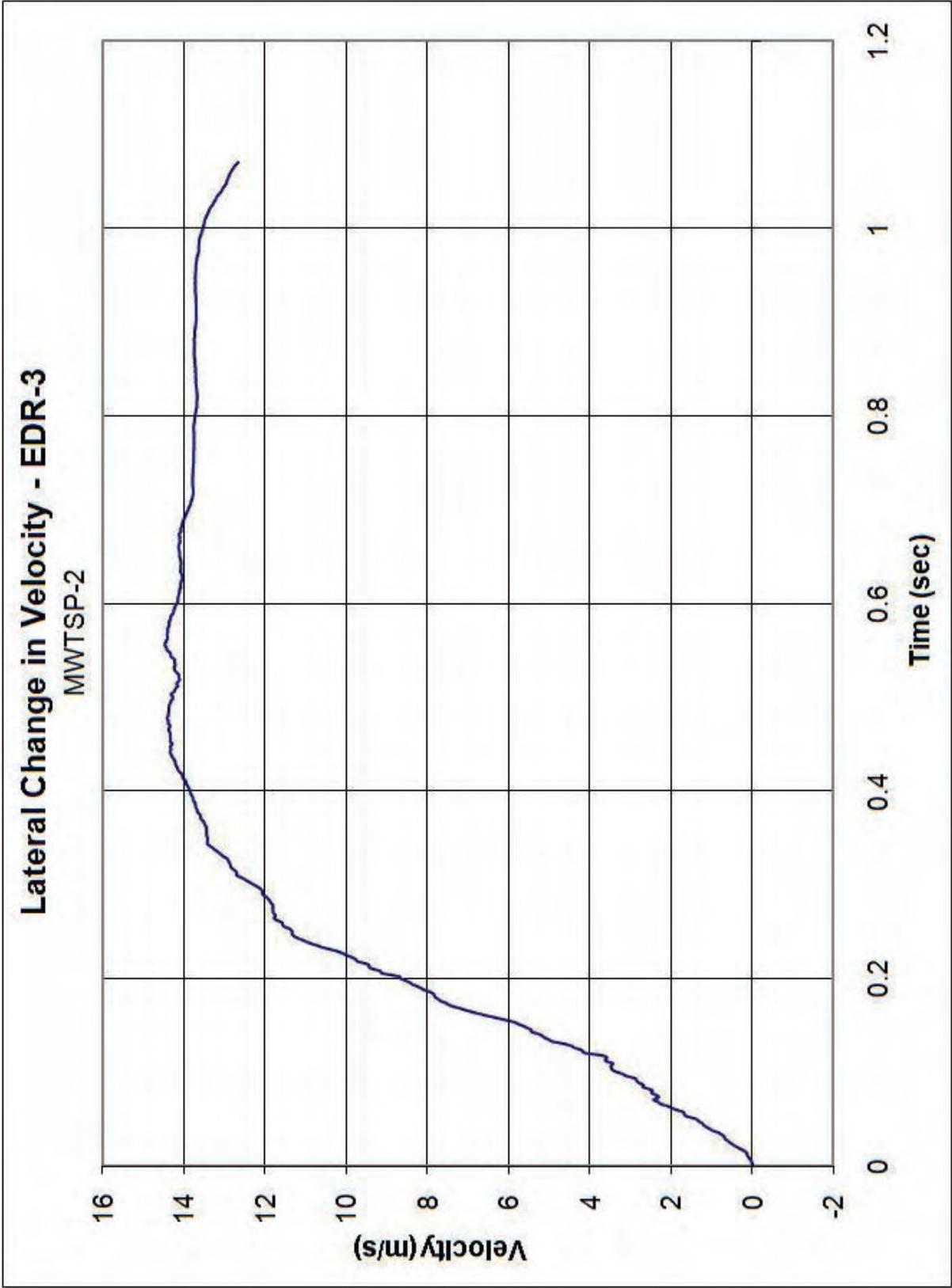
Figure H-5. Lateral Occupant Impact Velocity (EDR-3), Test No. MWTSP-2
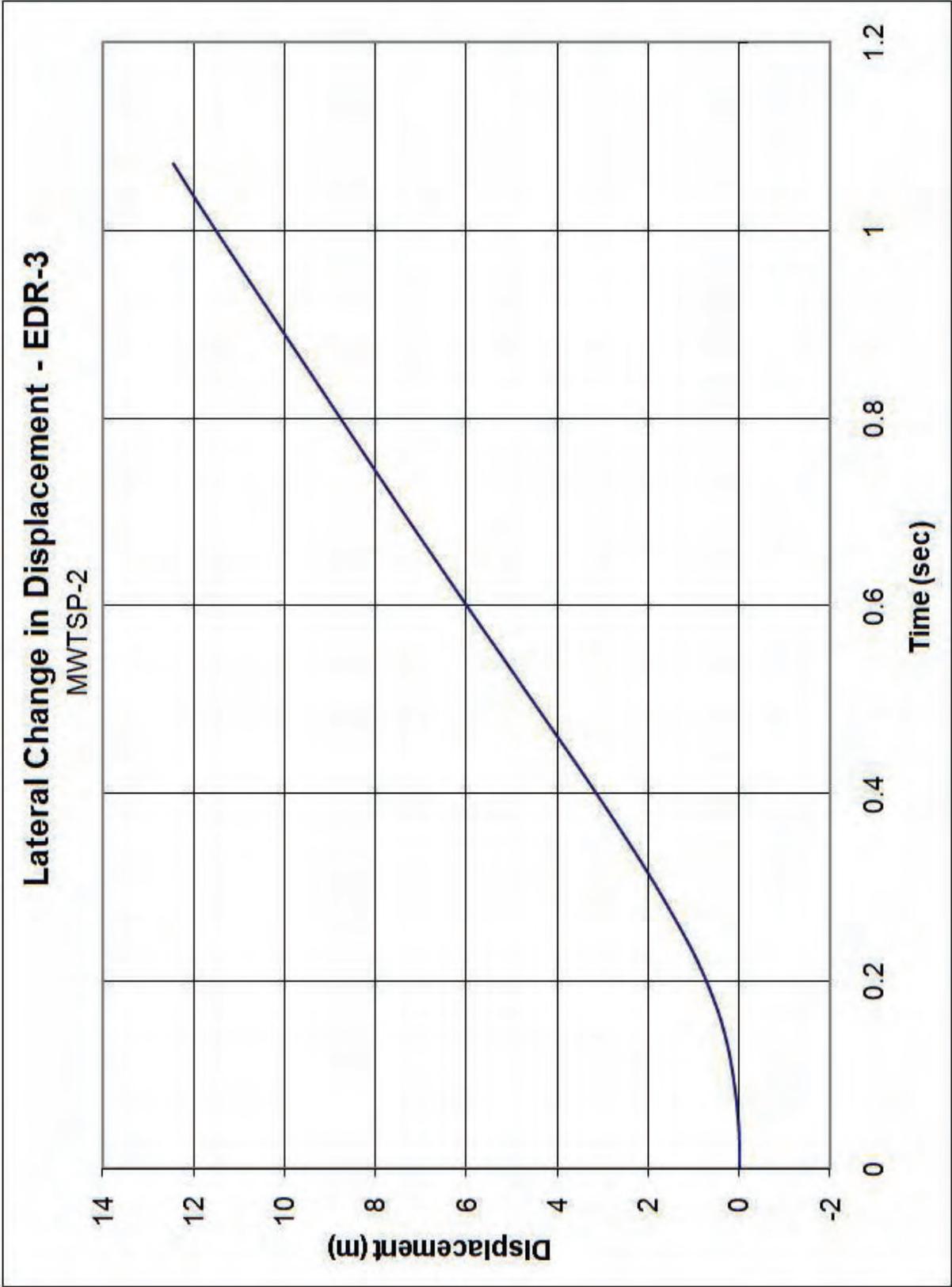
Figure H-6. Lateral Occupant Displacement (EDR-3), Test No. MWTSP-2
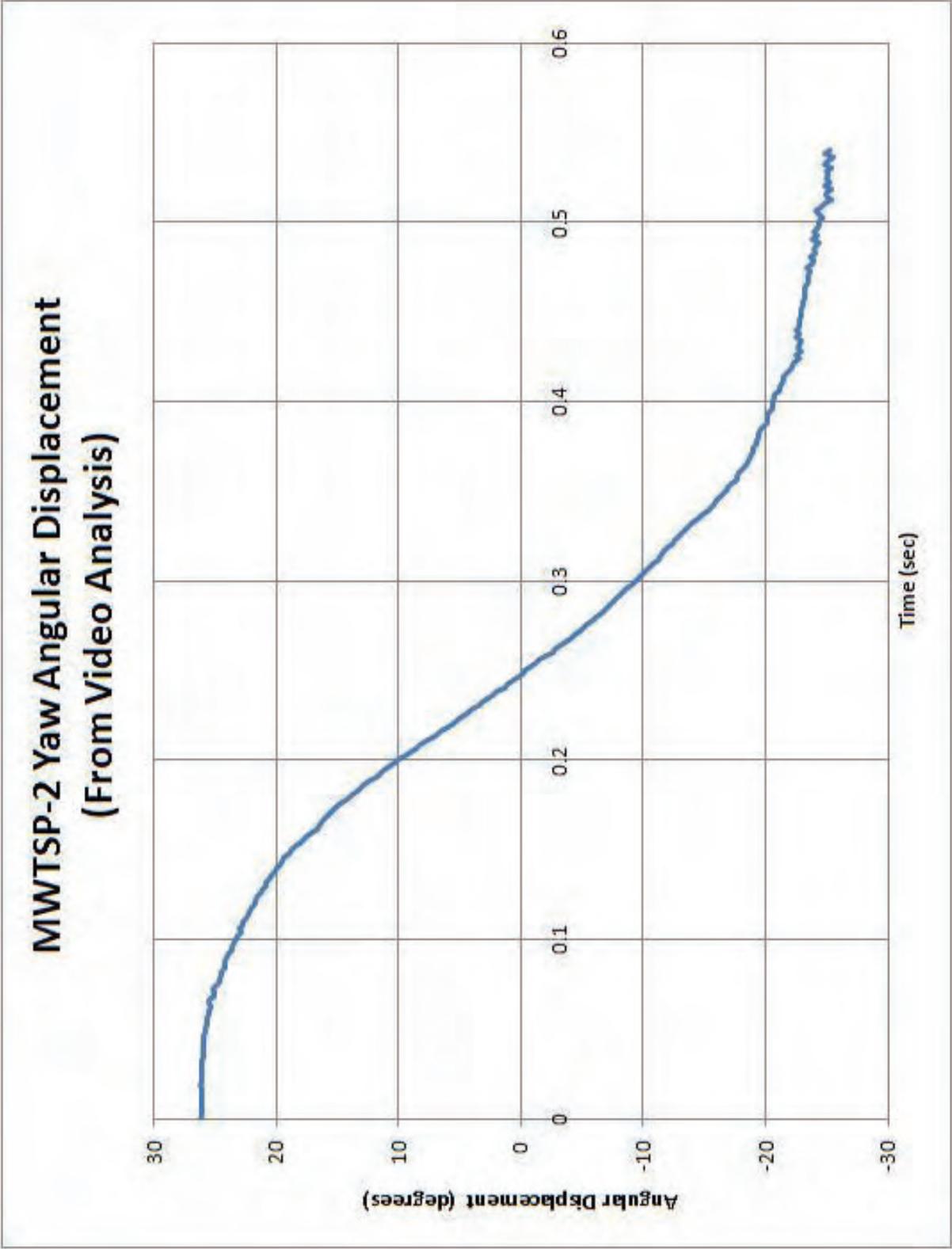
Figure H-7. Yaw Angular Displacements (Video Analysis), Test No. MWTSP-2
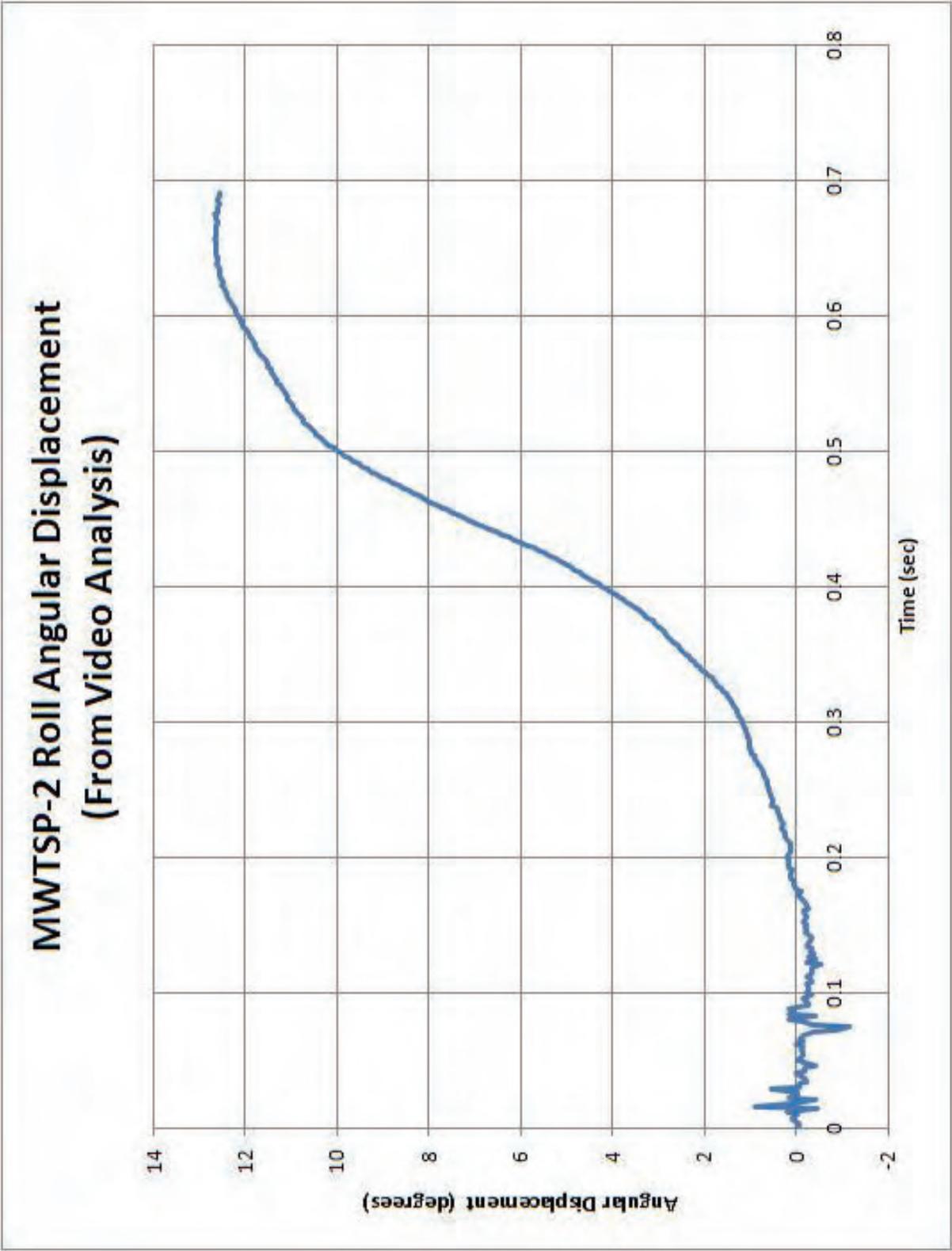
Figure H-8. Roll Angular Displacements (Video Analysis), Test No. MWTSP-2
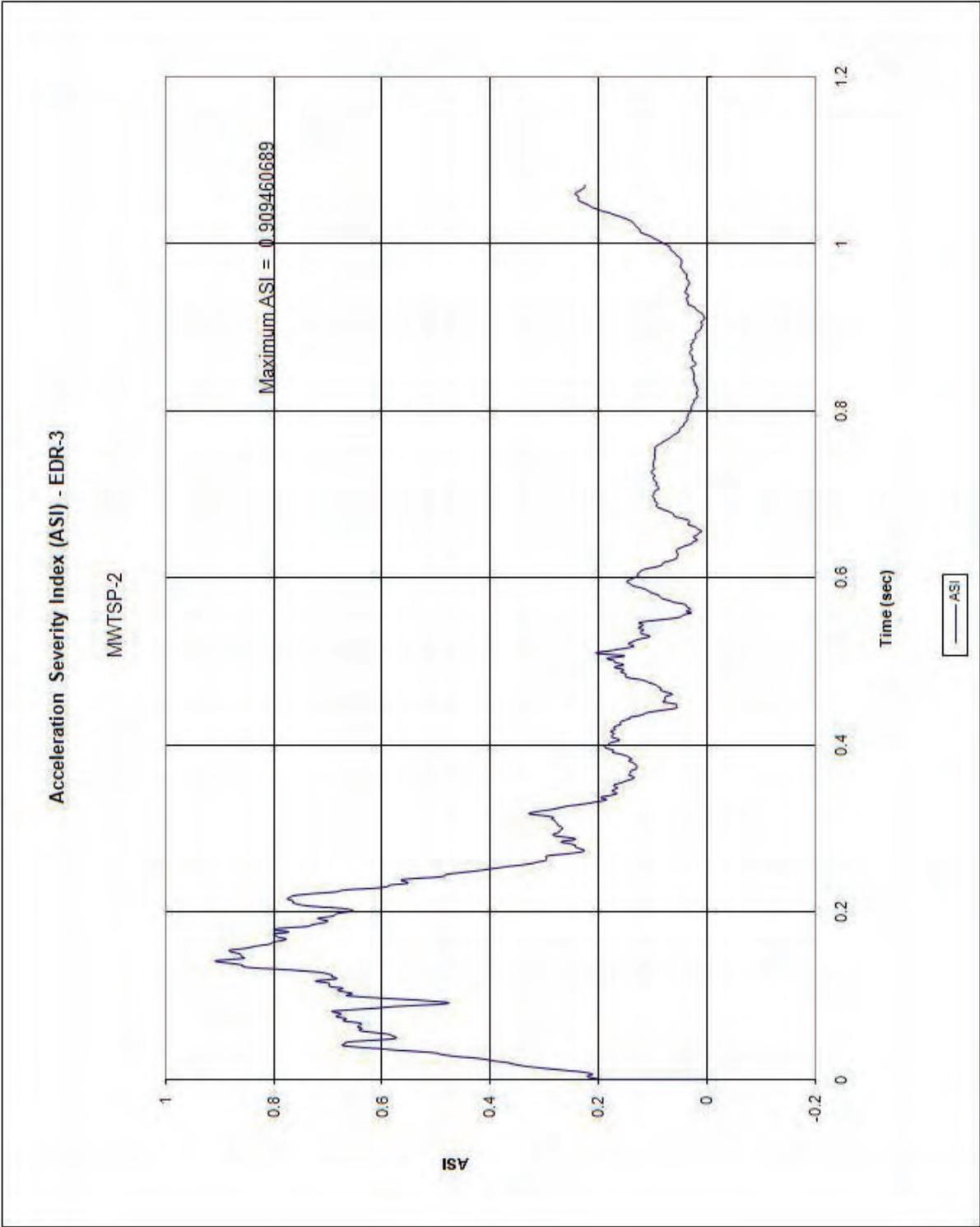
Figure H-9. Accident Severity Index (ASI) [EDR-3], Test No. MWTSP-2

Appendix I.   Accelerometer and Rate Transducer Data Plots, Test No. MWSTP-3
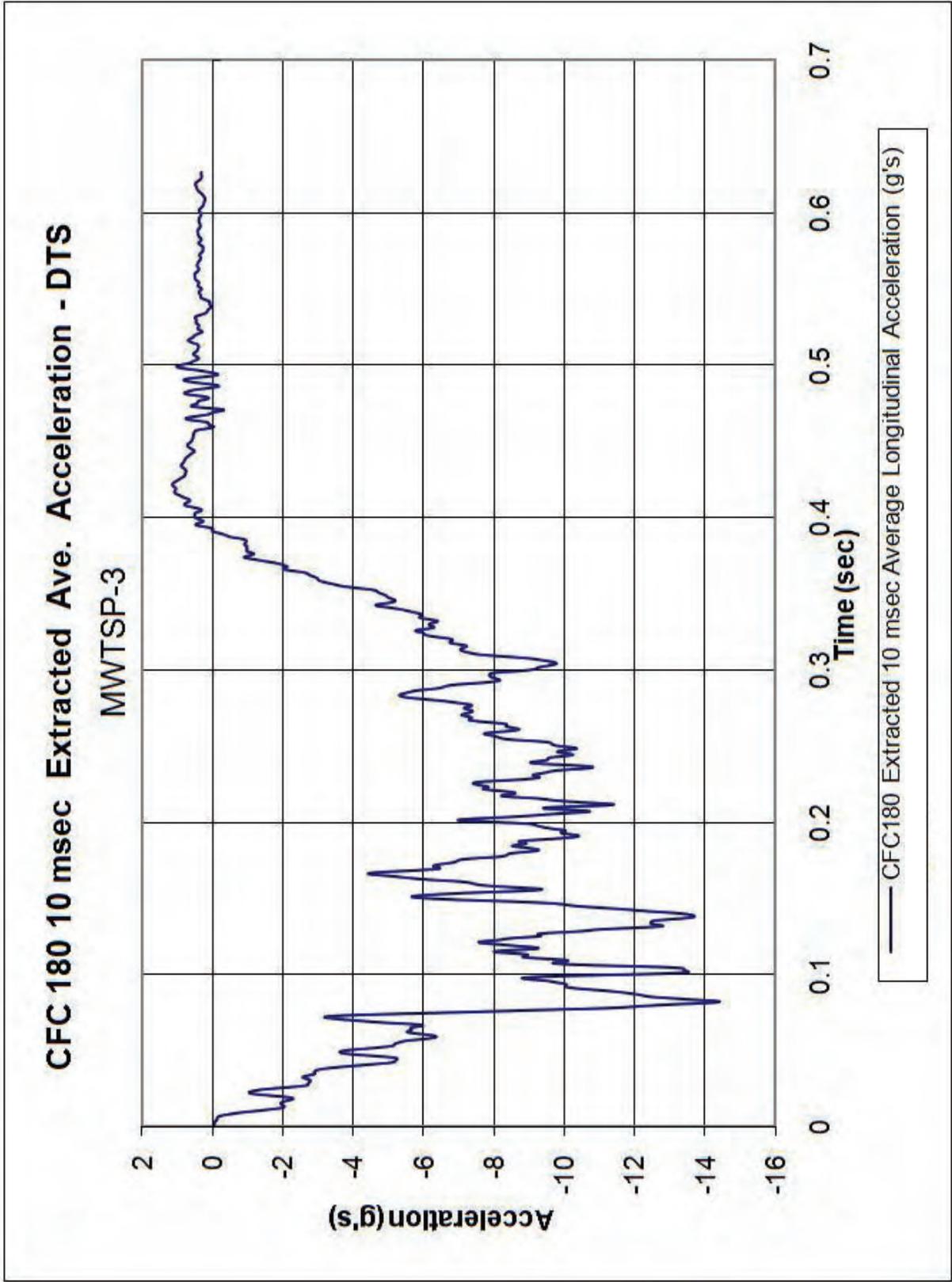
Figure I-1. 10-ms Average Longitudinal Deceleration (DTS), Test No. MWTSP-3
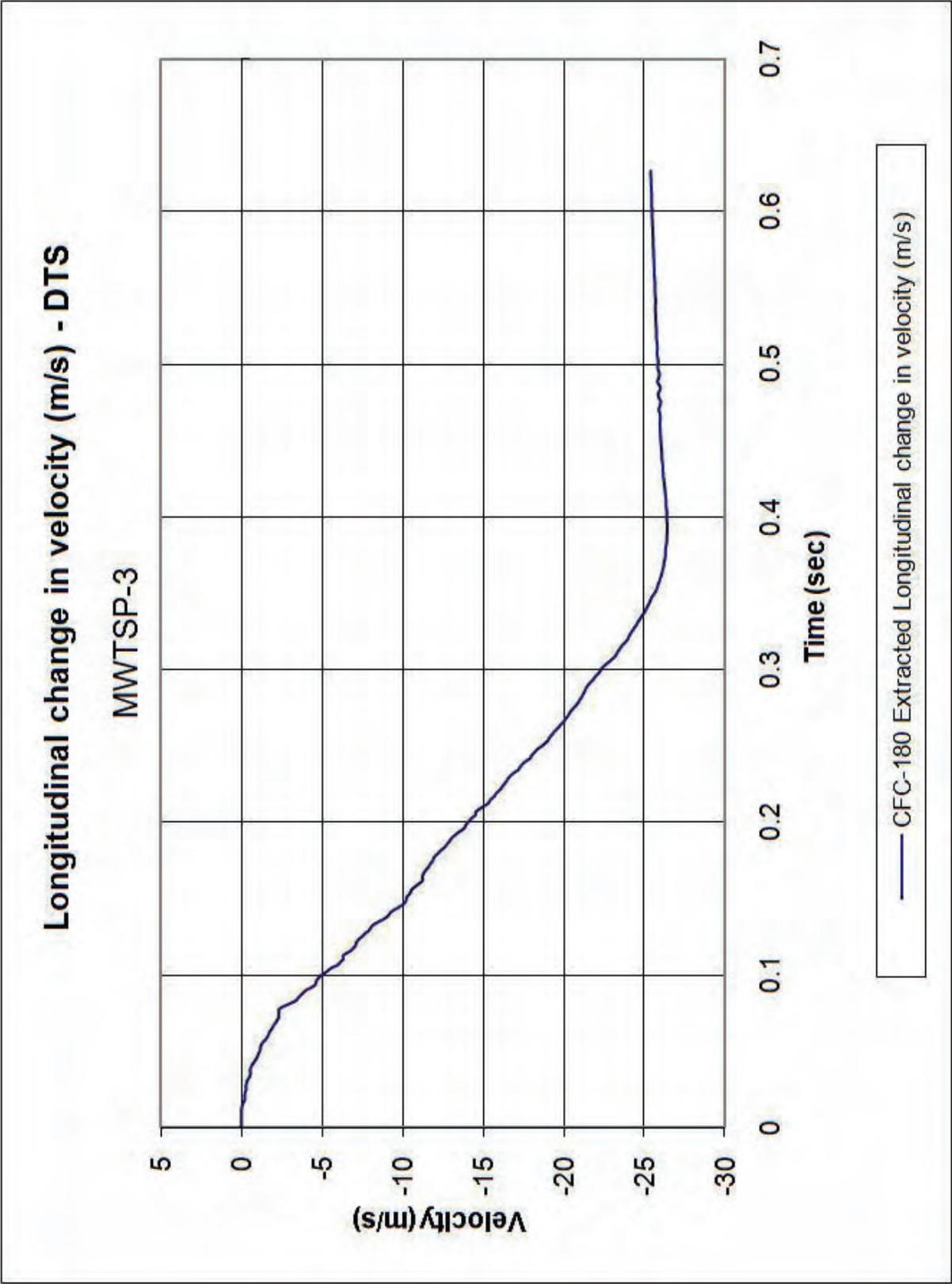
Figure I-2. Longitudinal Change in Velocity (DTS), Test No. MWTSP-3
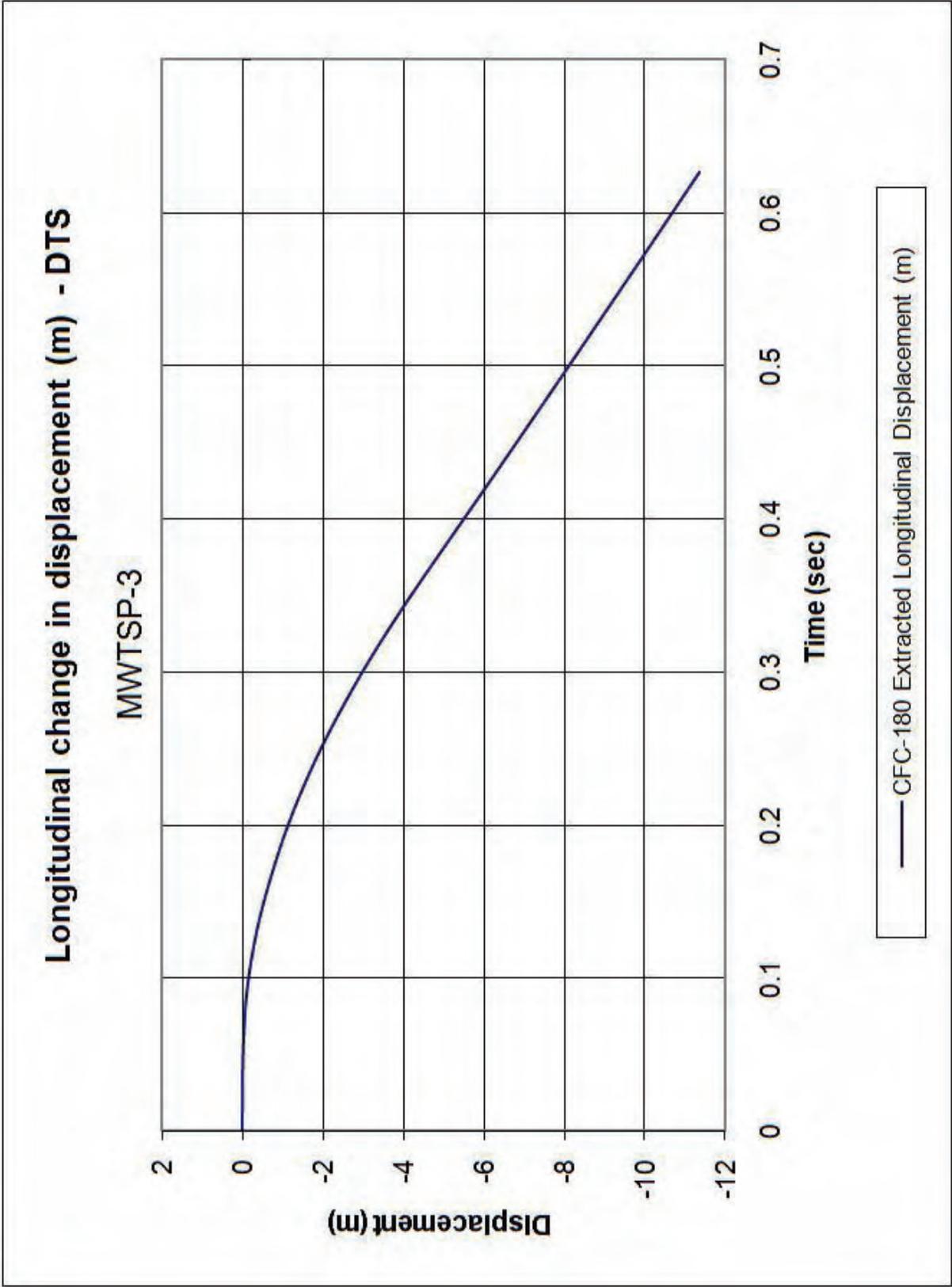
Figure I-3. Longitudinal Occupant Displacement (DTS), Test No. MWTSP-3
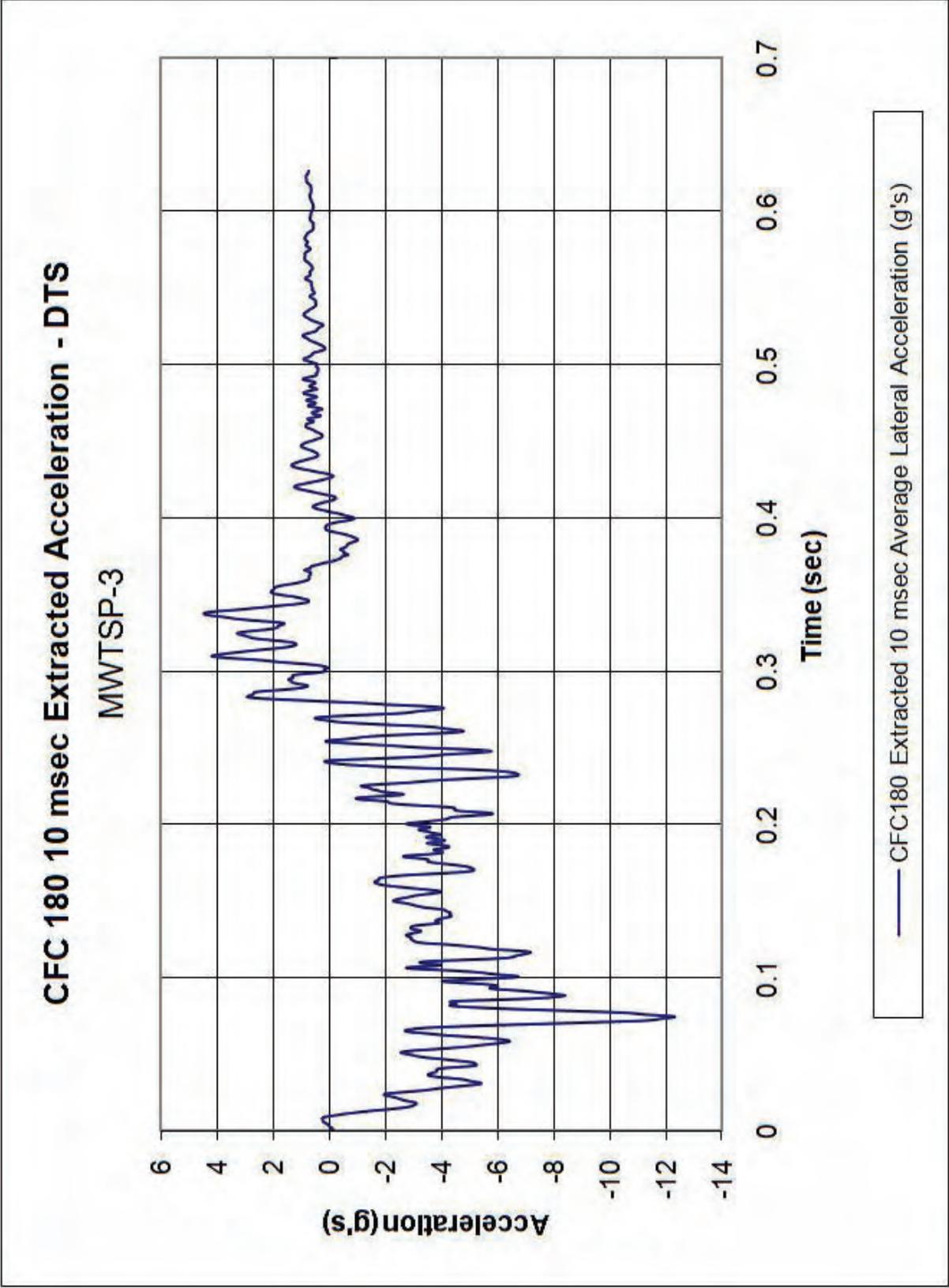
Figure I-4. 10-ms Average Lateral Deceleration (DTS), Test No. MWTSP-3
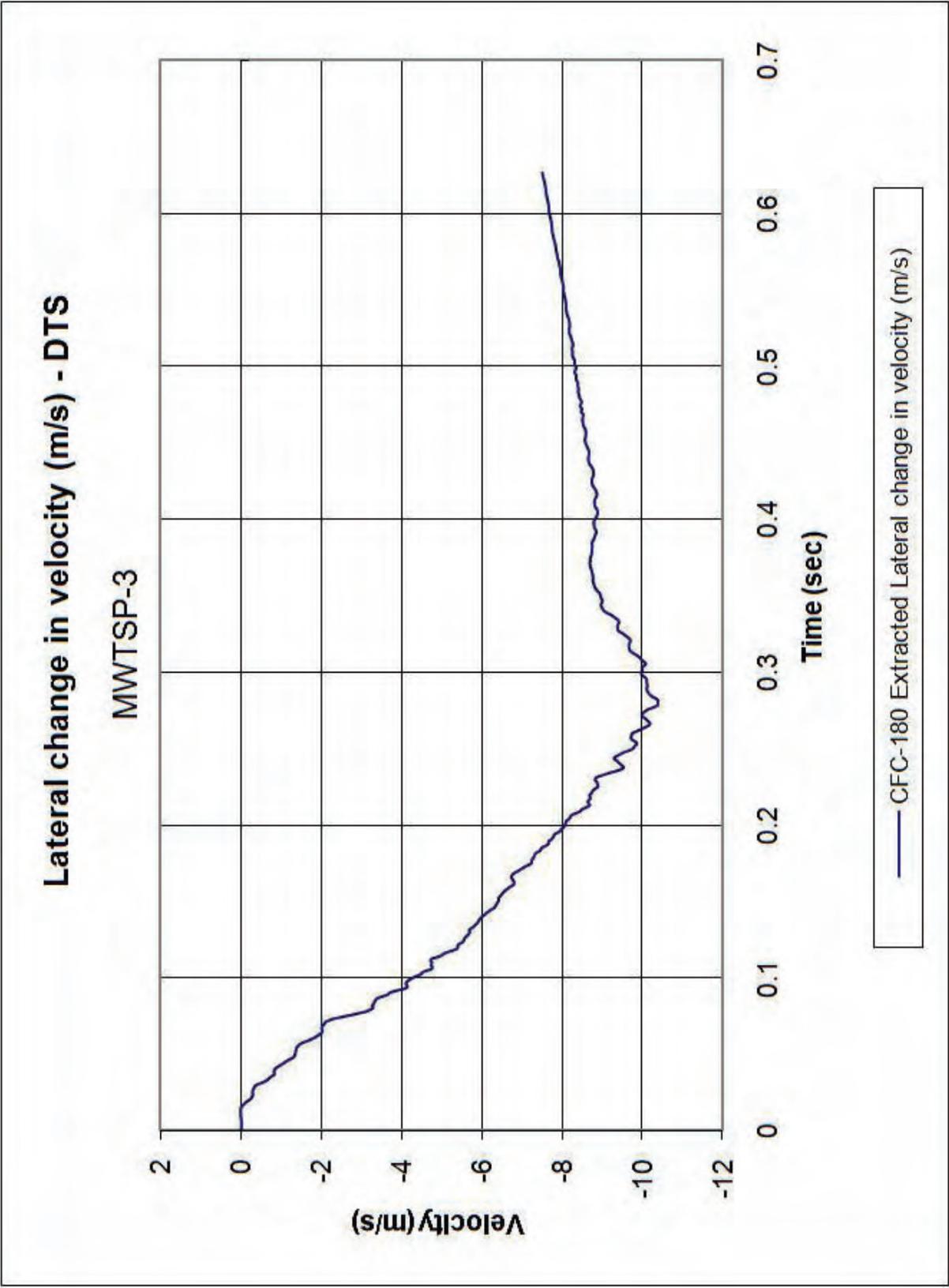
Figure I-5. Lateral Occupant Impact Velocity (DTS), Test No. MWTSP-3
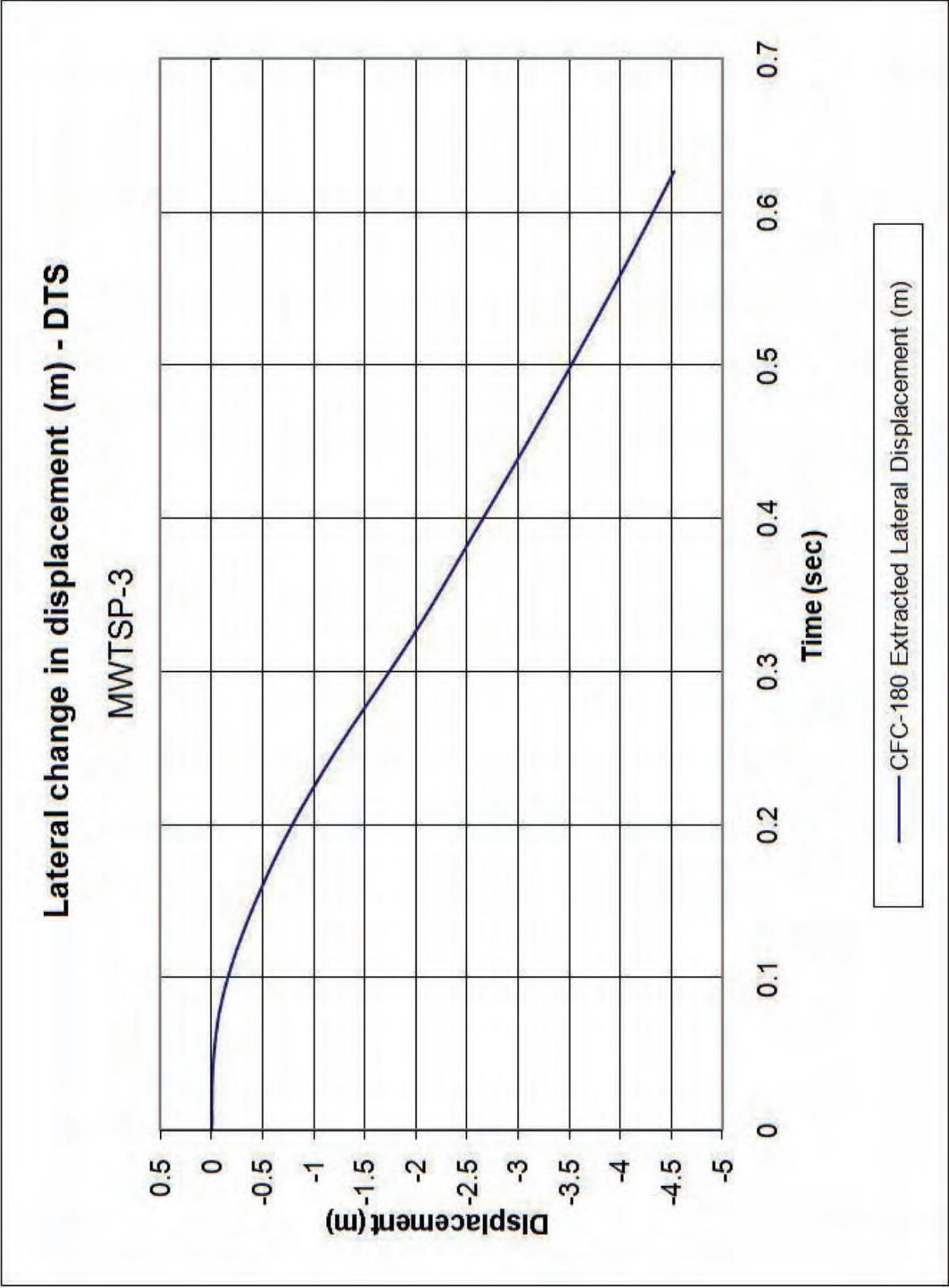
Figure I-6. Lateral Occupant Displacement (DTS), Test No. MWTSP-3
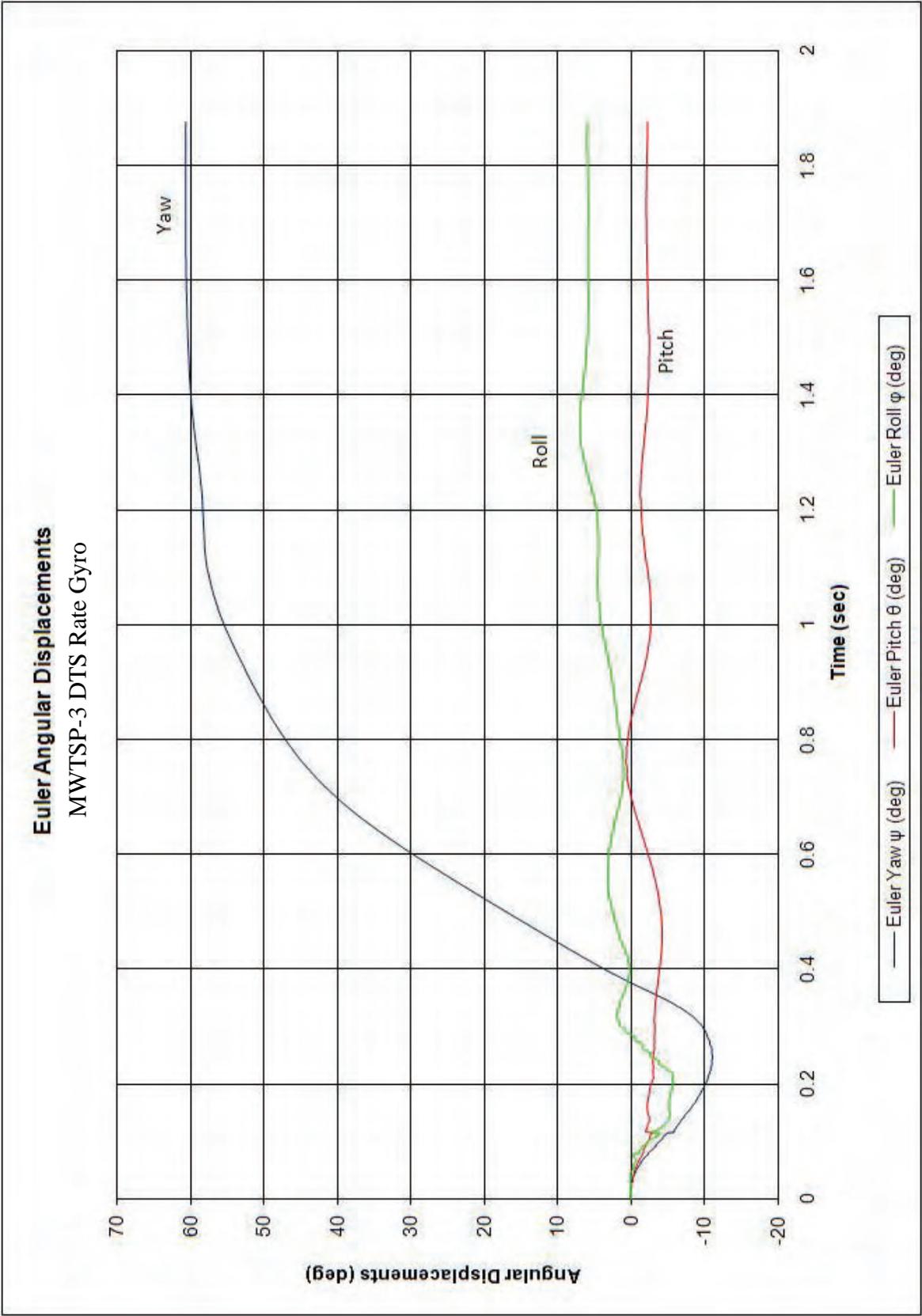
Figure I-7. Vehicle Angular Displacements (DTS), Test No. MWTSP-3
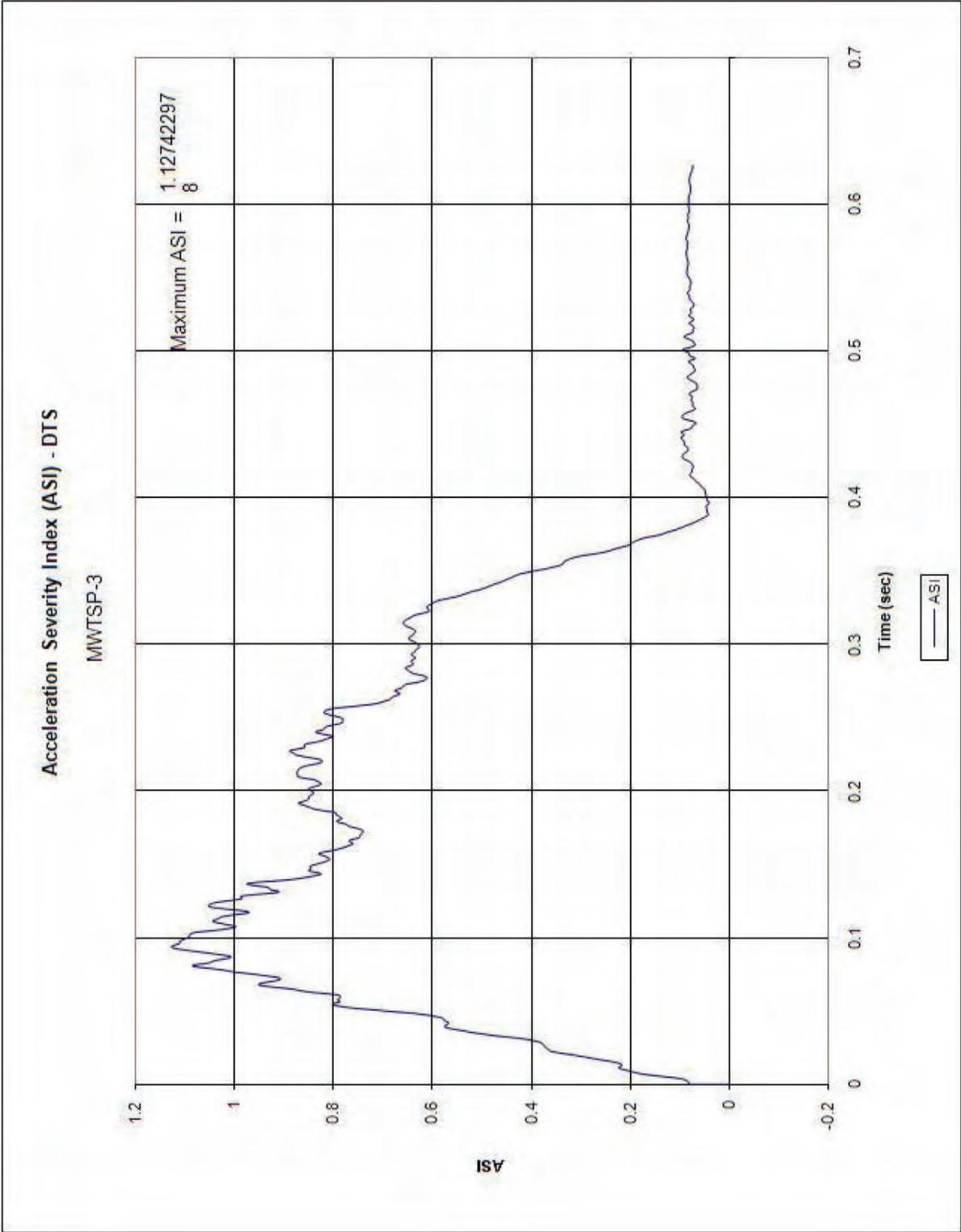
Figure I-8. Accident Severity Index (ASI) [DTS], Test No. MWTSP-3
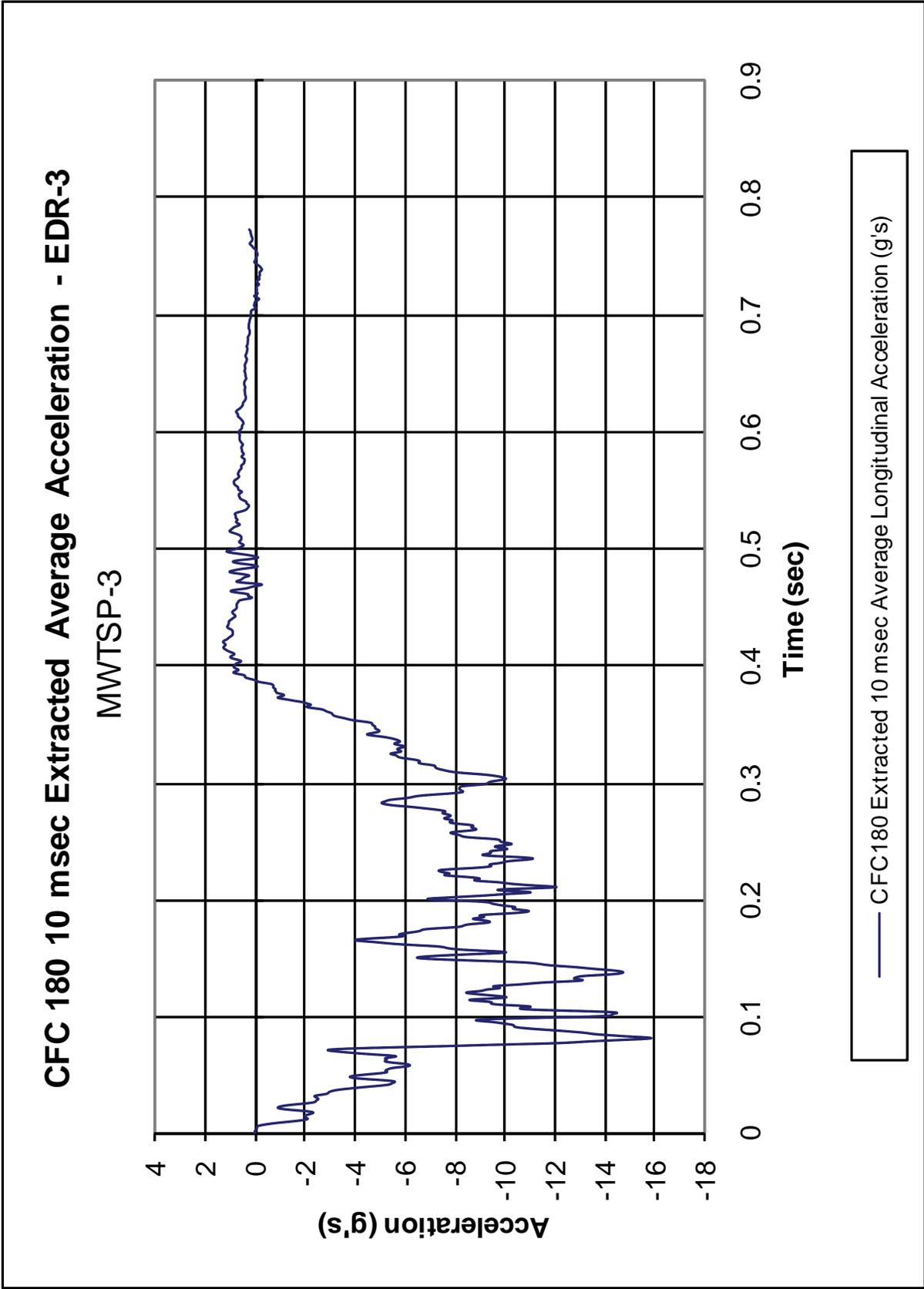
Figure I-9. 10-ms Average Longitudinal Deceleration (EDR-3), Test No. MWTSP-3
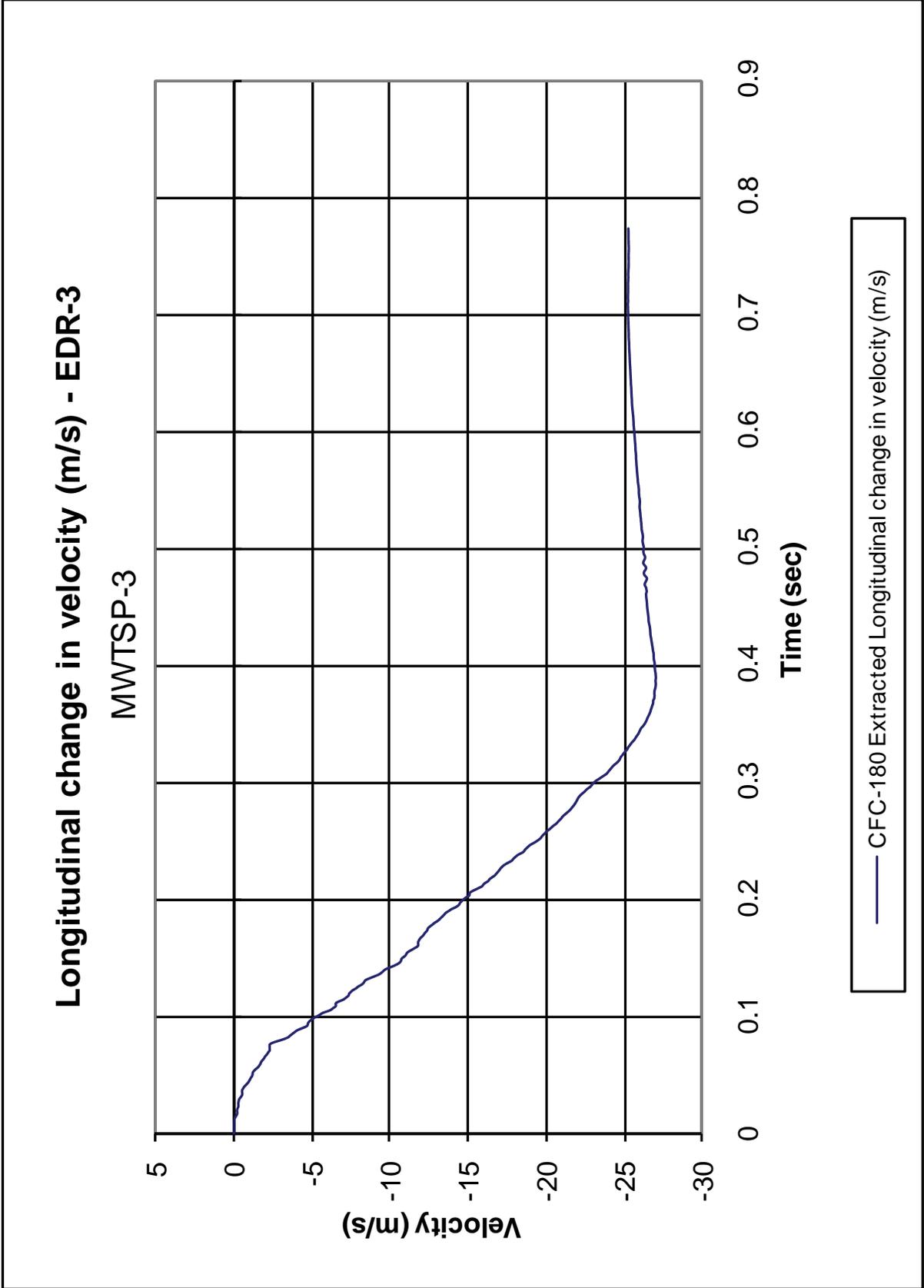
Figure I-10. Longitudinal Change in Velocity (EDR-3), Test No. MWTSP-3
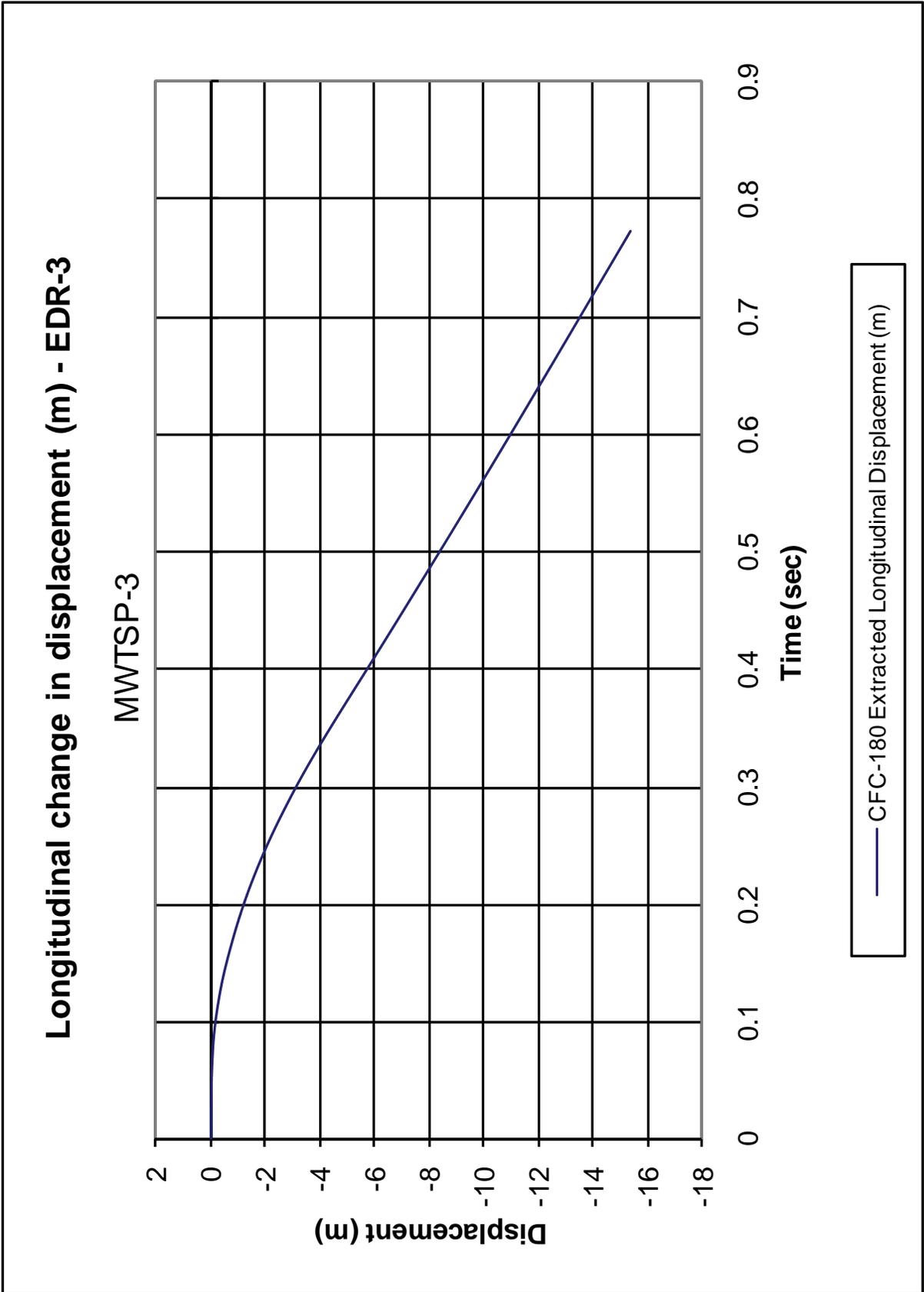
Figure I-11. Longitudinal Occupant Displacement (EDR-3), Test No. MWTSP-3
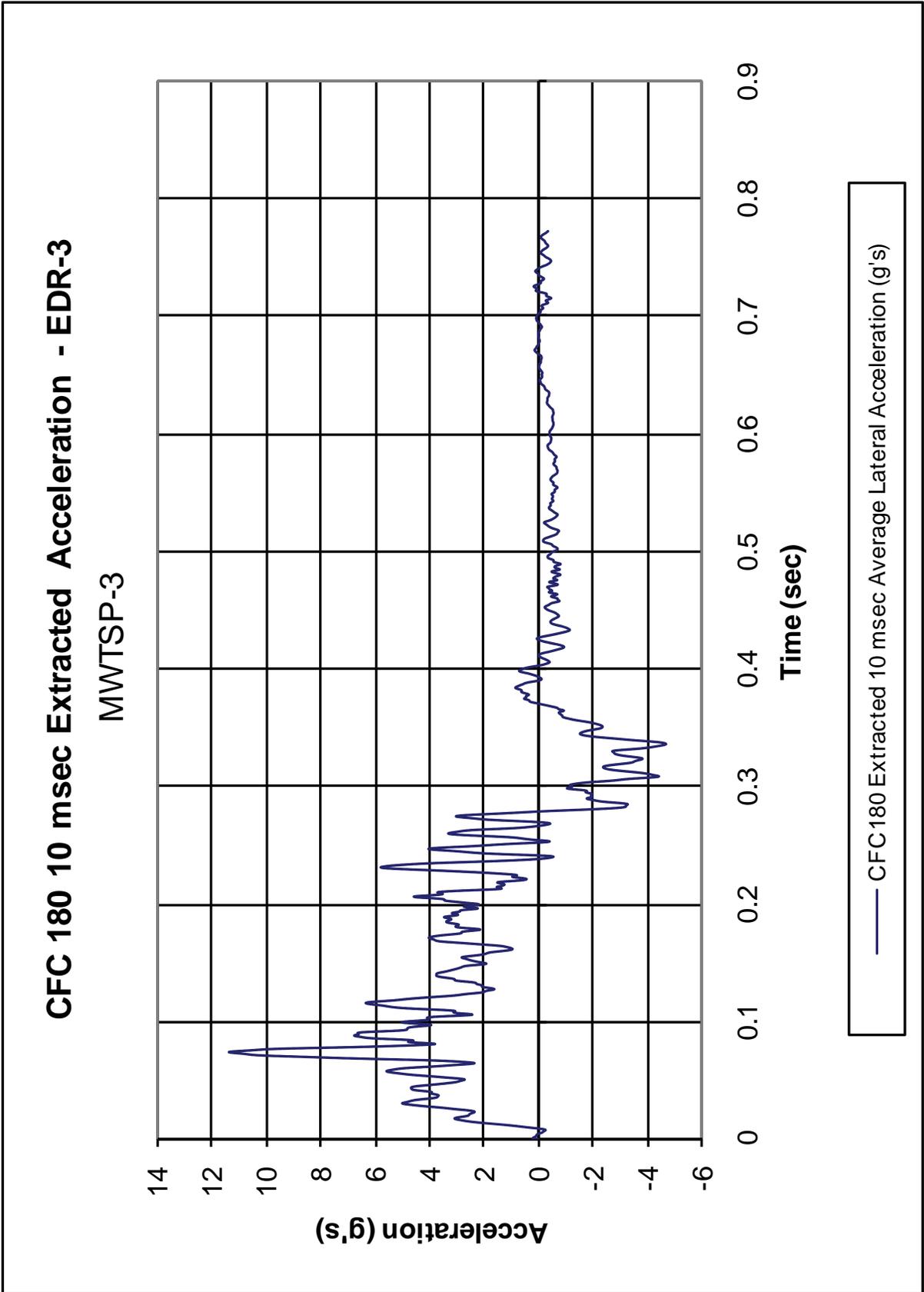
Figure I-12. 10-ms Average Lateral Deceleration (EDR-3), Test No. MWTSP-3
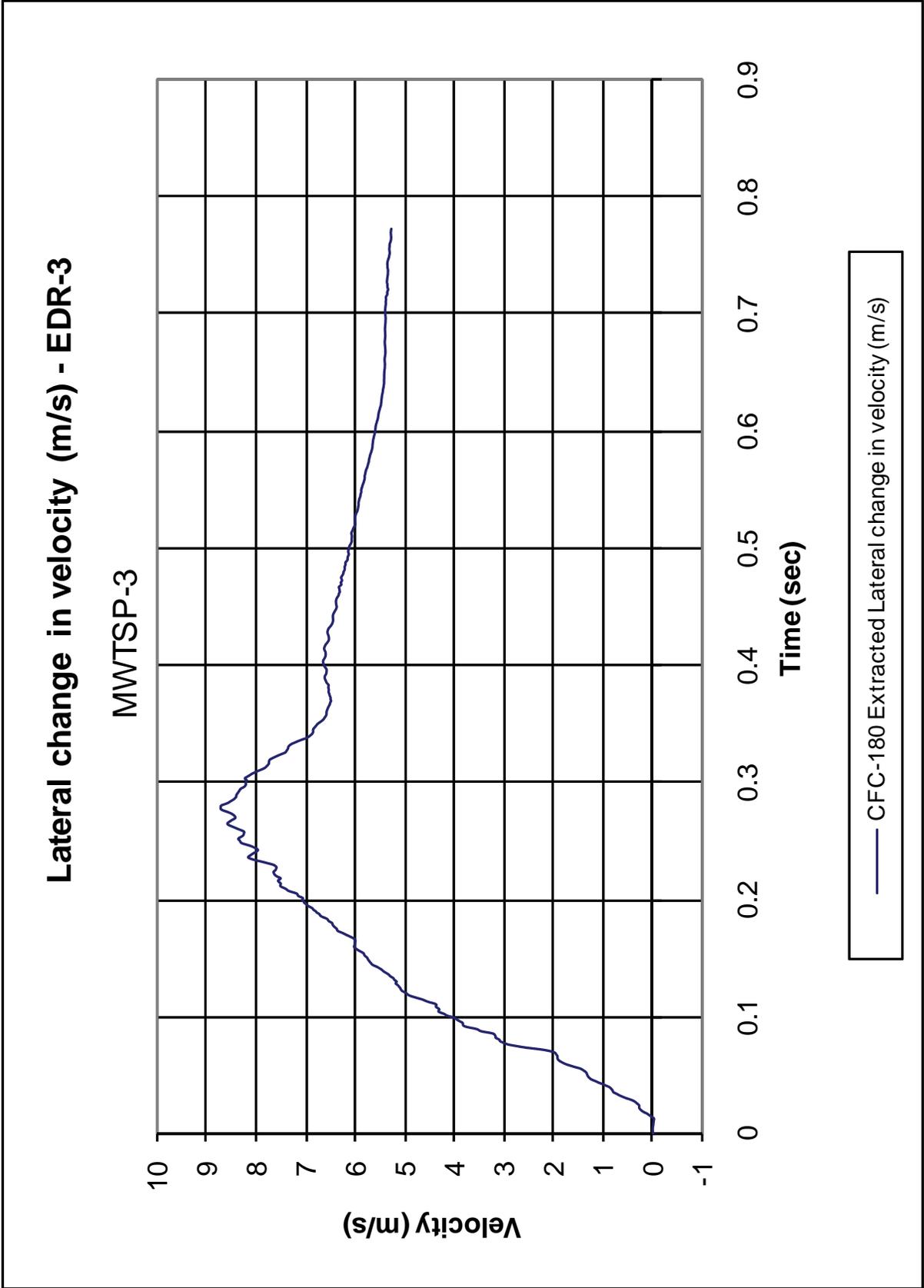
Figure I-13. Lateral Occupant Impact Velocity (EDR-3), Test No. MWTSP-3
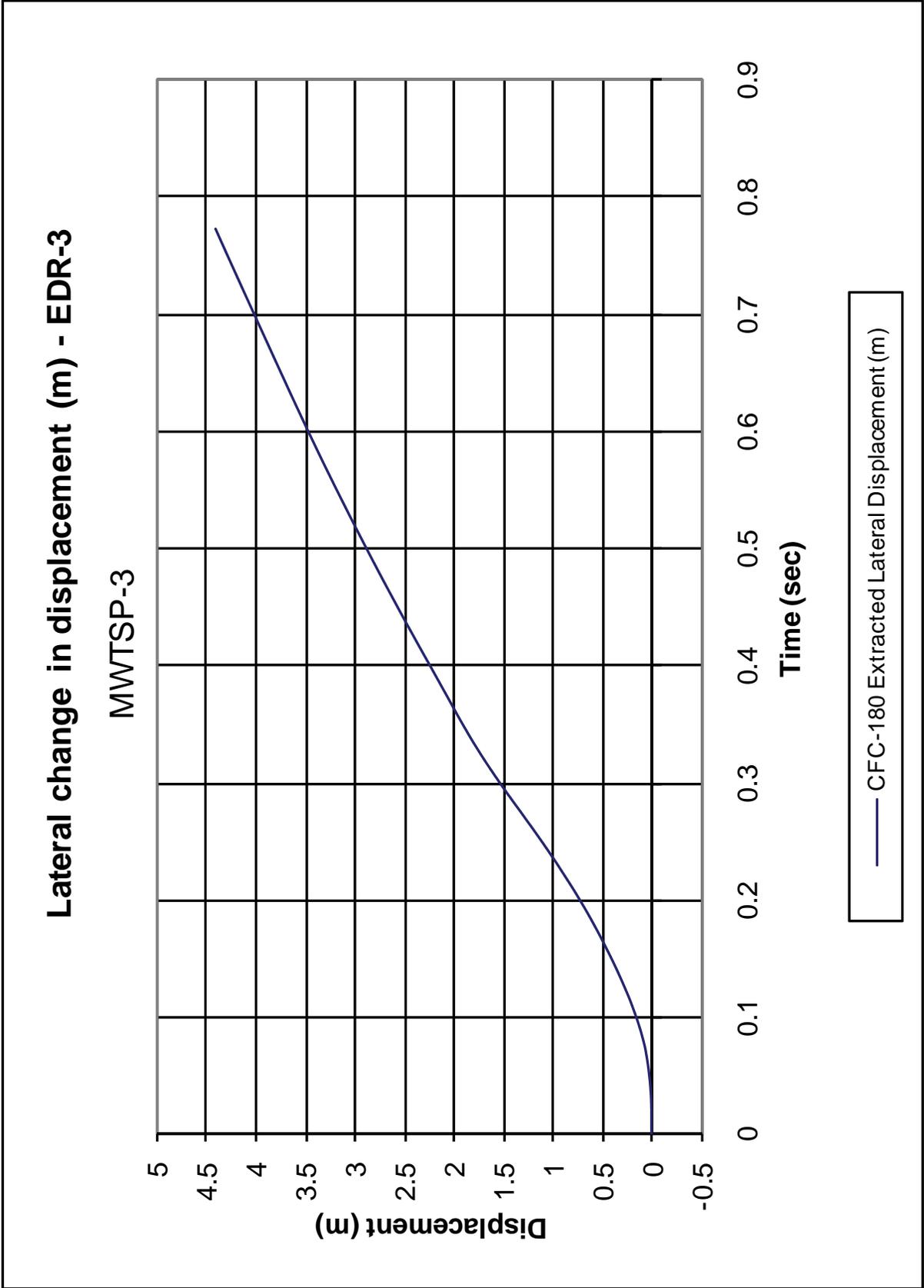
Figure I-14. Lateral Occupant Displacement (EDR-3), Test No. MWTSP-3
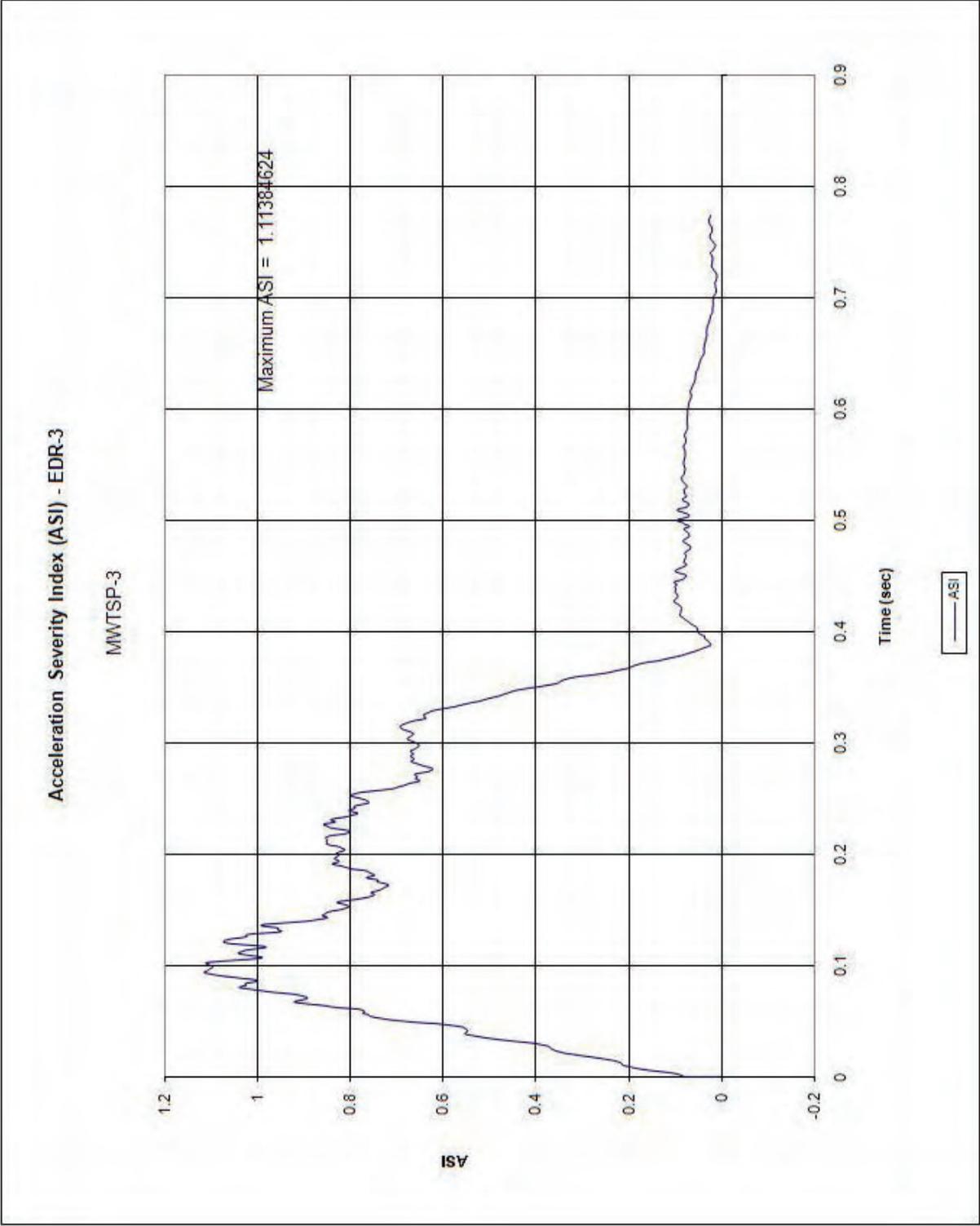
Figure I-15. Accident Severity Index (ASI) [EDR-3], Test No. MWTSP-3

END OF DOCUMENT